Boundaries of triangle-patches and the expander constant of fullerenes

Dissertation
zur Erlangung des Doktorgrades der Fakultät für Mathematik
an der Universität Bielefeld

vorgelegt von

Claudia Justus

Bielefeld, im Oktober 2007

Gutachter: Prof. Dr. Hans-Georg Carstens
Prof. Dr. Gunnar Brinkmann

Tag der mündlichen Prüfung: 21. Dezember 2007

Gedruckt auf alterungsbeständigem Papier nach ISO 9706

Contents

Chapter 1

Introduction

Fullerenes are spherically shaped molecules composed entirely of carbon, where each atom is directly bonded to three others in a way that only hexagonal and pentagonal rings occur. The first fullerene was discovered in 1985 by Kroto, Curl, and Smalley [31], who were awarded the 1996 Nobel Prize in chemistry for their discovery. That fullerene is still the most famous member of the family: It consists of 60 atoms and is called the *Buckminster fullerene* – named after the architect Richard Buckminster Fuller because its structure reminded of the *geodesic domes* that were popularized by Fuller. Later, the term *fullerene* was used for the whole class of molecules. In 1990, Krätschmer and Huffman [30] developed a technique that enabled fullerene synthesis in a large amount. Since then, these molecules and their promising chemical and physical properties (see e.g. [41], [42]) have been the topic of many studies.

Research in the field of fullerenes and related forms of carbon provides opportunities for collaboration between both chemists and mathematicians, since those molecules can be modeled as discrete mathematical structures where the application of graph theory can yield new insights. In mathematical terms, a fullerene is a trivalent convex polyhedron with pentagonal and hexagonal faces, which is commonly interpreted as a graph with the vertices standing for the atoms and the edges representing the bonds. Therefore in graph theory, the term fullerene refers to any 3-regular, plane graph with all faces of size 5 or 6. Its 3-dimensional representation can immediately be transferred into a 2-dimensional drawing where one of the faces becomes the unbounded outer face. Applying Euler's polyhedron formula to the graph of a fullerene, it follows that there are always exactly 12 pentagons. The smallest fullerene is the dodecahedron with 20 vertices. For larger n, the number of mathematically possible, non-isomorphic fullerenes C_n on n atoms grows extremely fast as a high power of n – for instance, the number of conceivable isomers C_{40} is 40, for C_{60} it is 1 812, for C_{80} there are already 31 924 possible isomers and for C_{100} even 285 913.

However, only few of these mathematically possible structures have already been found in experiment, and an important task in theoretical chemistry is to find criteria to determine which of the many theoretically possible fullerenes are actually stable enough to exist [18]. One factor is the so-called isolated-pentagon-rule: The *isolated-pentagon fullerenes*, that are fullerenes where none of the pentagonal faces are adjacent, typically show a greater chemical stability. The smallest isolated-pentagon fullerene – and the only one with 60 vertices – is the Buckminster fullerene; all others have at least 70 vertices.

Graph theory offers various concepts of stability. For instance, a graph is defined as *connected* if there exists a path between any two vertices, as *k-(vertex-)connected* if at least k vertices have to be removed to obtain a non-connected graph, and as *k-edge-connected* if at least k edges must be removed to destroy the connectivity. Since all fullerenes are 3-vertex- and 3-edge-connected but not 4-vertex- and 4-edge-connected, this concept does not enable us to distinguish different fullerenes due to their degrees of connectivity. However, there exists another, more complex measure of connectivity which is particularly reasonable for k-regular graphs and might provide a further criterion for the stability of a fullerene: the *expander constant*, also known as *Cheeger constant* or *isoperimetric constant* (see e.g. [1], [13], [33], [40]). In this work we use the term expander constant since it is fairly compatible with its meaning.

The computation of the expander constant of a graph requires for each subset of vertices to determine the ratio of the number of edges running between this set and its complement, and the size of the set or its complement (depending on which is smaller); then the minimal ratio over all subsets is determined. The idea behind this is that – in contrast to the common definition of connectivity – the number of edges running between two vertex sets is considered in relation to the size of these sets: If the expander constant is small, then there exists a ‘bottleneck’ where only a few edges join two large subsets of vertices, which makes the graph quite ‘unstable’, whereas in case of a large expander constant, every vertex set has many neighbours outside the set (hence the name ‘expander’). The problem to determine the expander constant of a graph is also common as the *sparsest cut problem.* Since so many subsets have to be considered, it is a very difficult problem – in fact it is known to be NP-hard (see e.g. [34]).

One aim of this thesis is to develop an approach for the computation of the expander constant of fullerenes. It is not known yet whether the expander constant has actually an influence on the chemical stability of a fullerene, but it might give a further hint for identifying the stable fullerenes (see also [18]). In particular, it would be interesting to know the fullerenes with the largest expander constant among all fullerenes with a fixed number of n vertices, and to compare them with the respective isolated-pentagon fullerenes in case they exist.

Besides these possible chemical results, the concept of the expander constant has applications in various fields, for instance in theoretical computer science, because it measures the quality of a network: A graph with a small expander constant is not suitable as a network since a large portion of the network can be removed by cutting only a few edges, while a network corresponding to a graph with a large expander constant cannot be ‘destroyed’ that easily. Since fullerenes are 3-regular, they are ‘sparse’ in the sense that for a fixed number of vertices, the number of edges is not too large. Therefore they are appropriate candidates for good networks, and it would be helpful to be able to determine and compare the expander constants of fullerenes in order to have a measure for their connectivity and pick out the ‘best’ ones.

As many other topics that are related with the mathematics behind carbon molecules, this also leads immediately to the theory of *patches*, that are 2-connected plane graphs which typically have all faces of the same size except the unbounded face and possibly some ‘defective faces’, and all vertices of the same degree except those lying in the unbounded face (these are called boundary vertices) and possibly some ‘defective vertices’. Although fullerenes contain patches with hexagonal and pentagonal faces, the main focus of the present thesis will lie on triangle-patches. The reason for this is that sometimes – and in particular in the context of the expander constant – it is easier to consider the *dual* graph of a fullerene, which is defined to be the plane graph that is obtained by drawing a vertex in each face and inserting an edge between two vertices lying in neighbouring faces for each edge the faces have in common. In the case of a fullerene, the dual is a triangulation of the plane with vertices of degree 5 and 6 (those of degree 5 correspond to the pentagons and so their number is also 12) – and this is exactly the definition of a geodesic dome, the structure for which the architect Fuller became famous, as already mentioned above.

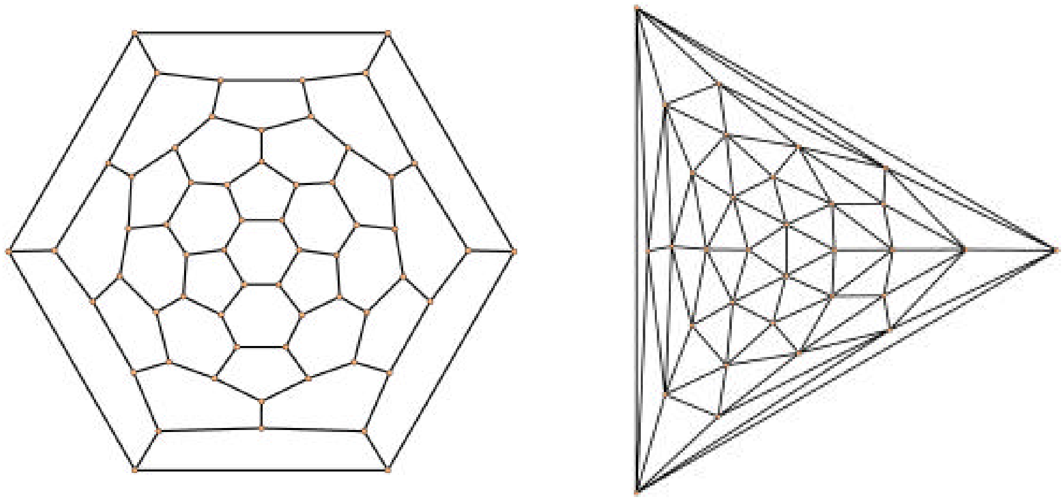

Figure 1.1: The Buckminster fullerene C_{60} (left figure), and its dual (right figure)

All topics and results of this thesis have in common that the *boundaries* of patches – mainly triangle-patches – are analysed, in particular in relation to their numbers of faces. One application of these studies consists in the investigation of the expander constant of fullerenes, since the ratio that has to be calculated for vertex sets in fullerenes becomes simply the quotient of boundary length divided by face number in triangle-patches when considering the dual. However, computing expander constants is not the only aim of this work. The results that are presented in the separate chapters have different applications and all are of mathematical interest on their own.

The number of faces of a triangle-, hexagon- or quadrangle-patch (the three cases that correspond to the Euclidean lattices of the plane) with respect to its boundary sequence, that is the cyclic sequence of vertex degrees in the outer face, has already been examined in several studies: In [26] and [5] it was shown for patches without disorder (that is, without defective faces or vertices) that the boundary sequence – although it does in general not determine the interior of a patch uniquely – does determine its number of faces. Furthermore, in [29] and [9] this result was extended to patches with exactly one defective face whose size is not a multiple of the regular face size, applying a technique based on the observation that when embedding the boundary of such a patch into the regular lattice, the disorder corresponds to a non-trivial rotation. The proof was carried out for quadrangle-patches but can be transferred to triangle- and hexagon-patches. Moreover, by translation to the dual it can be seen that a similar theorem holds if a defective vertex instead of a defective face exists. But it is also known that the statement is not true anymore if more than one defective face or vertex is allowed. However, if a fixed subpatch is given that determines the position of the defective faces or vertices, this might change again. In chapter 2 it is shown that indeed the number of faces of a triangle-patch with defective vertices is uniquely determined by its boundary sequence and a fixed subgraph that contains all defective vertices in case the disorder does not correspond to a trivial rotation. This generalizes the previous results since the case of no or one disorder is of course included. The corresponding result for the dual implies that two hexagon-patches with the same boundary and p pentagons as defective faces, where $p \bmod 6 \neq 0$, can only have a different number of faces if they do not contain isomorphic subpatches containing the pentagons. As two hexagon-pentagon-patches with the same boundary can be used to construct one fullerene from another by a patch replacement operation (see [7] and [8]), which enables fullerene growth in case the patches have different numbers of faces, one consequence of this outcome is that in such *growth patches* with $p \neq 6$ pentagons, the positions of the pentagons relative to each other must differ.

In chapter 3, various results on the minimality of the boundary length of patches with respect to their numbers of faces are provided. These will be helpful for the determination of the expander constant, but are also of mathematical interest on their own. There have already been several studies in this area (see e.g. [27], [3], [22], [15]) that deal mainly with hexagon-patches. Here we present first some explicit formulas on the minimal boundary lengths of disordered hexagon-patches containing triangles, quadrangles, and pentagons as defective faces in terms of their numbers of faces that extend [15]; afterwards these results are used to develop similar formulas for the duals, that are triangle-patches with defective vertices of degrees 3, 4, and 5. While [27] contains such a formula for triangle-patches without disorder, this study provides a complete list of formulas for minimal boundary lengths of all triangle-patches with t defective vertices of degree 3, s defective vertices of degree 4, and p defective vertices of degree 5 that fulfill $p + 2s + 3t \leq 6$. This includes the cases with $p \leq 6$ vertices of degree 5, which are the dual results to [3], but also other possible combinations of defective vertices that yield the curvature of a half-tube or a cone and hence allow the construction of arbitrarily large patches. Moreover, we prove that these minimal boundaries are attained when arranging the faces in a certain spiral way.

With these results, we are able to determine triangle-patches with a certain number of defective vertices that obtain a minimal boundary length for a fixed number of faces. However, sometimes patches with minimal boundary lengths are wanted which fulfill the additional requirement that the defective vertices have certain positions relative to each other. For this we consider disordered subpatches containing the defective vertices exactly as in chapter 2, and examine which patches with a given number of faces *and* containing that subpatch have minimal boundary length. This is the subject of the last two sections of chapter 3, and an approach for developing respective boundary formulas is presented that is applied later in chapter 5.

The technique demonstrated in chapter 2, together with some results of chapter 3, can be used for a further application that is of interest for chemists, which is contained in chapter 4: An important result in theoretical chemistry was the classification of *halftubes*, that are infinite hexagon-patches with exactly 6 pentagons. They describe the caps of nanotubes, a tube-type class of fullerenes which is very promising for various applications (see e.g. [41], [42], [46]). The classification of halftubes was enabled due to two results: On the one hand it was known that the boundary of a cap can be chosen in a certain way that can be described by special parameters [14], on the other hand one result of [3] is that such a boundary can only be filled with a finite number of patches. Now chemists are interested in classifying *nanocones*, that are in mathematical terms infinite hexagon-patches with $p < 6$ pentagons. Due to [3] there is also only a finite number of patches with $p < 6$ pentagons that correspond to a given boundary, but a parameterization of the boundary of such cones was still missing.

Here we prove – at first for triangle-cones with $p < 5$ vertices of degree 5 – that the boundary can be chosen in a certain way such that it can be described with two parameters (in case $p = 5$ even one parameter is sufficient). This result then is transferred to hexagon-cones which enables the desired classification.

Finally, chapter 5 contains several results regarding the determination of the expander constant of fullerenes. It is shown that the whole problem can be transferred to the dual – a geodesic dome with n faces – where the task is to find a patch with minimal ratio of boundary length and face number among all subpatches in the geodesic dome that contain at most $\frac{n}{2}$ faces. We will call such a patch *optimal* and derive some properties of optimal patches. Eventually we conclude with two different approaches to determine the expander constant of a fullerene: At first we present a technique of how to verify the expander constant of a class of symmetric fullerenes 'by hand', making use of the results on minimal boundary lengths developed in chapter 3. Afterwards we describe an algorithm that is based on the results of chapter 5 and can be used to calculate the expander constants of fullerenes by computer. A program has been implemented which enables us in particular to compute the maximal expander constant of all fullerenes with a certain number of faces. We present the results of that program, including a complete list of the maximal expander constants of fullerenes with up to 140 vertices and of the maximal expander constants of the respective isolated-pentagon fullerenes. Appendix A contains some figures of geodesic domes where the maximal expander constants are attained.

Chapter 2

Numbers of faces in disordered triangle-patches

2.1 Introduction

A *patch without disorder* is usually defined as a 2-connected plane graph with all faces of size k except one outer face, and all vertices of degree m except the vertices lying in the outer face which have degree at most m. In a *disordered patch*, additional faces of sizes different from k (*defective faces*) or vertices of degrees different from m (*defective vertices*) are allowed. The cases $(m, k) \in \{(3, 6), (4, 4), (6, 3)\}$ correspond to the three Euclidean lattices of the plane; we call all three of them the *Euclidean cases* and distinguish between the hexagonal, quadrangular, and triangular case, respectively.

In this chapter, we deal with the question whether the boundary of a patch, that is the sequence of vertex degrees in the outer face, determines its number of faces. For the non-Euclidean cases it follows easily with the help of Euler's formula that this is always true (see [29]). The three remaining cases are more interesting; in particular the case $(m, k) = (3, 6)$ has applications in Chemistry, but however all three Euclidean cases can be treated similarly.

In the Euclidean cases, patches without disorder are known to have the property that the number of faces is uniquely determined by the boundary. This has first been shown by Guo, Hansen and Zheng [26] for the hexagonal case, while the triangular case has been treated in [5] and the quadrangular case in [29]. Furthermore, the case of exactly *one* disorder is examined in [29] and [9]: It is proven that in case there exists one defective face whose size is not a multiple of k, the number of faces is still determined by the boundary of a patch. The proof is carried out for the quadrangular case but can easily be transferred to the two other cases. Moreover, transferring the outcome to the dual, it can be shown that the same holds in case of one defective vertex with a degree that is not a multiple of k.

Here we are generalizing these results further. We investigate disordered triangle-patches, which we define to be triangular patches with an arbitrary number of defective vertices. This includes disordered triangle-patches with defective vertices of degree 5, as they occur in geodesic domes, the duals of fullerenes. In case there are exactly p defective vertices of degree 5 and no other defective vertices, such a patch will be denoted as a *p-patch*. With this notation, the already mentioned results imply that in a 0-patch as well as in a 1-patch, the number of faces is uniquely determined by the boundary sequence.

For 2 or more defective vertices this is generally not the case, as can be seen in figure 2.1: The two 2-patches, which have been constructed as duals of the *Endo-Kroto patches* (see [16]), have the same boundary sequence, while the right one has two more faces than the left one. But we also observe that comparing the patches, the two degree 5 vertices – which will usually be emphasized by fat dots in this work – have different distances from each other. So the question that arises is: Would it also be possible to find two 2-patches with the same boundary sequence but a different number of faces where both contain, for instance, two *neighbouring* vertices of degree 5? Or more general, two disordered triangle-patches with the same boundary sequence and a different number of faces both containing the same 'configuration' of defective vertices?

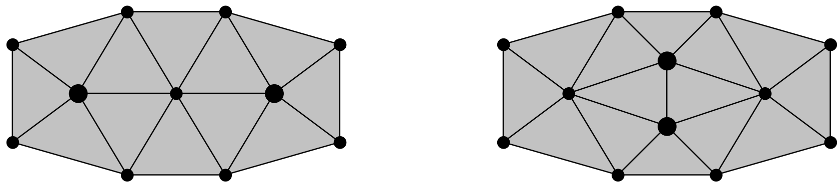

Figure 2.1: Two 2-patches with the same boundary but a different number of faces

In order to describe the 'configuration' of the defective vertices, we consider fixed subgraphs that contain all the defective vertices of the patch, which we will also call (disordered) subpatches. So the general question that we deal with is whether two disordered triangle-patches have the same number of faces if they have the same boundary sequence *and* contain isomorphic subpatches which in turn contain all defective vertices of the patches.

This investigation includes all cases considered before and hence generalizes the work from [29] and [9]; in particular, we re-prove the result for the case of one defective vertex, since for two patches with one defective vertex of the same degree we can always find isomorphic subgraphs containing that defective vertex.

The observation that the number of faces is *not* uniquely determined by the boundary in case there is one defective vertex with a degree that is a multiple of the 'regular' degrees must now be extended to more cases – for instance to all 6-patches: We can easily construct two patches with the same boundary sequence and a different number of faces, both containing the same small 6-patch; for an example see figure 2.2.

Nevertheless we will show in this chapter that in most of the cases – depending on a value that can immediately be computed from the defective vertex degrees – the number of faces of a disordered triangle-patch P with a given subgraph Q that contains all defective vertices is indeed determined by its boundary sequence. The proof adapts ideas of the proof that has been applied in [9] and [29] for single defective faces:

We define a closed directed cycle in P along the boundary of the outer face such that the outer face lies on its left hand side, add a path to one vertex in the boundary of Q, a path along the boundary of Q such that Q lies on its left hand side, and the same path back to the outer face using the inverse edges. This cycle 'cuts out' the patch Q in a way that all faces in $P - Q$ are enclosed on its right hand side. If we embed it into the triangular lattice, it forms a closed cycle and the number of faces in its interior can easily be counted (see figure 2.3 for an example). We will show that this method yields the same number of

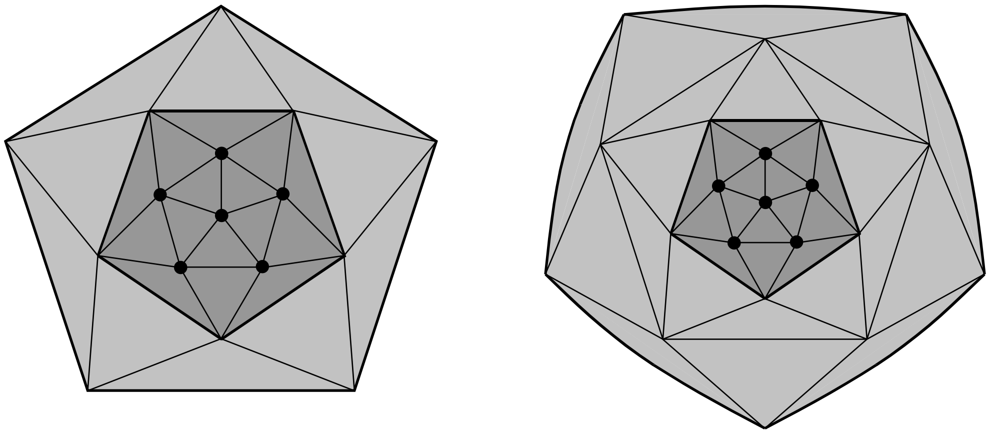

Figure 2.2: Two patches containing the same subgraph – in this case with $p = 6$ vertices of degree 5 – that have the same boundary but a different number of faces

faces for *any* disordered triangle-patch with the same boundary that contains Q by using that the boundary corresponds to a non-trivial rotation. (In the cases where the statement is not true, e.g. for 6 degree 5 vertices, we have a trivial rotation here.)

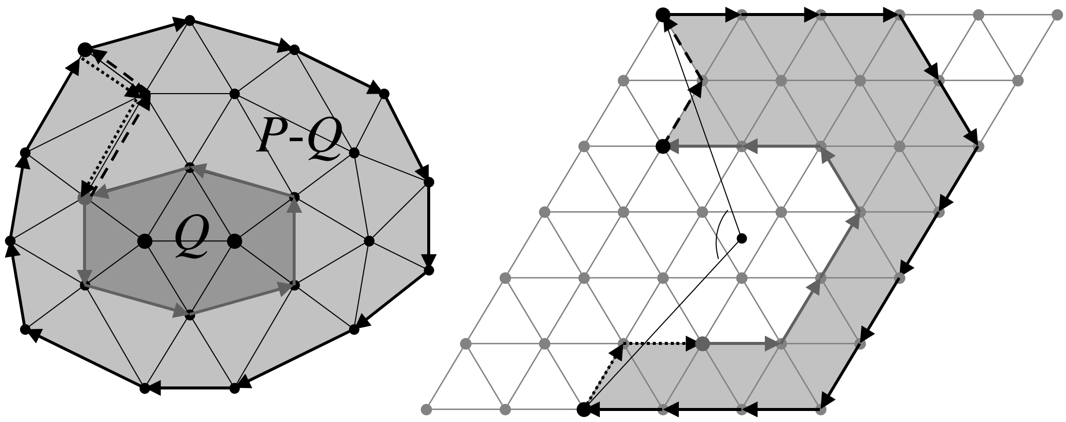

Figure 2.3: Cutting out a small patch containing the defective vertices and embedding the result into the lattice

Although this approach uses some techniques from the previous proofs, the essential step that was carried out in [9] and [29] does not work any more in this more general context, because it was based on the symmetry of the single disorder, which does not apply here. Therefore new techniques had to be found in order to prove the general theorem that we present here.

2.2 Disordered triangle-patches

We start with the definition of disordered triangle-patches and the notation that will be used in this context.

Definition 2.2.1 *A* disordered triangle-patch *is a 2-connected plane graph P where all faces have size 3 (these will be called* triangles*) except one face that is called the* outer face, *and all vertices that lie in the outer face have degree at most 6. Vertices that do not lie in the outer face and have a degree different from 6 are called* defective vertices.

Any face in P that is not the outer face is called bounded face. *We usually draw P such that the unbounded area is the outer face. The set of vertices will be denoted by $V(P)$, the set of edges by $E(P)$, and the set of bounded faces by $F(P)$. If there is no possibility of misunderstanding we also use just V, E, and F, respectively, and write $P = (V, E, F)$. Moreover, we define $v(P) := |V(P)|$, $e(P) := |E(P)|$, and $f(P) := |F(P)|$.*

The vertices and edges lying in the outer face are called boundary vertices *and* boundary edges, *respectively. Edges that are no boundary edges are called* inner edges, *vertices that are no boundary vertices are called* inner vertices. *The set of boundary vertices in P will be denoted by $V_b(P)$, the set of inner vertices by $V_i(P)$.*

The boundary cycle *of P is a directed cycle consisting of the boundary edges directed in a way such that the outer face lies on their left hand side. The* boundary length *of P is the number of boundary edges or vertices and denoted by $b(P)$. The cyclic sequence of vertex degrees in the boundary cycle is called the* boundary sequence *of P. Two patches are said to have the same boundary sequence (or simply the* same boundary*) if one boundary sequence can be obtained from the other by a cyclic reordering or inversion.*

For $i \in \mathbb{N}$ we denote the number of inner vertices in P that have degree i by $D_i(P)$. With this we define:

$$D(P) := \sum_{i \in \mathbb{N}} (6 - i)\, D_i(P) \tag{2.1}$$

A disordered triangle-patch with exactly p defective vertices of degree 5 and no other defective vertices is called p-patch.

Remark 2.2.2 *If P is a p-patch,* (2.1) *implies $D(P) = p$.*

Lemma 2.2.3 *For any disordered triangle-patch P we have*

$$\sum_{v \in V_b(P)} (4 - \deg(v)) \;=\; 6 - D(P)\;.$$

PROOF:

Let $e := e(P)$, $f := f(P)$, $v := v(P)$, and $b := b(P)$. By counting every vertex v exactly $\deg(v)$ times we get every edge twice, so

$$2e \;=\; \sum_{v \in V_i(P)} \deg(v) + \sum_{v \in V_b(P)} \deg(v) \;=\; \sum_{i \in \mathbb{N}} D_i(P) \cdot i + \sum_{v \in V_b(P)} \deg(v) \tag{2.2}$$

holds. Similarly, if we count every bounded face three times we get boundary edges once and all other edges twice, so we have

$$3f \;=\; 2e - b \stackrel{(2.2)}{=} \sum_{i\in\mathbb{N}} D_i(P)\cdot i + \sum_{v\in V_b(P)} \deg(v) - b \tag{2.3}$$

Furthermore we have by definition:

$$v \;=\; |V_i(P)| + |V_b(P)| \;=\; \sum_{i\in\mathbb{N}} D_i(P) + b \tag{2.4}$$

Now Euler's formula yields $v - e + f = 1$ (note that $F(P)$ does not include the outer face), or equivalently

$$6v - 6e + 6f \;=\; 6\,. \tag{2.5}$$

Inserting (2.2), (2.3), and (2.4) into (2.5) we get

$$\begin{aligned} 6 \;&=\; 6\big(\sum_{i\in\mathbb{N}} D_i(P) + b\big) \;-\; 3\big(\sum_{i\in\mathbb{N}} D_i(P)\cdot i + \sum_{v\in V_b(P)} \deg(v)\big) \\ &\qquad + 2\big(\sum_{i\in\mathbb{N}} D_i(P)\cdot i + \sum_{v\in V_b(P)} \deg(v) - b\big) \\ &=\; 6\sum_{i\in\mathbb{N}} D_i(P) \;-\; \sum_{i\in\mathbb{N}} D_i(P)\cdot i \;+\; 4b \;-\; \sum_{v\in V_b(P)} \deg(v) \\ &=\; \sum_{i\in\mathbb{N}} (6-i)\, D_i(P) \;+\; 4\,|V_b(P)| \;-\; \sum_{v\in V_b(P)} \deg(v) \\ &=\; D(P) \;+\; \sum_{v\in V_b(P)} (4 - \deg(v)) \end{aligned}$$

which immediately implies the statement of the lemma.

□

Corollary 2.2.4 *If P and P' are disordered triangle-patches with the same boundary, then we have $D(P) = D(P')$.*

PROOF:

If P and P' have the same boundary, they must in particular fulfill

$$\sum_{v\in V_b(P)} (4 - \deg(v)) \;=\; \sum_{v\in V_b(P')} (4 - \deg(v))$$

from which we get with lemma 2.2.3

$$6 - D(P) \;=\; 6 - D(P')$$

and hence $D(P) = D(P')$.

□

2.3 The triangular lattice

In this section we specify what we mean by 'the lattice', introduce further useful definitions, and prove some results that are essential for the later main proof of this chapter.

At first we define the *Coxeter coordinates*, a helpful notation which was applied by Coxeter in [12] in order to describe the construction of geodesic domes.

Definition 2.3.1 *By the* triangular lattice *(or simply also the* lattice*) we mean the infinite plane graph with all faces triangles and all vertices of degree* 6. *We usually draw the triangular lattice such that all triangles are equilateral.*

A segment *in the triangular lattice is a pair of two vertices* $\{v, w\}$ *of the lattice which is visualized by the straight line between them.*

As described e.g. in [20], *we assign* Coxeter coordinates $\mathrm{Cox}(\{v, w\}) = (p, q)$ *to a segment* $\{v, w\}$ *which does not coincide with a line of the lattice as follows: Take one of the vertices – w.l.o.g.* v *– as the origin, the edge that lies right of the segment as the unit vector in the* p *direction, and the edge left of the segment as the unit vector in the* q *direction. Then the Coxeter coordinates of the segment* $\{v, w\}$ *are given by the coordinates of the second vertex* w*. In case the segment coincides with a line of the lattice, its Coxeter coordinate is simply* (p) *where* p *is the number of edges of the segment. Figure* 2.4 *shows some examples of the Coxeter coordinates of different segments.*

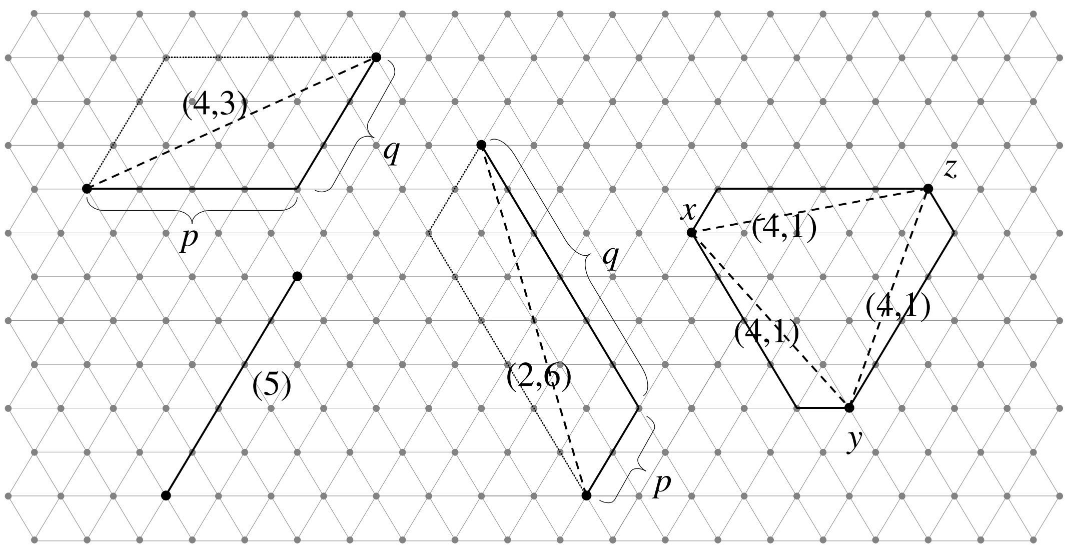

Figure 2.4: Segments in the triangular lattice with the respective Coxeter coordinates; note that the vertices x, y and z form an equilateral triangle

Note that if we start with the vertex w as the origin, we obtain the same coordinates (p, q). If the segment $\{v, w\}$ does not coincide with a line of the lattice and we draw the straight lines that correspond to their coordinates starting at both vertices we obtain a parallelogram that we will call the *parallelogram corresponding to* v *and* w.

The following lemma is of a geometrical type, so it is important to consider a drawing of the triangular lattice in the plane where indeed all basic triangles of the lattice are equilateral. Then it is guaranteed that if we have vertices x, y, z in the lattice with $\mathrm{Cox}(\{x,y\}) = \mathrm{Cox}(\{y,z\}) = \mathrm{Cox}(\{x,z\})$, they form an equilateral triangle, too.

Additionally we assume the length of the side of one basic triangle to be 1. Then by a *point* in the lattice we just mean a point in the plane – not necessarily a vertex of the lattice – and by the *distance* between two points we mean the length of the straight line joining them.

Lemma 2.3.2 *Let x, y, z be vertices in the triangular lattice which fulfill* $\mathrm{Cox}(\{x,y\}) = \mathrm{Cox}(\{y,z\}) = \mathrm{Cox}(\{x,z\}) = (p,q)$*, and c the* center *of the equilateral triangle formed by them, that is the point c in the lattice with equal distance to x, y, and z. Then c coincides with a vertex of the lattice if and only if* $|p-q| \bmod 3 = 0$*; otherwise, it lies in the center of a face.*

PROOF:

At first we consider the case $p = 0$, that means $\mathrm{Cox}(\{x,y\}) = \mathrm{Cox}(\{y,z\}) = \mathrm{Cox}(\{x,z\}) = (q)$. Then all lines of the triangle formed by x, y, and z coincide with lines of the lattice, and the sides are all of length q. The length of its altitude is $a = \frac{\sqrt{3}}{2}q^2$ and it is known that c divides a into parts of lengths $\frac{1}{3}a$ and $\frac{2}{3}a$; so since $\frac{\sqrt{3}}{2}$ is the altitude of a single face we obtain that c lies in a vertex of the lattice if and only if $q \bmod 3 = 0$. In case $q \bmod 3 \neq 0$ we can check in a similar way that c lies exactly in the center of a face of the lattice.

In case $p, q \neq 0$ we insert the parallelograms with sides of lengths p and q as can be seen in figure 2.5. Then we observe that c lies in the center of an equilateral triangle whose sides again coincide with lines of the lattice and have lengths $|p-q|$. With the result from above we obtain the statement of the lemma.

□

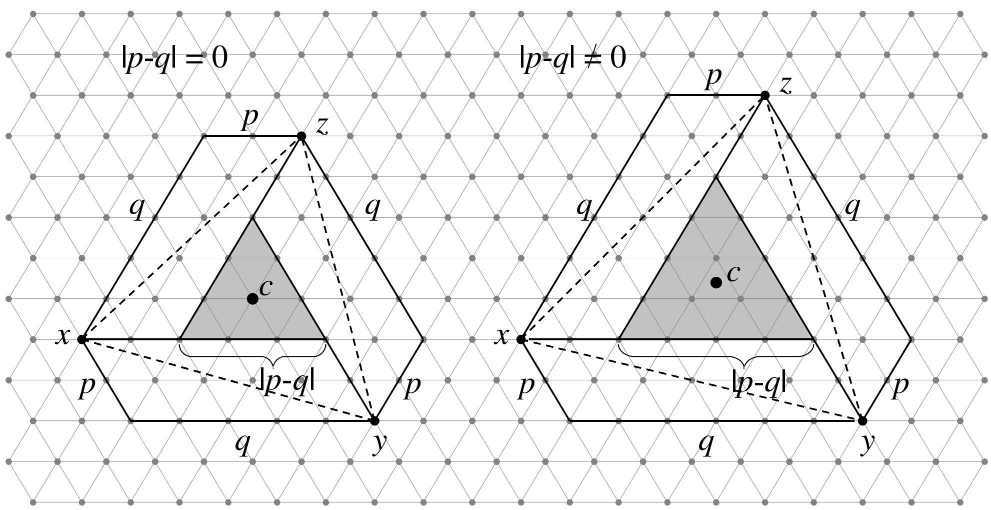

Figure 2.5: Two regular triangles in the lattice: In the left case we have $|p-q| \bmod 3 = 0$, in the right $|p-q| \bmod 3 \neq 0$.

In the following we will always consider the triangular lattice together with a coordinate system. The next definitions and results already occur in a similar way in [29] for the quadrangular case and have now just been transferred to the triangular case.

Definition 2.3.3 *By L we denote the triangular lattice equipped with a coordinate system such that the vertices are pairs (x, y) with $x, y \in \mathbb{Z}$ and there is an edge between (x, y) and (x', y') if and only if one of the following cases applies (see figure* 2.6*):*

1. $|x - x'| = 1$ *and* $y = y'$
2. $x = x'$ *and* $|y - y'| = 1$
3. $|x - x'| = |y - y'| = 1$ *and* $x + y = x' + y'$.

In the first case we will call the edge horizontal, *in the second* vertical *and in the third case* diagonal. *For a vertex $v = (a, b)$ we set $x(v) = a$ and $y(v) = b$.*

We will also consider directed edges in L, that are directed pairs (v, w) of adjacent vertices v and w. The set of directed edges in L is partitioned into six disjoint sets (see again figure 2.6*):*

$$\begin{aligned}
E_0 &:= \{(v, w) \mid x(v) + 1 = x(w),\ y(v) = y(w)\} \\
E_1 &:= \{(v, w) \mid x(v) + 1 = x(w),\ y(v) - 1 = y(w)\} \\
E_2 &:= \{(v, w) \mid x(v) = x(w),\ y(v) - 1 = y(w)\} \\
E_3 &:= \{(v, w) \mid x(v) - 1 = x(w),\ y(v) = y(w)\} \\
E_4 &:= \{(v, w) \mid x(v) - 1 = x(w),\ y(v) + 1 = y(w)\} \\
E_5 &:= \{(v, w) \mid x(v) = x(w),\ y(v) + 1 = y(w)\}
\end{aligned}$$

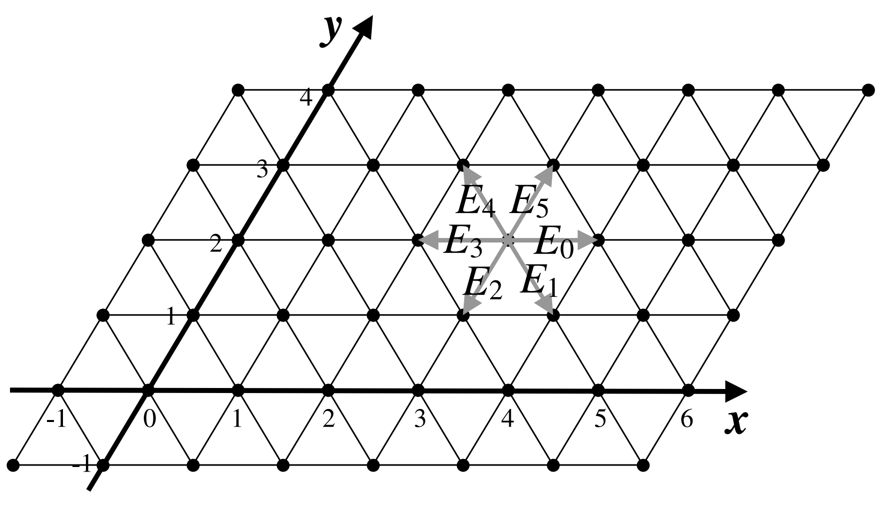

Figure 2.6: The triangular lattice of the plane with a coordinate system and examples of directed edges lying in $E_0, \ldots, E_5$

Definition 2.3.4 *Let M be a finite multiset of directed edges in L. For any directed edge $e = (v, w)$ in L we set $y(e) := y(v)$, i.e. the y-coordinate of an edge is defined as the y-coordinate of its starting point. Then we define:*

$$S_{rl}(M) := \sum_{e \in M \cap E_0} 2y(e) \;-\; \sum_{e \in M \cap E_3} 2y(e) \;+\; \sum_{e \in M \cap E_1} (2y(e) - 1) \;-\; \sum_{e \in M \cap E_4} (2y(e) + 1)$$

The index *'rl'* stands for *'right left'* – we will later see that this has to do with counting faces lying on the right resp. left hand side of closed cycles in the lattice.

Remark 2.3.5 (1) *If we denote the disjoint union of multisets by '+', for two multisets M, M' of directed edges in L we obviously have $S_{rl}(M + M') = S_{rl}(M) + S_{rl}(M')$.*

(2) *Furthermore, if M' consists of the same edges as M only with opposite direction, i.e. $M' = \{(v, w) \in L \mid (w, v) \in M\}$, definition* 2.3.4 *immediately implies*

$$S_{rl}(M') \;=\; -S_{rl}(M)\;.$$

Definition 2.3.6 *Given a disordered triangle-patch $P = (V, E, F)$ with boundary cycle C and a vertex v in C. By C_v we denote the directed path starting and ending at v and following the edges of C, such that P lies on its right hand side. Furthermore we denote $e_0, \ldots, e_{n-1}$ as the succeeding directed edges, and v_i as the ending point of e_{i-1} and starting point of e_i for $i = 1, \ldots, n-1$.*

An embedding *of C_v into the lattice L is a mapping φ that maps the directed edges $e_0, \ldots, e_{n-1}$ onto directed edges in L such that the following holds:*

- *The ending point of $\varphi(e_{i-1})$ is equal to the starting point of $\varphi(e_i)$ for all $i = 1, \ldots, n-1$;*
- *if $\varphi(e_{i-1}) \in E_j$ then $\varphi(e_i) \in E_{j-\deg(v_i)+4 \bmod 6}$ for all $i = 1, \ldots, n-1$.*

For an embedding φ of C_v we define the closure *as a mapping φ' of e_0 into L such that the starting point of $\varphi'(e_0)$ is the ending point of $\varphi(e_{n-1})$, and if $\varphi(e_{n-1}) \in E_j$ holds then we have $\varphi'(e_0) \in E_{j-\deg(v_0)+4 \bmod 6}$.*

The second part of the definition of the embedding makes sure that for two succeeding edges we have the same number of edges lying in the angle right of them in the embedding as in the patch (compare also figure 2.7). In particular, for two patches with the same boundary sequence there are always embeddings that map the boundary cycles onto the same image in L.

The closure is a kind of continuation of the embedding with which we can determine its degree of rotation with respect to $D(P)$:

Lemma 2.3.7 *Given a disordered triangle-patch P with boundary cycle C, a boundary vertex v and an embedding φ of C_v into L with closure φ'. Let e_0 be the first edge in C_v. Then we have for any $l \in \{0, \ldots, 5\}$:*

$$\varphi(e_0) \in E_l \;\;\Rightarrow\;\; \varphi'(e_0) \in E_{l-D(P) \bmod 6} \tag{2.6}$$

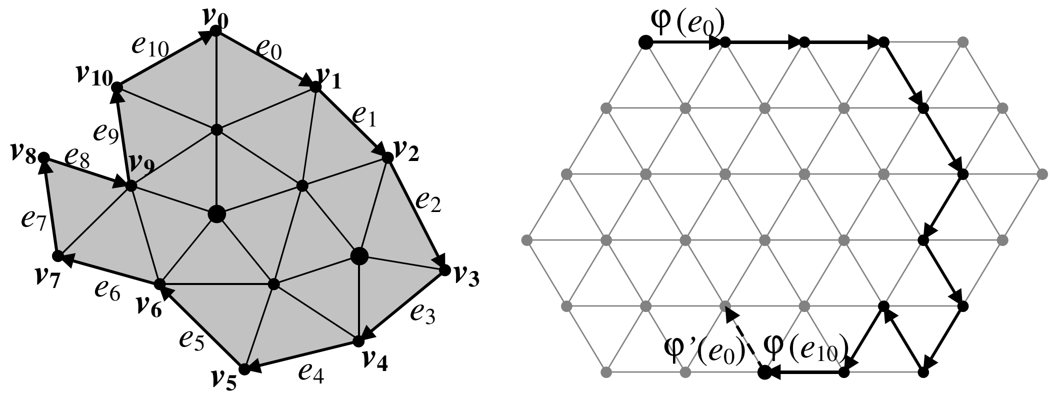

Figure 2.7: A 2-patch with boundary cycle and its embedding into the lattice

PROOF:

Let $v_0, \ldots, v_{n-1}$ and $e_1, \ldots, e_{n-1}$ as in definition 2.3.6, and define $d_i := \deg(v_i)$ for $i = 0, \ldots, n-1$. Then we have $\sum_{i=0}^{n-1}(4 - d_i) = 6 - D(P)$ (lemma 2.2.3) and hence

$$4n - 6 + D(P) = \sum_{i=0}^{n-1} d_i \ . \tag{2.7}$$

If $\varphi(e_0) \in E_l$ then the definition of the embedding yields

$$\begin{aligned}
& \varphi(e_1) \in E_{l-d_1+4 \bmod 6} \\
\Rightarrow\ & \varphi(e_2) \in E_{(l-d_1+4)-d_2+4 \bmod 6} \\
\Rightarrow\ & \ldots \\
\Rightarrow\ & \varphi(e_{n-1}) \in E_{l-\sum_{i=1}^{n-1} d_i+4(n-1) \bmod 6} \\
\Rightarrow\ & \varphi'(e_0) \in E_{l-\sum_{i=0}^{n-1} d_i+4n \bmod 6} \overset{(2.7)}{=} E_{l-(4n-6+D(P))+4n \bmod 6} \\
& = E_{l+6-D(P) \bmod 6} = E_{l-D(P) \bmod 6}
\end{aligned}$$

□

Lemma 2.3.8 *Given a disordered triangle-patch P with $D(P) \bmod 6 \neq 0$, boundary cycle C, a boundary vertex v, and e_0 the first edge in C_v. Let φ be an embedding of C_v into L with closure φ'. Then $\varphi'(e_0)$ is the image of a $D(P) \cdot 60$ degree counterclockwise rotation of $\varphi(e_0)$ around a point c in L which is uniquely determined.*

In case $D(P) \bmod 6 \in \{1, 5\}$, the center c is a vertex of L, in case $D(P) \bmod 6 \in \{2, 4\}$ it can be a vertex or the center of a face, and in case $D(P) \bmod 6 = 3$ it can be a vertex or the center of an edge.

PROOF:

Lemma 2.3.7 implies that in case of $D(P) \bmod 6 = 0$, the edge $\varphi'(e_0)$ is in the same class as $\varphi(e_0)$; in the other cases, $\varphi'(e_0)$ and $\varphi(e_0)$ will be in different classes, so they will definitely be different edges. More exactly, the formula (2.6) together with the definition of the classes $E_0, \ldots, E_5$ means that in the cases $D(P) \bmod 6 \neq 0$, the directed edge $\varphi'(e_0)$ is the image of a $D(P) \cdot 60$ degree counterclockwise rotation of $\varphi(e_0)$ (or equivalently, of a $(D(P) \bmod 6) \cdot 60$ degree counterclockwise rotation). Since it is a non-trivial rotation, the position of its center c is uniquely determined.

The type of c can be determined by geometrical means (see figure 2.8): Let u be the starting vertex of $\varphi(e_0)$ and v the starting vertex of $\varphi'(e_0)$. In case $D(P) \bmod 6 = 1$ or $D(P) \bmod 6 = 5$, the vertices u and v together with c form a regular triangle in the lattice. Hence, c has to be a vertex, too. In case $D(P) \bmod 6 = 2$ or $D(P) \bmod 6 = 4$, c is the center of a regular triangle formed by u, v, and a third vertex w of the lattice, so c might be a vertex or the center of a face (compare lemma 2.3.2). Finally, in case of $D(P) \bmod 6 = 3$, c lies exactly in the center of the line joining the vertices u and v, and hence it is either a vertex (this is the case if $\mathrm{Cox}(\{u, v\}) = (p, q)$ with p and q even), or the center of an edge (in any other case).

□

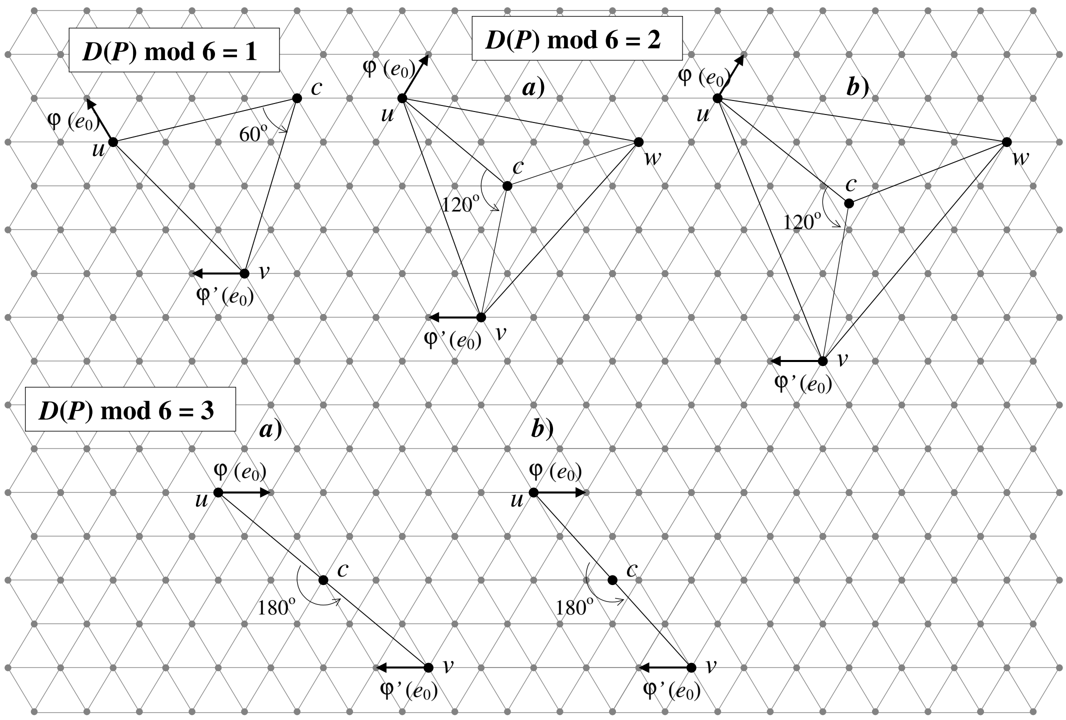

Figure 2.8: Different cases for the center of rotation (see lemma 2.3.8) with respect to $D(P)$ for the cases $D(P) \bmod 6 = 1$, $D(P) \bmod 6 = 2$, and $D(P) \bmod 6 = 3$. For $D(P) \bmod 6 = 4$ the situation is similar to $D(P) \bmod 6 = 2$, and for $D(P) \bmod 6 = 5$ similar to $D(P) \bmod 6 = 1$.

In case $D(P) \bmod 6 = 0$, $\varphi'(e_0)$ is obtained from $\varphi(e_0)$ by translation, so in general we do not have a rotation (and if so, it will be a trivial one, i.e. the edges are the same). We will return to this case later on.

2.4 General disordered triangle-patches

The idea of 'cutting out' a smaller patch leads us to patches that are connected but not necessarily 2-connected anymore, so we define:

Definition 2.4.1 *A* general disordered triangle-patch *is a connected plane graph P where all faces are triangles except one face called the* outer face*, and all vertices that lie in the outer face have degree at most* 6*. Vertices that do not lie in the outer face and have a degree different from* 6 *are called* defective vertices*. In case there are p defective vertices of degree* 5 *and no other defective vertices, P is called a* general p-patch*.*

Given a general disordered triangle-patch P with a combinatorial embedding in the plane (i.e. for every vertex we have a rotational order of the incident edges, which we will interpret as clockwise – see e.g. [25]*), we define the set of* angles *of a vertex $v \in V$ as*

$$A(v) := \{(e_1, e_2) \mid e_2 \textit{ follows } e_1 \textit{ in the rotational order around } v\} \ ,$$

and $A := \cup_{v \in V} A(v)$ as the set of angles in P. The face corresponding to an angle is the face that lies between the two edges in the order given.

A labeling *of P is a mapping l that assigns an integer $l(a) \in \{0, 1, 2, 3, 4, 5\}$ to every angle $a \in A$ such that $l(a) = 0$ holds for every angle a not corresponding to the outer face, and for every vertex $v \in V$ we have*

$$\sum_{a \in A(v)} l(a) + \deg(v) \mod 6 = 0 \ .$$

Figure 2.9 *gives an example of a possible labeling of a general triangle-patch.*

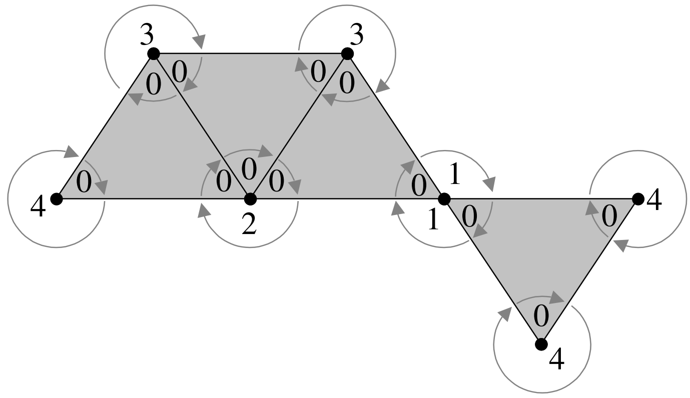

Figure 2.9: A general triangle-patch with angles and a labeling

The boundary cycle *of a general disordered triangle-patch P is defined to be the directed cycle of the edges in the outer face such that the outer face lies on its left hand side, where bridges occur twice. Furthermore we define an* enclosing cycle *of P as a directed cycle that has the same underlying undirected edges as the boundary cycle.*

Note that, in contrary to the boundary cycle, an enclosing cycle may cross itself at a cutvertex – see for instance figure 2.10.

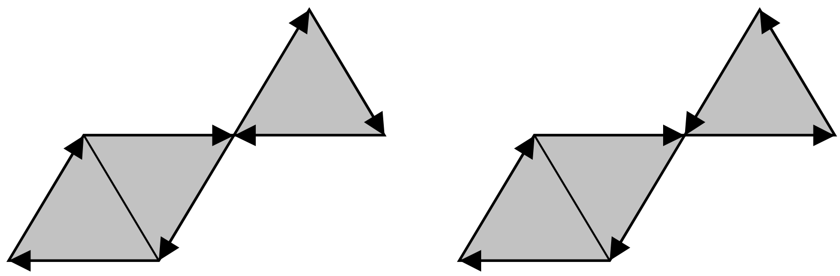

Figure 2.10: A general triangle-patch with boundary cycle (left) and the same patch with an enclosing cycle

It can be shown (see [29] and [9]) that edges of an enclosing cycle whose corresponding undirected edges form a simple cycle (that is, they lie in the boundary of a 2-connected component of the patch) form a directed subcycle. So given a general disordered triangle-patch P with an enclosing cycle C, for every bounded face of the patch there is a unique simple cycle surrounding it, such that it lies either on the right or left hand side of these edges. We call such a face *right* resp. *left* with respect to the patch and the enclosing cycle and denote the set of right faces as $F_r(P,C)$ and the set of left faces as $F_l(P,C)$. With this we define

$$F_{rl}(P,C) := |F_r(P,C)| - |F_l(P,C)|$$

as the number of right minus the number of left faces.

Note that in case C is the boundary cycle, $F_{rl}(P,C)$ is equal to the number of faces $|F(P)|$, because then all faces are right faces.

Definition 2.4.2 *Given a general disordered triangle-patch $P = (V,E,F)$ with a labeling l and an enclosing cycle C. Then let $e_0, e_1, \ldots, e_{n-1}$ be the directed edges of C such that the starting point of e_i is equal to the ending point of $e_{i-1 \bmod n}$ for $i = 0, 1, \ldots n-1$.*

A labeling *of C is a mapping l_C that assigns an integer from $\{0,\ldots,5\}$ to every pair $(e_{i-1 \bmod n}, e_i)$ of succeeding edges in C ($i = 0,\ldots n-1$), such that*

$$l_C(e_{i-1 \bmod n}, e_i) \;=\; \sum_{j=0}^{k-1} l(e^i_j, e^i_{j+1}) + (k-1) \bmod 6\ ,$$

where $e_{i-1 \bmod n} = e^i_0, e^i_1, \ldots, e^i_k = e_i$ denote the edges in rotational order around the common vertex of $e_{i-1 \bmod n}$ and e_i that lie between $e_{i-1 \bmod n}$ and e_i, including $e_{i-1 \bmod n}$ and e_i themselves; that means, $l_C(e_{i-1 \bmod n}, e_i)$ is the number of edges plus the sum of labels between $e_{i-1 \bmod n}$ and e_i (see figure 2.11 for an example).

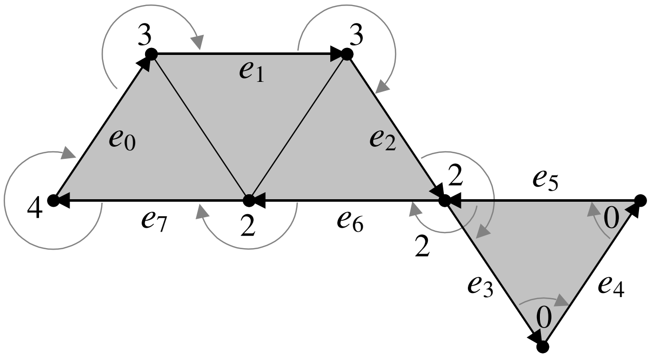

Figure 2.11: The general triangle-patch from figure 2.9 with an enclosing cycle and a labeling of the enclosing cycle (with respect to the angle labels given in figure 2.9)

In the following we consider a general triangle-patch without any defective vertices, i.e. a general 0-patch.

Definition 2.4.3 *Given a general* 0*-patch* P *with an enclosing cycle* C *consisting of edges* $e_0, \ldots, e_{n-1}$ *as above, and a labeling* l_C *of* C*. With respect to its labeling, an* embedding *of* C *into the lattice* L *is a mapping* φ *that maps* $e_0, \ldots, e_{n-1}$ *onto directed edges in* L *such that the following holds:*

- *For all* $i = 0, \ldots, n-1$*, the ending point of* $\varphi(e_{i-1 \bmod n})$ *is equal to the starting point of* $\varphi(e_i)$*;*
- *if for* $i = 1, \ldots, n-1$ *we have* $\varphi(e_{i-1 \bmod n}) \in E_j$*, then* $\varphi(e_i) \in E_k$ *with*

$$k \;=\; j + l_C(e_{i-1 \bmod n}, e_i) \;-\; 2 \mod 6 \;.$$

Figure 2.12 shows an embedding of the enclosing cycle from figure 2.11 into L.

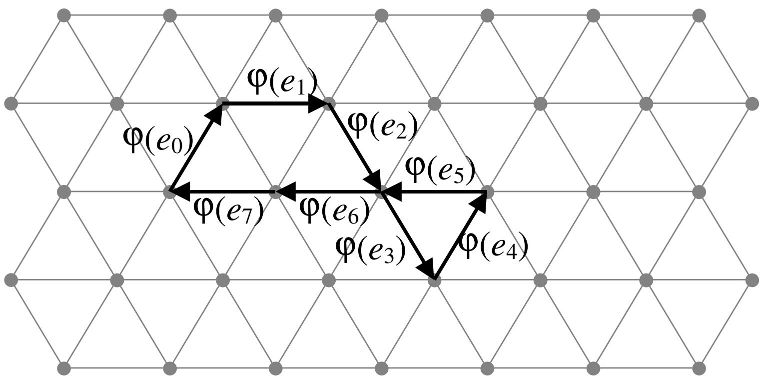

Figure 2.12: An embedding of the enclosing cycle from figure 2.11 with the given labels into the lattice.

Remark 2.4.4 *Definition* 2.4.3 *is an extension of definition* 2.3.6*: Assume the enclosing cycle C consists of disjoint subpaths C_1, C_2. Then an embedding φ of C induces embeddings of C_1 and C_2. In case C_1 is also equal to the boundary cycle C_v of some patch P cut at a vertex v, then $\varphi(C_1)$ is also an embedding of C_1 according to definition 2.3.6, because then all succeeding edges correspond to angles of the outer face and will get the label that was assigned to these angles in P. In particular, an angle a corresponding to a vertex v that occurs only once in the boundary cycle and hence has only one angle in the outer face will get a label with $l(a) + \deg(v) \bmod 6 = 0$; so if P is 2-connected, the labels of the outer face can be determined by the boundary degrees and vice versa. The definitions make sure that there is the same number of edges between two succeeding edges in both cases.*

The following lemma is essential for the main proof. A similar lemma can be found in [29] and [9] for the case of quadrangle-patches, but since in the triangular case we have a different lattice and a different definition of S_{rl}, we carry out the proof here for the present case.

Lemma 2.4.5 *Given a general* 0*-patch P with an enclosing cycle C and a labeling. Then there exists an embedding φ of C into L, and for each such φ we have:*

$$F_{rl}(P, C) = S_{rl}(\varphi(C))$$

PROOF:

We proceed by induction in the number of bounded faces $|F(P)| =: n$.

If $n = 0$ the patch is a tree, and $F_{rl}(P, C) = 0$ holds. This case can be proven by induction in the number of edges:

In case there is just one edge, the enclosing cycle consists of two opposite directed edges e_0, e_1, and at each of the two vertices we have one angle with label 5. By definition, any embedding φ of C into L must fulfill $\varphi(e_0) \in E_j \Rightarrow \varphi(e_1) \in E_{j+3 \bmod 6}$. Then we automatically have $\varphi(e_1) \in E_k \Rightarrow \varphi(e_0) \in E_{k+3 \bmod 6}$, so the second item of the definition is fulfilled. If (and only if) we choose $\varphi(e_0)$ and $\varphi(e_1)$ to be two arbitrary opposite directed edges in L that correspond to the same undirected edge, also the first item applies and we have an embedding of C into L. Then the definition of S_{rl} immediately implies $S_{rl}(\varphi(C)) = 0 = F_{rl}(P, C)$.

Now suppose there is more than one edge in the tree. Then consider a leaf v and its neighbouring vertex w; then C must contain the two succeeding edges $(v, w), (w, v)$. So if we delete v and the edge $\{v, w\}$, we easily obtain an enclosing cycle C' of the resulting tree by removing $(v, w), (w, v)$ from C and assigning the label $(a + b + 1) \bmod 6$ to the new angle at w, where a and b denote the labels of the former angles. By induction, this enclosing cycle has an embedding φ' into L, and it fulfills $S_{rl}(\varphi'(C')) = 0$. Now φ' can easily be extended to an embedding φ of C by just inserting two opposite directed edges at the angle with label $(a + b + 1) \bmod 6$, producing the correct angles corresponding to a and b, which ensures the existence of φ. On the other hand, reducing an embedding $\varphi(C)$ by $\varphi(v, w)$ and $\varphi(w, v)$ yields an embedding of C', so any embedding of C can be interpreted as an extension of $\varphi'(C')$. Furthermore, since the label of the angle next to v must be 5, any embedding must map (v, w) and (w, v) onto opposite directed edges, so $S_{rl}(\varphi(C))$ stays 0.

With this we have proven the lemma for the case of no bounded face. Now assume we have a general 0-patch P with enclosing cycle C and $n \geq 1$ bounded faces, and the lemma is true for any general 0-patch with $n-1$ bounded faces. W.l.o.g. we may assume there exists a right face in P. So consider a directed edge e in C that has a bounded face f on its right hand side. Then we remove e (and with this, f) and adapt the enclosing cycle and its labels as sketched in figure 2.13.

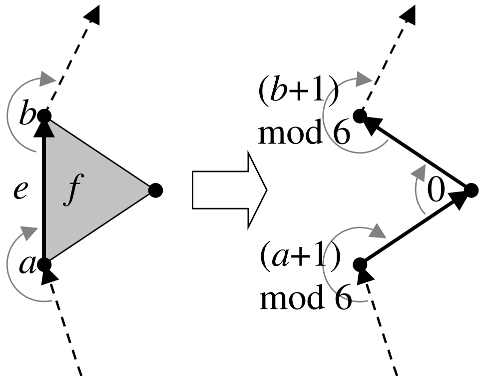

Figure 2.13: Removing a face in a general 0-patch

We obtain a general 0-patch P' with enclosing cycle C' and $n-1$ bounded faces. By induction there exists an embedding φ' of C' into L, and any such embedding fulfills $S_{rl}(\varphi'(C')) = F_{rl}(P', C')$. Again it can be extended to an embedding φ of C by inserting the edge between the two vertices in L that are the images of the endpoints of e (this is possible because the new label in P' is 0, so the two vertices are indeed neighbours in L). On the other hand a given embedding of C can be restricted to one of C', again implying that any embedding of C can be interpreted as an extension of $\varphi'(C')$.

Since we removed a right face we obviously have $F_{rl}(P', C') = F_{rl}(P, C) - 1$. Now it can be checked that $S_{rl}(\varphi'(C')) = S_{rl}(\varphi(C)) - 1$ holds: Let e_1, e_2 be the new edges in C' as depicted in figure 2.13, and assume $\varphi'(\bar{e}) = \varphi(\bar{e})$ for all edges $\bar{e} \in C - \{e\}$. Then if $\varphi(e) \in E_j$ for some $j \in \{0, 1, \ldots, 6\}$, we must have $\varphi'(e_1) \in E_{(j+1) \bmod 6}$ and $\varphi'(e_2) \in E_{(j-1) \bmod 6}$. In the different cases for $j = 0, \ldots, 5$ this implies, together with the definition of S_{rl}:

- $j = 0$: With $y(\varphi(e)) = y(\varphi'(e_1))$ we get

$$\begin{aligned} S_{rl}(\varphi(C)) - S_{rl}(\varphi'(C')) &= 2y(\varphi(e)) - \big(2y(\varphi'(e_1)) - 1\big) \\ &= 2y(\varphi(e)) - \big(2y(\varphi(e)) - 1\big) \ = \ 1 \end{aligned}$$

- $j = 1$: Then we have $y(\varphi(e)) = y(\varphi'(e_1)) = y(\varphi'(e_2)) + 1$ and hence

$$\begin{aligned} S_{rl}(\varphi(C)) - S_{rl}(\varphi'(C')) &= \big(2y(\varphi(e)) - 1\big) - 2y(\varphi'(e_2)) \\ &= 2y(\varphi(e)) - 1 - 2\big(y(\varphi(e)) - 1\big) \ = \ 1 \end{aligned}$$

- $j = 2$: Then $y(\varphi(e)) = y(\varphi'(e_1)) = y(\varphi'(e_2))$ holds, and with this we get

$$\begin{aligned} S_{rl}(\varphi(C)) - S_{rl}(\varphi'(C')) &= -\Big(- 2y(\varphi'(e_1)) + \big(2y(\varphi'(e_2)) - 1\big)\Big) \\ &= 2y(\varphi'(e_1)) - 2y(\varphi'(e_2)) + 1 \ = \ 1 \end{aligned}$$

- $j = 3$: Because of $y(\varphi(e)) = y(\varphi'(e_1))$ we have

$$\begin{aligned} S_{rl}(\varphi(C)) - S_{rl}(\varphi'(C')) &= -2y(\varphi(e)) + \bigl(2y(\varphi'(e_1)) + 1\bigr) \\ &= -2y(\varphi(e)) + \bigl(2y(\varphi(e)) + 1\bigr) \;=\; 1 \end{aligned}$$

- $j = 4$: Then we have $y(\varphi(e)) = y(\varphi'(e_1)) = y(\varphi'(e_2)) - 1$ and therefore

$$\begin{aligned} S_{rl}(\varphi(C)) - S_{rl}(\varphi'(C')) &= -\bigl(2y(\varphi(e)) + 1\bigr) + 2y(\varphi'(e_2)) \\ &= -2y(\varphi(e)) - 1 + 2\bigl(y(\varphi(e)) + 1\bigr) \;=\; 1 \end{aligned}$$

- $j = 5$: Then $y(\varphi(e)) = y(\varphi'(e_1)) = y(\varphi'(e_2))$ holds, and we obtain

$$\begin{aligned} S_{rl}(\varphi(C)) - S_{rl}(\varphi'(C')) &= -\Bigl(2y(\varphi'(e_1)) - \bigl(2y(\varphi'(e_2)) + 1\bigr)\Bigr) \\ &= -2y(\varphi'(e_1)) + 2y(\varphi'(e_2)) + 1 \;=\; 1 \end{aligned}$$

So in all cases we have shown $S_{rl}(\varphi(C)) - S_{rl}(\varphi'(C')) = 1$, and hence

$$S_{rl}(\varphi'(C')) = S_{rl}(\varphi(C)) - 1 \; .$$

Together with $F_{rl}(P', C') = F_{rl}(P, C) - 1$ and the induction we obtain

$$S_{rl}(\varphi(C)) = S_{rl}(\varphi'(C')) + 1 = F_{rl}(P', C') + 1 = F_{rl}(P, C)$$

and with this we have shown the lemma also for the patch P with $n > 0$ bounded faces.

□

Lemma 2.4.6 *Given a closed directed cycle C_L in L. Then there exists a general 0-patch P and an enclosing cycle C of P with a labeling such that C_L is the image of an embedding of C into L.*

PROOF:

This can be proved by composing the cycle C_L into simple cycles and taking the interior of those cycles to construct the patch P. A detailed proof of the corresponding lemma for quadrangle-patches can be found in [29] (Satz 4.20), which can easily be transferred to the present case of triangle-patches.

□

Corollary 2.4.7 *For a given enclosing cycle C of a general 0-patch P with an embedding φ into L, the value of $S_{rl}(\varphi(C))$ does not depend on φ, so we may define $S_{rl}(C) := S_{rl}(\varphi(C))$ for any embedding φ.*

Furthermore, given two closed cycles C_L, C'_L in the lattice where C'_L is a rotation or translation of C_L, $S_{rl}(C_L) = S_{rl}(C'_L)$ holds.

PROOF:

By lemma 2.4.5 we have $S_{rl}(\varphi(C)) = F_{rl}(P,C)$. Since $F_{rl}(P,C)$ does not depend on φ, this implies that indeed $S_{rl}(\varphi(C))$ does not depend on φ, either.

By lemma 2.4.6 we know that for any cycle C_L in the lattice we can find a general 0-patch $\bar{P}$ with an enclosing cycle $\bar{C}$ such that C_L is the image of an embedding of $\bar{C}$ into L. If C'_L is a rotation or translation of C_L, then it must also be the image of an embedding of $\bar{C}$ into L, so we have embeddings φ and φ' with $C_L = \varphi(\bar{C})$ and $C'_L = \varphi'(\bar{C})$. But then we have with the first part of this lemma:

$$S_{rl}(C_L) = S_{rl}(\varphi(\bar{C})) = S_{rl}(\bar{C}) = S_{rl}(\varphi'(\bar{C})) = S_{rl}(C'_L)$$

□

Corollary 2.4.8 *The number of faces of a general* 0*-patch is uniquely determined by its labeled boundary cycle.*

PROOF:

Given a general 0-patch P with enclosing cycle C and a labeling of C. By lemma 2.4.5, $F_{rl}(P,C)$ is equal to $S_{rl}(\varphi(C))$ for any embedding φ of C into L. Since $S_{rl}(\varphi(C))$ does not depend on the patch P but only on the labeled enclosing cycle C, this means that $F_{rl}(P,C)$ actually does not depend on P, either.

Now the boundary cycle of a general 0-patch is a special enclosing cycle where all faces are right faces. So if C is the boundary cycle, then – as we have noted before – $F_{rl}(P,C)$ is also equal to the number of bounded faces $|F(P)|$. Consequently we have

$$|F(P)| = F_{rl}(P,C) = S_{rl}(\varphi(C))$$

for any embedding φ of C into L – so indeed the number of faces of P is uniquely determined by C.

□

2.5 Patches with disordered subpatches

Now we come back to the original problem: We consider a disordered triangle-patch P and want to determine its number of faces with respect to its boundary and a fixed subgraph that contains all defective vertices.

In case $D(P) \bmod 6 \neq 0$, an embedding of the boundary cycle of P does *not* form a closed cycle in the lattice. But if we add a path that cuts out the defective vertices, we obtain the boundary cycle of a general 0-patch, which has an embedding into L due to lemma 2.4.5. So we define:

Definition 2.5.1 *Let P be a disordered triangle-patch and Q a* 2*-connected subgraph of P such that all defective vertices of P lie in the interior of Q. We call such a subgraph Q a* disordered subpatch *of P.*

A cutpath *in P relative to Q, a vertex v in the boundary of P, and a vertex w in the boundary of Q is a directed path XYZ in P consisting of subpaths X, Y, and Z with the following properties:*

- *X is a path starting at v and ending at w;*
- *Y is the path starting and ending at w and consisting of the boundary edges of Q directed such that Q lies on its left hand side;*
- *Z is the path starting at w and ending at v using the same edges as X with opposite direction.*

A disordered triangle-patch P with (labeled) boundary cycle C, disordered subpatch Q, and cutpath XYZ relative to Q, v and w as described above can be cut along XYZ to obtain a general 0-patch P' with boundary cycle C_vXYZ, where again C_v denotes the path consisting of the edges of C starting and ending at v (see figure 2.14).

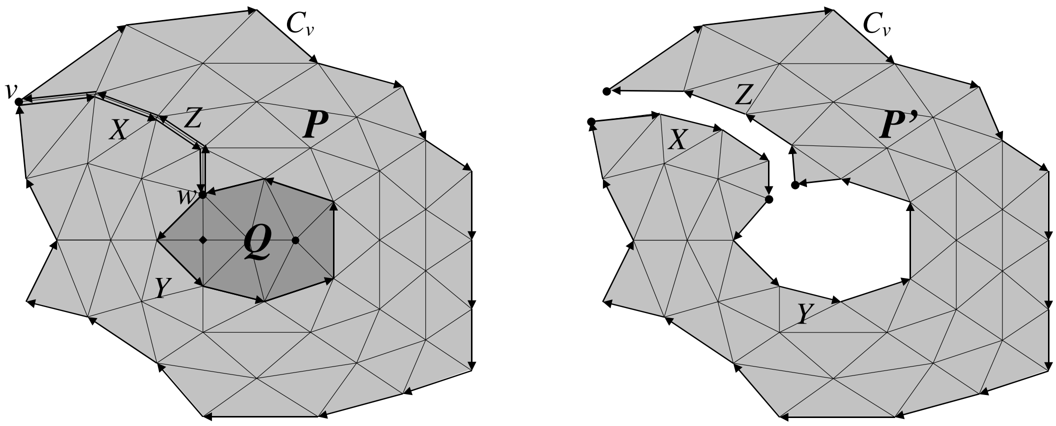

Figure 2.14: An example of a disordered triangle-patch P with disordered subpatch Q and a cutpath XYZ (left), and the corresponding general 0-patch P' with boundary cycle C_vXYZ (right)

Since C_vXYZ is the boundary cycle of a general 0-patch, it can be embedded into L and forms a closed cycle there. By construction, the number of bounded faces $F_{rl}(C_vXYZ)$ in P' is equal to the number of faces in $P - Q$. What is left to show is that this number is the same for *any* disordered triangle-patch with the same labeled boundary cycle C and the same disordered subpatch Q.

For this we need the following lemma which is based on the results on the rotation of embedded paths that were developed in the last section:

Lemma 2.5.2 *Given a disordered triangle-patch P with $D(P) \bmod 6 \neq 0$, boundary cycle C, disordered subpatch Q, and cutpath XYZ relative to Q, a vertex v in the boundary of P and a vertex w in the boundary of Q. Let P' be the corresponding general 0-patch with boundary cycle C_vXYZ, and φ an embedding of C_vXYZ into L. Then the inverse path of $\varphi(Z)$ (that is, $\varphi(Z)$ with opposite orientation of the edges) is the image of a clockwise* *rotation of $\varphi(X)$ by $D(P) \cdot 60$ degrees around a center c, which can be a vertex, the center of a face, or the center of an edge in L. Its position is uniquely determined by $\varphi(C_v)$.*

PROOF:

Let e_0 be the first edge in C_v, and φ' the closure with respect to the embedding φ of C_v. Then by lemma 2.3.8, there is a point c in L (a vertex, the center of a face, or the center of an edge) such that $\varphi'(e_0)$ is the image of a counterclockwise rotation of $\varphi(e_0)$ by $D(P) \cdot 60$ degrees, and it is uniquely determined by $\varphi(C_v)$. We show that this point is also the requested center of rotation for the paths. Let α denote the clockwise rotation by $D(P) \cdot 60$ degrees around c.

At first some simple remarks concerning the orientation of directed edges in L:

1. For any edge $e \in E_j$ we have $\alpha(e) \in E_{j+D(P) \bmod 6}$.
2. If $e \in E_j$ and e' is inverse to e, we must have $e' \in E_{j+3 \bmod 6}$.
3. Let e_{i-1}, e_i be succeeding edges in some enclosing cycle with labeling l and embedding φ. Then by definition 2.4.3 we have

$$\varphi(e_{i-1}) \in E_j \;\Rightarrow\; \varphi(e_i) \in E_{j+l(e_{i-1},e_i)-2 \bmod 6}$$

   and vice versa

$$\varphi(e_i) \in E_j \;\Rightarrow\; \varphi(e_{i-1}) \in E_{j-l(e_{i-1},e_i)+2 \bmod 6}\ .$$

Now let $v = v_1, \dots, v_k = w$ be the vertices in X such that $X = (v_1, v_2), \dots, (v_{k-1}, v_k)$ and $Z = (v_k, v_{k-1}), \dots, (v_2, v_1)$. Furthermore let $x_1, \dots, x_k, z_1, \dots, z_k$ be the corresponding vertices of the embedding in L, i.e. $\varphi(v_i, v_{i+1}) = (x_i, x_{i+1})$ and $\varphi(v_{i+1}, v_i) = (z_{i+1}, z_i)$ for $i = 1, \dots, k-1$.

Using this notation we have to show $\alpha(x_i) = z_i$ for $i = 1, \dots, k$. We proceed by induction in i (showing that provided that it holds for $i-2$ and $i-1$, we get the statement for i).

First we have to show $\alpha(x_1) = z_1$. If we let e_0 be the first edge of C_v, e_{n-1} the last one, and φ' the closure of the embedding, then the starting point of $\varphi'(e_0)$ is the ending point of $\varphi(e_{n-1})$ (that is x_1), and if $\varphi(e_{n-1}) \in E_j$ then $\varphi'(e_0) \in E_{j-\deg(v)+4 \bmod 6}$. By lemma 2.3.8 we have $\varphi'(e_0) = \alpha^{-1}(\varphi(e_0))$, hence $\alpha(\varphi'(e_0)) = \varphi(e_0)$ and in particular $\alpha(x_1) = z_1$.

Now we show $\alpha(x_2) = z_2$: Let $\varphi(e_0) \in E_j$. Then the definition of the embedding yields $(z_2, z_1) = \varphi(v_2, v_1) \in E_{j-l((v_2,v_1),e_0)+2 \bmod 6}$ (remark 3) and hence (with remark 2):

$$(z_1, z_2) \in E_{j-l((v_2,v_1),e_0)+5 \bmod 6} \tag{2.8}$$

Furthermore, due to lemma 2.3.7 and remark 1 we have $\varphi'(e_0) = \alpha^{-1}(\varphi(e_0)) \in E_{j-D(P) \bmod 6}$, so again with remark 3 and the definition of $\varphi'(e_0)$ we get

$$\varphi(e_{n-1}) \in E_{j-D(P)-l(e_{n-1},e_0)+2 \bmod 6}\ .$$

This again implies $(x_1, x_2) \in E_{j-D(P)-l(e_{n-1},e_0)+l(e_{n-1},(v_1,v_2)) \bmod 6}$ and therefore (with remark 1)

$$\alpha(x_1, x_2) \in E_{j-l(e_{n-1},e_0)+l(e_{n-1},(v_1,v_2)) \bmod 6}\ . \tag{2.9}$$

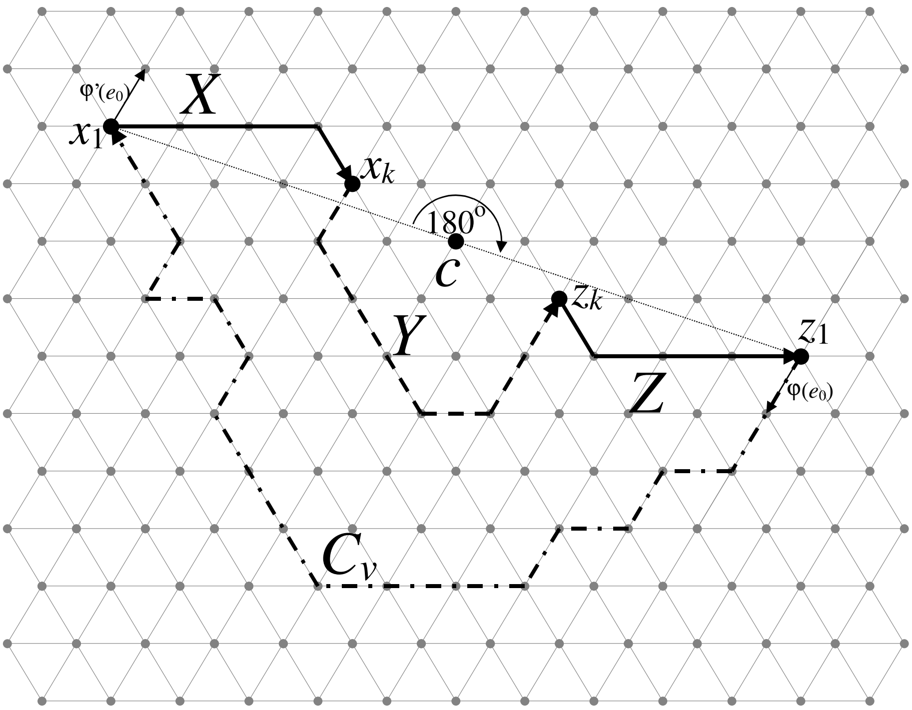

Figure 2.15: An embedding of the boundary cycle C_vXYZ of P' from figure 2.14 into the lattice with the notation used in the proof of lemma 2.5.2, demonstrating the idea of the proof (for simplification we denote the embeddings in the same way as the respective paths)

Now we have by definition of the labeling $l(e_{n-1},(v_1,v_2)) = l(e_{n-1},e_0)+1+m$, where m denotes the number of edges in rotational order between e_0 and (v_1,v_2). Then we also have $l((v_2,v_1),e_0)+m+2=6$ and hence $m=4-l((v_2,v_1),e_0)$. Inserting m we obtain

$$l(e_{n-1},e_0) = l(e_{n-1},(v_1,v_2)) + l((v_2,v_1),e_0) - 5\,. \tag{2.10}$$

If we insert (2.10) into (2.9) we get

$$\alpha(x_1,x_2) \in E_{j-l((v_2,v_1),e_0)+5 \bmod 6}$$

– so $\alpha(x_1,x_2)$ and (z_1,z_2) (compare (2.8)) are in the same class. Since we already know that $\alpha(x_1)=z_1$ this implies also $\alpha(x_2)=z_2$.

Now assume we have $\alpha(x_{i-2})=z_{i-2}$ and $\alpha(x_{i-1})=z_{i-1}$ for some $i\in\{2,\dots,k-1\}$. We have to show $\alpha(x_i)=z_i$.

Let $(x_{i-1},x_i)\in E_j$. Then we have by remark 3

$$(x_{i-2},x_{i-1}) \in E_{j-l((v_{i-2},v_{i-1}),(v_{i-1},v_i))+2 \bmod 6}$$

so it follows by induction and remark 2:

$$\begin{aligned} & (z_{i-2},z_{i-1}) \in E_{j+D(P)-l((v_{i-2},v_{i-1}),(v_{i-1},v_i))+2 \bmod 6} \\ \overset{\text{remark 3}}{\Rightarrow}\; & (z_{i-1},z_i) \in E_{j+D(P) \bmod 6} \end{aligned}$$

Because of $\alpha(x_{i-1}) = z_i$ this implies that we also have $\alpha(x_i) = z_i$.

□

Now consider two disordered triangle-patches P and $\bar{P}$ with the same boundary sequence and isomorphic disordered subpatches Q and $\bar{Q}$, and let v resp. $\bar{v}$ be boundary vertices that correspond to each other in the two respective boundary sequences. In order to show that the patches have the same number of faces, it would be helpful if we could choose the cutpaths such that there are embeddings that map not only the boundary cycles C_v and $C_{\bar{v}}$ onto the same paths, but also the paths Y and $\bar{Y}$ around the disordered subpatches. Indeed we use such an argument in [9]: There the disordered subpatch consists of a single face, so w.l.o.g. we may assume that the images of the paths around that face are equal (otherwise we extend one of the paths by an appropriate number of edges).

However, this argument cannot be applied anymore in case of an arbitrary disordered subpatch because in general its boundary does not have the appropriate rotational symmetry. Hence it can occur in different positions relative to the boundary symmetry, as e.g. in figure 2.16. In this case it is not possible to determine cutpaths such that the embedded paths corresponding to the boundary of P and $\bar{P}$ as well as those corresponding to the boundary of Q and $\bar{Q}$ are equal: Then the paths Y and $\bar{Y}$ around the boundaries of Q and $\bar{Q}$ would have to be chosen such that their starting points w and $\bar{w}$ correspond to each other with respect to the symmetry of the boundary, which means in this case that choosing a starting point of Y determines the one in $\bar{Y}$. But then their embeddings do not coincide, as we see in figure 2.17, where the paths from figure 2.16 are embedded.

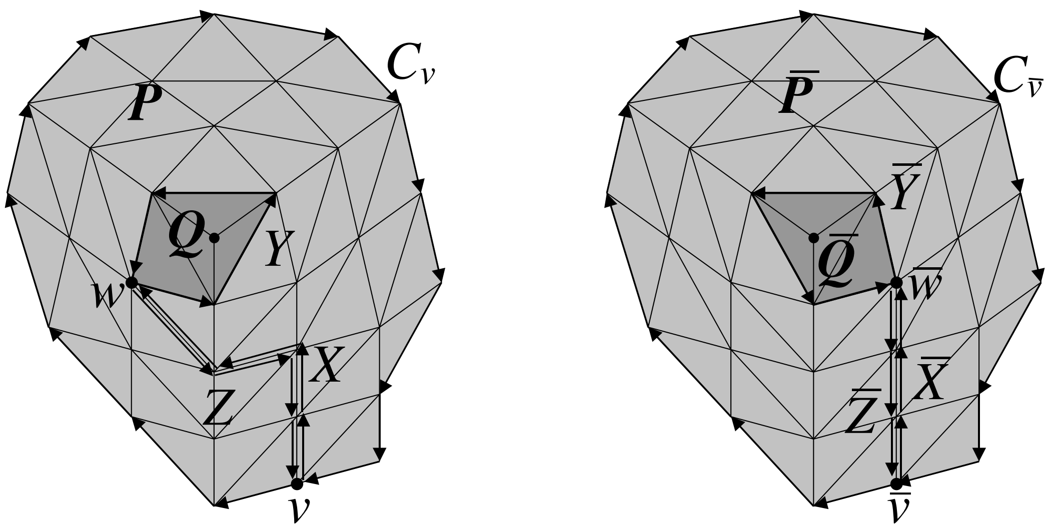

Figure 2.16: Two patches P, $\bar{P}$ with the same boundary (actually they are even the same patches) containing two isomorphic disordered subpatches Q, $\bar{Q}$, with cutpaths XYZ and $\bar{X}\bar{Y}\bar{Z}$, where the ending points w and $\bar{w}$ of X and $\bar{X}$ are chosen such that they correspond to each other with respect to the boundary of Q (in this case both are the only degree 2 vertices)

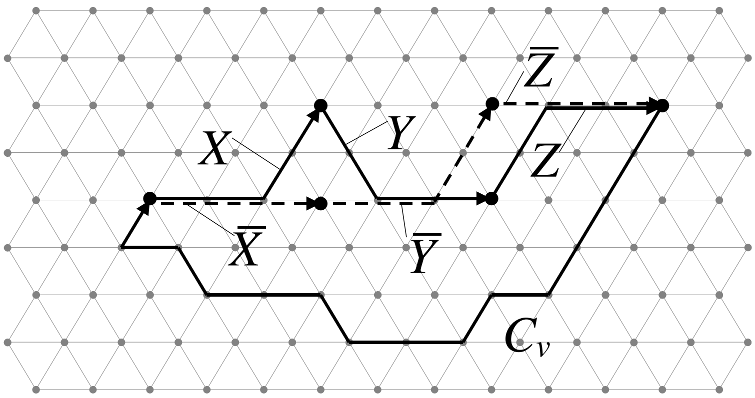

Figure 2.17: Embeddings of the paths from figure 2.16 into the lattice (again the embedded paths are denoted in the same way as the respective origin paths), where the embeddings of Y and $\bar{Y}$ do not coincide

For this reason, the proof of the following theorem requires some new ideas extending the approach that has been applied in the corresponding proof from [29] resp. [9].

Theorem 2.5.3 *Given two disordered triangle patches P and $\bar{P}$ with the same boundary sequence and disordered subpatches Q, $\bar{Q}$ that are isomorphic, where $D(Q) \bmod 6 = D(\bar{Q}) \bmod 6 \neq 0$. Then P and $\bar{P}$ have the same number of faces.*

PROOF:

Let v be a vertex in the boundary of P, w a vertex in the boundary of Q, and XYZ a cutpath in P relative to Q, v, and w. Then we choose $\bar{v}$ and $\bar{w}$ as vertices in the boundary of $\bar{P}$ resp. $\bar{Q}$ that correspond to v resp. w in the boundary sequence of the patches, and let $\bar{X}\bar{Y}\bar{Z}$ be a cutpath relative to $\bar{Q}$, $\bar{v}$, and $\bar{w}$ (see figure 2.18).

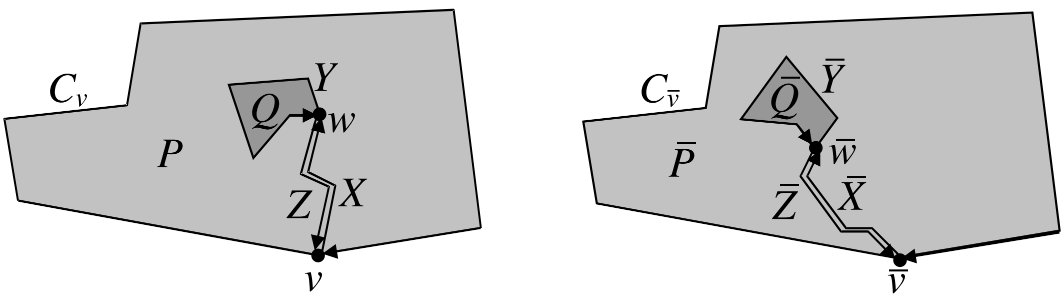

Figure 2.18: The patches P and $\bar{P}$ with cutpaths XYZ and $\bar{X}\bar{Y}\bar{Z}$

Furthermore let P' and $\bar{P}'$ be the corresponding general 0-patches with boundary cycles C_vXYZ and $C_{\bar{v}}\bar{X}\bar{Y}\bar{Z}$. By definition of F_{rl}, their numbers of faces are $F_{rl}(C_vXYZ)$ and $F_{rl}(C_{\bar{v}}\bar{X}\bar{Y}\bar{Z})$ (because all faces are right faces), and these are also the numbers of faces in $P - Q$ resp. $\bar{P} - \bar{Q}$. But since Q and $\bar{Q}$ are isomorphic they have the same number of faces, so it is sufficient to show that P' and $\bar{P}'$ have the same number of faces, or equivalently

$$F_{rl}(C_vXYZ) = F_{rl}(C_{\bar{v}}\bar{X}\bar{Y}\bar{Z})\,. \tag{2.11}$$

Now let φ and $\bar{\varphi}$ be embeddings of $C_v XYZ$ and $C_{\bar{v}}\bar{X}\bar{Y}\bar{Z}$ such that $\varphi(C_v) = \bar{\varphi}(C_{\bar{v}})$ – this is possible because P and $\bar{P}$ have the same boundary sequences and v and $\bar{v}$ are chosen as corresponding vertices, so C_v and $C_{\bar{v}}$ are the same labeled paths.

In order to simplify notation, we denote the embedded paths equal to the paths in the patch, so we have cycles $C_v XYZ$ and $C_v\bar{X}\bar{Y}\bar{Z}$ in L.

By lemma 2.4.5 we have $F_{rl}(C_v XYZ) = S_{rl}(C_v XYZ)$ and $F_{rl}(C_v\bar{X}\bar{Y}\bar{Z}) = S_{rl}(C_v\bar{X}\bar{Y}\bar{Z})$, so instead of (2.11) we may show:

$$S_{rl}(C_v XYZ) = S_{rl}(C_v\bar{X}\bar{Y}\bar{Z}) \tag{2.12}$$

In the lattice L we define the following vertices (see figure 2.19):
- v_1 as the starting point of X and $\bar{X}$;
- v_2 resp. $\bar{v_2}$ as the ending point of X resp. $\bar{X}$ and starting point of Y resp. $\bar{Y}$;
- v_3 resp. $\bar{v_3}$ as the ending point of Y resp. $\bar{Y}$ and starting point of Z resp. $\bar{Z}$;
- and v_4 as the ending point of Z and $\bar{Z}$.

Due to lemma 2.5.2, the inverse path of Z is the image of a clockwise rotation of X by $D(P)\cdot 60$ degrees around a center c – and since $D(P) \bmod 6 \neq 0$ and Z and $\bar{Z}$ have the same endpoints, the inverse path of $\bar{Z}$ is the image of a clockwise rotation of $\bar{X}$ by $D(P)\cdot 60$ degrees around the *same* point c. So if α denotes this rotation, we have $\alpha(v_1) = v_4$, $\alpha(v_2) = v_3$, and $\alpha(\bar{v_2}) = \bar{v_3}$.

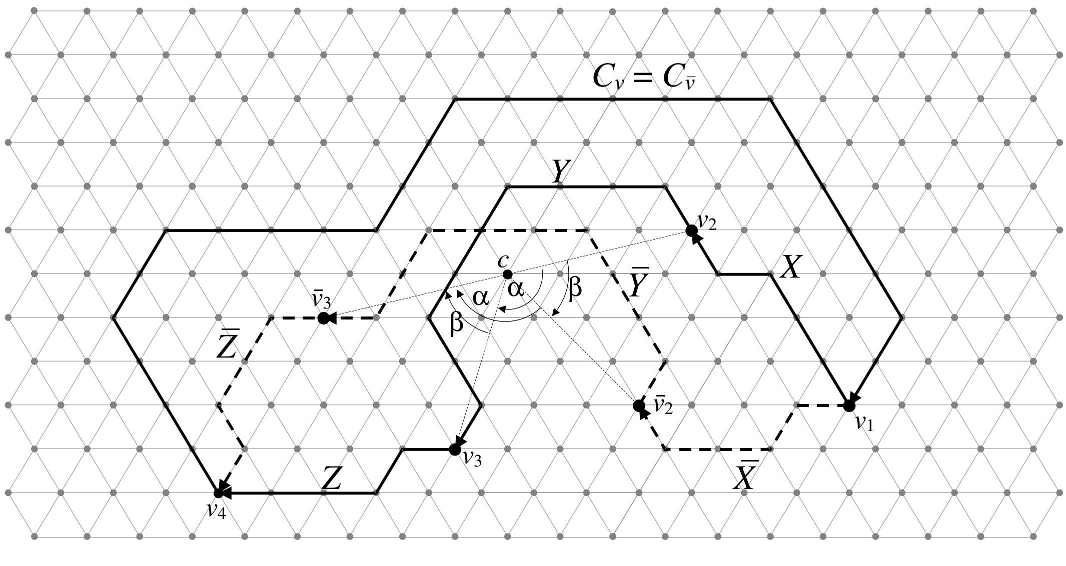

Figure 2.19: Embeddings of the cutpaths XYZ and $\bar{X}\bar{Y}\bar{Z}$ (compare figure 2.18) into L

As noted before, it is not always possible to ensure $Y = \bar{Y}$ in the lattice. But in any case we have $\beta(Y) = \bar{Y}$ for a rotation β around the center c: Let $\text{dist}(x, y)$ denote the distance between two points x and y in the lattice (not necessarily vertices), i.e. the length of the straight line joining them. Because of $\alpha(v_2) = v_3$ and $\alpha(\bar{v_2}) = \bar{v_3}$ we have $\text{dist}(v_2, c) = \text{dist}(v_3, c)$ and $\text{dist}(\bar{v_2}, c) = \text{dist}(\bar{v_3}, c)$. On the other hand $\text{dist}(v_2, v_3) = \text{dist}(\bar{v_2}, \bar{v_3})$ holds, since the paths Y from v_2 to v_3 and $\bar{Y}$ from $\bar{v_2}$ to $\bar{v_3}$ in the lattice are embeddings of the same labeled path. So v_2, v_3, c and $\bar{v_2}, \bar{v_3}, c$ form congruent triangles (both are isosceles, have the same angle α and the same length of the opposite side). But this means in particular that we have $\text{dist}(v_2, c) = \text{dist}(v_3, c) = \text{dist}(\bar{v_3}, c) = \text{dist}(\bar{v_2}, c)$, so there is a rotation β around c with $\beta(v_2) = \bar{v_2}$, $\beta(v_3) = \bar{v_3}$, and hence $\beta(Y) = \bar{Y}$.

At first consider the case where β is the trivial rotation, that means $Y = \bar{Y}$ indeed holds (and hence $v_2 = \bar{v_2}$ and $v_3 = \bar{v_3}$) – see figure 2.20. Then the proof works similarly to the one in [9]: Because the cycle $Z^{-1}\bar{Z}$ is just a rotation under α of $X\bar{X}^{-1}$ we have by corollary 2.4.7 and remark 2.3.5 (2)

$$S_{rl}(X\bar{X}^{-1}) = S_{rl}(Z^{-1}\bar{Z}) = -S_{rl}(Z\bar{Z}^{-1})$$

and therefore with the additivity of S_{rl} (remark 2.3.5 (1))

$$S_{rl}(C_v\bar{X}\bar{Y}\bar{Z}) = S_{rl}(C_v\bar{X}\bar{Y}\bar{Z}) + S_{rl}(X\bar{X}^{-1}) + S_{rl}(Z\bar{Z}^{-1}) = S_{rl}(C_vXYZ)$$

which is what we wanted to show.

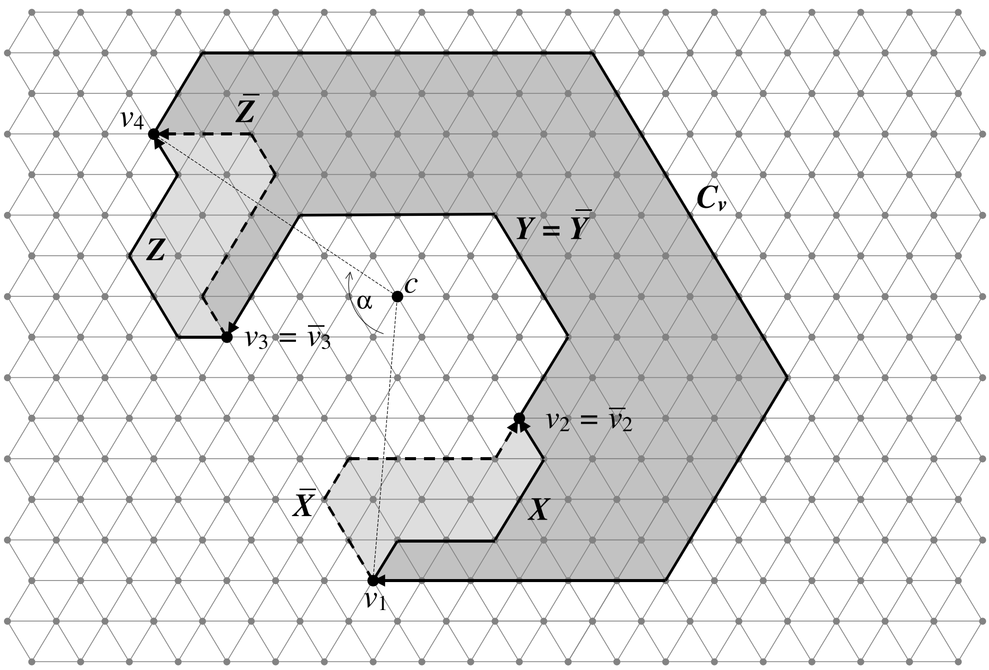

Figure 2.20: An example of the case $Y = \bar{Y}$

Now assume that $Y = \bar{Y}$ is not the case, that means $v_2 \neq \bar{v_2}$ and $v_3 \neq \bar{v_3}$. Then we have $\beta(Y) = \bar{Y}$ for a non-trivial rotation β around c (in particular $\beta(v_2) = \bar{v_2}$ and $\beta(v_3) = \bar{v_3}$). Because of the symmetry of the triangular lattice, the degree of rotation must be a multiple of 60 degrees. W.l.o.g. we may assume that β is a clockwise rotation of at most 180 degrees; otherwise define XYZ and $\bar{X}\bar{Y}\bar{Z}$ the other way around.

For simpler notation we will use α and β also as the size of the corresponding angle.

Let γ be the greatest common divisor of α and β. Since the vertices $v_2, v_3, \bar{v_2}, \bar{v_3}$ have the same distance to c, we may define a directed cycle H in the lattice with c on its left hand side, symmetry group $C_{\frac{360}{\gamma}}$ (with c as rotation center) and containing the vertices $v_2, v_3, \bar{v_2}, \bar{v_3}$. H can be chosen as a regular hexagon in case of $\gamma = 60$ and as a hexagon with the appropriate symmetry otherwise (see figure 2.21). Note that c is not always a vertex; if $\gamma = 120$, it might also be the center of a face and if $\gamma = 180$, it might be the center of an edge.

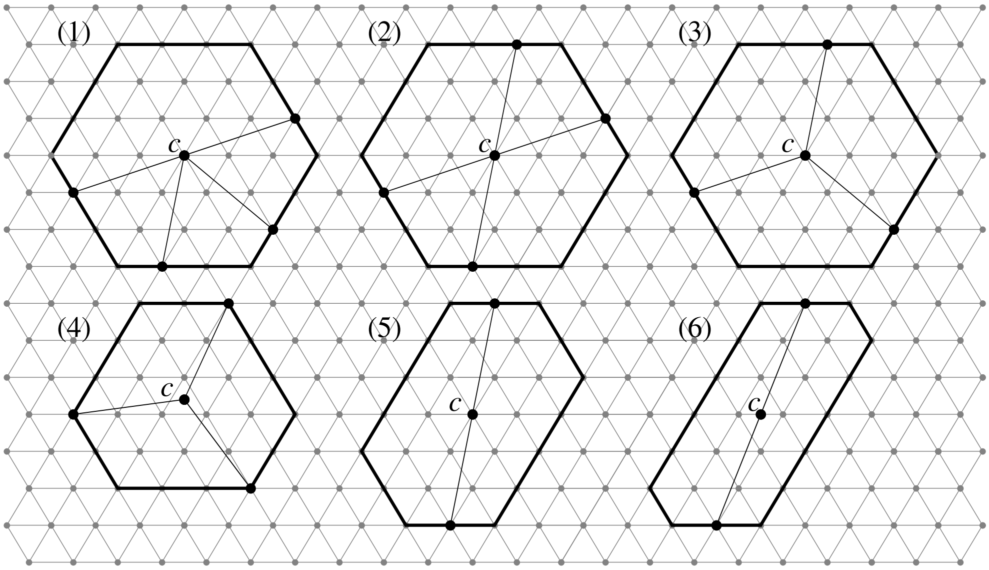

Figure 2.21: The possible configurations of $v_2, v_3, \bar{v_2}, \bar{v_3}$ in the lattice and the corresponding hexagon

The idea is now to replace the paths Y and $\bar{Y}$ by the appropriate paths along the hexagon. So we define Y_H as the path from v_2 to v_3 along H, and $\bar{Y}_H$ as the path from $\bar{v_2}$ to $\bar{v_3}$ along H (see also figure 2.22). By construction of H, Y_H and $\bar{Y}_H$ are the same labeled paths and we have $\beta(Y_H^{-1}Y) = \bar{Y}_H^{-1}\bar{Y}$, so by corollary 2.4.7 we get

$$S_{rl}({Y_H}^{-1}Y) = S_{rl}(\bar{Y}_H^{-1}\bar{Y})\ .$$

Because of $S_{rl}({Y_H}^{-1}Y) = -S_{rl}(Y_H Y^{-1})$ and $S_{rl}(\bar{Y}_H^{-1}\bar{Y}) = -S_{rl}(\bar{Y}_H\bar{Y}^{-1})$, this implies also $S_{rl}(Y_H Y^{-1}) + S_{rl}(\bar{Y}_H^{-1}\bar{Y}) = 0$ and $S_{rl}(\bar{Y}_H\bar{Y}^{-1}) + S_{rl}({Y_H}^{-1}Y) = 0$. With this and the additivity of S_{rl} we get

$$\begin{aligned}
& S_{rl}(C_v XYZ) - S_{rl}(C_v XY_H Z) \\
= \ & S_{rl}(C_v XYZ) + S_{rl}(Y_H Y^{-1}) + S_{rl}(\bar{Y}_H^{-1}\bar{Y}) - S_{rl}(C_v XY_H Z) \\
= \ & S_{rl}(C_v XY_H Z) + S(\bar{Y}_H^{-1}\bar{Y}) - S_{rl}(C_v XY_H Z) \\
= \ & S_{rl}(\bar{Y}_H^{-1}\bar{Y})
\end{aligned}$$

and

$$\begin{aligned}
& S_{rl}(C_v\bar{X}\bar{Y}\bar{Z}) - S_{rl}(C_v\bar{X}\bar{Y}_H\bar{Z}) \\
= \ & S_{rl}(C_v\bar{X}\bar{Y}\bar{Z}) + S_{rl}(\bar{Y}_H\bar{Y}^{-1}) + S_{rl}({Y_H}^{-1}Y) - S_{rl}(C_v\bar{X}\bar{Y}_H\bar{Z}) \\
= \ & S_{rl}(C_v\bar{X}\bar{Y}_H\bar{Z}) + S_{rl}(Y_H^{-1}Y) - S_{rl}(C_v\bar{X}\bar{Y}_H\bar{Z}) \\
= \ & S_{rl}(Y_H^{-1}Y) \\
= \ & S_{rl}(\bar{Y}_H^{-1}\bar{Y})\ ,
\end{aligned}$$

and hence

$$S_{rl}(C_v XYZ) - S_{rl}(C_v XY_H Z) \ = \ S_{rl}(C_v\bar{X}\bar{Y}\bar{Z}) - S_{rl}(C_v\bar{X}\bar{Y}_H\bar{Z})\ .$$

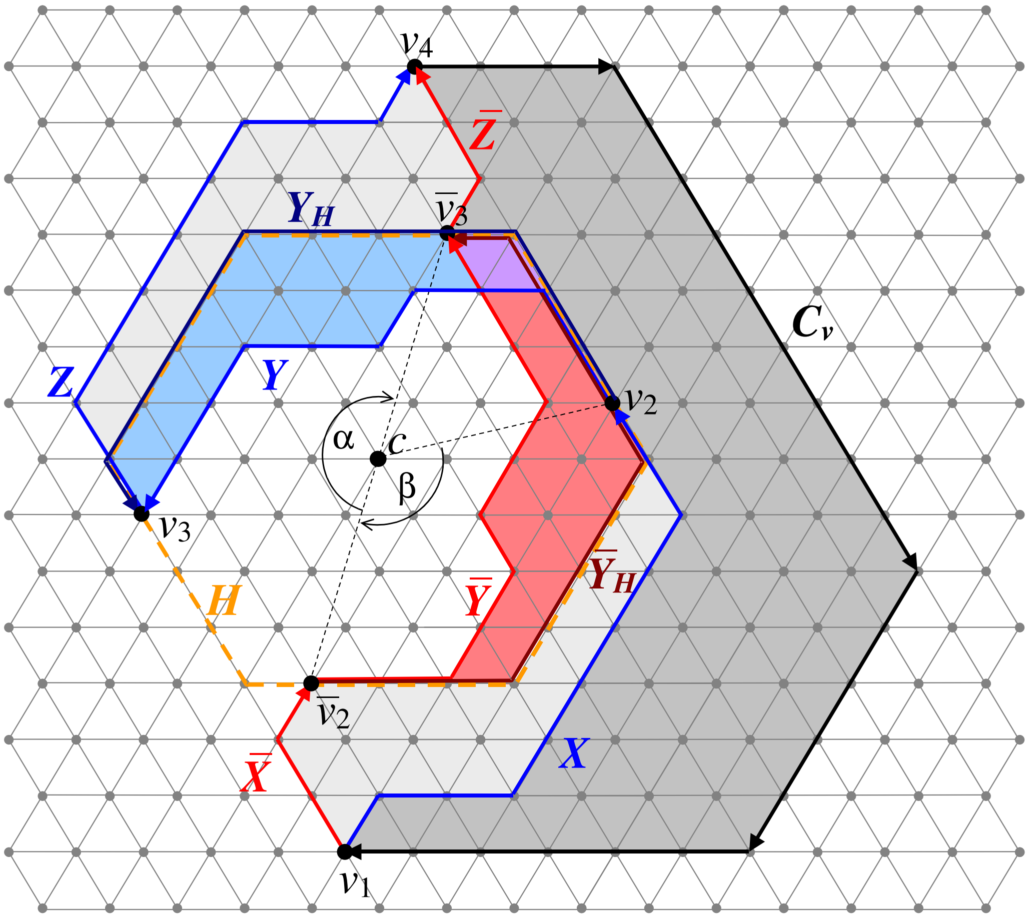

Figure 2.22: An example of two cutpaths with $Y \neq \bar{Y}$; the paths Y and $\bar{Y}$ may be replaced by Y_H and $\bar{Y}_H$ (the red area is a rotation of the blue area by β!)

Therefore it is sufficient to show

$$S_{rl}(C_v X Y_H Z) = S_{rl}(C_v \bar{X} \bar{Y}_H \bar{Z}) \tag{2.13}$$

instead of $S_{rl}(C_v XYZ) = S_{rl}(C_v \bar{X}\bar{Y}\bar{Z})$, because with (2.13) we obtain

$$\begin{aligned} S_{rl}(C_v XYZ) &= S_{rl}(C_v XYZ) - S_{rl}(C_v X Y_H Z) + S_{rl}(C_v X Y_H Z) \\ &= S_{rl}(C_v \bar{X}\bar{Y}\bar{Z}) - S_{rl}(C_v \bar{X}\bar{Y}_H \bar{Z}) + S_{rl}(C_v \bar{X}\bar{Y}_H \bar{Z}) \\ &= S_{rl}(C_v \bar{X}\bar{Y}\bar{Z})\ . \end{aligned}$$

So in the following we may w.l.o.g. assume $Y = Y_H$ and $\bar{Y} = \bar{Y}_H$. For the proof we distinguish whether $\alpha + \beta < 360$, $\alpha + \beta = 360$, or $\alpha + \beta > 360$.

1. $\alpha + \beta < 360$:

   Because of $\bar{v_3} = \alpha(\bar{v_2}) = \alpha(\beta(v_2))$ this means that $\bar{v_3}$ is a clockwise rotation of v_2 around c of less than 360 degrees. Hence, since $\bar{Y}$ is the (counterclockwise) path along the hexagon from $\bar{v_2}$ to $\bar{v_3}$ and Y is the corresponding path from v_2 to v_3, they must have a segment in common, namely the subpath from v_2 to $\bar{v_3}$. We define $\bar{Y}_1$ as the subpath of $\bar{Y}$ from $\bar{v}_2$ to v_2, $\bar{Y}_2 = Y_1$ as the common subpath from v_2 to $\bar{v_3}$, and Y_2 as the subpath of Y from $\bar{v_3}$ to v_3 (see also figure 2.23). Because of the symmetry of H, also $\bar{Y}_1$ and Y_2 are the same labeled paths.

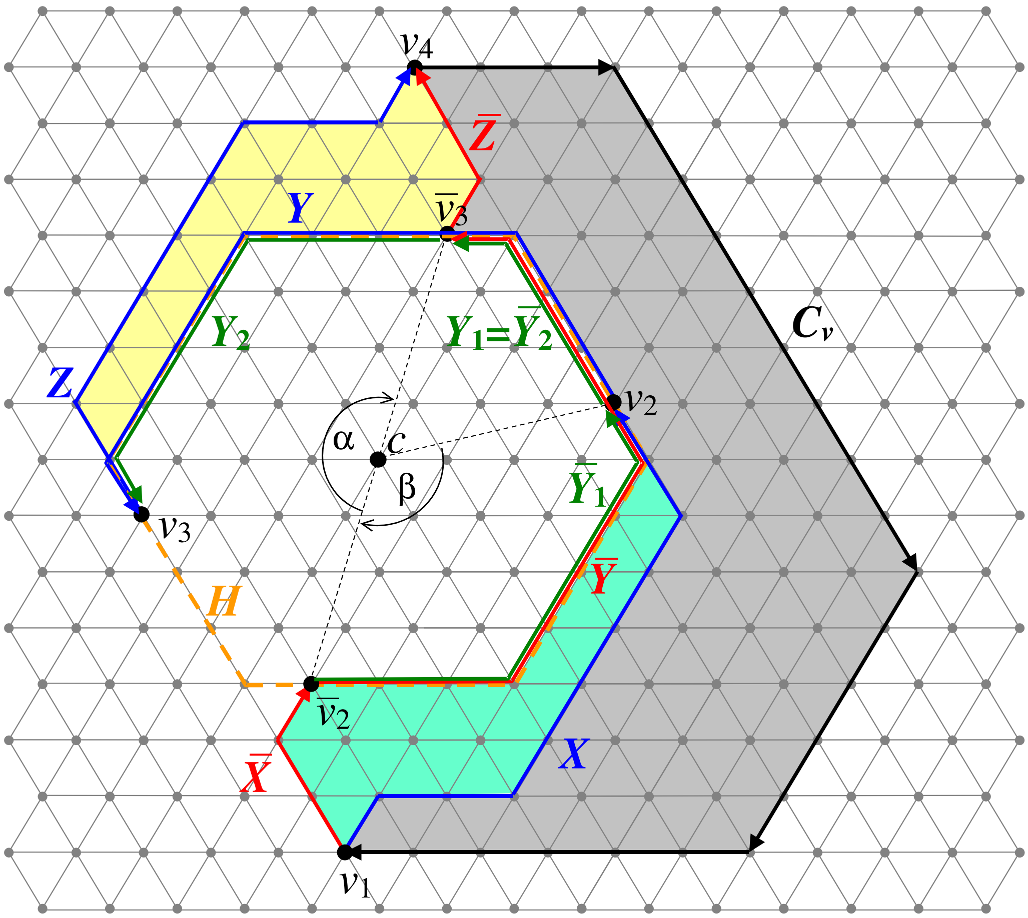

Figure 2.23: An example where $\alpha + \beta < 360$. Then $\bar{Y}$ and Y can be partitioned into $\bar{Y}_1\bar{Y}_2$ resp. Y_1Y_2 such that $Y_1 = \bar{Y}_2$, and it can be seen that $Z^{-1}Y_2^{-1}\bar{Z}$ is a rotation under α of $X\bar{Y}_1^{-1}\bar{X}^{-1}$

Now the situation is similar to the first case where $Y = \bar{Y}$: Due to the definition of α and the symmetry of H, the cycle $Z^{-1}Y_2^{-1}\bar{Z}$ is a rotation under α of $X\bar{Y}_1^{-1}\bar{X}^{-1}$, so we have

$$S(X\bar{Y}_1^{-1}\bar{X}^{-1}) + S(ZY_2\bar{Z}^{-1}) = 0$$

and therefore

$$\begin{aligned} S(C_v\bar{X}\bar{Y}\bar{Z}) &= S(C_v\bar{X}\bar{Y}_1\bar{Y}_2\bar{Z}) \\ &= S(C_v\bar{X}\bar{Y}_1\bar{Y}_2\bar{Z}) + S(X\bar{Y}_1^{-1}\bar{X}^{-1}) + S(ZY_2\bar{Z}^{-1}) \\ &= S(C_vX\bar{Y}_2Y_2Z) \\ &= S(C_vXYZ)\,. \end{aligned}$$

2. $\alpha + \beta = 360$:

   Then we have $\bar{v_3} = \alpha(\bar{v_2}) = \alpha(\beta(v_2)) = v_2$, i.e. the ending point of $\bar{Y}$ is the starting point of Y (see also figure 2.24). This means there are cycles $Z^{-1}Y^{-1}\bar{Z}$ and $X\bar{Y}^{-1}\bar{X}^{-1}$, where $\alpha(X\bar{Y}^{-1}\bar{X}^{-1}) = Z^{-1}Y^{-1}\bar{Z}$, so it follows that

   $$S(X\bar{Y}^{-1}\bar{X}^{-1}) + S(ZY\bar{Z}^{-1}) = 0$$

   and hence

   $$S(C_v\bar{X}\bar{Y}\bar{Z}) \;=\; S(C_v\bar{X}\bar{Y}\bar{Z}) + S(X\bar{Y}^{-1}\bar{X}^{-1}) + S(ZY\bar{Z}^{-1}) \;=\; S(C_vXYZ)\,.$$

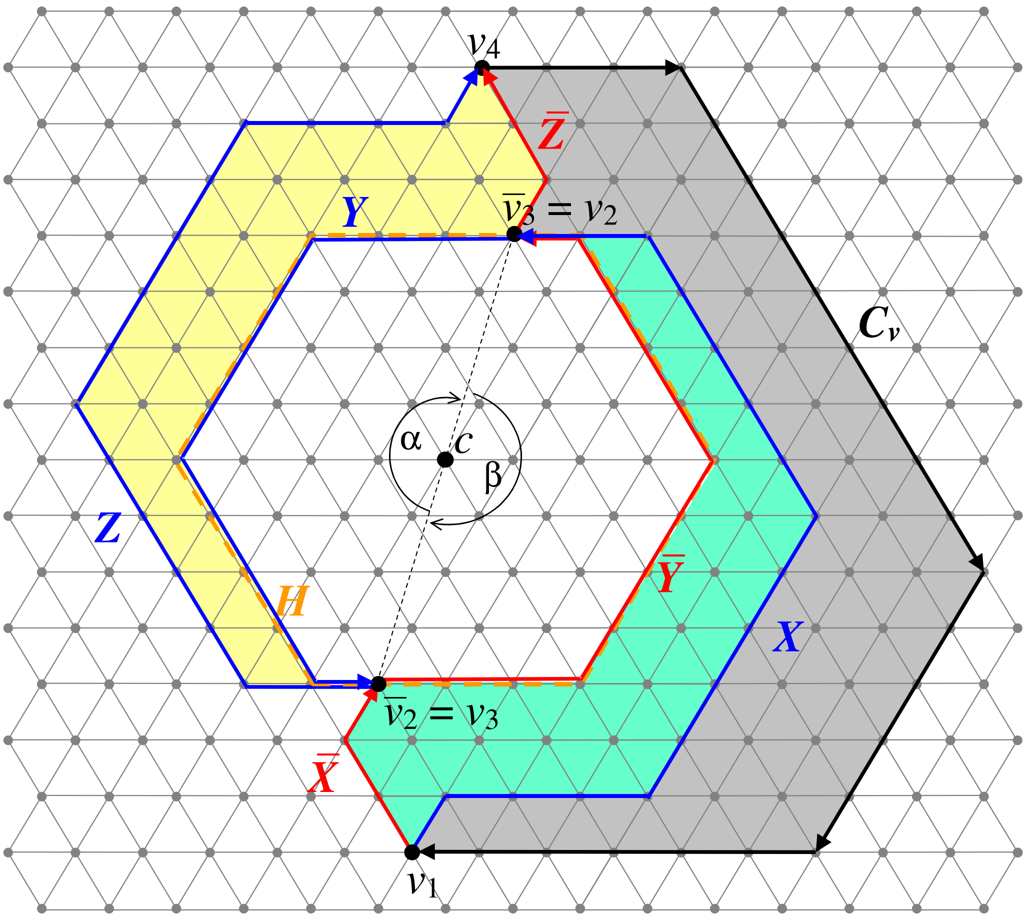

Figure 2.24: Here we have $\alpha + \beta = 360$ and hence $\bar{v_3} = v_2$. Then we get $\alpha(X\bar{Y}^{-1}\bar{X}^{-1}) = Z^{-1}Y^{-1}\bar{Z}$

3. $\alpha + \beta > 360$:

   Then Y and $\bar{Y}$ do not intersect, so we define a path A from $\bar{v_3}$ to v_2 following H and obtain cycles $\bar{X}\bar{Y}AX^{-1}$ and $\bar{Z}^{-1}AYZ$ (see figure 2.25). Because of the symmetry of H, $\bar{Y}A$ and AY are also the same labeled paths only rotated by α, so

   $$\alpha(\bar{X}\bar{Y}AX^{-1}) = \bar{Z}^{-1}AYZ$$

holds. Therefore we have

$$S(\bar{X}^{-1}\bar{Y}^{-1}A^{-1}X) + S(\bar{Z}^{-1}AYZ) = 0$$

and

$$\begin{aligned} S(C_v\bar{X}\bar{Y}\bar{Z}) &= S(C_v\bar{X}\bar{Y}\bar{Z}) + S(\bar{X}^{-1}\bar{Y}^{-1}A^{-1}X) + S(\bar{Z}^{-1}AYZ) \\ &= S(C_vXYZ)\ . \end{aligned}$$

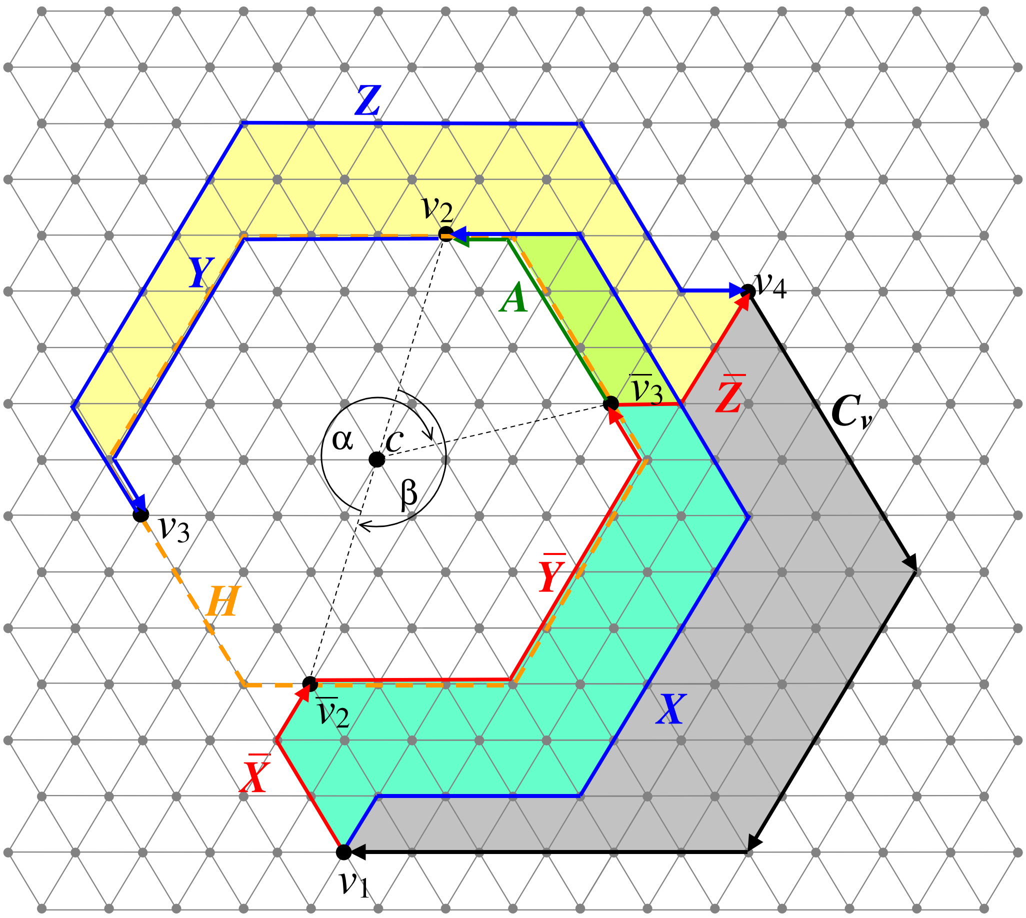

Figure 2.25: An example with $\alpha + \beta > 360$; then we define a path A from $\bar{v}_3$ to v_2

With this we have $S(C_v\bar{X}\bar{Y}\bar{Z}) = S(C_vXYZ)$ for all possible cases, which was what we wanted to show.

□

2.6 Further questions

There are several further interesting questions in this context that will not be investigated in this work but should be raised here:

In this chapter we have shown that two disordered triangle patches P and $\bar{P}$ with the same boundary sequence and disordered subpatches Q and $\bar{Q}$ that are isomorphic have the same number of faces if $D(Q) \bmod 6 = D(\bar{Q}) \bmod 6 \neq 0$. But what about the cases with $D(Q) \bmod 6 = 0$?

We know that the number of faces is also uniquely determined in case of $D(Q) = 0$ [26]. For $D(Q) = 6$ we know that this is *not* the case (see figure 2.2). However, in these kind of examples the closure of the embedding corresponds to a *translation* in the lattice and never to a rotation. But it can also happen that the image of the closure and the image of the first edge are equal such that we have a closed cycle in the lattice – figure 2.26 shows an example where this is the case. So the question is: Is the number of faces uniquely determined in this case?

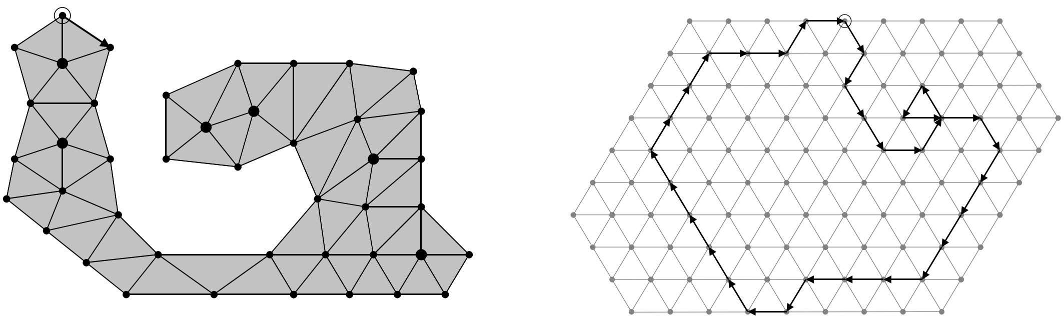

Figure 2.26: A patch with 6 degree 5 vertices whose boundary forms a closed cycle in the lattice

Finally, what about $D(Q) = 12$, for example 12 degree 5 vertices? If the patch is a subgraph of a geodesic dome this should be easy because the number of faces in the other cap with 0 degree 5 vertices is uniquely determined by the boundary, and the whole geodesic dome is uniquely determined by its signature which is obtained by the Coxeter coordinates between the degree 5 vertices ([19]). But what if the patch is not such a subgraph?

Chapter 3

Minimal boundary lengths of disordered patches

3.1 Introduction

In this chapter we investigate patches that have minimal boundary length while containing a fixed number of faces. We determine formulas for lower bounds on the boundary length in terms of the number of faces, and furthermore construct patches that indeed assume these minimal boundary lengths.

Harary and Harborth have already discussed similar problems in [27], but only for patches without disorder, that means patches where all bounded faces have the same size and all inner vertices the same degrees. This includes triangle-patches where all inner vertices have degree 6. We are basically interested in results on triangle-patches that allow also defective vertices with degrees different from 6 – in particular we are interested in the cases with inner vertices of degree 5 and 6, since these triangle-patches occur in geodesic domes, the duals of fullerenes.

Indeed there have already been investigations on the boundary lengths of the dual patches, that are hexagon-patches with pentagons as defective faces [3], and in [15] also with triangles and quadrangles. We discuss and extend these results in the first main section of this chapter (section 3.2). In section 3.3, we turn to disordered triangle-patches with a limited number of defective vertices. Using the results on hexagonal patches, we prove lower bounds on the boundary length of these patches with respect to their numbers of faces. Afterwards we define *spirals* and show that their boundary lengths are equal to the lower bounds computed before. This way we have determined disordered triangle-patches with minimal boundary lengths for a given number of certain defective vertices. However, the positions of the defective vertices are variable, and for application we are also interested in triangle-patches with minimal boundary lengths for a given *configuration* of defective vertices (e.g. with certain distances), or more general with a fixed subpatch containing the defective vertices. These problems are discussed in the sections 3.3.4 and 3.3.5, making use of the results established before.

3.2 The boundary length of disordered hexagon-patches

Since the duals of disordered triangle-patches are hexagonal patches with inner vertices of degree 3 where the disorder consists in faces whose sizes deviate from 6, we examine these patches in this section.

In [3], Bornhöft, Brinkmann, and Greinus consider pentagon-hexagon-patches, that are 2-connected plane graphs with all bounded faces pentagons or hexagons, all interior vertices of degree 3 and all boundary vertices of degree 2 or 3. They show that for a given number of pentagons and hexagons a minimal boundary length is reached by arranging the faces in a spiral way starting with the pentagons, and give explicit formulas for the boundary length of these spirals. This result is extended by Anke Egging in her diploma thesis [15] to patches where not only hexagons and pentagons, but also squares and triangles are allowed. Analogously to the disordered triangle-patches we introduce the following definitions for hexagonal patches:

Definition 3.2.1 *A* disordered hexagon-patch *is a* 2*-connected plane graph* P *with one distinguished face called the* outer face *where all vertices not lying in the outer face have degree* 3*, and all vertices that lie in the outer face have degree* 2 *or* 3*. Any face that is not the outer face is called* bounded face*, and a bounded face with size different from* 6 *is called* defective face*. We call a bounded face of size* 6 *a* hexagon*, a bounded face of size* 5 *a* pentagon*, a bounded face of size* 4 *a* square*, and a bounded face of size* 3 *a* triangle*. The vertices and edges in the outer face are called* boundary vertices *and* boundary edges*, respectively. The* boundary length *of* P *is defined as the number of boundary edges (or equivalently, boundary vertices) and denoted by* $b(P)$*.*

A disordered hexagon-patch with exactly p *pentagons,* s *squares,* t *triangles and no further defective faces will be called* (p, s, t)-hexagon-patch*. Moreover, we define for* $p, s, t \in \mathbb{N}_0$*:*

$$D(p, s, t) := p + 2s + 3t$$

We are particularly interested in (p, s, t)-hexagon-patches with $D(p, s, t) \leq 6$ because only these cases allow to construct patches with an arbitrary number of hexagons. Due to [15], there are 23 different possibilities to choose $p, s, t \in \mathbb{N}_0$ such that $D(p, s, t) \leq 6$ holds (see also table 3.1). For these cases, a (p, s, t)-hexagon-spiral is defined as a (p, s, t)-hexagon-patch where the faces are arranged in a spiral way, starting with the triangles and continuing with the squares, pentagons and finally the hexagons. We will denote a (p, s, t)-hexagon-spiral with h hexagons by $S^{\text{hex}}_{h,p,s,t}$. The detailed definition as well as the existence and uniqueness of such a spiral can be looked up in [15].

Furthermore, it is proven in [15] with the help of the technique applied in [3] that the spiral $S^{\text{hex}}_{h,p,s,t}$ has minimal boundary length among all (p, s, t)-hexagon-patches with h hexagons. The boundary length of $S^{\text{hex}}_{h,p,s,t}$ for given (p, s, t) is computed in terms of the number h of hexagons – however, with a few errors. In subsection 3.2.1 we give the correct formulas and the proofs for those that differ from [15].

Afterwards, in subsection 3.2.2, we introduce *general* disordered hexagon-patches – disordered hexagon-patches that are not necessarily 2-connected – which will be needed in section 3.3 for transferring the results to the dual. We show that general disordered hexagon-patches with minimal boundary length are 2-connected, which means that the proven formulas on the minimal boundary length of disordered hexagon-patches also hold for general disordered hexagon-patches.

3.2.1 Lower bounds on the boundary length of hexagon-patches

We start with a basic formula for hexagon-patches:

Lemma 3.2.2 *Let P be a (p,s,t)-hexagon-patch, and d_2 resp. d_3 the number of boundary vertices of P with degree 2 resp. 3. Then we have*

$$d_2 - d_3 \;=\; 6 - D(p,s,t)\;.$$

PROOF:

This follows by summing up on the one hand the vertices and on the other hand the edges for all the bounded faces, and inserting the obtained equations into Euler‘s formula (see [15], Lemma 2.11).

□

The following theorem corresponds to Theorem 4.1 and Lemma 4.4 in [15], where the incorrect formulas from Theorem 4.1 have been corrected in this place (see table 3.1). We give the proof only for these cases.

Theorem 3.2.3 *For given $h,p,s,t \in \mathbb{N}_0$ with $D(p,s,t) \leq 6$, the spiral $S^{hex}_{h,p,s,t}$ has minimal boundary length among all (p,s,t)-hexagon-patches with h hexagons. Its boundary length can be found in table 3.1. Thus, these formulas give lower bounds on the boundary length of any (p,s,t)-hexagon-patch.*

PROOF:

The proof of the minimality can be found in [15], lemma 4.4.

The formulas for the cases with $s = t = 0$ appear in [3] and are proven in detail in [22]. The proofs of the cases $(p,s,t) \in \{(0,1,0),(2,1,0),(4,1,0),(0,2,0),(2,2,0),(0,3,0),(0,0,1),(3,0,1),(0,1,1),(1,1,1),(0,0,2)\}$ are contained in [15]. Left are the formulas for

$$(p,s,t) \in \{(1,1,0),(3,1,0),(1,2,0),(1,0,1),(2,0,1)\}$$

which are not correct in [15] and will be proven in the following.

For each of the five cases for (p,s,t) that we consider, we define a *basic patch* as shown in figure 3.1. These patches are contained in any of the corresponding (p,s,t)-hexagon-spirals $S^{\text{hex}}_{h,p,s,t}$ and form the first faces in the spiral order – for the cases $(p,s,t) = (3,1,0)$ and $(p,s,t) = (2,0,1)$ we have to assume $h \geq 1$, but this is no problem since the formulas can easily be checked by hand for the case $h = 0$.

The set of faces with minimal distance d to one of the faces in the basic patch will be called the dth layer of the spiral. The dth layer is called complete if the unbounded face has a distance of more than d from any of the faces in the basic patch.

(p,s,t)	$D(p,s,t)$	$b\,(S^{\text{hex}}_{h,p,s,t})$
$(0,0,0)$	0	$2\lceil\sqrt{12h-3}\rceil$
$(1,0,0)$	1	$2\lceil\sqrt{10h+\frac{25}{4}}+\frac{1}{2}\rceil-1$
$(2,0,0)$	2	$2\lceil\sqrt{8h+16}\rceil$
$(3,0,0)$	3	$2\lceil\sqrt{6h+\frac{81}{4}}+\frac{1}{2}\rceil-1$
$(4,0,0)$	4	$2\lceil\sqrt{4h+25}\rceil$
$(5,0,0)$	5	$2\lceil\sqrt{2h+\frac{113}{4}}+\frac{1}{2}\rceil-1$
$(6,0,0)$	6	10 if $\frac{h}{5}\in\mathbb{N}_0$ 12 else
$(0,1,0)$	2	$2\lceil\sqrt{8h+4}\rceil$
$(1,1,0)$	3	$2\lceil\sqrt{6h+\frac{49}{4}}+\frac{1}{2}\rceil-1$
$(2,1,0)$	4	$2\lceil\sqrt{4h+16}\rceil$
$(3,1,0)$	5	$2\lceil\sqrt{2h+\frac{73}{4}}+\frac{1}{2}\rceil-1$
$(4,1,0)$	6	8 if $\frac{h}{4}\in\mathbb{N}_0$ 10 else
$(0,2,0)$	4	$2\lceil\sqrt{4h+9}\rceil$
$(1,2,0)$	5	$2\lceil\sqrt{2h+\frac{49}{4}}+\frac{1}{2}\rceil-1$
$(2,2,0)$	6	8
$(0,3,0)$	6	6 if $\frac{h}{3}\in\mathbb{N}_0$ 8 else
$(0,0,1)$	3	$2\lceil\sqrt{6h+\frac{9}{4}}+\frac{1}{2}\rceil-1$
$(1,0,1)$	4	$2\lceil\sqrt{4h+8}\rceil$
$(2,0,1)$	5	$2\lceil\sqrt{2h+\frac{41}{4}}+\frac{1}{2}\rceil-1$
$(3,0,1)$	6	6 if $\frac{h}{3}\in\mathbb{N}_0$ 8 else
$(0,1,1)$	5	$2\lceil\sqrt{2h+\frac{25}{4}}+\frac{1}{2}\rceil-1$
$(1,1,1)$	6	6
$(0,0,2)$	6	4 if $\frac{h}{2}\in\mathbb{N}_0$ 6 else

Table 3.1: The 23 combinations of $p,s,t\in\mathbb{N}_0$ with $D(p,s,t)\leq 6$, and the boundary length $b(S^{\text{hex}}_{h,p,s,t})$ of the spiral $S^{\text{hex}}_{h,p,s,t}$ with h hexagons in each case.

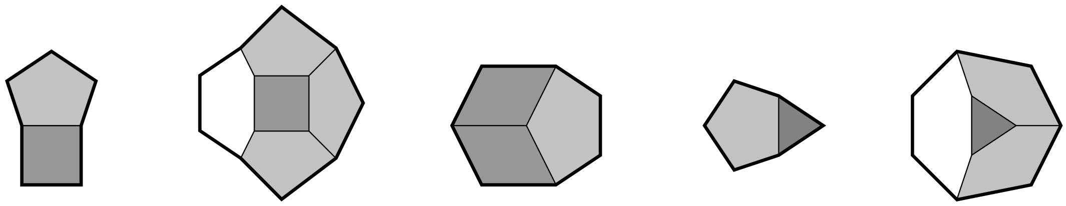

Figure 3.1: The basic patches for the cases $(p,s,t) = (1,1,0)$, $(p,s,t) = (3,1,0)$, $(p,s,t) = (1,2,0)$, $(p,s,t) = (1,0,1)$, and $(p,s,t) = (2,0,1)$

Now we insert a small *lemma*: Let S be a spiral consisting of a basic patch, $l \geq 1$ complete layers and no further faces, and let $\bar{S}$ be the spiral consisting of the same basic patch, $l-1$ complete layers and no further faces. Then in case $l \geq 2$, the lth complete layer contains $6 - D(p,s,t)$ more faces than the $(l-1)$st complete layer. Furthermore, we have $b(S) = b(\bar{S}) + 2(6 - D(p,s,t))$.

Proof: For $j = 2,3$, let d_j resp. $\bar{d}_j$ be the number of boundary vertices with degree j in S resp. $\bar{S}$. Since in each layer every face has exactly two neighbouring faces, $\bar{d}_2 = d_3$ gives the number of faces in the lth layer, while $\bar{d}_3$ is the number of faces in the $(l-1)$st layer. Furthermore, by lemma 3.2.2 we have $d_2 - d_3 = \bar{d}_2 - \bar{d}_3 = 6 - D(p,s,t)$. We obtain

$$d_3 - \bar{d}_3 \;=\; \bar{d}_2 - \bar{d}_3 \;=\; 6 - D(p,s,t)$$

and

$$\begin{aligned} b(S) \;=\; d_2 + d_3 &= d_2 + d_3 + \bar{d}_2 - \bar{d}_2 + \bar{d}_3 - \bar{d}_3 \\ &= (\bar{d}_2 + \bar{d}_3) + (d_2 - \bar{d}_2) + (d_3 - \bar{d}_3) \\ &= (\bar{d}_2 + \bar{d}_3) + (d_2 - d_3) + (\bar{d}_2 - \bar{d}_3) \\ &= b(\bar{S}) + 2(6 - D(p,s,t)) \; . \end{aligned}$$

The case (p,s,t)=(1,1,0)

At first we want to determine the boundary length of the spiral $S^{\text{hex}}_{h,1,1,0}$ with respect to its number of hexagons $h \in \mathbb{N}$ (see figure 3.2). For this assume it has l complete layers, and let a be the number of additional hexagons that do not lie in a complete layer.

Since the first layer contains 5 faces and for $d \geq 2$, the dth complete layer contains $6 - D(1,1,0) = 3$ more faces than the $(d-1)$st layer, we have

$$\begin{aligned} h &= \sum_{i=1}^{l} (3i+2) + a \\ &= 3\,\frac{l(l+1)}{2} + 2l + a \\ &= \frac{3}{2}\,l^2 + \frac{7}{2}\,l + a \; . \end{aligned}$$

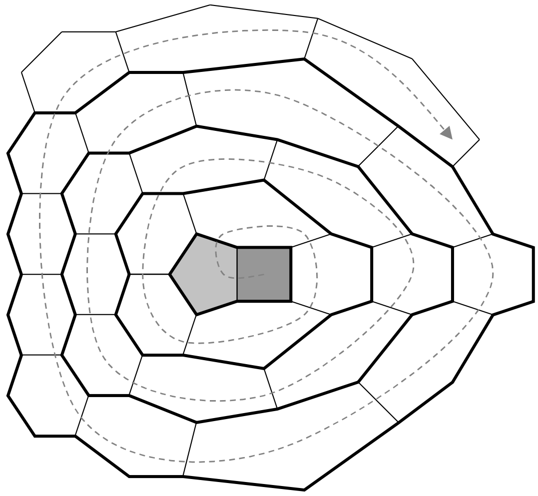

Figure 3.2: The spiral $S^{\text{hex}}_{h,1,1,0}$ – here with $l = 3$ layers and $a = 3$ additional faces

In case $a = 0$ we have $b(S^{\text{hex}}_{h,1,1,0}) = 6l + 7$, since the basic patch has boundary length 7, and with each complete layer the boundary length grows by $2(6 - D(1,1,0)) = 6$. On the other hand, we get by inserting h into the stated formula:

$$\begin{aligned} 2\lceil\sqrt{6h + \frac{49}{4}} + \frac{1}{2}\rceil - 1 &= 2\lceil\sqrt{9l^2 + 21l + \frac{49}{4}} + \frac{1}{2}\rceil - 1 \\ &= 2\lceil(3l + \frac{7}{2}) + \frac{1}{2}\rceil - 1 \\ &= 6l + 7 = b(S^{\text{hex}}_{h,1,1,0}) \end{aligned}$$

Now let $a \neq 0$. Then we have

$$b(S^{\text{hex}}_{h,1,1,0}) = 6l + 7 + \begin{cases} 2 & , \quad 1 \leq a \leq l + 1 \\ 4 & , \quad l + 2 \leq a \leq 2l + 3 \\ 6 & , \quad 2l + 4 \leq a \leq 3l + 4 \,. \end{cases}$$

In case $1 \leq a \leq l + 1$ we get:

$$\begin{aligned} \frac{3}{2}l^2 + \frac{7}{2}l + 1 &\leq h \leq \frac{3}{2}l^2 + \frac{9}{2}l + 1 \\ \Leftrightarrow\quad 9l^2 + 21l + \frac{73}{4} &\leq 6h + \frac{49}{4} \leq 9l^2 + 27l + \frac{73}{4} \\ \Rightarrow\quad 9l^2 + 21l + \frac{49}{4} &< 6h + \frac{49}{4} \leq 9l^2 + 27l + \frac{81}{4} \\ \Rightarrow\quad 3l + \frac{7}{2} &< \sqrt{6h + \frac{49}{4}} \leq 3l + \frac{9}{2} \\ \Leftrightarrow\quad 3l + 4 &< \sqrt{6h + \frac{49}{4}} + \frac{1}{2} \leq 3l + 5 \end{aligned}$$

This implies:

$$\begin{aligned}
\lceil\sqrt{6h+\frac{49}{4}}+\frac{1}{2}\rceil &= 3l+5 \\
\Leftrightarrow\ 2\lceil\sqrt{6h+\frac{49}{4}}+\frac{1}{2}\rceil-1 &= 6l+9 \ = \ b(S^{\text{hex}}_{h,1,1,0})
\end{aligned}$$

In case $l+2 \le a \le 2l+3$ we have

$$\begin{aligned}
\frac{3}{2}l^2+\frac{9}{2}l+2 \ &\le \ h \ \le \ \frac{3}{2}l^2+\frac{11}{2}l+3 \\
\Leftrightarrow\ 9l^2+27l+\frac{97}{4} \ &\le \ 6h+\frac{49}{4} \ \le \ 9l^2+33l+\frac{121}{4} \\
\Rightarrow\ 9l^2+27l+\frac{81}{4} \ &< \ 6h+\frac{49}{4} \ \le \ 9l^2+33l+\frac{121}{4} \\
\Rightarrow\ 3l+\frac{9}{2} \ &< \ \sqrt{6h+\frac{49}{4}} \ \le \ 3l+\frac{11}{2} \\
\Leftrightarrow\ 3l+5 \ &< \ \sqrt{6h+\frac{49}{4}}+\frac{1}{2} \ \le \ 3l+6
\end{aligned}$$

and therefore we get:

$$\begin{aligned}
\lceil\sqrt{6h+\frac{49}{4}}+\frac{1}{2}\rceil &= 3l+6 \\
\Leftrightarrow\ 2\lceil\sqrt{6h+\frac{49}{4}}+\frac{1}{2}\rceil-1 &= 6l+11 \ = \ b(S^{\text{hex}}_{h,1,1,0})
\end{aligned}$$

Finally, if $2l+4 \le a \le 3l+4$ we have

$$\begin{aligned}
\frac{3}{2}l^2+\frac{11}{2}l+4 \ &\le \ h \ \le \ \frac{3}{2}l^2+\frac{13}{2}l+4 \\
\Leftrightarrow\ 9l^2+33l+\frac{145}{4} \ &\le \ 6h+\frac{49}{4} \ \le \ 9l^2+39l+\frac{145}{4} \\
\Rightarrow\ 9l^2+33l+\frac{121}{4} \ &< \ 6h+\frac{49}{4} \ \le \ 9l^2+39l+\frac{169}{4} \\
\Rightarrow\ 3l+\frac{11}{2} \ &< \ \sqrt{6h+\frac{49}{4}} \ \le \ 3l+\frac{13}{2} \\
\Leftrightarrow\ 3l+6 \ &< \ \sqrt{6h+\frac{49}{4}}+\frac{1}{2} \ \le \ 3l+7
\end{aligned}$$

so it follows that:

$$\begin{aligned}
\lceil\sqrt{6h+\frac{49}{4}}+\frac{1}{2}\rceil &= 3l+7 \\
\Leftrightarrow\ 2\lceil\sqrt{6h+\frac{49}{4}}+\frac{1}{2}\rceil-1 &= 6l+13 \ = \ b(S^{\text{hex}}_{h,1,1,0})
\end{aligned}$$

Hence we have shown in all cases:

$$b(S^{\text{hex}}_{h,1,1,0}) \ = \ 2\lceil\sqrt{6h+\frac{49}{4}}+\frac{1}{2}\rceil-1$$

The case (p,s,t)=(3,1,0)

Now consider $S^{\text{hex}}_{h,3,1,0}$ with $h \in \mathbb{N}$ (see figure 3.3). Assume S has l complete layers, and let a be the number of additional faces not lying in a complete layer (nor in the basic patch).

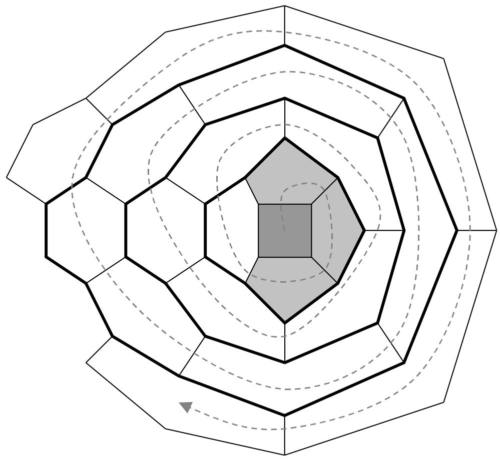

Figure 3.3: The spiral $S^{\text{hex}}_{h,3,1,0}$ – here with $l = 2$ layers and $a = 5$ additional faces

Note that the basic patch contains one hexagon, the first layer contains 5 faces and for $d \geq 2$, the dth complete layer contains $6 - D(3,1,0) = 1$ more face than the $(d-1)$st layer. Therefore the number of hexagons is

$$\begin{aligned} h &= 1 + \sum_{i=1}^{l}(i+4) + a \\ &= 1 + \frac{l(l+1)}{2} + 4l + a \\ &= 1 + \frac{1}{2}l^2 + \frac{9}{2}l + a \; . \end{aligned}$$

In case $a = 0$ we have $b(S^{\text{hex}}_{h,3,1,0}) = 2l + 9$, since the basic patch has boundary length 9, and with each complete layer the boundary length grows by $2(6 - D(3,1,0)) = 2$. On the other hand, we get by inserting h into the stated formula:

$$\begin{aligned} 2\lceil\sqrt{2h + \frac{73}{4}} + \frac{1}{2}\rceil - 1 &= 2\lceil\sqrt{2 + l^2 + 9l + \frac{73}{4}} + \frac{1}{2}\rceil - 1 \\ &= 2\lceil(l + \frac{9}{2}) + \frac{1}{2}\rceil - 1 \\ &= 2l + 9 \;=\; b(S^{\text{hex}}_{h,3,1,0}) \end{aligned}$$

Now let $a \neq 0$. Since the dth complete layer contains $d + 4$ hexagons, the $(l + 1)$st layer would contain $l + 5$ faces if it was complete, so $1 \leq a \leq l + 4$ must hold. For any such a we have

$$b(S^{\text{hex}}_{h,3,1,0}) = 2l + 9 + 2 = 2l + 11 \; .$$

With $1 \leq a \leq l+4$ we get:

$$\begin{array}{rcccl} & \frac{1}{2}l^2+\frac{9}{2}l+2 & \leq & h & \leq & \frac{1}{2}l^2+\frac{11}{2}l+5 \\ \Leftrightarrow & l^2+9l+\frac{89}{4} & \leq & 2h+\frac{73}{4} & \leq & l^2+11l+\frac{113}{4} \\ \Rightarrow & l^2+9l+\frac{81}{4} & < & 2h+\frac{73}{4} & \leq & l^2+11l+\frac{121}{4} \\ \Rightarrow & l+\frac{9}{2} & < & \sqrt{2h+\frac{73}{4}} & \leq & l+\frac{11}{2} \\ \Leftrightarrow & l+5 & < & \sqrt{2h+\frac{73}{4}}+\frac{1}{2} & \leq & l+6 \end{array}$$

This implies:

$$\begin{array}{rcl} \lceil\sqrt{2h+\frac{73}{4}}+\frac{1}{2}\rceil & = & l+6 \\ \Leftrightarrow \; 2\lceil\sqrt{2h+\frac{73}{4}}+\frac{1}{2}\rceil-1 & = & 2l+11 \; = \; b(S^{\text{hex}}_{h,3,1,0}) \end{array}$$

So we have proven

$$b(S^{\text{hex}}_{h,3,1,0}) \; = \; 2\lceil\sqrt{2h+\frac{73}{4}}+\frac{1}{2}\rceil-1\,.$$

The case (p,s,t)=(1,2,0)

Now we determine the boundary length of the spiral $S^{\text{hex}}_{h,1,2,0}$ with $h \in \mathbb{N}$ (see figure 3.4). Assume it has l complete layers and a additional faces not lying in a complete layer or the basic patch.

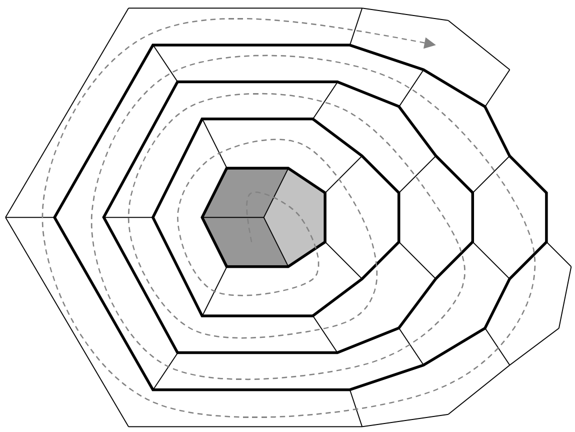

Figure 3.4: The spiral $S^{\text{hex}}_{h,1,2,0}$ – here with $l=3$ layers and $a=5$ additional faces

Since the first layer contains 4 faces and for $d \geq 2$, the dth complete layer contains $6 - D(1,2,0) = 1$ more face than the $(d-1)$st layer, the number of hexagons is

$$\begin{aligned} h &= \sum_{i=1}^{l}(i+3) + a \\ &= \frac{l(l+1)}{2} + 3l + a \\ &= \frac{1}{2}l^2 + \frac{7}{2}l + a \,. \end{aligned}$$

In case $a = 0$ we have $b(S^{\text{hex}}_{h,1,2,0}) = 2l + 7$, because the basic patch has boundary length 7, and with each complete layer the boundary length grows by $2(6 - D(1,2,0)) = 2$. On the other hand, we get by inserting h into the stated formula:

$$\begin{aligned} 2\lceil\sqrt{2h + \frac{49}{4}} + \frac{1}{2}\rceil - 1 &= 2\lceil\sqrt{l^2 + 7l + \frac{49}{4}} + \frac{1}{2}\rceil - 1 \\ &= 2\lceil(l + \frac{7}{2}) + \frac{1}{2}\rceil - 1 \\ &= 2l + 7 \;=\; b(S^{\text{hex}}_{h,1,2,0}) \end{aligned}$$

Now let $a \neq 0$. Since the dth complete layer contains $d + 3$ hexagons, the $(l+1)$st layer would contain $l + 4$ faces if it was complete, so $1 \leq a \leq l + 3$ must hold. For any such a we have

$$b(S^{\text{hex}}_{h,1,2,0}) = 2l + 7 + 2 = 2l + 9 \,.$$

With $1 \leq a \leq l + 3$ we get:

$$\begin{aligned} \frac{1}{2}l^2 + \frac{7}{2}l + 1 \;&\leq\; h \;\leq\; \frac{1}{2}l^2 + \frac{9}{2}l + 3 \\ \Leftrightarrow\; l^2 + 7l + \frac{57}{4} \;&\leq\; 2h + \frac{49}{4} \;\leq\; l^2 + 9l + \frac{73}{4} \\ \Rightarrow\; l^2 + 7l + \frac{49}{4} \;&<\; 2h + \frac{49}{4} \;\leq\; l^2 + 9l + \frac{81}{4} \\ \Rightarrow\; l + \frac{7}{2} \;&<\; \sqrt{2h + \frac{49}{4}} \;\leq\; l + \frac{9}{2} \\ \Leftrightarrow\; l + 4 \;&<\; \sqrt{2h + \frac{49}{4}} + \frac{1}{2} \;\leq\; l + 5 \end{aligned}$$

This implies:

$$\begin{aligned} \lceil\sqrt{2h + \frac{49}{4}} + \frac{1}{2}\rceil &= l + 5 \\ \Leftrightarrow\; 2\lceil\sqrt{2h + \frac{49}{4}} + \frac{1}{2}\rceil - 1 &= 2l + 9 \;=\; b(S^{\text{hex}}_{h,1,2,0}) \end{aligned}$$

Hence we have shown

$$b(S^{\text{hex}}_{h,1,2,0}) \;=\; 2\lceil\sqrt{2h + \frac{49}{4}} + \frac{1}{2}\rceil - 1 \,.$$

The case (p,s,t)=(1,0,1)

Now consider $S^{\text{hex}}_{h,1,0,1}$ with $h \in \mathbb{N}$ as shown in figure 3.5. Assume $S^{\text{hex}}_{h,1,0,1}$ has l complete layers and a additional faces not lying in a complete layer.

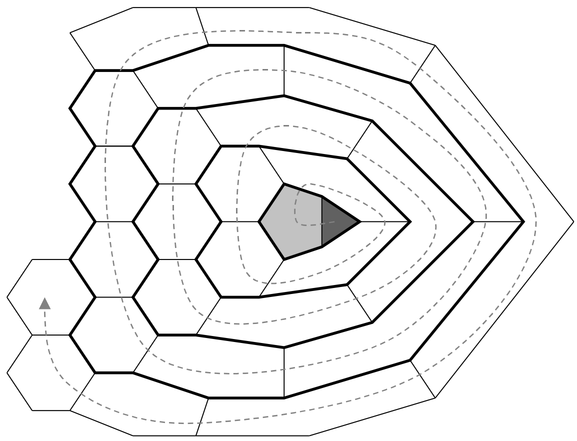

Figure 3.5: The spiral $S^{\text{hex}}_{h,1,0,1}$ – here with $l = 3$ layers and $a = 7$ additional faces

Since the first layer contains 4 faces and for $d \geq 2$, the dth complete layer contains $6 - D(1,0,1) = 2$ more faces than the $(d-1)$st layer, the number of hexagons is

$$\begin{aligned} h &= \sum_{i=1}^{l}(2i+2) + a \\ &= l(l+1) + 2l + a \\ &= l^2 + 3l + a \,. \end{aligned}$$

In case $a = 0$ we have $b(S^{\text{hex}}_{h,1,0,1}) = 4l+6$, because the basic patch has boundary length 6, and with each complete layer the boundary length grows by $2(6 - D(1,0,1)) = 4$. Furthermore we have

$$\begin{aligned} \sqrt{4h+8} &= \sqrt{4l^2+12l+8} \\ &> \sqrt{4l^2+8l+4} \\ &= 2l+2 \end{aligned}$$

and on the other hand

$$\begin{aligned} \sqrt{4h+8} &= \sqrt{4l^2+12l+8} \\ &\leq \sqrt{4l^2+12l+9} \\ &= 2l+3 \end{aligned}$$

which implies

$$2\lceil\sqrt{4h+8}\rceil \;=\; 2(2l+3) \;=\; 4l+6 \;=\; b(S^{\text{hex}}_{h,1,0,1}) \,.$$

Now let $a \neq 0$. Then we have

$$b(S^{\text{hex}}_{h,1,0,1}) = 4l + 6 + \begin{cases} 2 & , \quad 1 \leq a \leq l+2 \\ 4 & , \quad l+3 \leq a \leq 2l+3 \,. \end{cases}$$

In case $1 \leq a \leq l+2$ we get:

$$\begin{array}{rcccl} l^2+3l+1 & \leq & h & \leq & l^2+4l+2 \\ \Leftrightarrow \; 4l^2+12l+12 & \leq & 4h+8 & \leq & 4l^2+16l+16 \\ \Rightarrow \; 4l^2+12l+9 & < & 4h+8 & \leq & 4l^2+16l+16 \\ \Rightarrow \; 2l+3 & < & \sqrt{4h+8} & \leq & 2l+4 \end{array}$$

This implies:

$$\begin{array}{rcccl} \lceil\sqrt{4h+8}\rceil & = & 2l+4 & & \\ \Leftrightarrow \; 2\lceil\sqrt{4h+8}\rceil & = & 4l+8 & = & b(S^{\mathrm{hex}}_{h,1,0,1}) \end{array}$$

If $l+3 \leq a \leq 2l+3$ we obtain

$$\begin{array}{rcccl} l^2+4l+3 & \leq & h & \leq & l^2+5l+3 \\ \Leftrightarrow \; 4l^2+16l+20 & \leq & 4h+8 & \leq & 4l^2+20l+20 \\ \Rightarrow \; 4l^2+16l+16 & < & 4h+8 & \leq & 4l^2+20l+25 \\ \Rightarrow \; 2l+4 & < & \sqrt{4h+8} & \leq & 2l+5 \end{array}$$

and hence we have

$$\begin{array}{rcccl} \lceil\sqrt{4h+8}\rceil & = & 2l+5 & & \\ \Leftrightarrow \; 2\lceil\sqrt{4h+8}\rceil & = & 4l+10 & = & b(S^{\mathrm{hex}}_{h,1,0,1})\ . \end{array}$$

With this we have proven

$$b(S^{\mathrm{hex}}_{h,1,0,1}) \;=\; 2\lceil\sqrt{4h+8}\rceil$$

for all cases.

The case (p,s,t)=(2,0,1)

Finally we consider the spiral $S^{\mathrm{hex}}_{h,2,0,1}$ for some $h \in \mathbb{N}$ (see figure 3.6). We assume it has l complete layers and let a denote the number of additional faces not lying in a complete layer or the basic patch.

The basic patch contains one hexagon, the first layer contains 4 faces and for $d \geq 2$, the dth complete layer contains $6 - D(2,0,1) = 1$ more face than the $(d-1)$st layer. Hence the number of hexagons is

$$\begin{aligned} h &= 1 + \sum_{i=1}^{l}(i+3) + a \\ &= 1 + \frac{l(l+1)}{2} + 3l + a \\ &= 1 + \frac{1}{2}l^2 + \frac{7}{2}l + a\ . \end{aligned}$$

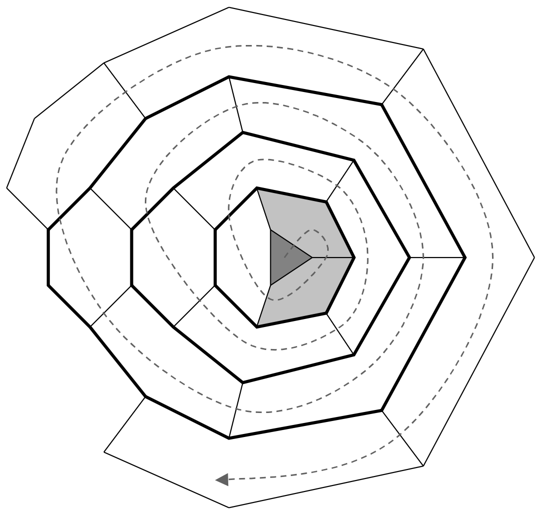

Figure 3.6: The spiral $S^{\text{hex}}_{h,2,0,1}$ – here with $l = 2$ layers and $a = 4$ additional faces

In case $a = 0$ we have $b(S) = 2l + 7$, since the basic patch has boundary length 7, and with each complete layer the boundary length grows by $2(6 - D(2, 0, 1)) = 2$. On the other hand, we get by inserting h into the stated formula:

$$\begin{aligned} 2\lceil\sqrt{2h + \frac{41}{4}} + \frac{1}{2}\rceil - 1 &= 2\lceil\sqrt{2 + l^2 + 7l + \frac{41}{4}} + \frac{1}{2}\rceil - 1 \\ &= 2\lceil(l + \frac{7}{2}) + \frac{1}{2}\rceil - 1 \\ &= 2l + 7 \;=\; b(S^{\text{hex}}_{h,2,0,1}) \end{aligned}$$

Now let $a \neq 0$. Since the dth complete layer contains $d + 3$ hexagons, the $(l + 1)$st layer would contain $l + 4$ faces if it was complete, so $1 \leq a \leq l + 3$ must hold. For any such a we have

$$b(S^{\text{hex}}_{h,2,0,1}) = 2l + 7 + 2 = 2l + 9 \,.$$

Now $1 \leq a \leq l + 3$ implies:

$$\begin{aligned} \frac{1}{2}l^2 + \frac{7}{2}l + 2 \;&\leq\; h \;\leq\; \frac{1}{2}l^2 + \frac{9}{2}l + 4 \\ \Leftrightarrow\; l^2 + 7l + \frac{57}{4} \;&\leq\; 2h + \frac{41}{4} \;\leq\; l^2 + 9l + \frac{73}{4} \\ \Rightarrow\; l^2 + 7l + \frac{49}{4} \;&<\; 2h + \frac{41}{4} \;\leq\; l^2 + 9l + \frac{81}{4} \\ \Rightarrow\; l + \frac{7}{2} \;&<\; \sqrt{2h + \frac{41}{4}} \;\leq\; l + \frac{9}{2} \\ \Leftrightarrow\; l + 4 \;&<\; \sqrt{2h + \frac{41}{4}} + \frac{1}{2} \;\leq\; l + 5 \end{aligned}$$

We get:

$$\begin{aligned} \lceil\sqrt{2h+\frac{41}{4}}+\frac{1}{2}\rceil &= l+5 \\ \Leftrightarrow\ 2\lceil\sqrt{2h+\frac{41}{4}}+\frac{1}{2}\rceil-1 &= 2l+9 \ = \ b(S^{\text{hex}}_{h,2,0,1}) \end{aligned}$$

Thus we have shown

$$b(S^{\text{hex}}_{h,2,0,1}) \ = \ 2\lceil\sqrt{2h+\frac{41}{4}}+\frac{1}{2}\rceil-1\ .$$

□

3.2.2 General disordered hexagon-patches

In the second main section of this chapter, we are going to investigate minimal boundary lengths of triangular patches. There we want to make use of the 'duality' between triangle- and hexagon-patches and apply the formulas for disordered hexagon-patches that were given in the previous subsection to the inner duals of triangle-patches in order to derive new relations for triangle-patches. However, the inner dual of a triangle-patch is not necessarily 2-connected. For this reason we want to show now that the established bounds on the boundary length of disordered hexagon-patches are still correct if we omit the requirement to be 2-connected. Therefore we define disordered hexagon-patches that are connected but not necessarily 2-connected:

Definition 3.2.4 *A* general disordered hexagon-patch *is a connected plane graph P with one distinguished face (the* outer face*), all vertices not lying in the outer face (*inner vertices*) of degree* 3*, and all vertices that lie in the outer face (*boundary vertices*) of degree* 2 *or* 3*. Again all faces different from the outer face are called* bounded faces*, and all bounded faces that are no hexagons are called* defective faces*. Edges lying in the outer face are called* boundary edges*, and the set of boundary edges in P is denoted by $E_b(P)$. A* bridge *in P is an edge $e \in E(P)$ such that $P-\{e\}$ is not connected.*

We define the boundary length *of a general disordered hexagon-patch P as the number of boundary edges but with bridges counted twice, and denote it by $b(P)$:*

$$b(P) \ := \ |\{e \in E_b(P)\}| + |\{e \in E_b(P) : e \text{ is bridge in } P\}|$$

A general disordered hexagon-patch with exactly p pentagons, s squares, t triangles and no other defective faces will be called general (p,s,t)-hexagon-patch*. A general (p,s,t)-hexagon-patch with h hexagons is called* boundary-minimal *if it has minimal boundary length among all general (p,s,t)-hexagon-patches with h hexagons.*

The following lemma implies that the bounds on the boundary length of (p,s,t)-hexagon-patches that we obtain from table 3.1 also hold for general (p,s,t)-hexagon-patches.

Lemma 3.2.5 *A general (p, s, t)-hexagon-patch with $D(p, s, t) \leq 6$ that is boundary-minimal is 2-connected.*

PROOF:

Assume that P is a general (p, s, t)-hexagon-patch with $D(p, s, t) \leq 6$ that is boundary-minimal but not 2-connected. Since all vertices have degree at most 3, the existence of a cutvertex implies the existence of a bridge; so P contains at least one bridge. Let b be the number of bridges in P and remove all these bridges. Then the resulting graph consists only of 2-connected patches. Choose two of them and denote them by C^1 and C^2. Suppose that C^i is a (p^i, s^i, t^i)-hexagon-patch for $i = 1, 2$, and let d_j^i be the number of boundary vertices with degree j in C^i. By lemma 3.2.2 we have:

$$d_2^i - d_3^i = 6 - D(p^i, s^i, t^i)$$

In case $D(p^i, s^i, t^i) \leq 5$ this implies that there must be two succeeding vertices of degree 2 in the boundary cycle of C^i. If this holds for both $i = 1$ and $i = 2$, we may glue C^1 and C^2 together by choosing two succeeding boundary vertices of degree 2 for both and identifying the two edges between the degree 2 vertices.

Otherwise we must have w.l.o.g. $D(p^1, s^1, t^1) = 6$ and $D(p^2, s^2, t^2) = 0$, and may assume that in C^1 the boundary vertices of degree 2 and 3 are alternating. Then C^2 consists only of hexagons. We take *all* these hexagons of C^2 and arrange them around C^1 in rings (see figure 3.7) – this extends the boundary length of C^1 by at most 2, while the boundary length of C^2 must have been at least 6.

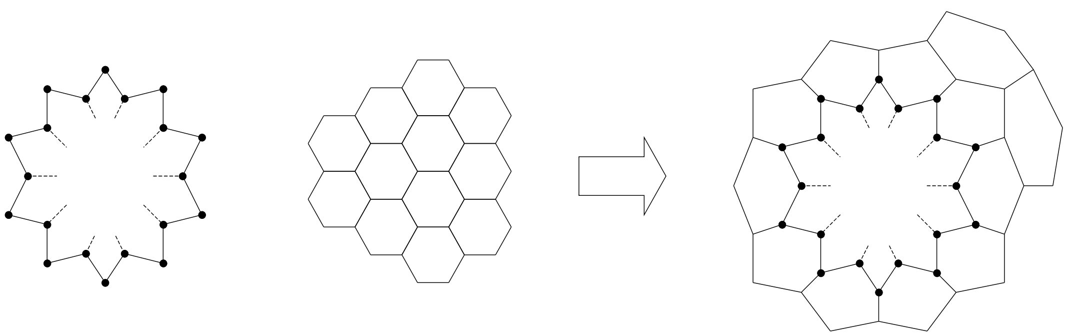

Figure 3.7: An example of the case where the boundary of C^1 contains the same number of degree 2 and degree 3 vertices such that the vertices are alternating (left) and C^2 consists only of hexagons (middle); then the faces can be rearranged to one patch whose boundary length is smaller than the sum of the boundary lengths of C^1 and C^2 (right).

In both cases the total boundary length has been reduced. Now we may join the single components by inserting one bridge between two different components again (this is possible since each component contains at least two vertices of degree 2) – the total boundary length is still smaller than in the beginning. Hence P could not have been boundary-minimal.

□

3.3 The boundary length of disordered triangle-patches

This section contains various results on the boundary length of disordered triangle-patches. Basically we are interested in disordered triangle-patches where, apart from the inner vertices of degree 6, only p defective vertices of degree 5 are allowed – that means, with the notation introduced in chapter 2, p-patches.

At first we deduce formulas for lower bounds on the boundary length of a p-patch with $p \leq 6$ relative to its number of faces by applying the known formulas for the hexagonal case to the dual (subsection 3.3.1). Afterwards, we define *spirals* as special disordered triangle-patches (subsection 3.3.2) and compute their boundary lengths (subsection 3.3.3), which turn out to be exactly the lower bounds established before, implying that spirals are triangle-patches with minimal boundary length for a given number of faces.

With this we have completely solved the dual cases to those investigated in [3]: We are able to determine the smallest possible boundary length of any p-patch with $p \leq 6$ and n faces – we will provide the exact formulas with respect to n for each $p = 0, \ldots, 6$, which will also be helpful later in this work – and moreover, we may even construct a respective p-patch with n faces where this minimal boundary length is achieved. We will see that in such a patch, the p vertices of degree 5 lie close together in the interior of the patch.

However, for some applications p-patches with minimal boundary length (or the respective boundary formulas) are needed where the vertices of degree 5 may not be placed arbitrarily in the patch, but must lie in fixed positions relative to each other. Then the lower bounds on the boundary lengths that hold for all p-patches may not be precise enough, so we want to determine patches with minimal boundary and derive formulas for the boundary length using the additional information on the 'configurations' of the degree 5 vertices. Similarly to chapter 2, we deal with these configurations by considering fixed subpatches that contain the defective vertices. Hence the task that arises is to determine p-patches with minimal boundary length that contain a certain number of faces and a given p-patch as a subgraph.

In subsection 3.3.4 we solve this task in case the subgraph has a boundary of a particular type; subsection 3.3.5 contains a further generalization, where also parts of chapter 2 are used. The proof of the main theorem in subsection 3.3.4 can be reduced to the results from the subsections before by replacing the subgraph by a different subgraph where the defective vertices lie 'closer together'. But it turns out that for the cases $p = 2$, $p = 3$ and $p = 4$, not all subgraphs can be replaced by an appropriate p-patch such that the previous results can be applied, because there exist two different types of boundaries. This problem can be solved by proving the first mentioned results on the minimal boundary length of triangle-patches (subsections 3.3.1 and 3.3.3) not only for the cases with p defective vertices of degree 5, but also for three further cases – representing the respective other boundary type – where also defective vertices with degree 4 are allowed.

For this reason, we consider in the following not only p-patches, but in a more general way disordered triangle-patches with p defective vertices of degree 5, s defective vertices of degree 4, and t defective vertices of degree 3, and carry out the computations in the next subsections for the cases with $s = t = 0$ as well as for the three further cases. For the sake of completeness we even give in table 3.2 all formulas of minimal boundaries for all possible cases that allow to build spirals of unlimited size (these are the cases with $p + 2s + 3t \leq 6$ that occur already in the last section – compare also table 3.1).

3.3.1 Lower bounds on the boundary length of triangle-patches

One result of [27] is that a 2-connected patch with all bounded faces triangles and all inner vertices of degree 6 which is subgraph of the triangular lattice (a so-called *triangular animal*) has a minimal number of edges – and with this also a minimal boundary length – if the triangles are arranged in a spiral fashion. This follows with the help of a formula that determines a lower bound on the number of edges, which in turn is proven by applying a similar formula for hexagonal patches to the inner dual of the triangular animal.

In this subsection we are using a similar technique to transfer the results on the boundary length of disordered hexagon-patches that have been discussed in the previous section to the dual, that is to triangle-patches which may contain inner vertices of degree 3, 4, 5 and 6 and are not necessarily subgraph of a lattice.

The following pages deal with triangle-patches that contain only inner vertices of degree 5 and 6 (p-patches), and hence can be seen as a translation of the results of [3] to the dual. We develop bounds on the boundary length of such patches for each of the different cases with $p = 0, \ldots, 6$ vertices of degree 5 that are summarized in theorem 3.3.2; later on we will show that these inequations are fulfilled as equalities if the patches are also of a spiral type.

Of the more general cases that allow also inner vertices of degree 3 and 4, we actually need only three for the later application, where defective vertices of degree 5 and 4 occur. We also establish bounds on the boundary length for these cases, which can be found in theorem 3.3.5. Again, we will see later that certain spirals fulfill these formulas as equalities.

A disordered triangle-patch has already been defined in section 2.2 to be a 2-connected plane graph P where all faces are triangles except the outer face, and all vertices that lie in the outer face have degree at most 6. Arbitrary inner vertices with degree different from 6 (defective vertices) have been allowed.

Now we focus on those disordered triangle-patches where only defective vertices of degree 5, 4, and 3 occur – similarly to the sizes of the defective faces in the previous section. For these we continue applying the notation that has already been introduced in definition 2.2.1.

Definition 3.3.1 *A disordered triangle-patch with exactly p inner vertices of degree 5, s inner vertices of degree 4, and t inner vertices of degree 3 is called a* (p, s, t)-triangle-patch, *or just* (p, s, t)-patch.

In accordance to definition 2.2.1, a $(p, 0, 0)$-patch is also denoted as p-patch.

For $p, s, t \in \mathbb{N}_0$ we let

$$D(p, s, t) := p + 2s + 3t \,.$$

The inner dual *of P is defined as the dual of P with the vertex corresponding to the outer face removed. It will be denoted as P^*.*

In the following we will deduce some formulas establishing connections between different sizes that occur in (p, s, t)-patches, which will prove helpful afterwards when determining lower bounds on the boundary lengths for the different cases of (p, s, t) with the help of the dual results.

We let P be a (p,s,t)-patch with n bounded faces. If q denotes the number of inner edges and e the total number of edges in P, we get by summing up the edges of all bounded faces separately

$$3n = e + q \tag{3.1}$$

and hence for the boundary length of P:

$$b(P) = e - q = 3n - 2q \tag{3.2}$$

Now consider the inner dual P^* of P. Then P^* is a general (p,s,t)-hexagon-patch with n vertices and q edges. Let h be its number of hexagons, and q_i the number of edges that lie in i bounded faces. Then we have

$$q = q_0 + q_1 + q_2 \ , \tag{3.3}$$

$$b(P^*) = 2q_0 + q_1 \ , \tag{3.4}$$

and by counting the edges of the bounded faces:

$$6h + 5p + 4s + 3t = q_1 + 2q_2 \tag{3.5}$$

With this we get

$$b(P^*) \overset{(3.4)}{=} 2q_0 + q_1 \overset{(3.3)}{=} 2q - (q_1 + 2q_2) \overset{(3.5)}{=} 2q - (6h + 5p + 4s + 3t) \ . \tag{3.6}$$

Euler's formula applied to P^* yields

$$n - q + h + p + s + t = 1 \quad \Leftrightarrow \quad h = 1 - n + q - p - s - t \ . \tag{3.7}$$

From (3.2) we get $q = \frac{3}{2}n - \frac{1}{2}b(P)$; inserting this into (3.7) we obtain

$$\begin{aligned} h &= 1 - n + \big(\frac{3}{2}n - \frac{1}{2}b(P)\big) - p - s - t \\ &= \frac{1}{2}n - \frac{1}{2}b(P) - p - s - t + 1 \end{aligned} \tag{3.8}$$

and furthermore by inserting (3.7) into (3.6):

$$\begin{aligned} b(P^*) &= 2q - 6(1 - n + q - p - s - t) - 5p - 4s - 3t \\ &= 6n - 4q - 6 + p + 2s + 3t \\ &= 6n - 4q - \big(6 - D(p,s,t)\big) \end{aligned} \tag{3.9}$$

Now inserting (3.2) into (3.9) yields:

$$b(P^*) = 2b(P) - \big(6 - D(p,s,t)\big) \tag{3.10}$$

$$\Rightarrow \ \frac{1}{4}b(P^*)^2 = \Big(b(P) - \frac{6 - D(p,s,t)}{2}\Big)^2$$

$$\Leftrightarrow \ b(P)^2 = \frac{1}{4}b(P^*)^2 + \big(6 - D(p,s,t)\big)\, b(P) - \frac{\big(6 - D(p,s,t)\big)^2}{4} \tag{3.11}$$

At first we let P be a (p, s, t)-patch P with $s = t = 0$, that means P is a p-patch. We distinguish the different cases $p = 0, 1, \ldots, 6$ and determine a lower bound on the boundary length relative to the number n of bounded faces for the respective case.

The case p=0

Assume we have a 0-patch P with inner dual P^*. According to [3] (see also theorem 3.2.3 and table 3.1), the boundary length of the spiral $S^{\text{hex}}_{h,0,0,0}$ consisting of h hexagons is given by

$$b(S^{\text{hex}}_{h,0,0,0}) \;=\; 2\lceil\sqrt{12h-3}\,\rceil\;.$$

Since this is the minimal boundary length that a $(0, 0, 0)$-hexagon-patch can obtain, the formula gives us a bound on the boundary length of any $(0, 0, 0)$-hexagon-patch. By lemma 3.2.5, a general $(0, 0, 0)$-hexagon-patch that is not 2-connected cannot be boundary-minimal, so the bound holds also for general $(0, 0, 0)$-hexagon-patches – in particular for P^*. We obtain

$$\begin{aligned} b(P^*) &\;\geq\; 2\lceil\sqrt{12h-3}\,\rceil \\ \Rightarrow\; b(P^*) &\;\geq\; 2\sqrt{12h-3} \\ &\stackrel{(3.8)}{=}\; 2\sqrt{6n-6b(P)+9} \end{aligned} \tag{3.12}$$

and hence

$$\begin{aligned} b(P)^2 &\stackrel{(3.11)}{=} \frac{1}{4}\,b(P^*)^2 + 6\,b(P) - \frac{36}{4} \\ &\stackrel{(3.12)}{\geq} (6n-6b(P)+9) + 6\,b(P) - 9 \\ &= 6n \\ \Rightarrow\; b(P) &\geq \sqrt{6n} \end{aligned} \tag{3.13}$$

This can even be improved by using (3.2) and the fact that certain variables are integers: We have

$$2\,(2n-q)-n \;=\; 3n-2q \;\stackrel{(3.2)}{=}\; b(P) \;\stackrel{(3.13)}{\geq}\; \sqrt{6n} \;=\; 2\,(\frac{1}{2}(n+\sqrt{6n}))-n\;,$$

and since $q, n \in \mathbb{N}$ (and hence $2n - q \in \mathbb{N}$) this implies

$$b(P) \;\geq\; 2\,\lceil\frac{1}{2}(n+\sqrt{6n})\rceil - n\;. \tag{3.14}$$

The case p=1

Now consider a 1-patch P with inner dual P^*. Then P^* is a general $(1, 0, 0)$-hexagon-patch. The boundary length of the spiral $S^{\text{hex}}_{h,1,0,0}$ consisting of h hexagons and 1 pentagon is

$$b(S^{\text{hex}}_{h,1,0,0}) \;=\; 2\lceil\sqrt{10h+\frac{25}{4}}+\frac{1}{2}\rceil - 1\;.$$

With the minimality and lemma 3.2.5 this gives us a bound on the boundary length of P^*, so we have

$$\begin{aligned} b(P^*) &\geq 2\lceil\sqrt{10h+\frac{25}{4}}+\frac{1}{2}\rceil - 1 \\ \Rightarrow b(P^*) &\geq 2\left(\sqrt{10h+\frac{25}{4}}+\frac{1}{2}\right) - 1 \\ &= 2\sqrt{10h+\frac{25}{4}} \\ &\overset{(3.8)}{=} 2\sqrt{5n-5b(P)+\frac{25}{4}} \end{aligned} \tag{3.15}$$

and hence, by inserting this into (3.11):

$$\begin{aligned} b(P)^2 &\overset{(3.11)}{=} \frac{1}{4}\,b(P^*)^2 + 5\,b(P) - \frac{25}{4} \\ &\overset{(3.15)}{\geq} (5n-5b(P)+\frac{25}{4}) + 5\,b(P) - \frac{25}{4} \\ &= 5n \\ \Rightarrow b(P) &\geq \sqrt{5n} \end{aligned} \tag{3.16}$$

Again this can still be improved: We have

$$2\,(2n-q)-n \;=\; 3n-2q \overset{(3.2)}{=} b(P) \overset{(3.16)}{\geq} \sqrt{5n} \;=\; 2\,(\frac{1}{2}(n+\sqrt{5n}))-n$$

which yields because of $q, n \in \mathbb{N}$

$$b(P) \;\geq\; 2\,\lceil\frac{1}{2}(n+\sqrt{5n})\rceil - n\;. \tag{3.17}$$

The case p=2

Now let P be a 2-patch and P^* its inner dual, a general $(2,0,0)$-hexagon-patch. The boundary length of the spiral $S^{\text{hex}}_{h,2,0,0}$ with h hexagons and 2 pentagons is

$$b(S^{\text{hex}}_{h,2,0,0}) \;=\; 2\lceil\sqrt{8h+16}\rceil\;,$$

and this is the minimal boundary length that a $(2,0,0)$-hexagon-patch with h hexagons – and by lemma 3.2.5 also a general $(2,0,0)$-hexagon-patch with h hexagons – can obtain. Hence we have

$$\begin{aligned} b(P^*) &\geq 2\lceil\sqrt{8h+16}\rceil \\ \Rightarrow b(P^*) &\geq 2\sqrt{8h+16} \\ &\overset{(3.8)}{=} 2\sqrt{4n-4b(P)+8} \end{aligned} \tag{3.18}$$

which implies

$$\begin{aligned} b(P)^2 &\overset{(3.11)}{=} \frac{1}{4}\, b(P^*)^2 + 4\, b(P) - 4 \\ &\overset{(3.18)}{\geq} (4n - 4b(P) + 8) + 4b(P) - 4 \\ &= 4n + 4 \\ \Rightarrow\ b(P) &\geq \sqrt{4n+4} \end{aligned} \tag{3.19}$$

With this we get

$$2\,(2n - q) - n \ = \ 3n - 2q \overset{(3.2)}{=} b(P) \overset{(3.19)}{\geq} \sqrt{4n+4} \ = \ 2\,(\frac{1}{2}(n + \sqrt{4n+4})) - n$$

and hence because of $q, n \in \mathbb{N}$:

$$b(P) \ \geq \ 2\,\lceil \frac{1}{2}(n + \sqrt{4n+4}) \rceil - n\ . \tag{3.20}$$

The case p=3

If P is a 3-patch, the inner dual P^* is a general $(3, 0, 0)$-hexagon-patch. For the spiral $S^{\text{hex}}_{h,3,0,0}$ with h hexagons and 3 pentagons we have the boundary length

$$b(S^{\text{hex}}_{h,3,0,0}) \ = \ 2\lceil \sqrt{6h + \frac{81}{4}} + \frac{1}{2} \rceil - 1\ ,$$

and with the minimality of the boundary length and lemma 3.2.5 we get:

$$\begin{aligned} b(P^*) &\geq 2\,\lceil \sqrt{6h + \frac{81}{4}} + \frac{1}{2} \rceil - 1 \\ \Rightarrow\ b(P^*) &\geq 2\left(\sqrt{6h + \frac{81}{4}} + \frac{1}{2}\right) - 1 \\ &= 2\sqrt{6h + \frac{81}{4}} \\ &\overset{(3.8)}{=} 2\sqrt{3n - 3b(P) + \frac{33}{4}} \end{aligned} \tag{3.21}$$

This implies

$$\begin{aligned} b(P)^2 &\overset{(3.11)}{=} \frac{1}{4}\, b(P^*)^2 + 3b(P) - \frac{9}{4} \\ &\overset{(3.21)}{\geq} (3n - 3b(P) + \frac{33}{4}) + 3b(P) - \frac{9}{4} \\ &= 3n + 6 \\ \Rightarrow\ b(P) &\geq \sqrt{3n+6} \end{aligned} \tag{3.22}$$

Hence we have

$$2\,(2n - q) - n \ = \ 3n - 2q \overset{(3.2)}{=} b(P) \overset{(3.22)}{\geq} \sqrt{3n+6} \ = \ 2\,(\frac{1}{2}(n + \sqrt{3n+6})) - n$$

and with $q, n \in \mathbb{N}$

$$b(P) \;\geq\; 2\left\lceil \frac{1}{2}(n + \sqrt{3n+6})\right\rceil - n \; . \tag{3.23}$$

The case p=4

Now let P be a 4-patch with dual P^*, a general $(4,0,0)$-hexagon-patch. The boundary length of the spiral $S^{\text{hex}}_{h,4,0,0}$ is

$$b(S^{\text{hex}}_{h,4,0,0}) \;=\; 2\lceil\sqrt{4h+25}\rceil \; .$$

Since the spiral has minimal boundary length, we get with lemma 3.2.5 a bound for the boundary length of P^*:

$$\begin{aligned} b(P^*) &\;\geq\; 2\lceil\sqrt{4h+25}\rceil \\ \Rightarrow\; b(P^*) &\;\geq\; 2\sqrt{4h+25} \\ &\overset{(3.8)}{=}\; 2\sqrt{2n - 2b(P) + 13}\; . \end{aligned} \tag{3.24}$$

We obtain

$$\begin{aligned} b(P)^2 &\overset{(3.11)}{=} \frac{1}{4}\, b(P^*)^2 + 2b(P) - 1 \\ &\overset{(3.24)}{\geq} (2n - 2b(P) + 13) + 2b(P) - 1 \\ &= 2n + 12 \\ \Rightarrow\; b(P) &\geq \sqrt{2n+12} \end{aligned} \tag{3.25}$$

and

$$2\,(2n-q) - n \;=\; 3n - 2q \overset{(3.2)}{=} b(P) \overset{(3.25)}{\geq} \sqrt{2n+12} \;=\; 2\,(\frac{1}{2}\,(n + \sqrt{2n+12})) - n$$

which yields because of $q, n \in \mathbb{N}$:

$$b(P) \;\geq\; 2\left\lceil \frac{1}{2}\,(n + \sqrt{2n+12})\right\rceil - n \tag{3.26}$$

The case p=5

If P is a 5-patch, its inner dual P^* is a general $(5,0,0)$-hexagon-patch. We have

$$b(S^{\text{hex}}_{h,5,0,0}) \;=\; 2\left\lceil\sqrt{2h + \frac{113}{4}} + \frac{1}{2}\right\rceil - 1\; ,$$

and by using the minimality of the spiral's boundary length and applying again lemma 3.2.5 we get the corresponding bound for the inner dual P^*:

$$\begin{aligned} b(P^*) &\;\geq\; 2\left\lceil\sqrt{2h + \frac{113}{4}} + \frac{1}{2}\right\rceil - 1 \\ \Rightarrow\; b(P^*) &\;\geq\; 2\left(\sqrt{2h + \frac{113}{4}} + \frac{1}{2}\right) - 1 \\ &\;=\; 2\sqrt{2h + \frac{113}{4}} \\ &\overset{(3.8)}{=}\; 2\sqrt{n - b(P) + \frac{81}{4}} \end{aligned} \tag{3.27}$$

This implies

$$\begin{aligned} b(P)^2 &\overset{(3.11)}{=} \frac{1}{4}\,b(P^*)^2 + b(P) - \frac{1}{4} \\ &\overset{(3.27)}{\geq} (n - b(P) + \frac{81}{4}) + b(P) - \frac{1}{4} \\ &= n + 20 \\ \Rightarrow \quad b(P) &\geq \sqrt{n+20} \end{aligned} \tag{3.28}$$

and hence

$$2\,(2n-q) - n \;=\; 3n - 2q \overset{(3.2)}{=} b(P) \overset{(3.28)}{\geq} \sqrt{n+20} \;=\; 2\,(\frac{1}{2}(n + \sqrt{n+20})) - n\;.$$

With $q, n \in \mathbb{N}$ we obtain

$$b(P) \;\geq\; 2\,\lceil \frac{1}{2}(n + \sqrt{n+20}) \rceil - n\;. \tag{3.29}$$

The case p=6

Finally let P be a 6-patch and P^* its inner dual, a general $(6,0,0)$-hexagon-patch. We have for the spiral $S^{\text{hex}}_{h,6,0,0}$ with h hexagons and 6 pentagons:

$$b(S^{\text{hex}}_{h,6,0,0}) \;=\; \begin{cases} 10 & \text{if } \frac{h}{5} \in \mathbb{N}_0 \\ 12 & \text{else} \end{cases}$$

Due to the minimality of its boundary length and lemma 3.2.5 we get

$$b(P^*) \;\geq\; \begin{cases} 10 & \text{if } \frac{h}{5} \in \mathbb{N}_0 \\ 12 & \text{else}\;. \end{cases}$$

This yields

$$b(P) \overset{(3.10)}{=} \frac{1}{2}\,b(P^*) \;\geq\; \begin{cases} 5 & \text{if } \frac{h}{5} \in \mathbb{N}_0 \\ 6 & \text{else} \end{cases}$$

and hence

$$2\,(2n-q) - n \;=\; 3n - 2q \overset{(3.2)}{=} b(P) \;\geq\; 5 \;=\; 2\,(\frac{1}{2}(n+5)) - n\;.$$

Since $q, n \in \mathbb{N}$ we get

$$b(P) \;\geq\; 2\,\lceil \frac{1}{2}(n+5) \rceil - n\;. \tag{3.30}$$

In case n is even, $n+5$ is odd so we have

$$\lceil \frac{1}{2}(n+5) \rceil = \frac{1}{2}(n+6)$$

and hence (3.30) implies

$$b(P) \;\geq\; 2\,(\frac{1}{2}(n+6)) - n \;=\; 6\;.$$

Now assume we have $b(P) = 5$. Then $\frac{h}{5} \in \mathbb{N}_0$ must hold, that means there is $k \in \mathbb{N}$ with $h = 5(k-1)$. In that case we get with (3.8)

$$\begin{aligned} 5(k-1) &= h \overset{(3.8)}{=} \frac{1}{2}n - \frac{1}{2}b(P) - 5 \;=\; \frac{1}{2}n - \frac{15}{2} \\ \Leftrightarrow\; n &= 5 + 10k \end{aligned}$$

and hence $n \in \{5 + 10k \mid k \in \mathbb{N}\}$.

Consequently, in case n is odd and $n \notin \{5 + 10k \mid k \in \mathbb{N}\}$ we cannot have $b(P) = 5$. So $b(P) \geq 6$ must hold and we get

$$2\,(2n - q) - n \;=\; 3n - 2q \;\overset{(3.2)}{=}\; b(P) \;\geq\; 6 \;=\; 2\,(\frac{1}{2}(n+6)) - n$$

and because of $q, n \in \mathbb{N}$

$$b(P) \;\geq\; 2\,\lceil \frac{1}{2}(n+6) \rceil - n\,. \tag{3.31}$$

For odd n (and hence odd $n+6$) we have

$$\lceil \frac{1}{2}(n+6) \rceil = \frac{1}{2}(n+7)$$

so (3.31) implies

$$b(P) \;\geq\; 2\,(\frac{1}{2}(n+7)) - n \;=\; 7\,.$$

We obtain:

$$b(P) \;\geq\; \begin{cases} 6 & \text{if } n \text{ is even} \\ 7 & \text{if } n \text{ is odd and } n \notin \{5+10k \mid k \in \mathbb{N}\} \\ 5 & \text{else}\,. \end{cases} \tag{3.32}$$

Summing up all cases we get the following theorem:

Theorem 3.3.2 *Given a p-patch P with n faces. Then we have*

- *in case $p = 0$:* $\quad b(P) \;\geq\; 2\,\lceil \frac{1}{2}(n + \sqrt{6n}) \rceil - n$
- *in case $p = 1$:* $\quad b(P) \;\geq\; 2\,\lceil \frac{1}{2}(n + \sqrt{5n}) \rceil - n$
- *in case $p = 2$:* $\quad b(P) \;\geq\; 2\,\lceil \frac{1}{2}(n + \sqrt{4n+4}) \rceil - n$
- *in case $p = 3$:* $\quad b(P) \;\geq\; 2\,\lceil \frac{1}{2}(n + \sqrt{3n+6}) \rceil - n$
- *in case $p = 4$:* $\quad b(P) \;\geq\; 2\,\lceil \frac{1}{2}\,(n + \sqrt{2n+12}) \rceil - n$
- *in case $p = 5$:* $\quad b(P) \;\geq\; 2\,\lceil \frac{1}{2}(n + \sqrt{n+20}) \rceil - n$
- *in case $p = 6$:* $\quad b(P) \;\geq\; \begin{cases} 6 & \textit{if } n \textit{ is even} \\ 7 & \textit{if } n \textit{ is odd and } n \notin \{5+10k \mid k \in \mathbb{N}\} \\ 5 & \textit{else}\,. \end{cases}$

The improvement of the first obtained inequations for each p with the help of the ceiling function to the formulas listed in theorem 3.3.2 is important because, as we will see in the next subsection, these formulas are sharp for certain patches. However, for other applications the weaker inequations will be useful (they have the advantage that the formulas on the right hand side are monotonously increasing in the number of faces), so we want to sum them up here as well:

Corollary 3.3.3 *For any p-patch P with* $0 \le p \le 5$ *we have*

- $b(P) \ge \sqrt{6f(P)}$ *in case* $p = 0$ (3.13)*;*
- $b(P) \ge \sqrt{5f(P)}$ *in case* $p = 1$ (3.16)*;*
- $b(P) \ge \sqrt{4f(P)+4} \ge \sqrt{4f(P)}$ *in case* $p = 2$ (3.19)*;*
- $b(P) \ge \sqrt{3f(P)+6} \ge \sqrt{3f(P)}$ *in case* $p = 3$ (3.22)*;*
- $b(P) \ge \sqrt{2f(P)+12} \ge \sqrt{2f(P)}$ *in case* $p = 4$ (3.25)*;*
- $b(P) \ge \sqrt{f(P)+20} \ge \sqrt{f(P)}$ *in case* $p = 5$ (3.28)*.*

Moreover, we obtain the following useful corollary:

Corollary 3.3.4 *For any p-patch P with* $0 \le p \le 5$ *we have*

$$b(P) \ge \sqrt{(6-p)f(P)} \tag{3.33}$$

$$\text{and} \qquad f(P) \le \frac{b(P)^2}{6-p}\,. \tag{3.34}$$

PROOF:

While (3.33) follows immediately from the formulas given in corollary 3.3.3, the second inequation (3.34) is obtained from (3.33) by taking the square.

□

Thus, we have not only proven lower bounds on the boundary length of a given p-patch with respect to its number of faces, but with (3.34) – at least for the cases $0 \le p \le 5$ – also upper bounds on the number of faces relative to a given boundary length. This result will prove useful later on.

Now, as already explained in the beginning of this section, for the application in subsection 3.3.4 we have to extend the investigation of the boundary length of disordered triangle-patches to cases where not only defective vertices of degree 5, but also of degree 4 are allowed. Therefore we will now consider (p, s, t)-triangle-patches for three further cases – we will see later that they correspond to the boundary types that are missing so far – and that are the cases $(p,s,t) = (0,1,0)$, $(p,s,t) = (1,1,0)$, and $(p,s,t) = (2,1,0)$.

For this, we need the following formulas for a general (p,s,t)-hexagon-patch P^* with h hexagons that follow by theorem 3.2.3 and lemma 3.2.5:

1. In case $(p,s,t) = (0,1,0)$:

$$b(P^*) \;\geq\; 2\lceil\sqrt{8h+4}\rceil \tag{3.35}$$

2. In case $(p,s,t) = (1,1,0)$:

$$b(P^*) \;\geq\; 2\lceil\sqrt{6h+\frac{49}{4}}+\frac{1}{2}\rceil - 1 \tag{3.36}$$

3. In case $(p,s,t) = (2,1,0)$:

$$b(P^*) \geq 2\lceil\sqrt{4h+16}\rceil \tag{3.37}$$

The case (p,s,t)=(0,1,0)

At first consider a $(0,1,0)$-patch P with inner dual P^*. Then P^* is a general $(0,1,0)$-hexagon-patch, so we have by (3.35)

$$\begin{aligned} b(P^*) &\;\geq\; 2\lceil\sqrt{8h+4}\,\rceil \\ \Rightarrow\; b(P^*) &\;\geq\; 2\sqrt{8h+4} \\ &\overset{(3.8)}{=}\; 2\sqrt{4n-4b(P)+4} \end{aligned} \tag{3.38}$$

and hence

$$\begin{aligned} b(P)^2 &\overset{(3.11)}{=} \frac{1}{4}\,b(P^*)^2 + 4b(P) - 4 \\ &\geq (4n - 4b(P) + 4) + 4b(P) - 4 \\ &= 4n \\ \Rightarrow\; b(P) &\geq \sqrt{4n}\,. \end{aligned} \tag{3.39}$$

It follows that

$$2\,(2n-q) - n \;=\; 3n - 2q \overset{(3.2)}{=} b(P) \overset{(3.39)}{\geq} \sqrt{4n} \;=\; 2\,(\frac{1}{2}(n+\sqrt{4n})) - n\,,$$

and as $q, n \in \mathbb{N}$ holds, this implies

$$b(P) \;\geq\; 2\,\lceil\frac{1}{2}(n+\sqrt{4n})\rceil - n\,. \tag{3.40}$$

The case (p,s,t)=(1,1,0)

Now assume P is a $(1,1,0)$-patch and P^* its inner dual. Then we have with (3.36)

$$\begin{aligned} b(P^*) &\geq 2\lceil\sqrt{6h+\frac{49}{4}}+\frac{1}{2}\rceil-1 \\ \Rightarrow\ b(P^*) &\geq 2\sqrt{6h+\frac{49}{4}} \\ &\stackrel{(3.8)}{=} 2\sqrt{3n-3b(P)+\frac{25}{4}} \end{aligned} \tag{3.41}$$

and hence

$$\begin{aligned} b(P)^2 &\stackrel{(3.11)}{=} \frac{1}{4}\,b(P^*)^2+3b(P)-\frac{9}{4} \\ &\geq (3n-3b(P)+\frac{25}{4})+3b(P)-\frac{9}{4} \\ &= 3n+4 \\ \Rightarrow\ b(P) &\geq \sqrt{3n+4} \end{aligned} \tag{3.42}$$

So we get

$$2\,(2n-q)-n \;=\; 3n-2q \;\stackrel{(3.2)}{=}\; b(P) \;\stackrel{(3.42)}{\geq}\; \sqrt{3n+4} \;=\; 2\,(\frac{1}{2}(n+\sqrt{3n+4}))-n\;,$$

and with $q,n\in\mathbb{N}$

$$b(P)\;\geq\;2\,\lceil\frac{1}{2}(n+\sqrt{3n+4})\rceil-n\;. \tag{3.43}$$

The case (p,s,t)=(2,1,0)

Finally suppose we have a $(2,1,0)$-patch P with inner dual P^*. Then by (3.37) we have

$$\begin{aligned} b(P^*) &\geq 2\lceil\sqrt{4h+16}\rceil \\ \Rightarrow\ b(P^*) &\geq 2\sqrt{4h+16} \\ &\stackrel{(3.8)}{=} 2\sqrt{2n-2b(P)+8} \end{aligned} \tag{3.44}$$

and hence

$$\begin{aligned} b(P)^2 &\stackrel{(3.11)}{=} \frac{1}{4}\,b(P^*)^2+2b(P)-1 \\ &\geq (2n-2b(P)+8)+2b(P)-1 \\ &= 2n+7 \\ \Rightarrow\ b(P) &\geq \sqrt{2n+7} \end{aligned} \tag{3.45}$$

We obtain

$$2\,(2n-q)-n \;=\; 3n-2q \;\stackrel{(3.2)}{=}\; b(P) \;\stackrel{(3.45)}{\geq}\; \sqrt{2n+7} \;=\; 2\,(\frac{1}{2}(n+\sqrt{2n+7}))-n\;,$$

and since $q, n \in \mathbb{N}$

$$b(P) \ \geq \ 2\lceil \frac{1}{2}(n + \sqrt{2n+7}) \rceil - n \ . \tag{3.46}$$

So we have proven the following theorem:

Theorem 3.3.5 *Given a (p,s,t)-patch P with n faces. We have*

- *in case* $(p,s,t) = (0,1,0)$: $\quad b(P) \ \geq \ 2\lceil \frac{1}{2}(n + \sqrt{4n}) \rceil - n$
- *in case* $(p,s,t) = (1,1,0)$: $\quad b(P) \ \geq \ 2\lceil \frac{1}{2}(n + \sqrt{3n+4}) \rceil - n$
- *in case* $(p,s,t) = (2,1,0)$: $\quad b(P) \ \geq \ 2\lceil \frac{1}{2}(n + \sqrt{2n+7}) \rceil - n$

3.3.2 Spirals

In the previous subsection we have established lower bounds on the boundary length of disordered triangle-patches in terms of their numbers of faces. However, we do not know yet if these bounds can still be improved or if there exist patches that fulfill the proven inequations as equalities. In the following we will show that the latter is the case: There are indeed (p,s,t)-triangle-patches whose boundary lengths are equal to the given lower bounds, which implies that they have minimal boundary length among all (p,s,t)-patches with the same number of faces.

Similar to the hexagonal case, those patches are obtained by arranging the faces in a spiral way; however, the situation is a bit different because now we do not have defective faces, but defective vertices. The spirals that we will define consist of a fixed basic patch that contains the defective vertices, and further triangles that are built around that patch in a certain spiral way.

In this section, we will first show some helpful properties of (p,s,t)-patches, then we come to the spiral definition. In the section afterwards we will determine the boundary length of certain spirals which will turn out to be minimal.

Definition 3.3.6 *Given a (p,s,t)-triangle-patch P. As before, we denote the set of vertices by $V(P)$, the set of edges by $E(P)$, and the set of bounded faces by $F(P)$. The set of boundary vertices in P is denoted by $V_b(P)$, the set of inner vertices by $V_i(P)$, and the number of inner vertices by $v_i(P) := |V_i(P)|$.*

A boundary face *is defined as a face that contains at least one boundary vertex. We denote the set of boundary faces of P by $F_b(P)$, and the number of boundary faces in P by $f_b(P) := |F_b(P)|$. A face that is no boundary face and not the outer face is called* inner face*. The set of inner faces of P is denoted by $F_i(P)$ and the number of inner faces by $f_i(P) := |F_i(P)|$. We say two faces are* neighbouring *or* neighbours *if they share a common edge.*

Lemma 3.3.7 *For any (p, s, t)-triangle-patch P we have*

$$\sum_{v \in V_b(P)} (4 - \deg(v)) \;=\; 6 - D(p, s, t) \; .$$

PROOF:

Since for any (p, s, t)-triangle-patch P we have by definition $D(P) = D(p, s, t)$ (compare formula (2.1)), this lemma follows immediately from lemma 2.2.3.

□

Definition 3.3.8 *Given a (p, s, t)-patch P. If there are only boundary vertices of degree 3 and 4, we say P has a* nice boundary*. In case of at least one vertex of degree 3 we call a (possibly closed) path $v_0, \ldots, v_n$ $(n \geq 1)$ of succeeding vertices in the boundary cycle a* side *of P if $\deg(v_0) = \deg(v_n) = 3$ and $\deg(v_i) = 4$ for $0 < i < n$.*

Remark 3.3.9 *Applying lemma 3.3.7, we observe that a (p, s, t)-patch with a nice boundary can only exist for $0 \leq D(p, s, t) \leq 6$, and that its boundary contains exactly $6 - D(p, s, t)$ vertices of degree 3 and $6 - D(p, s, t)$ sides. In case $D(p, s, t) = 6$ it has no degree 3 vertices and no sides at all.*

The following lemma implies that in patches with a nice boundary, all faces can only occur once in the boundary cycle:

Lemma 3.3.10 *Let P be a (p, s, t)-patch with a nice boundary. Then any edge $\{v, w\} \in E(P)$ with $v, w \in V_b(P)$ must be a boundary edge of P (i.e. lies in the outer face).*

PROOF:

For two boundary vertices x, y we denote by $d_b(x, y)$ the length of the path from x to y following the boundary cycle, and define $d_b\{x, y\} := \min\{d_b(x, y), d_b(y, x)\}$.

Now assume the contrary of the statement: Let $\{v, w\} \in E(P)$ with $v, w \in V_b(P)$ be an edge that does not lie in the outer face. W.l.o.g. we may choose $\{v, w\}$ with this property such that $d_b\{v, w\}$ is minimal, that means any edge $\{v', w'\} \in E(P)$ with $v', w' \in V_b(P)$ and $d_b\{v', w'\} < d_b\{v, w\}$ must be a boundary edge.

Since $\{v, w\}$ does not lie in the outer face, it must lie in two bounded faces which we denote by f_1 and f_2 as shown in figure 3.8. Let w' be the third vertex in f_1 and v' the third vertex in f_2. Both faces must have further bounded faces as neigbours because v' or w' would have degree 2. So let f_3 be a further face neigbouring to f_1, w.l.o.g. such that it contains v. Since v is a boundary vertex it has at most degree 4, so it cannot lie in a further bounded face apart from f_2, f_1 and f_3. Hence the neighbouring face f_4 of f_2 must contain the vertex w (see again figure 3.8). Then we have $\deg(v) = \deg(w) = 4$, so the edges $\{w, w'\}$ and $\{v, v'\}$ must be boundary edges, and consequently w' and v' are boundary vertices. But then we have $d_b(v', w) < d_b(v, w)$ and $d_b(w', v) < d_b(w, v)$.

In case $\min\{d_b(v, w), d_b(w, v)\} = d_b(v, w)$ this implies

$$\min\{d_b(v', w), d_b(w, v')\} < \min\{d_b(v, w), d_b(w, v)\}$$

and in case $\min\{d_b(v,w), d_b(w,v)\} = d_b(w,v)$ we get

$$\min\{d_b(v,w'), d_b(w',v)\} < \min\{d_b(v,w), d_b(w,v)\} ;$$

that means either $d_b\{v',w\} < d_b\{v,w\}$ or $d_b\{v,w'\} < d_b\{v,w\}$ holds. Then by assumption, one of the edges $\{v',w\}$ and $\{v,w'\}$ must be a boundary edge. But this is a contradiction since by construction, $\{v',w\}$ lies in the bounded faces f_2 and f_4, $\{v,w'\}$ lies in the bounded faces f_1 and f_3. Consequently, the assumption was wrong and such an edge $\{v,w\}$ cannot exist.

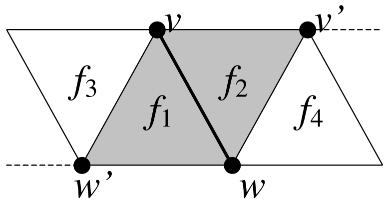

Figure 3.8: The situation in a hypothetical counterexample

□

Definition 3.3.11 *Let P be a (p,s,t)-patch with a nice boundary. A (p,s,t)-patch Q is called the* extension *of P if it contains P, if $F_b(Q) = F(Q) - F(P)$ holds, and if every boundary face in Q has exactly two boundary faces as neighbours (see figure* 3.9 *for an example). Then we write $Q = P^+$ and say Q has been obtained by* adding a ring around *P.*

Furthermore, if for $k \geq 2$ we have (p,s,t)-patches $P_0, P_1, \ldots, P_k$ with $P_i = P_{i-1}^+$ for all $i = 1, \ldots, k$, we define $P_0^{k+} := P_k$ and say P_0^{k+} has been constructed by adding k rings around *P_0. For consistent notation we let $P^{0+} := P$ and $P^{1+} := P^+$. The set of faces in $P^{k+} - P^{(k-1)+}$ $(k \geq 1)$ is called the* kth ring *around P.*

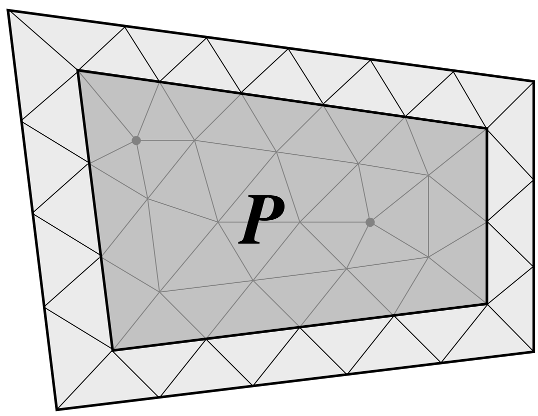

Figure 3.9: An example of a (p,s,t)-patch Q obtained by adding a ring around a (p,s,t)-patch P (in this case we have $(p,s,t) = (2,0,0)$)

Remark 3.3.12 *For any (p, s, t)-patch P with a nice boundary, the extension Q with the properties from definition* 3.3.11 *exists and is uniquely determined, so the notation $Q = P^+$ is justified. Furthermore, Q has a nice boundary, which implies that P^{k+} is well-defined for any $k \in \mathbb{N}$, too.*

PROOF:

The extension Q can be constructed in the following way: At first, we add a triangle to each boundary edge of P by inserting one new vertex for each boundary edge and joining it with both vertices incident to that edge. This way we obtain $b(P)$ new vertices of degree 2 which are alternating in the boundary cycle with the former boundary vertices of P. Let F_1 denote the set of the new faces. The boundary vertices of P with degree 3 now have degree 5, those with degree 4 have degree 6. In a second step, we insert one triangle at every boundary vertex v of degree 6 – making the degree 6 vertex an inner vertex – by joining the two degree 2 vertices that are adjacent to v, and furthermore we add two new triangles at every boundary vertex w of degree 5 by inserting a new vertex and joining it with w and the two degree 2 vertices adjacent to w, such that the degree 5 vertex obtains degree 6 and becomes also an inner vertex. We denote the set of faces that have been constructed in this second step by F_2, and the new constructed patch by Q.

Then Q has a nice boundary because by construction, the boundary vertices of P lie in the interior of Q, so the boundary vertices of Q have all been inserted by the operation – and those inserted in step 1 have (after carrying out step 2) degree 4, while those inserted in step 2 have degree 3. The boundary faces of P are no boundary faces of Q as they do not contain any of the new inserted vertices, and since each face in F_1 contains exactly one boundary edge of P and one boundary vertex of Q while each face in F_2 contains exactly one boundary vertex of P and one boundary edge of Q, we have

$$F_b(Q) = F_1 \cup F_2 = F(Q) - F(P),$$

and every boundary face in Q has exactly two boundary faces as neighbours.

Furthermore, Q is the only patch fulfilling the required properties: Suppose there is a (p, s, t)-patch Q' with $Q' = P^+$. By definition it must contain P, and since $F_b(Q') = F(Q') - F(P)$ all faces in P must be inner faces in Q' – in particular all boundary vertices of P must be inner vertices of Q'. This means Q' has to contain all faces in F_1 and F_2 that lie in Q by construction. Consequently, Q must be subgraph of Q'. But on the other hand, if there was a face in Q' that does not lie in Q, this would be a boundary face of Q' (since it cannot lie in P) while all faces in $Q - P$ must remain boundary faces – hence there would be at least one boundary face in Q' with three neighbouring boundary faces, which is a contradiction to the definition. We obtain $Q' = Q$, so consequently the patch $Q = P^+$ is uniquely determined.

□

Lemma 3.3.13 *Given a (p, s, t)-patch P with a nice boundary, and consider P^{k+} for some $k \in \mathbb{N}_0$. Then the following equations hold:*

$$(i) \qquad b(P^{k+}) = b(P) + k(6 - D(p, s, t))$$

$$(ii) \qquad f_b(P^{k+}) = 2b(P) + (2k - 1)(6 - D(p, s, t))$$

$$(iii) \qquad f(P^{k+}) = f(P) + 2kb(P) + k^2(6 - D(p, s, t))$$

PROOF:

Denote the number of boundary vertices of P^{k+} that have degree 3 by d_3, and the number of those with degree 4 by d_4. Then we have $d_3 + d_4 = b(P^{k+})$ and by lemma 3.3.7 $d_3 = 6 - D(p, s, t)$. If every boundary vertex with degree 4 is counted 3 times and every boundary vertex with degree 3 twice, we obtain each boundary face with x boundary vertices x times. By lemma 3.3.10, any edge between two boundary vertices must be a boundary edge. Consequently there are no faces with three boundary vertices, and all faces with two boundary vertices must contain a boundary edge. This means that there exist only boundary faces with one boundary edge and two boundary vertices, which are counted twice, and boundary faces with no boundary edge and one boundary vertex, which are counted once. So the number of boundary faces is

$$\begin{aligned} f_b(P^{k+}) &= 3d_4 + 2d_3 - b(P^{k+}) \\ &= 3(d_3 + d_4) - d_3 - b(P^{k+}) \\ &= 2b(P^{k+}) - (6 - D(p, s, t)) . \end{aligned} \tag{3.47}$$

This already proves (ii) for the case $k = 0$. Since (i) and (iii) are clear in case $k = 0$, we may from now on assume that $k \geq 1$ holds. Then by definition, each boundary face in P^{k+} is neighbouring to exactly two other boundary faces, so a boundary face that contains only one boundary vertex must have one neighbour that is not the outer face nor a boundary face, that means that lies in P. Hence each boundary face must contain either exactly one boundary edge of P^{k+}, or exactly one boundary edge of $P^{(k-1)+}$. Therefore we obtain:

$$\begin{aligned} b(P^{k+}) + b(P^{(k-1)+}) &= f_b(P^{k+}) \\ &\overset{(3.47)}{=} 2b(P^{k+}) - (6 - D(p, s, t)) \\ \Leftrightarrow \quad b(P^{(k-1)+}) + (6 - D(p, s, t)) &= b(P^{k+}) \end{aligned} \tag{3.48}$$

By induction in k, (3.48) immediately implies (i).

Inserting (i) into (3.47) we get

$$\begin{aligned} f_b(P^{k+}) &= 2\big(b(P) + k(6 - D(p, s, t))\big) - (6 - D(p, s, t)) \\ &= 2b(P) + (2k - 1)(6 - D(p, s, t)) \end{aligned}$$

so we have proven (ii).

Finally, the number of faces in P^{k+} can be determined by summing up the faces in P and the rings around P separately:

$$\begin{aligned} f(P^{k+}) &= f(P) + \sum_{i=1}^{k} f_b(P^{i+}) \\ &\overset{(ii)}{=} f(P) + \sum_{i=1}^{k} \big(2b(P) + (2i - 1)(6 - D(p, s, t))\big) \\ &= f(P) + 2kb(P) + k^2(6 - D(p, s, t)) \end{aligned}$$

□

Definition 3.3.14 *Let P be a (p,s,t)-patch with a nice boundary, $D(p,s,t) \leq 5$, and let $s_0,\dots,s_{m-1}$ (with $m := 6 - D(p,s,t)$) be the sides of P such that for $i = 0,\dots,m-1$ the sides s_i and $s_{(i+1) \bmod m}$ have a vertex in common. Furthermore let l_i $(i = 0,\dots,m-1)$ be the length of side s_i. Then the* boundary segmentation *of P is defined as*

$$B(P) := (l_0,\dots,l_{m-1}) \ .$$

The boundary segmentations $(l_0,\dots,l_{m-1})$ and $(l'_0,\dots,l'_{m-1})$ are identified with each other if there is a cyclic reordering or inversion $(l''_0,\dots,l''_{m-1})$ of $(l'_0,\dots,l'_{m-1})$ such that $l_i = l''_i$ for all $i = 0,\dots,m-1$.

For a (p,s,t)-patch P with nice boundary and $B(P) = (l_0,\dots,l_{m-1})$ we denote the maximal length of the sides by

$$\max{}_B(P) := \max\{l_0,\dots,l_{m-1}\}$$

and the minimal length of the sides by

$$\min{}_B(P) := \min\{l_0,\dots,l_{m-1}\} \ .$$

Furthermore we define

$$\Delta(P) := \max{}_B(P) - \min{}_B(P) \ .$$

Definition 3.3.15 *Let P be a (p,s,t)-patch with a nice boundary, and $B(P) = (l_0,\dots,l_{m-1})$ in case $D(p,s,t) \leq 5$. Then P is called* regular *if one of the following cases applies:*

- $D(p,s,t) \in \{5,6\}$
- $0 \leq D(p,s,t) \leq 4$ *and* $\Delta(P) = 0$
- $2 \leq D(p,s,t) \leq 4$ *and* $\sum_{i=0}^{m-1}(\max_B(P) - l_i) = 1$

That means either all sides of the boundary have the same length, or – for $2 \leq D(p,s,t) \leq 4$ – we have one side of length $\max_B(P) - 1$ and all others have length $\max_B(P)$ (then in particular, $\Delta(P) = 1$ holds).

We will see later that it makes sense to allow only these two cases (and not, for instance, also the case with one side of length $\max_B(P)$ and all others have length $\max_B(P) - 1$) because every patch with a nice boundary can be extended to such a regular patch.

Remark 3.3.16 *Consider a (p,s,t)-patch P with a nice boundary. In case $D(p,s,t) \leq 5$ let $B(P) = (l_0,\dots,l_{m-1})$. Then with the help of the construction described in remark* 3.3.12*, we notice that $B(P^+) = (l_0+1,\dots,l_{m-1}+1)$ and hence $B(P^{k+}) = (l_0+k,\dots,l_{m-1}+k)$ for all $k \in \mathbb{N}$. In particular we have $\Delta(P^{k+}) = \Delta(P)$, so P^{k+} is regular if and only if P is regular. In case of $D(p,s,t) = 6$, all boundary vertices in P have degree* 4*, so the described construction yields $b(P^{k+}) = b(P^+) = b(P)$.*

Definition 3.3.17 *Given a regular (p,s,t)-patch P and some $n \in \mathbb{N}_0$. Then we define a* spiral with respect to P and n *as a (p,s,t)-patch $S = S(P,n)$ consisting of P and n further faces which can be numbered with $1,\ldots,n$ such that the following holds:*

- *For $i = 1,\ldots,n-1$, face i and $i+1$ are neighbours.*
- *If $n \geq 1$, face number 1 contains a boundary edge e of P and a degree 3 vertex v of P in case there is one; furthermore, for $D(p,s,t) \leq 5$ the edge e lies in a side of P which has length $\max_B(P)$, and if there is also a side of length $\max_B(P) - 1$ then it contains the vertex v, too. In case $n \geq 2$, face number 2 does not contain the vertex v.*
- *For $2 \leq i \leq n-1$, face $i+1$ either contains a boundary vertex of P, or – in case all boundary vertices of P are inner vertices in the subgraph S_i induced by P and the faces $1,\ldots,i$ – it shares a vertex with the face which has the lowest number among the boundary faces of S_i that have a common vertex with face i.*

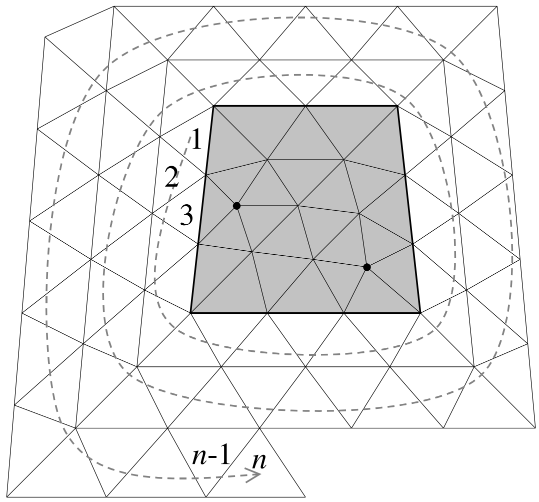

Figure 3.10: A spiral $S(P,n)$ with respect to a regular (p,s,t)-patch P (here $(p,s,t) = (2,0,0)$) and $n \in \mathbb{N}$

We make sure that for any regular (p,s,t)-patch P and any $n \in \mathbb{N}_0$, a spiral $S(P,n)$ exists:

Obviously the faces of P^{k+} can be labeled in the desired spiral way (start with face 1 and 2 as the definition requires, and continue with the respective neighbouring faces in the first ring, then in the second ring, and so on). So given a regular (p,s,t)-patch P and $n \in \mathbb{N}_0$, we choose k maximal with

$$n \;\geq\; f(P^{k+}) - f(P) \;\overset{3.3.13(iii)}{=}\; 2kb(P) + k^2(6 - D(p,s,t)) \;:=\; m$$

and label the faces in P^{k+} with $1,\ldots,m$ in the way described above. Then we add $a := n-m$ additional faces with labels $m+1,\ldots,n$ such that face i and $i+1$ are neighbours for $i = m,\ldots,n-1$ and all faces $m+1,\ldots,n$ have a vertex with P^{k+} in common. This is possible because k was chosen maximal, so together with the $(k+1)$st ring we would have more than n faces.

Furthermore, the last item of the spiral definition implies that for a given boundary of P – disregarding its interior – the position of the faces in $S(P, n) - P$ is uniquely determined up to the symmetry of the boundary.

However, note that with respect to the same n and P, there may exist non-isomorphic spirals if the symmetry of the patch P itself is lower than the symmetry of its boundary (see for instance figure 3.11). Nevertheless, by abuse of language we will use the term *the* spiral $S(P, n)$, meaning one arbitrary of the possible spirals; this is justified since the properties we discuss are invariant under reflections and rotations of the interior of P.

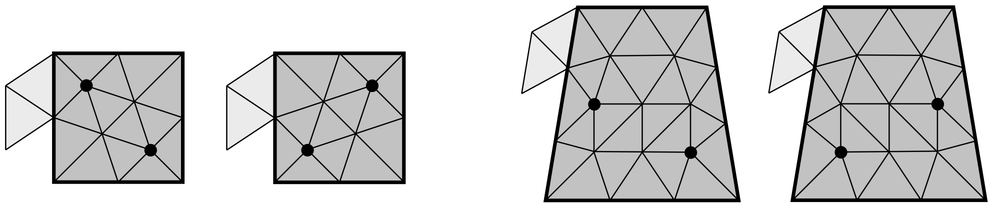

Figure 3.11: Two pairs of non-isomorphic spirals with respect to the same P and n. In the left case, one spiral can be transferred into the other by a rotation of the interior of P, in the right case by a reflection.

The uniqueness implies that any spiral can be constructed in the way described before: If $n \geq f(P^{k+}) - f(P) =: m$, the patch P^{k+} must be subgraph of $S(P, n)$. So we may choose k maximal such that P^{k+} is subgraph of $S(P, n)$ and get $S(P, n) = S(P^{k+}, a)$ with $a = n - m$ additional faces, where $0 \leq a \leq f_b(P^{(k+1)+}) = b(P^{k+}) + (6 - D(p, s, t))$ (lemma 3.3.13(ii)). Figure 3.12 shows again the spiral $S(P, n)$ from figure 3.10; we observe that in this case, P^{2+} is subgraph of $S(P, n)$ and $a = n - m$ additional faces are left, such that $S(P, n) = S(P^{2+}, a)$.

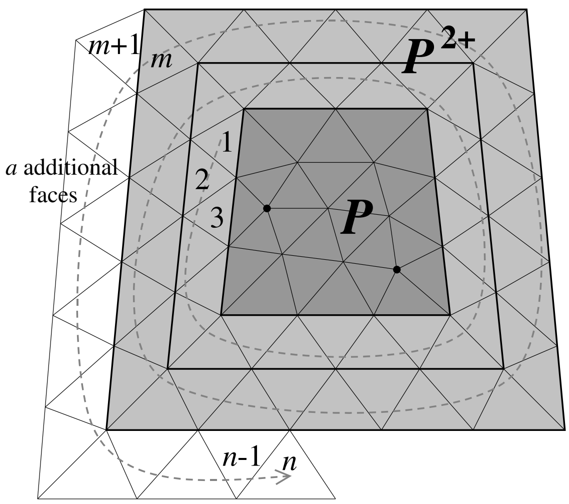

Figure 3.12: The spiral $S(P, n)$ from figure 3.10, which can also be written as $S(P^{2+}, a)$.

3.3.3 The boundary length of spirals

In this section we determine formulas giving the boundary length of some spirals in terms of their number of faces. For this we consider certain regular (p, s, t)-patches that we denote by $P_{p,s,t}$ as shown in figure 3.13.

Furthermore we denote the spiral containing $P_{p,s,t}$ and a total number of $n \geq f(P_{p,s,t})$ faces by

$$S_{n,p,s,t} := S(P_{p,s,t},\, n - f(P_{p,s,t}))\ .$$

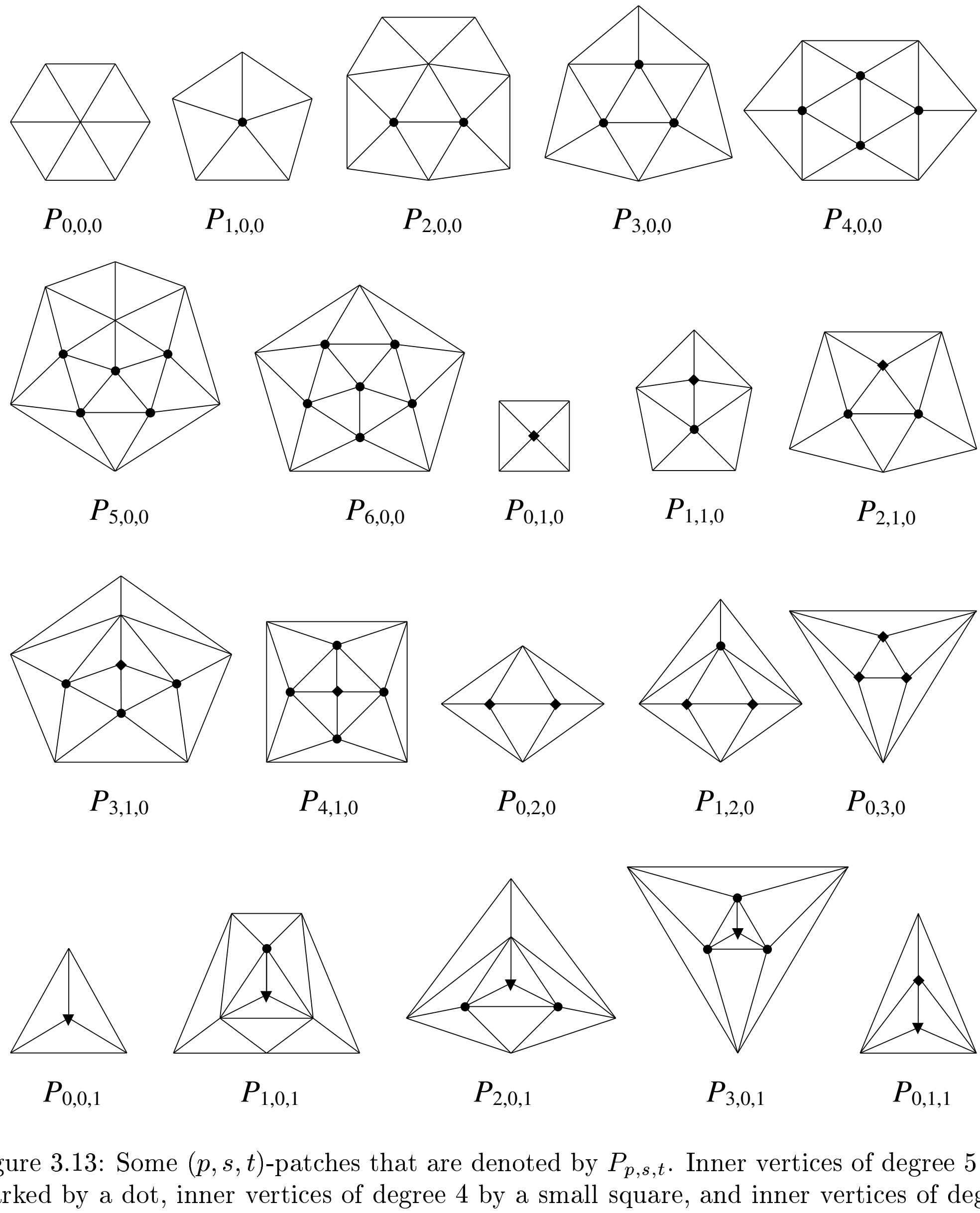

Figure 3.13: Some (p, s, t)-patches that are denoted by $P_{p,s,t}$. Inner vertices of degree 5 are marked by a dot, inner vertices of degree 4 by a small square, and inner vertices of degree 3 by a small triangle.

We will see later that in our context it is sufficient to consider the spirals with respect to the first 10 patches of the figure, that are the cases $(p, s, t) = (p, 0, 0)$ for $p = 0, 1, \ldots, 6$, and the cases $(p, s, t) = (p, 1, 0)$ for $p = 0, 1, 2$. The reason is that the boundary of each of these patches represents a special boundary type of a regular patch: By adding rings around $P_{0,0,0}$, $P_{1,0,0}$, $P_{0,1,0}$, $P_{3,0,0}$, $P_{4,0,0}$ and $P_{5,0,0}$ we obtain regular patches with boundary segmentations of the types (l, l, l, l, l, l), (l, l, l, l, l), (l, l, l, l), (l, l, l), (l, l) and (l), respectively; and on the other hand, adding an appropriate number of rings around $P_{2,0,0}$, $P_{1,1,0}$ and $P_{2,1,0}$ yields the boundary segmentations $(l, l, l, l-1)$, $(l, l, l-1)$ and $(l, l-1)$.

Since (p, s, t)-patches with $D(p, s, t) = 6$ have the property that adding rings does not change the boundary length, we may not construct such patches with arbitrary boundary length by building rings around $P_{6,0,0}$. However, this is the 6-patch with shortest boundary length, which forms a special case, for we will later see that all other cases with $p = 6$ can be solved with the help of the case $p = 5$.

For these 10 cases we will now determine the boundary length and thereby prove that they have minimal boundary length among all respective (p, s, t)-patches with the same number of faces. Nevertheless, we will later also give the formulas for the boundary lengths of the other spirals, which are minimal, too.

Spirals with p inner vertices of degree 5

At first we consider the different p-patches, i.e. the (p, s, t)-patches with $s = t = 0$, and show that the corresponding spirals fulfill the inequations from theorem 3.3.2 as equalities.

The case p=0

Lemma 3.3.18 *For $n \geq 6$ consider the spiral $S_{n,0,0,0}$ containing $P_{0,0,0}$ and a total number of n faces. Its boundary length is given by*

$$b(S_{n,0,0,0}) = 2\left\lceil \frac{1}{2}(n + \sqrt{6n}) \right\rceil - n\ .$$

PROOF:

The case of this spiral (see figure 3.14), where all inner vertices have degree 6, has already been examined in [27]. There it is stated that the number e of edges in the spiral with n faces is given by

$$e \;=\; n + \left\lceil \frac{1}{2}(n + \sqrt{6n}) \right\rceil\ . \qquad (3.49)$$

Now if q denotes the number of inner edges, we have for the boundary length $b(P)$ of any triangle-patch P with n faces and e edges:

$$b(P) \;=\; e - q \;\stackrel{(3.1)}{=}\; e - (3n - e) \;=\; 2e - 3n \qquad (3.50)$$

In case of $P = S_{n,0,0,0}$, we get by inserting (3.49) into (3.50):

$$b(S_{n,0,0,0}) \;=\; 2e - 3n \;=\; 2\left(n + \left\lceil \frac{1}{2}(n + \sqrt{6n}) \right\rceil\right) - 3n \;=\; 2\left\lceil \frac{1}{2}(n + \sqrt{6n}) \right\rceil - n$$

□

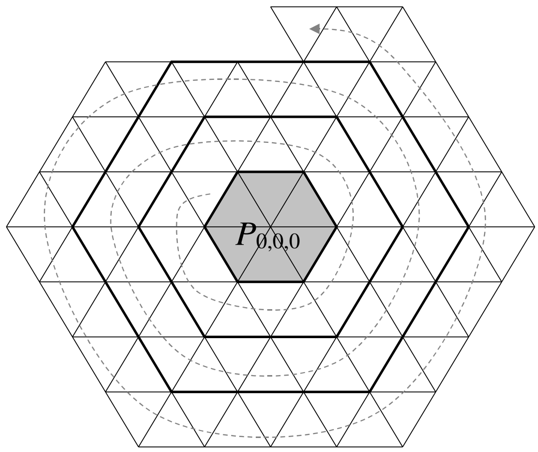

Figure 3.14: The spiral $S_{n,0,0,0}$

The case p=1

Lemma 3.3.19 *For $n \geq 5$, the boundary length of the spiral $S_{n,1,0,0}$ which contains the 1-patch $P_{1,0,0}$ and has a total number of n faces is given by*

$$b(S) = 2\left\lceil \frac{1}{2}(n + \sqrt{5n}) \right\rceil - n\ .$$

PROOF:

Let $k \in \mathbb{N}$ be maximal such that the patch $P_{1,0,0}^{(k-1)+}$ with boundary length $5k$ and $5k^2$ faces is contained in $S_{n,1,0,0}$, and let a be the number of additional faces. We observe that in case a is even, the boundary length is obtained by

$$b(S_{n,1,0,0}) = 5k + \begin{cases} 0 & , \quad a = 0 \\ 2 & , \quad 0 < a \leq 4k \\ 4 & , \quad 4k+2 \leq a \leq 8k+2 \\ 6 & , \quad 8k+4 \leq a \leq 10k+4 \end{cases}$$

and in case a is odd we have

$$b(S_{n,1,0,0}) = 5k + \begin{cases} 1 & , \quad 1 \leq a \leq 2k-1 \\ 3 & , \quad 2k+1 \leq a \leq 6k+1 \\ 5 & , \quad 6k+3 \leq a \leq 10k+3\ . \end{cases}$$

Note that since $n = 5k^2 + a$, one of the following four cases applies:

1. a even, k even, n even;
2. a even, k odd, n odd;
3. a odd, k even, n odd;
4. a odd, k odd, n even.

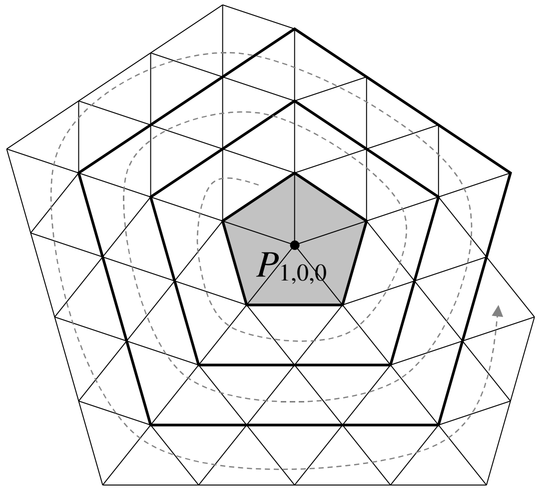

Figure 3.15: The spiral $S_{n,1,0,0}$

Now we confirm the formula for the different cases:

- In case $a = 0$ we have $n = 5k^2$ and hence
$$2\lceil\frac{1}{2}(n+\sqrt{5n})\rceil - n \;=\; 2\lceil\frac{1}{2}(5k^2+5k)\rceil - 5k^2 \;=\; 5k \;=\; b(S_{n,1,0,0})$$
since $5k^2 + 5k = 5k(k+1)$ is even for all $k \in \mathbb{N}!$ – so the lemma is correct in this case.

- If a is even and $0 < a \le 4k$ we have:
$$\begin{array}{rrcccl} & 5k^2 & < & n & \le & 5k^2+4k \\ \Leftrightarrow & 25k^2 & < & 5n & \le & 25k^2+20k \\ \Rightarrow & 25k^2 & < & 5n & \le & 25k^2+20k+4 \\ \Rightarrow & 5k & < & \sqrt{5n} & \le & 5k+2 \\ \Leftrightarrow & \frac{1}{2}n+\frac{5}{2}k & < & \frac{1}{2}(n+\sqrt{5n}) & \le & \frac{1}{2}n+\frac{5}{2}k+1 \end{array}$$
Since a is even we have that either n and k are both even, or both are odd – in any case $n + 5k$ is even and hence $\frac{1}{2}n + \frac{5}{2}k = \frac{1}{2}(n + 5k) \in \mathbb{N}$, so we get:
$$\begin{array}{rrcccl} & \lceil\frac{1}{2}(n+\sqrt{5n})\rceil & = & \frac{1}{2}n+\frac{5}{2}k+1 & & \\ \Leftrightarrow & 2\lceil\frac{1}{2}(n+\sqrt{5n})\rceil - n & = & 5k+2 & = & b(S_{n,1,0,0}) \end{array}$$

- Now let a be even and $4k + 2 \le a \le 8k + 2$. Then we have
$$\begin{array}{rrcccl} & 5k^2+4k+2 & \le & n & \le & 5k^2+8k+2 \\ \Leftrightarrow & 25k^2+20k+10 & \le & 5n & \le & 25k^2+40k+10 \\ \Rightarrow & 25k^2+20k+4 & < & 5n & \le & 25k^2+40k+16 \\ \Rightarrow & 5k+2 & < & \sqrt{5n} & \le & 5k+4 \\ \Leftrightarrow & \frac{1}{2}n+\frac{5}{2}k+1 & < & \frac{1}{2}(n+\sqrt{5n}) & \le & \frac{1}{2}n+\frac{5}{2}k+2 \end{array}$$

and again $\frac{1}{2}n + \frac{5}{2}k = \frac{1}{2}(n+5k) \in \mathbb{N}$ because a is even, so we obtain:

$$\begin{aligned} \lceil \frac{1}{2}(n+\sqrt{5n}) \rceil &= \frac{1}{2}n + \frac{5}{2}k + 2 \\ \Leftrightarrow \quad 2\lceil \frac{1}{2}(n+\sqrt{5n}) \rceil - n &= 5k+4 = b(S_{n,1,0,0}) \end{aligned}$$

- If a is even and $8k+4 \leq a \leq 10k+4$ holds, we have:

$$\begin{aligned} 5k^2+8k+4 &\leq n \leq 5k^2+10k+4 \\ \Leftrightarrow \quad 25k^2+40k+20 &\leq 5n \leq 25k^2+50k+20 \\ \Rightarrow \quad 25k^2+40k+16 &< 5n \leq 25k^2+60k+36 \\ \Rightarrow \quad 5k+4 &< \sqrt{5n} \leq 5k+6 \\ \Leftrightarrow \quad \frac{1}{2}n+\frac{5}{2}k+2 &< \frac{1}{2}(n+\sqrt{5n}) \leq \frac{1}{2}n+\frac{5}{2}k+3 \end{aligned}$$

With $\frac{1}{2}n + \frac{5}{2}k = \frac{1}{2}(n+5k) \in \mathbb{N}$ we get:

$$\begin{aligned} \lceil \frac{1}{2}(n+\sqrt{5n}) \rceil &= \frac{1}{2}n + \frac{5}{2}k + 3 \\ \Leftrightarrow \quad 2\lceil \frac{1}{2}(n+\sqrt{5n}) \rceil - n &= 5k+6 = b(S_{n,1,0,0}) \end{aligned}$$

- Now assume a is odd and $1 \leq a \leq 2k-1$. Then we get:

$$\begin{aligned} 5k^2+1 &\leq n \leq 5k^2+2k-1 \\ \Leftrightarrow \quad 25k^2+5 &\leq 5n \leq 25k^2+10k-5 \\ \Rightarrow \quad 25k^2-10k+2 &< 5n \leq 25k^2+10k+1 \\ \Rightarrow \quad 5k-1 &< \sqrt{5n} \leq 5k+1 \\ \Leftrightarrow \quad \frac{1}{2}n+\frac{5}{2}k-\frac{1}{2} &< \frac{1}{2}(n+\sqrt{5n}) \leq \frac{1}{2}n+\frac{5}{2}k+\frac{1}{2} \end{aligned}$$

Since a is odd we have either k even and n odd, or k odd and n even. In both cases $n+k$ is odd and hence $\frac{1}{2}n + \frac{5}{2}k + \frac{1}{2} = \frac{1}{2}(n+k+1) \in \mathbb{N}$, so we have

$$\begin{aligned} \lceil \frac{1}{2}(n+\sqrt{5n}) \rceil &= \frac{1}{2}n + \frac{5}{2}k + \frac{1}{2} \\ \Leftrightarrow \quad 2\lceil \frac{1}{2}(n+\sqrt{5n}) \rceil - n &= 5k+1 = b(S_{n,1,0,0}) \ . \end{aligned}$$

- If a is odd and $2k+1 \leq k \leq 6k+1$ we have

$$\begin{aligned} 5k^2+2k+1 &\leq n \leq 5k^2+6k+1 \\ \Leftrightarrow \quad 25k^2+10k+5 &\leq 5n \leq 25k^2+30k+5 \\ \Rightarrow \quad 25k^2+10k+1 &< 5n \leq 25k^2+30k+9 \\ \Rightarrow \quad 5k+1 &< \sqrt{6n} \leq 5k+3 \\ \Leftrightarrow \quad \frac{1}{2}n+\frac{5}{2}k+\frac{1}{2} &< \frac{1}{2}(n+\sqrt{5n}) \leq \frac{1}{2}n+\frac{5}{2}k+\frac{3}{2} \end{aligned}$$

and as before, $n+k$ is odd and hence $\frac{1}{2}n+\frac{5}{2}k+\frac{3}{2}=\frac{1}{2}(n+k+3)\in\mathbb{N}$, so we obtain

$$\begin{aligned} \lceil\frac{1}{2}(n+\sqrt{5n})\rceil &= \frac{1}{2}n+\frac{5}{2}k+\frac{3}{2} \\ \Leftrightarrow\ 2\lceil\frac{1}{2}(n+\sqrt{5n})\rceil-n &= 5k+3 = b(S_{n,1,0,0})\ . \end{aligned}$$

- Now let a be odd and $6k+3\le k\le 10k+3$. Then we have:

$$\begin{aligned} 5k^2+6k+3 &\le n \le 5k^2+10k+3 \\ \Leftrightarrow\ 25k^2+30k+15 &\le 5n \le 25k^2+50k+15 \\ \Rightarrow\ 25k^2+30k+9 &< 5n \le 25k^2+50k+25 \\ \Rightarrow\ 5k+3 &< \sqrt{5n} \le 5k+5 \\ \Leftrightarrow\ \frac{1}{2}n+\frac{5}{2}k+\frac{3}{2} &< \frac{1}{2}(n+\sqrt{5n}) \le \frac{1}{2}n+\frac{5}{2}k+\frac{5}{2} \end{aligned}$$

With $n+k$ odd we have $\frac{1}{2}n+\frac{5}{2}k+\frac{5}{2}=\frac{1}{2}(n+k+5)\in\mathbb{N}$ and hence

$$\begin{aligned} \lceil\frac{1}{2}(n+\sqrt{5n})\rceil &= \frac{1}{2}n+\frac{5}{2}k+\frac{5}{2} \\ \Leftrightarrow\ 2\lceil\frac{1}{2}(n+\sqrt{5n})\rceil-n &= 5k+5 = b(S_{n,1,0,0})\ . \end{aligned}$$

□

The case p=2

Lemma 3.3.20 *For $n\ge 11$, let $S_{n,2,0,0}$ be the spiral with respect to $P_{2,0,0}$ that contains n faces. Then the boundary length of $S_{n,2,0,0}$ is given by*

$$b(S_{n,2,0,0})=2\lceil\frac{1}{2}(n+\sqrt{4n+4})\rceil-n\ .$$

PROOF:

Let $k\in\mathbb{N}$ be maximal such that $P_{2,0,0}^{(k-2)+}$ – the 2-patch consisting of $P_{2,0,0}$ and $k-2$ rings, whose boundary has three sides of length k and one of length $k-1$ – is subgraph of $S_{n,2,0,0}$. Obviously its boundary length is $b(P_{2,0,0}^{(k-2)+})=4k-1$, and its number of faces can be determined with lemma 3.3.13 as

$$\begin{aligned} f(P_{2,0,0}^{(k-2)+}) &= f(P_{2,0,0})+2(k-2)b(P_{2,0,0})+4(k-2)^2 \\ &= 11+14(k-2)+4k^2-16k+16 \\ &= 4k^2-2k-1\ . \end{aligned}$$

Now let a be the number of additional faces. Then we have in case a is even

$$b(S)=4k-1+\begin{cases} 0 & ,\quad a=0 \\ 2 & ,\quad 0<a\le 4k \\ 4 & ,\quad 4k+2\le a\le 8k \end{cases}$$

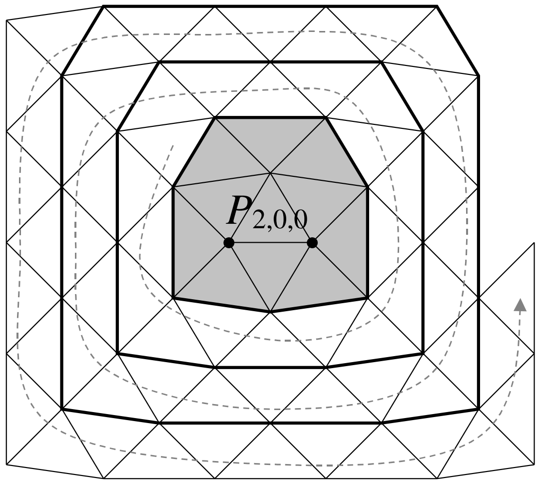

Figure 3.16: The spiral $S_{n,2,0,0}$

and in case a is odd

$$b(S) = 4k - 1 + \begin{cases} 1 & , \quad 1 \le a \le 2k-1 \\ 3 & , \quad 2k+1 \le a \le 6k+1 \\ 5 & , \quad 6k+3 \le a \le 8k+1 \ . \end{cases}$$

Since $n = (4k^2 - 2k - 1) + a$ holds, n is even (odd) if and only if a is odd (even).

- In case $a = 0$ we have $n = 4k^2 - 2k - 1$. This implies

$$\begin{aligned} \frac{1}{2}(n + \sqrt{4n+4}) &= \frac{1}{2}(4k^2 - 2k - 1 + \sqrt{16k^2 - 8k}) \\ &\le \frac{1}{2}(4k^2 - 2k - 1 + \sqrt{16k^2 - 8k + 1}) \\ &= \frac{1}{2}(4k^2 - 2k - 1 + (4k - 1)) \\ &= 2k^2 + k - 1 \end{aligned}$$

and on the other hand

$$\begin{aligned} \frac{1}{2}(n + \sqrt{4n+4}) &= \frac{1}{2}(4k^2 - 2k - 1 + \sqrt{16k^2 - 8k}) \\ &> \frac{1}{2}(4k^2 - 2k - 1 + \sqrt{16k^2 - 24k + 9}) \\ &= \frac{1}{2}(4k^2 - 2k - 1 + (4k - 3)) \\ &= 2k^2 + k - 2 \ , \end{aligned}$$

which means we have

$$\begin{aligned} \lceil \frac{1}{2}(n + \sqrt{4n+4}) \rceil &= 2k^2 + k - 1 \\ \Leftrightarrow \quad 2 \lceil \frac{1}{2}(n + \sqrt{4n+4}) \rceil - n &= 2(2k^2 + k - 1) - (4k^2 - 2k - 1) \\ &= 4k - 1 \quad = \quad b(S_{n,2,0,0}) \ . \end{aligned}$$

- If a is even and $2 \leq a \leq 4k$ we have:

$$\begin{array}{rrcl} & 4k^2-2k+1 & \leq\ n\ \leq & 4k^2+2k-1 \\ \Leftrightarrow & 16k^2-8k+8 & \leq\ 4n+4\ \leq & 16k^2+8k \\ \Rightarrow & 16k^2-8k+1 & <\ 4n+4\ \leq & 16k^2+8k+1 \\ \Rightarrow & 4k-1 & <\ \sqrt{4n+4}\ \leq & 4k+1 \\ \Leftrightarrow & \frac{1}{2}n+2k-\frac{1}{2} & <\ \frac{1}{2}(n+\sqrt{4n+4})\ \leq & \frac{1}{2}n+2k+\frac{1}{2} \end{array}$$

Since a is even, n must be odd and hence $\frac{1}{2}n+2k+\frac{1}{2} = \frac{1}{2}(n+1)+2k \in \mathbb{N}$, so we get:

$$\begin{array}{rrcl} & \lceil\frac{1}{2}(n+\sqrt{4n+4})\rceil & = & \frac{1}{2}n+2k+\frac{1}{2} \\ \Leftrightarrow & 2\lceil\frac{1}{2}(n+\sqrt{4n+4})\rceil-n & = & 4k+1 \ = \ b(S_{n,2,0,0}) \end{array}$$

- Now let a even and $4k+2 \leq a \leq 8k$. Then

$$\begin{array}{rrcl} & 4k^2+2k+3 & \leq\ n\ \leq & 4k^2+6k-1 \\ \Leftrightarrow & 16k^2+8k+16 & \leq\ 4n+4\ \leq & 16k^2+24k \\ \Rightarrow & 16k^2+8k+1 & <\ 4n+4\ \leq & 16k^2+24k+9 \\ \Rightarrow & 4k+1 & <\ \sqrt{4n+4}\ \leq & 4k+3 \\ \Leftrightarrow & \frac{1}{2}n+2k+\frac{1}{2} & <\ \frac{1}{2}(n+\sqrt{4n+4})\ \leq & \frac{1}{2}n+2k+\frac{3}{2} \end{array}$$

and since a is even, n is odd, so we have $\frac{1}{2}n+2k+\frac{3}{2} = \frac{1}{2}(n+3)+2k \in \mathbb{N}$ and hence

$$\begin{array}{rrcl} & \lceil\frac{1}{2}(n+\sqrt{4n+4})\rceil & = & \frac{1}{2}n+2k+\frac{3}{2} \\ \Leftrightarrow & 2\lceil\frac{1}{2}(n+\sqrt{4n+4})\rceil-n & = & 4k+3 \ = \ b(S_{n,2,0,0})\ . \end{array}$$

- In case a is odd and $1 \leq a \leq 2k-1$, we have:

$$\begin{array}{rrcl} & 4k^2-2k & \leq\ n\ \leq & 4k^2-2 \\ \Leftrightarrow & 16k^2-8k+4 & \leq\ 4n+4\ \leq & 16k^2-4 \\ \Rightarrow & 16k^2-16k+4 & <\ 4n+4\ \leq & 16k^2 \\ \Rightarrow & 4k-2 & <\ \sqrt{4n+4}\ \leq & 4k \\ \Leftrightarrow & \frac{1}{2}n+2k-1 & <\ \frac{1}{2}(n+\sqrt{4n+4})\ \leq & \frac{1}{2}n+2k \end{array}$$

Since a is odd, n is even and hence $\frac{1}{2}n+2k \in \mathbb{N}$, which implies

$$\begin{array}{rrcl} & \lceil\frac{1}{2}(n+\sqrt{4n+4})\rceil & = & \frac{1}{2}n+2k \\ \Leftrightarrow & 2\lceil\frac{1}{2}(n+\sqrt{4n+4})\rceil-n & = & 4k \ = \ b(S_{n,2,0,0})\ . \end{array}$$

- If a is odd and $2k+1 \leq a \leq 6k+1$, we have:

$$\begin{array}{rcccl} & 4k^2 & \leq & n & \leq & 4k^2+4k \\ \Leftrightarrow & 16k^2+4 & \leq & 4n+4 & \leq & 16k^2+16k+4 \\ \Rightarrow & 16k^2 & < & 4n+4 & \leq & 16k^2+16k+4 \\ \Rightarrow & 4k & < & \sqrt{4n+4} & \leq & 4k+2 \\ \Leftrightarrow & \frac{1}{2}n+2k & < & \frac{1}{2}(n+\sqrt{4n+4}) & \leq & \frac{1}{2}n+2k+1 \end{array}$$

Since a is odd, n is even, so we have $\frac{1}{2}n+2k+1 \in \mathbb{N}$ and therefore

$$\begin{array}{rcl} \lceil \frac{1}{2}(n+\sqrt{4n+4}) \rceil & = & \frac{1}{2}n+2k+1 \\ \Leftrightarrow \quad 2\lceil \frac{1}{2}(n+\sqrt{4n+4}) \rceil - n & = & 4k+2 \quad = \quad b(S_{n,2,0,0}) \; . \end{array}$$

- Finally consider the case where a is odd and $6k+3 \leq a \leq 8k+1$. Then

$$\begin{array}{rcccl} & 4k^2+4k+2 & \leq & n & \leq & 4k^2+12k+1 \\ \Leftrightarrow & 16k^2+16k+12 & \leq & 4n+4 & \leq & 16k^2+48k+8 \\ \Rightarrow & 16k^2+16k+4 & < & 4n+4 & \leq & 16k^2+48k+16 \\ \Rightarrow & 4k+2 & < & \sqrt{4n+4} & \leq & 4k+4 \\ \Leftrightarrow & \frac{1}{2}n+2k+1 & < & \frac{1}{2}(n+\sqrt{4n+4}) & \leq & \frac{1}{2}n+2k+2 \end{array}$$

and again n is even, so $\frac{1}{2}n+2k+2 \in \mathbb{N}$ holds, and hence

$$\begin{array}{rcl} \lceil \frac{1}{2}(n+\sqrt{4n+4}) \rceil & = & \frac{1}{2}n+2k+2 \\ \Leftrightarrow \quad 2\lceil \frac{1}{2}(n+\sqrt{4n+4}) \rceil - n & = & 4k+4 \quad = \quad b(S_{n,2,0,0}) \; . \end{array}$$

□

The case p=3

Lemma 3.3.21 *For $n \in \mathbb{N}$, $n \geq 10$, let $S_{n,3,0,0}$ be the spiral with respect to $P_{3,0,0}$ that contains n faces. Then the boundary length of $S_{n,3,0,0}$ is given by*

$$b(S_{n,3,0,0}) = 2\lceil \frac{1}{2}(n+\sqrt{3n+6}) \rceil - n \; .$$

PROOF:

Let $k \in \mathbb{N}$ be maximal such that $P_{3,0,0}^{(k-2)+}$, the 3-patch consisting of $P_{3,0,0}$ and $k-2$ rings whose boundary has three sides of length k, is subgraph of $S_{n,3,0,0}$. Its boundary length is $b(P_{3,0,0}^{(k-2)+}) = 3k$ and its number of faces

$$\begin{array}{rcl} f(P_{3,0,0}^{(k-2)+}) & = & f(P_{3,0,0}) + 2(k-2)b(P_{3,0,0}) + 3(k-2)^2 \\ & = & 10 + 12(k-2) + 3k^2 - 12k + 12 \\ & = & 3k^2 - 2 \; . \end{array}$$

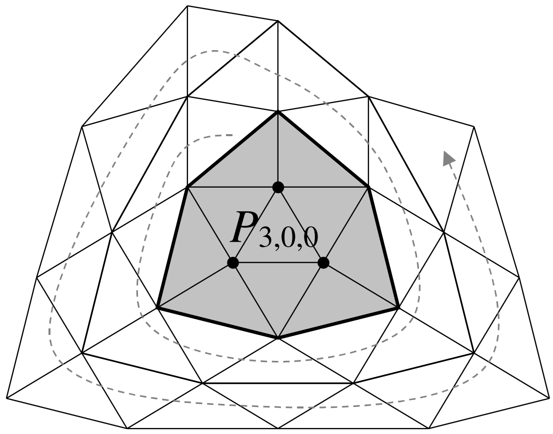

Figure 3.17: The spiral $S_{n,3,0,0}$

Furthermore let a be the number of additional faces. Then we have in case a is even

$$b(S_{n,3,0,0}) = 3k + \begin{cases} 0 & , \quad a = 0 \\ 2 & , \quad 0 < a \leq 4k \\ 4 & , \quad 4k+2 \leq a \leq 6k+2 \end{cases}$$

and in case a is odd

$$b(S_{n,3,0,0}) = 3k + \begin{cases} 1 & , \quad 1 \leq a \leq 2k-1 \\ 3 & , \quad 2k+1 \leq a \leq 6k+1 \ . \end{cases}$$

Since $n = 3k^2 - 2 + a$ holds, one of the following cases must apply:

1. a even, k even, n even;
2. a even, k odd, n odd;
3. a odd, k even, n odd;
4. a odd, k odd, n even.

- In case $a = 0$ we have $n = 3k^2 - 2$ and hence

$$\begin{aligned} 2\lceil\frac{1}{2}(n+\sqrt{3n+6})\rceil - n &= 2\lceil\frac{1}{2}(3k^2-2+\sqrt{9k^2})\rceil - 3k^2 + 2 \\ &= 2\lceil\frac{3}{2}(k^2+k)-1\rceil - 3k^2 + 2 \\ &= 2\,(\frac{3}{2}(k^2+k)-1) - 3k^2 + 2 \quad (k^2+k \text{ is always even}) \\ &= 3k \ = \ b(S_{n,3,0,0}) \ . \end{aligned}$$

- If a is even and $2 \leq a \leq 4k$ we have:

$$\begin{array}{rcccl} & 3k^2 & \leq & n & \leq & 3k^2+4k-2 \\ \Leftrightarrow & 9k^2+6 & \leq & 3n+6 & \leq & 9k^2+12k \\ \Rightarrow & 9k^2 & < & 3n+6 & \leq & 9k^2+12k+4 \\ \Rightarrow & 3k & < & \sqrt{3n+6} & \leq & 3k+2 \\ \Leftrightarrow & \frac{1}{2}n+\frac{3}{2}k & < & \frac{1}{2}(n+\sqrt{3n+6}) & \leq & \frac{1}{2}n+\frac{3}{2}k+1 \end{array}$$

Since a is even, k and n must be either both even or both odd – in any case $n+3k$ is even and hence $\frac{1}{2}n+\frac{3}{2}k = \frac{1}{2}(n+3k) \in \mathbb{N}$, so we get

$$\begin{array}{rcccl} & \lceil \frac{1}{2}(n+\sqrt{3n+6}) \rceil & = & \frac{1}{2}n+\frac{3}{2}k+1 & \\ \Leftrightarrow & 2\lceil \frac{1}{2}(n+\sqrt{3n+6}) \rceil - n & = & 3k+2 & = & b(S_{n,3,0,0}) \, . \end{array}$$

- If a is even and $4k+2 \leq a \leq 6k+2$ we have:

$$\begin{array}{rcccl} & 3k^2+4k & \leq & n & \leq & 3k^2+6k \\ \Leftrightarrow & 9k^2+12k+6 & \leq & 3n+6 & \leq & 9k^2+18k+6 \\ \Rightarrow & 9k^2+12k+4 & < & 3n+6 & \leq & 9k^2+24k+16 \\ \Rightarrow & 3k+2 & < & \sqrt{3n+6} & \leq & 3k+4 \\ \Leftrightarrow & \frac{1}{2}n+\frac{3}{2}k+1 & < & \frac{1}{2}(n+\sqrt{3n+6}) & \leq & \frac{1}{2}n+\frac{3}{2}k+2 \end{array}$$

Again $n+3k$ must be even and hence $\frac{1}{2}n+\frac{3}{2}k \in \mathbb{N}$, so we obtain:

$$\begin{array}{rcccl} & \lceil \frac{1}{2}(n+\sqrt{3n+6}) \rceil & = & \frac{1}{2}n+\frac{3}{2}k+2 & \\ \Leftrightarrow & 2\lceil \frac{1}{2}(n+\sqrt{3n+6}) \rceil - n & = & 3k+4 & = & b(S_{n,3,0,0}) \end{array}$$

- Now let a be odd and $1 \leq a \leq 2k-1$. Then we have:

$$\begin{array}{rcccl} & 3k^2-1 & \leq & n & \leq & 3k^2+2k-3 \\ \Leftrightarrow & 9k^2+3 & \leq & 3n+6 & \leq & 9k^2+6k-3 \\ \Rightarrow & 9k^2-6k+1 & < & 3n+6 & \leq & 9k^2+6k+1 \\ \Rightarrow & 3k-1 & < & \sqrt{3n+6} & \leq & 3k+1 \\ \Leftrightarrow & \frac{1}{2}n+\frac{3}{2}k-\frac{1}{2} & < & \frac{1}{2}(n+\sqrt{3n+6}) & \leq & \frac{1}{2}n+\frac{3}{2}k+\frac{1}{2} \end{array}$$

Since a is odd, either k is even and n odd, or k is odd and n even. In both cases $n+3k$ is odd and hence $\frac{1}{2}n+\frac{3}{2}k+\frac{1}{2} = \frac{1}{2}(n+3k+1) \in \mathbb{N}$. We get:

$$\begin{array}{rcccl} & \lceil \frac{1}{2}(n+\sqrt{3n+6}) \rceil & = & \frac{1}{2}n+\frac{3}{2}k+\frac{1}{2} & \\ \Leftrightarrow & 2\lceil \frac{1}{2}(n+\sqrt{3n+6}) \rceil - n & = & 3k+1 & = & b(S_{n,3,0,0}) \end{array}$$

- In case a is odd and $2k+1 \le a \le 6k+1$ we have:

$$\begin{array}{rrcl} & 3k^2+2k-1 & \le \; n \; \le & 3k^2+6k-1 \\ \Leftrightarrow & 9k^2+6k+3 & \le \; 3n+6 \; \le & 9k^2+18k+3 \\ \Rightarrow & 9k^2+6k+1 & < \; 3n+6 \; \le & 9k^2+18k+9 \\ \Rightarrow & 3k+1 & < \; \sqrt{3n+6} \; \le & 3k+3 \\ \Leftrightarrow & \frac{1}{2}n+\frac{3}{2}k+\frac{1}{2} & < \; \frac{1}{2}(n+\sqrt{3n+6}) \; \le & \frac{1}{2}n+\frac{3}{2}k+\frac{3}{2} \end{array}$$

Again $n+3k$ is odd in any case, so we have $\frac{1}{2}n+\frac{3}{2}k+\frac{3}{2} = \frac{1}{2}(n+3k+3) \in \mathbb{N}$ and obtain

$$\begin{array}{rrcl} & \lceil \frac{1}{2}(n+\sqrt{3n+6}) \rceil & = & \frac{1}{2}n+\frac{3}{2}k+\frac{3}{2} \\ \Leftrightarrow & 2\lceil \frac{1}{2}(n+\sqrt{3n+6}) \rceil - n & = & 3k+3 \;=\; b(S_{n,3,0,0}) \,. \end{array}$$

□

The case p=4

Lemma 3.3.22 *For $n \ge 12$, the boundary length of the spiral $S_{n,4,0,0}$ with respect to $P_{4,0,0}$ that contains n faces is*

$$b(S) = 2\lceil \frac{1}{2}(n+\sqrt{2n+12}) \rceil - n \,.$$

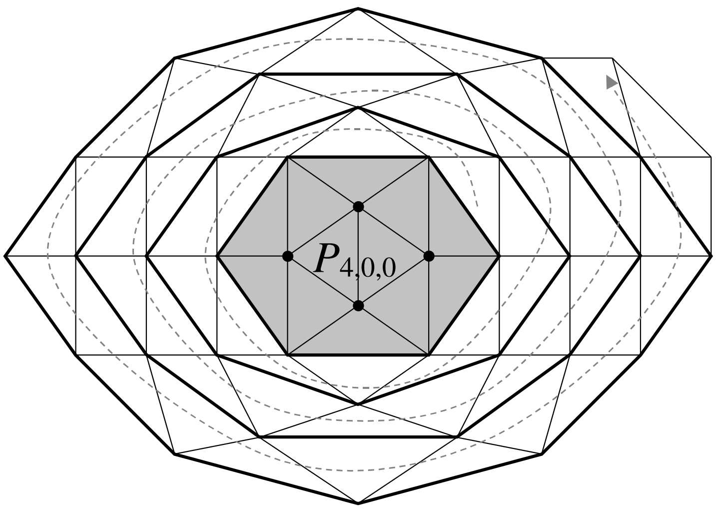

Figure 3.18: The spiral $S_{n,4,0,0}$

PROOF:

Let $k \in \mathbb{N}$ be maximal such that $P_{4,0,0}^{(k-3)+}$ – the 4-patch consisting of $P_{4,0,0}$ and $k-3$ rings with two sides of length k – is subgraph of $S_{n,4,0,0}$. Its boundary length is $b(P_{4,0,0}^{(k-3)+}) = 2k$

and its number of faces

$$\begin{aligned} f(P_{4,0,0}^{(k-3)+}) &= f(P_{4,0,0}) + 2(k-3)b(P_{4,0,0}) + 2(k-3)^2 \\ &= 12 + 12(k-3) + 2k^2 - 12k + 18 \\ &= 2k^2 - 6 \,. \end{aligned}$$

Furthermore let a be the number of additional faces. Then we have in case a is even

$$b(S_{n,4,0,0}) = 2k + \begin{cases} 0 & , \quad a = 0 \\ 2 & , \quad 0 < a \leq 4k \end{cases}$$

and in case a is odd

$$b(S_{n,4,0,0}) = 2k + \begin{cases} 1 & , \quad 1 \leq a \leq 2k-1 \\ 3 & , \quad 2k+1 \leq a \leq 4k+1 \,. \end{cases}$$

Because of $n = 2k^2 - 6 + a$, n is even (odd) if and only if a is even (odd).

- In case $a = 0$ we have $n = 2k^2 - 6$ and hence

$$\begin{aligned} 2\left\lceil \frac{1}{2}(n + \sqrt{2n+12})\right\rceil - n &= 2\left\lceil \frac{1}{2}(2k^2 - 6 + \sqrt{4k^2})\right\rceil - 2k^2 + 6 \\ &= 2\left\lceil k^2 - 3 + k \right\rceil - 2k^2 + 6 \\ &= 2\,(k^2 - 3 + k) - 2k^2 + 6 \\ &= 2k \;=\; b(S_{n,4,0,0}) \,. \end{aligned}$$

- If a is even and $2 \leq a \leq 4k$ we have:

$$\begin{aligned} & 2k^2 - 4 \leq n \leq 2k^2 + 4k - 6 \\ \Leftrightarrow\; & 4k^2 + 4 \leq 2n + 12 \leq 4k^2 + 8k \\ \Rightarrow\; & 4k^2 < 2n + 12 \leq 4k^2 + 8k + 4 \\ \Rightarrow\; & 2k < \sqrt{2n+12} \leq 2k + 2 \\ \Leftrightarrow\; & \frac{1}{2}n + k < \frac{1}{2}(n + \sqrt{2n+12}) \leq \frac{1}{2}n + k + 1 \end{aligned}$$

  Since a – and hence n – is even, we have $\frac{1}{2}n \in \mathbb{N}$ and therefore

$$\begin{aligned} & \left\lceil \frac{1}{2}(n + \sqrt{2n+12})\right\rceil = \frac{1}{2}n + k + 1 \\ \Leftrightarrow\; & 2\left\lceil \frac{1}{2}(n + \sqrt{2n+12})\right\rceil - n = 2k + 2 = b(S_{n,4,0,0}) \,. \end{aligned}$$

- If a is odd and $1 \leq a \leq 2k - 1$ we get:

$$\begin{aligned} & 2k^2 - 5 \leq n \leq 2k^2 + 2k - 7 \\ \Leftrightarrow\; & 4k^2 + 2 \leq 2n + 12 \leq 4k^2 + 4k - 2 \\ \Rightarrow\; & 4k^2 - 4k + 1 < 2n + 12 \leq 4k^2 + 4k + 1 \\ \Rightarrow\; & 2k - 1 < \sqrt{2n+12} \leq 2k + 1 \\ \Leftrightarrow\; & \frac{1}{2}n + k - \frac{1}{2} < \frac{1}{2}(n + \sqrt{2n+12}) \leq \frac{1}{2}n + k + \frac{1}{2} \end{aligned}$$

Since n is odd, $\frac{1}{2}n + \frac{1}{2} = \frac{1}{2}(n+1) \in \mathbb{N}$ holds and hence

$$\begin{aligned} \lceil \frac{1}{2}(n + \sqrt{2n+12}) \rceil &= \frac{1}{2}n + k + \frac{1}{2} \\ \Leftrightarrow\ 2\lceil \frac{1}{2}(n + \sqrt{2n+12}) \rceil - n &= 2k+1 = b(S_{n,4,0,0})\ . \end{aligned}$$

- Let a odd and $2k+1 \leq a \leq 4k+1$. Then

$$\begin{aligned} 2k^2+2k-5 &\leq n \leq 2k^2+4k-5 \\ \Leftrightarrow\ 4k^2+4k+2 &\leq 2n+12 \leq 4k^2+8k+2 \\ \Rightarrow\ 4k^2+4k+1 &< 2n+12 \leq 4k^2+12k+9 \\ \Rightarrow\ 2k+1 &< \sqrt{2n+12} \leq 2k+3 \\ \Leftrightarrow\ \frac{1}{2}n+k+\frac{1}{2} &< \frac{1}{2}(n+\sqrt{2n+12}) \leq \frac{1}{2}n+k+\frac{3}{2} \end{aligned}$$

and since n is odd, $\frac{1}{2}n + \frac{3}{2} = \frac{1}{2}(n+3) \in \mathbb{N}$. We get:

$$\begin{aligned} \lceil \frac{1}{2}(n + \sqrt{2n+12}) \rceil &= \frac{1}{2}n + k + \frac{3}{2} \\ \Leftrightarrow\ 2\lceil \frac{1}{2}(n + \sqrt{2n+12}) \rceil - n &= 2k+3 = b(S_{n,4,0,0}) \end{aligned}$$

□

The case p=5

Lemma 3.3.23 *For $n \geq 16$ let $S_{n,5,0,0}$ be the spiral with respect to $P_{5,0,0}$ that contains n faces. Then the boundary length of $S_{n,5,0,0}$ is given by*

$$b(S_{n,5,0,0}) = 2\lceil \frac{1}{2}(n + \sqrt{n+20}) \rceil - n$$

PROOF:

Let $k \in \mathbb{N}$ be maximal such that $P_{5,0,0}^{(k-6)+}$ – the 5-patch consisting of $P_{5,0,0}$ and $k-6$ rings, which has boundary length k – is subgraph of $S_{n,5,0,0}$. Its number of faces is

$$\begin{aligned} f(P_{5,0,0}^{(k-6)+}) &= f(P_{5,0,0}) + 2(k-6)b(P_{5,0,0}) + (k-6)^2 \\ &= 16 + 12(k-6) + k^2 - 12k + 36 \\ &= k^2 - 20\ . \end{aligned}$$

If a denotes the number of additional faces, we have in case a is even

$$b(S_{n,5,0,0}) = k + \begin{cases} 0 & , \quad a = 0 \\ 2 & , \quad 0 < a \leq 2k \end{cases}$$

and in case a is odd (and hence $1 \leq a \leq 2k-1$):

$$b(S_{n,5,0,0}) = k + 1$$

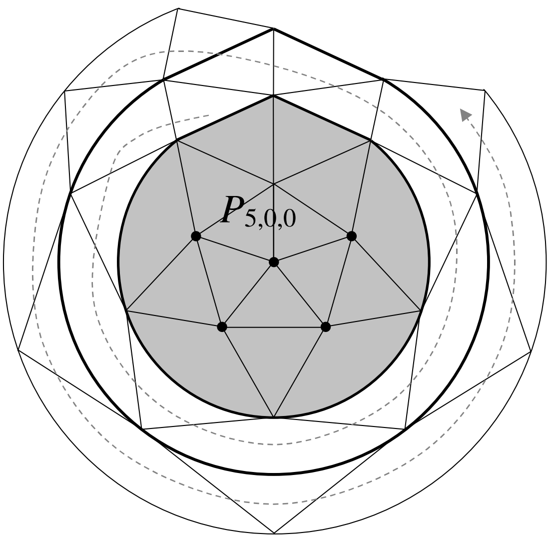

Figure 3.19: The spiral $S_{n,5,0,0}$

Because of $n = k^2 - 20 + a$, one of the following cases applies:

1. a even, k even, n even;
2. a even, k odd, n odd;
3. a odd, k even, n odd;
4. a odd, k odd, n even.

- In case $a = 0$ we have $n = k^2 - 20$ and hence

$$\begin{aligned}
2\lceil\frac{1}{2}(n+\sqrt{n+20})\rceil - n &= 2\lceil\frac{1}{2}(k^2-20+\sqrt{k^2})\rceil - k^2 + 20 \\
&= 2\lceil\frac{1}{2}(k^2+k) - 10\rceil - k^2 + 20 \\
&= 2\,(\frac{1}{2}(k^2+k) - 10) - k^2 + 20 \quad (k^2 + k \text{ is always even}) \\
&= k = b(S_{n,5,0,0})\,.
\end{aligned}$$

- If a is even and $2 \leq a \leq 2k$ we have:

$$\begin{aligned}
k^2 - 18 &\leq n \leq k^2 + 2k - 20 \\
\Leftrightarrow\; k^2 + 2 &\leq n + 20 \leq k^2 + 2k \\
\Rightarrow\; k^2 &< n + 20 \leq k^2 + 4k + 4 \\
\Rightarrow\; k &< \sqrt{n+20} \leq k + 2 \\
\Leftrightarrow\; \frac{1}{2}n + \frac{1}{2}k &< \frac{1}{2}(n + \sqrt{n+20}) \leq \frac{1}{2}n + \frac{1}{2}k + 1
\end{aligned}$$

Since a is even, k and n are either both even, or both odd. In both cases we have $\frac{1}{2}n + \frac{1}{2}k = \frac{1}{2}(n+k) \in \mathbb{N}$, and therefore

$$\begin{aligned} \lceil \frac{1}{2}(n+\sqrt{n+20}) \rceil &= \frac{1}{2}n + \frac{1}{2}k + 1 \\ \Leftrightarrow \quad 2\lceil \frac{1}{2}(n+\sqrt{n+20}) \rceil - n &= k+2 \;=\; b(S_{n,5,0,0}) \;. \end{aligned}$$

- If a is odd and $1 \leq a \leq 2k-1$ we get:

$$\begin{aligned} k^2 - 19 &\leq n \leq k^2 + 2k - 21 \\ \Leftrightarrow \quad k^2 + 1 &\leq n + 20 \leq k^2 + 2k - 1 \\ \Rightarrow \quad k^2 - 2k + 1 &< n + 20 \leq k^2 + 2k + 1 \\ \Rightarrow \quad k - 1 &< \sqrt{n+20} \leq k + 1 \\ \Leftrightarrow \quad \frac{1}{2}n + \frac{1}{2}k - \frac{1}{2} &< \frac{1}{2}(n+\sqrt{n+20}) \leq \frac{1}{2}n + \frac{1}{2}k + \frac{1}{2} \end{aligned}$$

Since a is odd, we have either k even and n odd, or k odd and n even. In both cases $\frac{1}{2}n + \frac{1}{2}k + \frac{1}{2} = \frac{1}{2}(n+k+1) \in \mathbb{N}$ holds, and hence

$$\begin{aligned} \lceil \frac{1}{2}(n+\sqrt{n+20}) \rceil &= \frac{1}{2}n + \frac{1}{2}k + \frac{1}{2} \\ \Leftrightarrow \quad 2\lceil \frac{1}{2}(n+\sqrt{n+20}) \rceil - n &= k+1 \;=\; b(S_{n,5,0,0}) \;. \end{aligned}$$

□

The case p=6

Lemma 3.3.24 *For $n \geq 15$, let $S_{n,6,0,0}$ be the spiral with respect to $P_{6,0,0}$ which has a total number of n faces. Its boundary length is given by*

$$b(S_{n,6,0,0}) = \begin{cases} 6 & \text{if } n \text{ is even} \\ 7 & \text{if } n \text{ is odd and } n \notin \{5+10k \mid k \in \mathbb{N}\} \\ 5 & \text{else .} \end{cases}$$

PROOF:

Let $k \in \mathbb{N}$ be maximal such that $P_{6,0,0}^{k+}$, the 6-patch consisting of $P_{6,0,0}$ and k rings, is subgraph of $S_{n,6,0,0}$. It has, without respect to k, boundary length 5, and its total number of faces is

$$\begin{aligned} f(P_{6,0,0}^{(k-5)+}) &= f(P_{6,0,0}) + 2kb(P_{6,0,0}) \\ &= 15 + 10k \;. \end{aligned}$$

If a denotes the number of additional faces, we have in case a is even

$$b(S_{n,6,0,0}) = 5 + \begin{cases} 0 & , \quad a = 0 \\ 2 & , \quad 0 < a \leq 8 \end{cases}$$

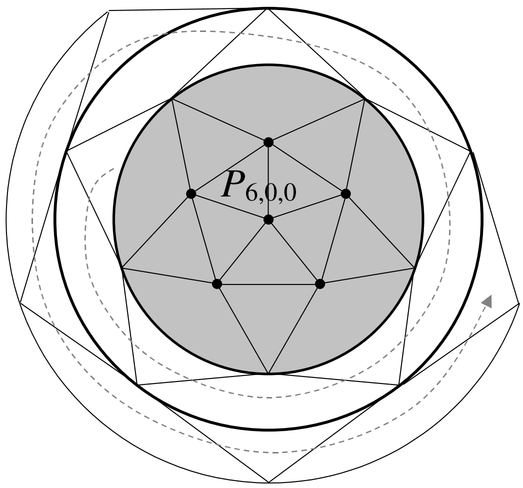

Figure 3.20: The spiral $S_{n,6,0,0}$

and in case a is odd (and hence $1 \leq a \leq 9$)

$$b(S_{n,6,0,0}) = 6 .$$

Because of $n = 10k + 15 + a$, n is even if and only if a is odd, so $b(S_{n,6,0,0}) = 6$ holds if n is even. If n is odd and $n \notin \{5 + 10k \mid k \in \mathbb{N}\}$, we have $a \neq 0$ and hence $b(S_{n,6,0,0}) = 5 + 2 = 7$; otherwise we have $n = 5 + 10k$, $a = 0$ and $b(S_{n,6,0,0}) = 5$. So the stated formula is correct in all cases.

□

Spirals with p inner vertices of degree 5 and s inner vertices of degree 4

Now we consider the three (p, s, t)-patches $P_{0,1,0}$, $P_{1,1,0}$, and $P_{2,1,0}$ with $(p, s, t) = (0, 1, 0)$, $(p, s, t) = (1, 1, 0)$, and $(p, s, t) = (2, 1, 0)$, respectively (see figure 3.13), and examine the boundary lengths of the corresponding spirals.

The case (p,s,t)=(0,1,0)

Lemma 3.3.25 *For $n \geq 4$, let $S_{n,0,1,0}$ be the spiral with respect to $P_{0,1,0}$ that contains n faces. Then its boundary length is given by*

$$b(S_{n,0,1,0}) = 2 \left\lceil \frac{1}{2}(n + \sqrt{4n}) \right\rceil - n .$$

PROOF:

Let $k \in \mathbb{N}$ be maximal such that $P_{0,1,0}^{(k-1)+}$ – the $(0, 1, 0)$-patch consisting of $P_{0,1,0}$ and $k - 1$ rings with four sides of length k – is subgraph of S. Obviously it has boundary length $4k$, and its number of faces is

$$f(P_{0,1,0}^{(k-1)+}) = 4k^2 .$$

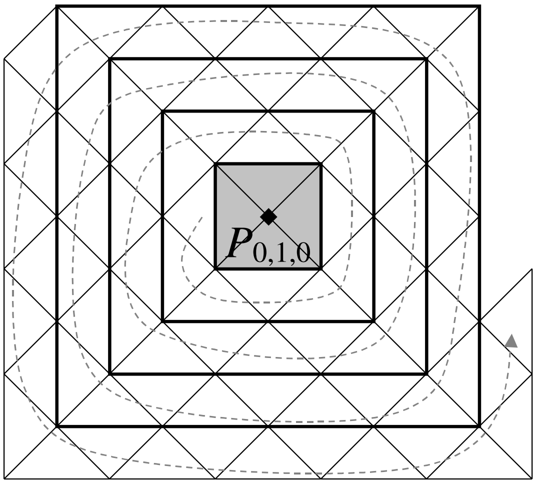

Figure 3.21: The spiral $S_{n,0,1,0}$

If a denotes the number of additional faces, we have in case a is even

$$b(S_{n,0,1,0}) = 4k + \begin{cases} 0 & , \quad a = 0 \\ 2 & , \quad 0 < a \leq 4k \\ 4 & , \quad 4k+2 \leq a \leq 8k+2 \end{cases}$$

and in case a is odd

$$b(S_{n,0,1,0}) = 4k + \begin{cases} 1 & , \quad 1 \leq a \leq 2k-1 \\ 3 & , \quad 2k+1 \leq a \leq 6k+1 \\ 5 & , \quad 6k+3 \leq a \leq 8k+3 \; . \end{cases}$$

Because of $n = 4k^2 + a$, n is even (odd) if and only if a is even (odd).

- In case $a = 0$ we have $n = 4k^2$ and hence

$$\begin{aligned} 2\,\lceil \frac{1}{2}(n + \sqrt{4n}) \rceil - n &= 2\,\lceil \frac{1}{2}(4k^2 + 4k) \rceil - 4k^2 \\ &= 2\,(2k^2 + 2k) - 4k^2 \\ &= 4k \\ &= b(S_{n,0,1,0}) \; . \end{aligned}$$

- If a is even and $0 < a \leq 4k$ we get:

$$\begin{aligned} & 4k^2 < n \leq 4k^2 + 4k \\ \Leftrightarrow\ & 16k^2 < 4n \leq 16k^2 + 16k \\ \Rightarrow\ & 16k^2 < 4n \leq 16k^2 + 16k + 4 \\ \Rightarrow\ & 4k < \sqrt{4n} \leq 4k + 2 \\ \Leftrightarrow\ & \frac{1}{2}n + 2k < \frac{1}{2}(n + \sqrt{4n}) \leq \frac{1}{2}n + 2k + 1 \end{aligned}$$

Since a is even, n is also even, so $\frac{1}{2}n \in \mathbb{N}$ and hence

$$\begin{aligned} \lceil \frac{1}{2}(n+\sqrt{4n}) \rceil &= \frac{1}{2}n + 2k + 1 \\ \Leftrightarrow \quad 2\lceil \frac{1}{2}(n+\sqrt{4n}) \rceil - n &= 4k+2 = b(S_{n,0,1,0}) \; . \end{aligned}$$

- If a is even and $4k+2 \leq a \leq 8k+2$ we have:

$$\begin{aligned} 4k^2+4k+2 &\leq n \leq 4k^2+8k+2 \\ \Leftrightarrow \quad 16k^2+16k+8 &\leq 4n \leq 16k^2+32k+8 \\ \Rightarrow \quad 16k^2+16k+4 &< 4n \leq 16k^2+32k+16 \\ \Rightarrow \quad 4k+2 &< \sqrt{4n} \leq 4k+4 \\ \Leftrightarrow \quad \frac{1}{2}n+2k+1 &< \frac{1}{2}(n+\sqrt{4n}) \leq \frac{1}{2}n+2k+2 \end{aligned}$$

Again n is even, so $\frac{1}{2}n \in \mathbb{N}$ holds and we have

$$\begin{aligned} \lceil \frac{1}{2}(n+\sqrt{4n}) \rceil &= \frac{1}{2}n + 2k + 2 \\ \Leftrightarrow \quad 2\lceil \frac{1}{2}(n+\sqrt{4n}) \rceil - n &= 4k+4 = b(S_{n,0,1,0}) \; . \end{aligned}$$

- In case a is odd and $1 \leq a \leq 2k-1$ we have:

$$\begin{aligned} 4k^2+1 &\leq n \leq 4k^2+2k-1 \\ \Leftrightarrow \quad 16k^2+4 &\leq 4n \leq 16k^2+8k-4 \\ \Rightarrow \quad 16k^2-8k+1 &< 4n \leq 16k^2+8k+1 \\ \Rightarrow \quad 4k-1 &< \sqrt{4n} \leq 4k+1 \\ \Leftrightarrow \quad \frac{1}{2}n+2k-\frac{1}{2} &< \frac{1}{2}(n+\sqrt{4n}) \leq \frac{1}{2}n+2k+\frac{1}{2} \end{aligned}$$

Now n is odd, so we have $\frac{1}{2}n + \frac{1}{2} \in \mathbb{N}$ and hence

$$\begin{aligned} \lceil \frac{1}{2}(n+\sqrt{4n}) \rceil &= \frac{1}{2}n + 2k + \frac{1}{2} \\ \Leftrightarrow \quad 2\lceil \frac{1}{2}(n+\sqrt{4n}) \rceil - n &= 4k+1 = b(S_{n,0,1,0}) \; . \end{aligned}$$

- In case a is odd and $2k+1 \leq a \leq 6k+1$ we have:

$$\begin{aligned} 4k^2+2k+1 &\leq n \leq 4k^2+6k+1 \\ \Leftrightarrow \quad 16k^2+8k+4 &\leq 4n \leq 16k^2+24k+4 \\ \Rightarrow \quad 16k^2+8k+1 &< 4n \leq 16k^2+24k+9 \\ \Rightarrow \quad 4k+1 &< \sqrt{4n} \leq 4k+3 \\ \Leftrightarrow \quad \frac{1}{2}n+2k+\frac{1}{2} &< \frac{1}{2}(n+\sqrt{4n}) \leq \frac{1}{2}n+2k+\frac{3}{2} \end{aligned}$$

Since n is odd, we have $\frac{1}{2}n + \frac{3}{2} \in \mathbb{N}$ and hence

$$\begin{aligned} \lceil \frac{1}{2}(n+\sqrt{4n}) \rceil &= \frac{1}{2}n + 2k + \frac{3}{2} \\ \Leftrightarrow \quad 2\lceil \frac{1}{2}(n+\sqrt{4n}) \rceil - n &= 4k+3 = b(S_{n,0,1,0}) \ . \end{aligned}$$

- Now let a is odd and $6k+3 \leq a \leq 8k+3$. Then we have:

$$\begin{array}{rcccl} 4k^2+6k+3 & \leq & n & \leq & 4k^2+8k+3 \\ \Leftrightarrow \quad 16k^2+24k+12 & \leq & 4n & \leq & 16k^2+32k+12 \\ \Rightarrow \quad 16k^2+24k+9 & < & 4n & \leq & 16k^2+40k+25 \\ \Rightarrow \quad 4k+3 & < & \sqrt{4n} & \leq & 4k+5 \\ \Leftrightarrow \quad \frac{1}{2}n+2k+\frac{3}{2} & < & \frac{1}{2}(n+\sqrt{4n}) & \leq & \frac{1}{2}n+2k+\frac{5}{2} \end{array}$$

Since n is odd, we have $\frac{1}{2}n + \frac{5}{2} \in \mathbb{N}$ and therefore

$$\begin{aligned} \lceil \frac{1}{2}(n+\sqrt{4n}) \rceil &= \frac{1}{2}n + 2k + \frac{5}{2} \\ \Leftrightarrow \quad 2\lceil \frac{1}{2}(n+\sqrt{4n}) \rceil - n &= 4k+5 = b(S_{n,0,1,0}) \ . \end{aligned}$$

□

The case (p,s,t)=(1,1,0)

Lemma 3.3.26 *For $n \geq 7$ consider the spiral $S_{n,1,1,0}$ with respect to $P_{1,1,0}$ that contains n faces. Then the boundary length of $S_{n,1,1,0}$ is given by*

$$b(S_{n,1,1,0}) = 2\lceil \frac{1}{2}(n+\sqrt{3n+4}) \rceil - n \ .$$

PROOF:

Let $k \in \mathbb{N}$ be maximal such that $P_{1,1,0}^{(k-2)+}$ – the $(1,1,0)$-patch consisting of $P_{1,1,0}$ and $k-2$ rings, which has two sides of length k and one of length $k-1$ – is subgraph of S. It has boundary length $3k-1$, and its number of faces is

$$\begin{aligned} f(P_{1,1,0}^{(k-2)+}) &= f(P_{1,1,0}) + 2(k-2)b(P_{1,1,0}) + 3(k-2)^2 \\ &= 7 + 10(k-2) + 3k^2 - 12k + 12 \\ &= 3k^2 - 2k - 1 \ . \end{aligned}$$

If a denotes the number of additional faces, we have in case a is even

$$b(S_{n,1,1,0}) = 3k - 1 + \begin{cases} 0 & , \quad a = 0 \\ 2 & , \quad 0 < a \leq 4k \\ 4 & , \quad 4k+2 \leq a \leq 6k \end{cases}$$

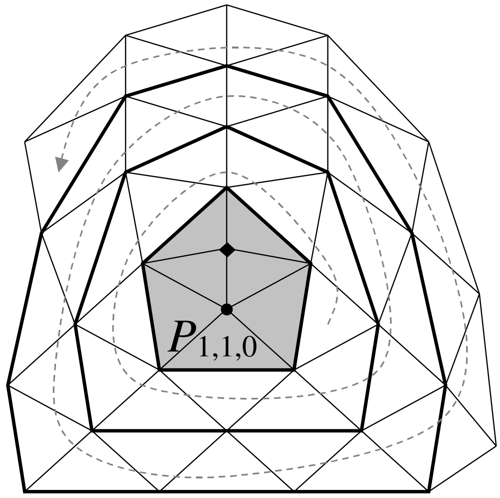

Figure 3.22: The spiral $S_{n,1,1,0}$

and in case a is odd

$$b(S_{n,1,1,0}) = 3k - 1 + \begin{cases} 1 & , \quad 1 \le a \le 2k-1 \\ 3 & , \quad 2k+1 \le a \le 6k+1. \end{cases}$$

Because of $n = 3k^2 - 2k - 1 + a$, one of the following cases applies:

1. a even, k even, n odd;
2. a even, k odd, n even;
3. a odd, k even, n even;
4. a odd, k odd, n odd.

- In case $a = 0$ we have $n = 3k^2 - 2k - 1$ and hence

$$\begin{aligned} 2\lceil \frac{1}{2}(n + \sqrt{3n+4})\rceil - n &= 2\lceil \frac{1}{2}(3k^2 - 2k - 1 + \sqrt{9k^2 - 6k + 1})\rceil - 3k^2 + 2k + 1 \\ &= 2\lceil \frac{1}{2}(3k^2 + k - 2)\rceil - 3k^2 + 2k + 1 \\ &= 2(\frac{1}{2}(3k^2 + k) - 1) - 3k^2 + 2k + 1 \quad (3k^2 + k \text{ is always even}) \\ &= 3k - 1 \;=\; b(S_{n,1,1,0}) . \end{aligned}$$

- If a is even and $0 < a \le 4k$ we get:

$$\begin{aligned} 3k^2 - 2k - 1 &< n \le 3k^2 + 2k - 1 \\ \Leftrightarrow 9k^2 - 6k + 1 &< 3n + 4 \le 9k^2 + 6k + 1 \\ \Rightarrow 3k - 1 &< \sqrt{3n+4} \le 3k + 1 \\ \Leftrightarrow \frac{1}{2}n + \frac{3}{2}k - \frac{1}{2} &< \frac{1}{2}(n + \sqrt{3n+4}) \le \frac{1}{2}n + \frac{3}{2}k + \frac{1}{2} \end{aligned}$$

Since a is even, either n is even and k odd, or n is odd and k even. In both cases we have $\frac{1}{2}n + \frac{3}{2}k + \frac{1}{2} = \frac{1}{2}(n + 3k + 1) \in \mathbb{N}$. We get

$$\begin{aligned} \lceil \frac{1}{2}(n + \sqrt{3n+4}) \rceil &= \frac{1}{2}n + \frac{3}{2}k + \frac{1}{2} \\ \Leftrightarrow \quad 2 \lceil \frac{1}{2}(n + \sqrt{3n+4}) \rceil - n &= 3k + 1 = b(S_{n,1,1,0}) \ . \end{aligned}$$

- If a is even and $4k + 2 \leq a \leq 6k$ we have:

$$\begin{aligned} 3k^2 + 2k + 1 &\leq n \leq 3k^2 + 4k - 1 \\ \Leftrightarrow \quad 9k^2 + 6k + 7 &\leq 3n + 4 \leq 9k^2 + 12k + 1 \\ \Rightarrow \quad 9k^2 + 6k + 1 &< 3n + 4 \leq 9k^2 + 18k + 9 \\ \Rightarrow \quad 3k + 1 &< \sqrt{3n+4} \leq 3k + 3 \\ \Leftrightarrow \quad \frac{1}{2}n + \frac{3}{2}k + \frac{1}{2} &< \frac{1}{2}(n + \sqrt{3n+4}) \leq \frac{1}{2}n + \frac{3}{2}k + \frac{3}{2} \end{aligned}$$

Again either n is even and k odd, or n is odd and k even. In both cases we have $\frac{1}{2}n + \frac{3}{2}k + \frac{3}{2} = \frac{1}{2}(n + 3k + 3) \in \mathbb{N}$ and get

$$\begin{aligned} \lceil \frac{1}{2}(n + \sqrt{3n+4}) \rceil &= \frac{1}{2}n + \frac{3}{2}k + \frac{3}{2} \\ \Leftrightarrow \quad 2 \lceil \frac{1}{2}(n + \sqrt{3n+4}) \rceil - n &= 3k + 3 = b(S_{n,1,1,0}) \ . \end{aligned}$$

- Now assume a is odd and $1 \leq a \leq 2k - 1$. We get:

$$\begin{aligned} 3k^2 - 2k &\leq n \leq 3k^2 - 2 \\ \Leftrightarrow \quad 9k^2 - 6k + 4 &\leq 3n + 4 \leq 9k^2 - 2 \\ \Rightarrow \quad 9k^2 - 12k + 4 &< 3n + 4 \leq 9k^2 \\ \Rightarrow \quad 3k - 2 &< \sqrt{3n+4} \leq 3k \\ \Leftrightarrow \quad \frac{1}{2}n + \frac{3}{2}k - 1 &< \frac{1}{2}(n + \sqrt{3n+4}) \leq \frac{1}{2}n + \frac{3}{2}k \end{aligned}$$

Since a is odd, n and k must be both even or both odd. In both cases we have $\frac{1}{2}n + \frac{3}{2}k = \frac{1}{2}(n + 3k) \in \mathbb{N}$, so we get

$$\begin{aligned} \lceil \frac{1}{2}(n + \sqrt{3n+4}) \rceil &= \frac{1}{2}n + \frac{3}{2}k \\ \Leftrightarrow \quad 2 \lceil \frac{1}{2}(n + \sqrt{3n+4}) \rceil - n &= 3k = b(S_{n,1,1,0}) \ . \end{aligned}$$

- If a is odd and $2k + 1 \leq a \leq 6k + 1$, we have:

$$\begin{aligned} 3k^2 &\leq n \leq 3k^2 + 4k \\ \Leftrightarrow \quad 9k^2 + 4 &\leq 3n + 4 \leq 9k^2 + 12k + 4 \\ \Rightarrow \quad 9k^2 &< 3n + 4 \leq 9k^2 + 12k + 4 \\ \Rightarrow \quad 3k &< \sqrt{3n+4} \leq 3k + 2 \\ \Leftrightarrow \quad \frac{1}{2}n + \frac{3}{2}k &< \frac{1}{2}(n + \sqrt{3n+4}) \leq \frac{1}{2}n + \frac{3}{2}k + 1 \end{aligned}$$

Again we have $\frac{1}{2}n + \frac{3}{2}k = \frac{1}{2}(n+3k) \in \mathbb{N}$ and therefore obtain

$$\begin{aligned} \lceil \frac{1}{2}(n+\sqrt{3n+4})\rceil &= \frac{1}{2}n + \frac{3}{2}k + 1 \\ \Leftrightarrow \quad 2\lceil \frac{1}{2}(n+\sqrt{3n+4})\rceil - n &= 3k+2 = b(S_{n,1,1,0}) \,. \end{aligned}$$

□

The case (p,s,t)=(2,1,0)

Lemma 3.3.27 *Let $n \geq 9$ and $S_{n,2,1,0}$ be the spiral with respect to $P_{2,1,0}$ containing n faces. Its boundary length is*

$$b(S) = 2\lceil \frac{1}{2}(n+\sqrt{2n+7})\rceil - n \,.$$

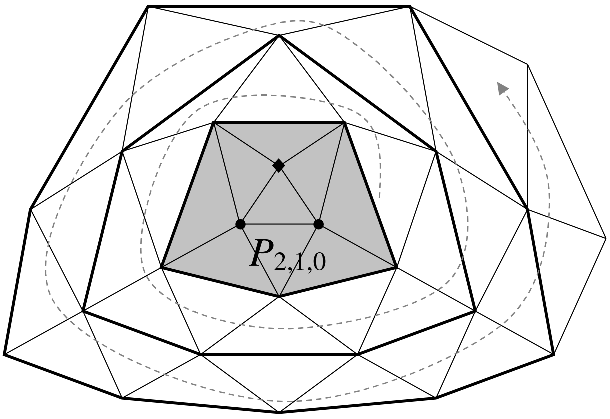

Figure 3.23: The spiral $S_{n,2,1,0}$

PROOF:

Let $k \in \mathbb{N}$ be maximal such that $P_{2,1,0}^{(k-3)+}$ – the $(2,1,0)$-patch consisting of $P_{2,1,0}$ and $k-3$ rings, which has one side of length k and one of length $k-1$ – is subgraph of S. Its boundary length is $2k-1$ and its number of faces

$$\begin{aligned} f(P_{2,1,0}^{(k-3)+}) &= f(P_{2,1,0}) + 2(k-3)b(P_{2,1,0}) + 2(k-3)^2 \\ &= 9 + 10(k-3) + 2k^2 - 12k + 18 \\ &= 2k^2 - 2k - 3 \,. \end{aligned}$$

If a denotes the number of additional faces, we have in case a is even

$$b(S_{n,2,1,0}) = 2k - 1 + \begin{cases} 0 & , \quad a = 0 \\ 2 & , \quad 0 < a \leq 4k-2 \end{cases}$$

and in case a is odd

$$b(S_{n,2,1,0}) = 2k - 1 + \begin{cases} 1 & , \quad 1 \leq a \leq 2k-1 \\ 3 & , \quad 2k+1 \leq a \leq 4k-1. \end{cases}$$

Because of $n = 2k^2 - 2k - 3 + a$, n is even (odd) if and only if a is odd (even).

- In case $a = 0$ we have $n = 2k^2 - 2k - 3$ and hence

$$\begin{aligned} 2\lceil\frac{1}{2}(n+\sqrt{2n+7})\rceil - n &= 2\lceil\frac{1}{2}(2k^2-2k-3+\sqrt{4k^2-4k+1})\rceil - 2k^2+2k+3 \\ &= 2\lceil\frac{1}{2}(2k^2-4)\rceil - 2k^2+2k+3 \\ &= 2(k^2-2) - 2k^2+2k+3 \\ &= 2k-1 \;=\; b(S_{n,2,1,0})\ . \end{aligned}$$

- If a is even and $0 < a \le 4k-2$ we get:

$$\begin{aligned} 2k^2-2k-3 &< n \le 2k^2+2k-5 \\ \Leftrightarrow\ 4k^2-4k+1 &< 2n+7 \le 4k^2+4k-3 \\ \Rightarrow\ 4k^2-4k+1 &< 2n+7 \le 4k^2+4k+1 \\ \Rightarrow\ 2k-1 &< \sqrt{2n+7} \le 2k+1 \\ \Leftrightarrow\ \frac{1}{2}n+k-\frac{1}{2} &< \frac{1}{2}(n+\sqrt{2n+7}) \le \frac{1}{2}n+k+\frac{1}{2} \end{aligned}$$

Since a is even, n is odd, so we have $\frac{1}{2}n+k+\frac{1}{2} = \frac{1}{2}(n+2k+1) \in \mathbb{N}$. We get

$$\begin{aligned} \lceil\frac{1}{2}(n+\sqrt{2n+7})\rceil &= \frac{1}{2}n+k+\frac{1}{2} \\ \Leftrightarrow\ 2\lceil\frac{1}{2}(n+\sqrt{2n+7})\rceil - n &= 2k+1 \;=\; b(S_{n,2,1,0})\ . \end{aligned}$$

- In case a is odd and $1 \le a \le 2k-1$ we have:

$$\begin{aligned} 2k^2-2k-2 &\le n \le 2k^2-4 \\ \Leftrightarrow\ 4k^2-4k+3 &\le 2n+7 \le 4k^2-1 \\ \Rightarrow\ 4k^2-8k+4 &< 2n+7 \le 4k^2 \\ \Rightarrow\ 2k-2 &< \sqrt{2n+7} \le 2k \\ \Leftrightarrow\ \frac{1}{2}n+k-1 &< \frac{1}{2}(n+\sqrt{2n+7}) \le \frac{1}{2}n+k \end{aligned}$$

Since a is odd, n is even and hence $\frac{1}{2}n \in \mathbb{N}$. We get

$$\begin{aligned} \lceil\frac{1}{2}(n+\sqrt{2n+7})\rceil &= \frac{1}{2}n+k \\ \Leftrightarrow\ 2\lceil\frac{1}{2}(n+\sqrt{2n+7})\rceil - n &= 2k \;=\; b(S_{n,2,1,0})\ . \end{aligned}$$

- In case a is odd and $2k+1 \le a \le 4k-1$ we have:

$$\begin{aligned} 2k^2-2 &\le n \le 2k^2+2k-4 \\ \Leftrightarrow\ 4k^2+3 &\le 2n+7 \le 4k^2+4k-1 \\ \Rightarrow\ 4k^2 &< 2n+7 \le 4k^2+8k+4 \\ \Rightarrow\ 2k &< \sqrt{2n+7} \le 2k+2 \\ \Leftrightarrow\ \frac{1}{2}n+k &< \frac{1}{2}(n+\sqrt{2n+7}) \le \frac{1}{2}n+k+1 \end{aligned}$$

Again n is even and hence $\frac{1}{2}n \in \mathbb{N}$, so we get

$$\begin{aligned} \lceil \frac{1}{2}(n + \sqrt{2n+7}) \rceil &= \frac{1}{2}n + k + 1 \\ \Leftrightarrow \quad 2 \lceil \frac{1}{2}(n + \sqrt{2n+7}) \rceil - n &= 2k + 2 = b(S_{n,2,1,0}) \; . \end{aligned}$$

□

With the previous results we obtain now:

Theorem 3.3.28 *Let* $(p, s, t) \in \{ (0,0,0), (1,0,0), (2,0,0), (3,0,0), (4,0,0), (5,0,0), (6,0,0), (0,1,0), (1,1,0), (2,1,0) \}$ *and* $n \in \mathbb{N}$ *with* $n \geq f(P_{p,s,t})$. *Then the spiral* $S_{n,p,s,t}$ *which contains* $P_{p,s,t}$ *and a total number of* n *faces has minimal boundary length among all* (p, s, t)*-patches with* n *faces.*

PROOF:

This follows from theorem 3.3.2, theorem 3.3.5, and the lemmas 3.3.18 to 3.3.27, since the lemmas show that the respective spirals fulfill the inequations from the theorems as equalities.

□

As mentioned before, we studied only the special cases for (p, s, t) which occur in theorem 3.3.28 because these are the cases we need for the application in the next section.

However, it is possible to solve the other cases for p, s, t with $D(p, s, t) \leq 6$ in the same way: Deduce lower bounds on the boundary of a (p, s, t)-patch by applying the respective result on hexagonal patches to the inner dual, then determine the correct spiral and show that its boundary length fulfills the obtained formula as an equality. For the sake of completeness we give all the formulas that can be obtained this way in table 3.2.

In order to check the correctness of the formulas, we have confirmed independently with a computer program building the respective spirals with up to 100 000 faces (following definition 3.3.17) that their boundary lengths are indeed given by the formulas listed in table 3.2.

Note that in figure 3.13, there do not occur (p, s, t)-patches for all 23 cases of (p, s, t) with $D(p, s, t) \leq 6$ – the cases $(p, s, t) = (2, 2, 0)$, $(p, s, t) = (1, 1, 1)$, and $(p, s, t) = (0, 0, 2)$ are missing. The reason for this is that for these cases, no *regular* patches exist from which spirals with minimal boundary length can be built. Instead, the patches with minimal boundary for the cases $(p, s, t) = (2, 2, 0)$ and $(p, s, t) = (1, 1, 1)$ can be constructed as indicated in figure 3.24 – actually the faces are also arranged in a spiral way, but since none of the subgraphs is regular these are no spirals in the sense of our definition. By abuse of notation we nevertheless denote these structures by $S_{n,2,2,0}$ and $S_{n,1,1,1}$ and complete table 3.2 with the corresponding boundary formulas.

The case $(p, s, t) = (0, 0, 2)$ is special in a different way: There we have the problem that starting with two neighbouring vertices of degree 3, as the result on the dual suggests, yields

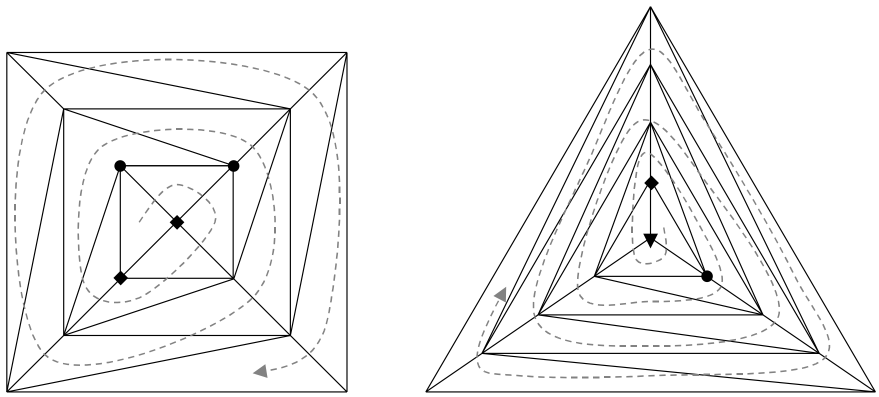

Figure 3.24: The 'spirals' $S_{n,2,2,0}$ and $S_{n,1,1,1}$

a double edge (see figure 3.25). If we nevertheless define this structure to be $P_{0,0,2}$ and build a spiral around it which allows double edges (see figure 3.26), we find that it has minimal boundary length among all plane graphs (possibly with double edges) with two inner vertices of degree 3, all other inner vertices of degree 6, and all inner faces triangles. So we include this case into table 3.2 as well.

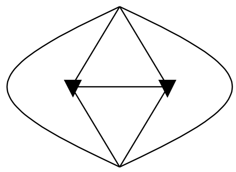

Figure 3.25: The patch $P_{0,0,2}$ which contains a double edge

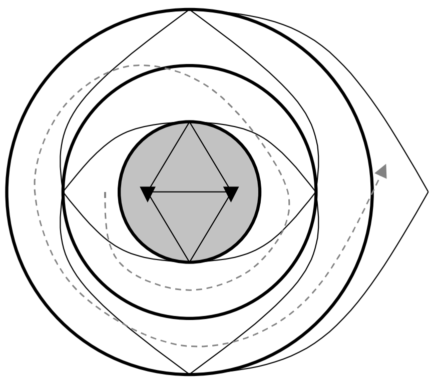

Figure 3.26: The 'spiral' $S_{n,0,0,2}$

(p,s,t)	$D(p,s,t)$	$b(S_{n,p,s,t})$
$(0,0,0)$	0	$2\lceil\frac{1}{2}(n+\sqrt{6n})\rceil - n$
$(1,0,0)$	1	$2\lceil\frac{1}{2}(n+\sqrt{5n})\rceil - n$
$(2,0,0)$	2	$2\lceil\frac{1}{2}(n+\sqrt{4n+4})\rceil - n$
$(3,0,0)$	3	$2\lceil\frac{1}{2}(n+\sqrt{3n+6})\rceil - n$
$(4,0,0)$	4	$2\lceil\frac{1}{2}(n+\sqrt{2n+12})\rceil - n$
$(5,0,0)$	5	$2\lceil\frac{1}{2}(n+\sqrt{n+20})\rceil - n$
$(6,0,0)$	6	6 if n is even 7 if n is odd and $n \notin \{5+10k \mid k \in \mathbb{N}\}$ 5 else
$(0,1,0)$	2	$2\lceil\frac{1}{2}(n+\sqrt{4n})\rceil - n$
$(1,1,0)$	3	$2\lceil\frac{1}{2}(n+\sqrt{3n+4})\rceil - n$
$(2,1,0)$	4	$2\lceil\frac{1}{2}(n+\sqrt{2n+7})\rceil - n$
$(3,1,0)$	5	$2\lceil\frac{1}{2}(n+\sqrt{n+12})\rceil - n$
$(4,1,0)$	6	5 if n is odd 6 if n is even and $n \notin \{4+8k \mid k \in \mathbb{N}\}$ 4 else
$(0,2,0)$	4	$2\lceil\frac{1}{2}(n+\sqrt{2n+4})\rceil - n$
$(1,2,0)$	5	$2\lceil\frac{1}{2}(n+\sqrt{n+8})\rceil - n$
$(2,2,0)$	6	4 if n is even 5 if n is odd
$(0,3,0)$	6	4 if n is even 5 if n is odd and $n \notin \{1+6k \mid k \in \mathbb{N}\}$ 3 else
$(0,0,1)$	3	$2\lceil\frac{1}{2}(n+\sqrt{3n})\rceil - n$
$(1,0,1)$	4	$2\lceil\frac{1}{2}(n+\sqrt{2n+3})\rceil - n$
$(2,0,1)$	5	$2\lceil\frac{1}{2}(n+\sqrt{n+6})\rceil - n$
$(3,0,1)$	6	4 if n is even 5 if n is odd and $n \notin \{3+6k \mid k \in \mathbb{N}\}$ 3 else
$(0,1,1)$	5	$2\lceil\frac{1}{2}(n+\sqrt{n+4})\rceil - n$
$(1,1,1)$	6	3 if n is odd 4 if n is even
$(0,0,2)$	6	3 if n is odd 4 if n is even and $n \notin \{4k \mid k \in \mathbb{N}\}$ 2 else

Table 3.2: Different cases for $p,s,t \in \mathbb{N}$ with $D(p,s,t) \leq 6$, and the boundary length $b(S_{n,p,s,t})$ of the spiral $S_{n,p,s,t}$ with n faces

3.3.4 Triangle-patches with fixed regular subgraphs

So far we know that for $0 \leq p \leq 6$ and $n \geq f(P_{p,0,0})$, we obtain a p-patch with n faces and minimal boundary length by arranging the appropriate number of faces in a spiral way around the patch $P_{p,0,0}$. Table 3.2 gives the boundary lengths of these spirals with respect to their numbers of faces and therefore lower bounds for the boundary lengths of arbitrary p-patches. However, in those spirals the degree 5 vertices lie close together in the center, and if we consider p-patches where the degree 5 vertices lie further apart, the given formulas are bad estimations for the boundary length. Indeed we will see in chapter 5 that sometimes it is desirable to have a sharper bound on the boundary length that takes the respective positions of the degree 5 vertices into account.

In this subsection we will at first show that given a fixed regular p-patch P, the spiral with respect to P has minimal boundary length among all p-patches containing P. Moreover, the idea of the proof provides a very useful method how a formula for the boundary length of such a spiral – that means for the minimal boundary length of a p-patch containing P – can be developed. With that technique we are able to determine lower bounds for the boundary length of p-patches containing any fixed regular p-patch P which improve those in table 3.2 for the respective case.

The cases $\mathbf{p \leq 5}$

At first we consider triangle-patches with $p \leq 5$ inner vertices of degree 5. With the already proven results, we are able to show that given a regular p-patch P with $p \leq 5$, the spiral $S(P, n)$ has minimal boundary length among all p-patches containing P and n further faces (theorem 3.3.32): The idea is to replace the patch P by a certain (p, s, t)-patch with the same boundary. For this we need lemma 3.3.31, which states that we can always find a patch with the same boundary segmentation that consists of one of the examined patches $P_{p,s,t}$ from the previous section and possibly a number of rings built around it, which in turn requires the following:

Lemma 3.3.29 *Any p-patch P with* $p \in \{2, 3, 4, 5\}$ *fulfills* $b(P) > 5$.

PROOF:

Let $n := f(P)$. Then the existence of at least two inner vertices with degree 5 already implies $n \geq 8$, since one degree 5 vertex must lie in 5 faces and the second one can only have at most two common faces with the first one, so there must be at least 3 further faces.

With $n \geq 8$ we obtain in the different cases $p = 2, 3, 4, 5$:

- If $p = 2$ we get with (3.19) $b(P) \geq \sqrt{4n + 4} \geq \sqrt{4 \cdot 8 + 4} = \sqrt{36} = 6$.
- In case $p = 3$, (3.22) implies $b(P) \geq \sqrt{3n + 6} \geq \sqrt{3 \cdot 8 + 6} = \sqrt{30} > 5$.
- For $p = 4$ we have with (3.25) $b(P) \geq \sqrt{2n + 12} \geq \sqrt{2 \cdot 8 + 12} = \sqrt{28} > 5$.
- Finally, if $p = 5$ then by (3.28) we have $b(P) \geq \sqrt{n + 20} \geq \sqrt{8 + 20} = \sqrt{28} > 5$.

□

Corollary 3.3.30 *Given a p-patch P.*

(*i*) *In case* $2 \leq p \leq 5$ *we have* $b(P) \geq 6$.

(*ii*) $B(P) = (l, l, l)$ *implies* $l \geq 2$.

(*iii*) $B(P) = (l, l)$ *or* $B(P) = (l, l-1)$ *implies* $l \geq 3$.

PROOF:

Because of $b(P) \in \mathbb{N}$, item (*i*) follows immediately from lemma 3.3.29. The items (*ii*) and (*iii*) in turn are direct consequences of (*i*). □

Lemma 3.3.31 *For any regular* $\bar{p}$*-patch P with* $0 \leq \bar{p} \leq 5$, *there exists* $k \in \mathbb{N}_0$ *and*

$$(p, s, t) \in \{(0,0,0), (1,0,0), (2,0,0), (3,0,0), (4,0,0), (5,0,0), (0,1,0), (1,1,0), (2,1,0)\}$$

such that $B(P) = B(P^{k+}_{p,s,t})$.

PROOF:

Let $B(P) = (l_0, \ldots, l_{m-1})$. By the definition of regular patches, we have either $\Delta(P) = 0$, or $2 \leq \bar{p} \leq 4$ and $\sum_{i=0}^{m-1}(\max_B(P) - l_i) = 1 = \Delta(P)$. This leads to the following cases:

1. $\bar{p} = 0$ and $\Delta(P) = 0$, i.e. $B(P) = (l, l, l, l, l, l)$ for some $l \in \mathbb{N}$:
   Then we may choose $k = l - 1$ to obtain $B(P) = B(P^{k+}_{0,0,0})$.
2. $\bar{p} = 1$ and $\Delta(P) = 0$, i.e. $B(P) = (l, l, l, l, l)$ for some $l \in \mathbb{N}$:
   Again we choose $k = l - 1$ and get $B(P) = B(P^{k+}_{1,0,0})$.
3. $\bar{p} = 2$ and $\Delta(P) = 0$, i.e. $B(P) = (l, l, l, l)$ for some $l \in \mathbb{N}$:
   Then with $k = l - 1$ we have $B(P) = B(P^{k+}_{0,1,0})$.
4. $\bar{p} = 2$ and $\Delta(P) = 1$, i.e. $B(P) = (l, l, l, l-1)$ for some $l \in \mathbb{N}$, $l \geq 2$:
   Then we choose $k = l - 2$ and obtain $B(P) = B(P^{k+}_{2,0,0})$.
5. $\bar{p} = 3$ and $\Delta(P) = 0$, i.e. $B(P) = (l, l, l)$ for some $l \in \mathbb{N}$, $l \geq 2$ (corollary 3.3.30 (*ii*)):
   Then with $k = l - 2$ we have $B(P) = B(P^{k+}_{3,0,0})$.
6. $\bar{p} = 3$ and $\Delta(P) = 1$, i.e. $B(P) = (l, l, l-1)$ for some $l \in \mathbb{N}$, $l \geq 2$:
   Then let $k = l - 2$ – this implies $B(P) = B(P^{k+}_{1,1,0})$.
7. $\bar{p} = 4$ and $\Delta(P) = 0$, i.e. $B(P) = (l, l)$ for some $l \in \mathbb{N}$, $l \geq 3$ (corollary 3.3.30 (*iii*)):
   Then choose $k = l - 3$ to obtain $B(P) = B(P^{k+}_{4,0,0})$.
8. $\bar{p} = 4$ and $\Delta(P) = 1$, i.e. $B(P) = (l, l-1)$ for some $l \in \mathbb{N}$, $l \geq 3$ (corollary 3.3.30 (*iii*)):
   Then choose $k = l - 3$ such that $B(P) = B(P^{k+}_{2,1,0})$.
9. $\bar{p} = 5$, i.e. $B(P) = (l)$ for some $l \in \mathbb{N}$, $l \geq 6$ (corollary 3.3.30 (*i*)):
   Then we let $k = l - 6$ and get $B(P) = B(P^{k+}_{5,0,0})$.

□

Theorem 3.3.32 *Let P be a regular $\bar{p}$-patch with $0 \leq \bar{p} \leq 5$, and $n \in \mathbb{N}_0$. Then the spiral $S(P,n)$ has minimal boundary length among all $\bar{p}$-patches containing P and n further faces.*

PROOF:

By lemma 3.3.31 we know that there is a (p,s,t)-patch $P' = P^{k+}_{p,s,t}$ with the same boundary segmentation as P, where $k \in \mathbb{N}_0$ and $(p,s,t) \in \{(q,0,0) \,|\, q \in \mathbb{N}_0, 0 \leq q \leq 5\} \cup \{(q,1,0) \,|\, q \in \mathbb{N}_0, 0 \leq q \leq 2\}$. Now let Q be an arbitrary $\bar{p}$-patch containing P and n further faces. Then we may replace P in Q by the (p,s,t)-patch P' with the same boundary segmentation. The result is a (p,s,t)-patch Q'. Let $m := f(Q') = f(P') + n$ be the number of faces in Q'.

Due to theorem 3.3.28, the spiral $S_{m,p,s,t}$ has minimal boundary length among all (p,s,t)-patches with m faces – in particular this means $b(S_{m,p,s,t}) \leq b(Q')$. $S_{m,p,s,t}$ even contains the patch $P' = P^{k+}_{p,s,t}$, because $f(S_{m,p,s,t}) = m = f(P') + n \geq f(P')$, so we have $S_{m,p,s,t} = S(P',n)$. Hence we may replace P' in $S_{m,p,s,t}$ by P and obtain the spiral $S(P,n)$ consisting of P and n further faces. With this we have shown:

$$b(Q) = b(Q') \geq b(S_{m,p,s,t}) = b(S(P,n))$$

□

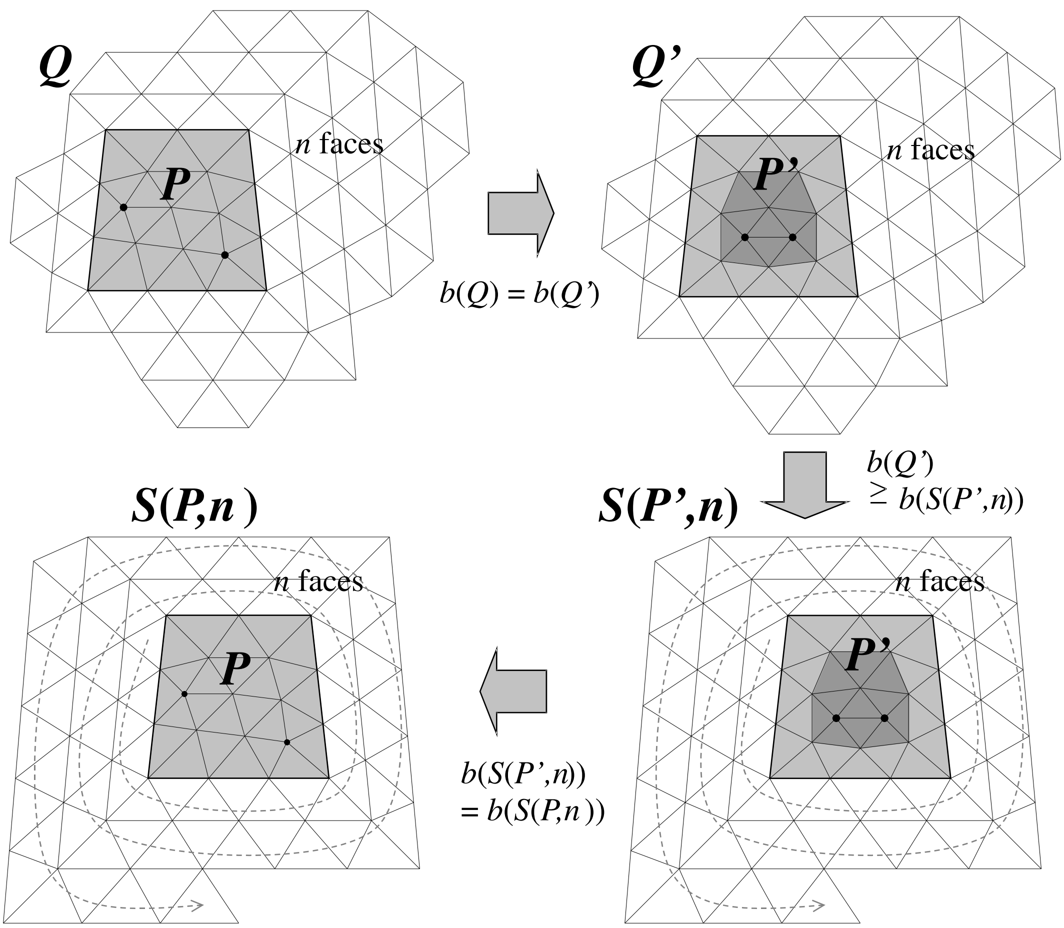

Figure 3.27: An example which demonstrates the idea of the proof of theorem 3.3.32

Following the technique applied in the proof of theorem 3.3.32, for a given regular $\bar{p}$-patch P with $\bar{p} \leq 5$ we may even deduce formulas for the boundary length of the respective spiral (and hence also bounds on the boundary length of all $\bar{p}$-patches containing P) with the help of the known formulas from table 3.2: We only need to determine the patch $P' = P^{k+}_{p,s,t}$ with the same boundary segmentation as P – which exists by lemma 3.3.31 – and compute the difference $C := f(P') - f(P)$ of the number of faces. In detail this works as follows:

Let $S := S(P, n - f(P))$ be the spiral containing P which has a total number of $n \geq f(P)$ faces. If we replace P by P', the number of faces grows by C while the boundary length stays the same. The resulting spiral is $S_{n',p,s,t}$ with $n' = n + C$, whose boundary length in terms of n' can be looked up in table 3.2. If we just replace n' in the formula by $n + C$, we obtain the desired formula for $b(S)$ depending only on the number of faces n in S.

We demonstrate this technique with the help of an example: Let P be the regular 2-patch shown in figure 3.28 on the left. It has boundary segmentation $B(P) = (3, 3, 3, 3)$ and we determine $P' = P^{2+}_{0,1,0}$ as the corresponding (p, s, t)-patch with the same boundary segmentation (see figure 3.28, right).

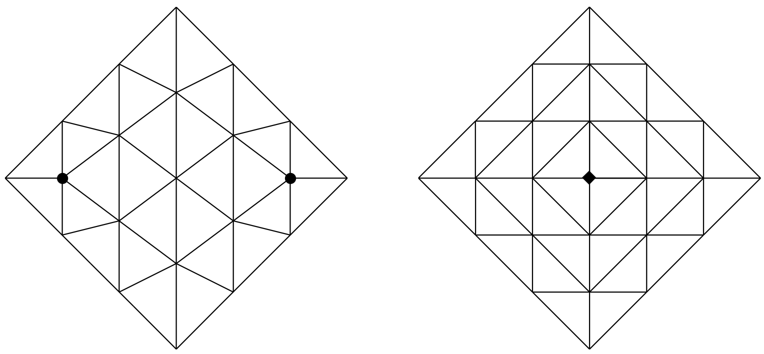

Figure 3.28: A 2-patch P (left) and the patch $P' = P^{2+}_{0,1,0}$ (right) which has the same boundary segmentation

We observe that $f(P) = 28$, $f(P') = 36$, and hence $C = f(P') - f(P) = 8$.

Now let $S := S(P, n - f(P))$ be the spiral containing P and a total number of $n \geq 28$ faces. Replacing P by P' yields the spiral $S_{n',0,1,0}$ with $n' = n + 8$.

We apply the respective formula from table 3.2 to $S_{n',0,1,0}$ and obtain:

$$\begin{aligned} b(S) = b(S_{n',0,1,0}) &= 2\left\lceil \frac{1}{2}(n' + \sqrt{4n'}) \right\rceil - n' \\ &= 2\left\lceil \frac{1}{2}(n + 8 + \sqrt{4(n+8)}) \right\rceil - (n + 8) \\ &= 2\left\lceil \frac{1}{2}(n + \sqrt{4n + 32}) \right\rceil - n \qquad (3.51) \end{aligned}$$

With this we have developed a formula for $b(S)$ in terms of the total number n of faces in S. Moreover, since S has minimal boundary length among all 2-patches containing P, (3.51) serves also as a lower bound for the number of faces in an arbitrary 2-patch that contains P and has a total number of $n \geq 28$ faces.

The case p=6

The problem in this case is that adding rings around $P_{6,0,0}$ or any other 6-patch does not change the boundary length. Therefore we cannot replace an arbitrary 6-patch by an extension of $P_{6,0,0}$, so the whole idea does not work. Instead, we solve the case $p = 6$ with the help of the already proven case $p = 5$.

Lemma 3.3.33 *If P is a regular 6-patch that does not contain $P_{6,0,0}$, then we have $b(P) \geq 6$.*

PROOF:

Suppose there is a counterexample with $b(P) < 6$. Then we must have $b(P) = 5$ because of the minimality of the boundary length of the spiral $S_{n,6,0,0}$ which fulfills $b(S_{n,6,0,0}) \geq 5$ (theorem 3.3.28).

W.l.o.g. we may assume that P cannot be reduced to a smaller regular 6-patch by removing rings, because in case there is a 6-patch P_0 and $k \in \mathbb{N}$ with $P = P_0^{k+}$, we have $b(P) = b(P_0)$ by lemma 3.3.13, so we could consider P_0 instead of P.

So we have five boundary edges such that the five inner vertices $v_1, \ldots, v_5$ which lie opposite to the boundary edges (see figure 3.29) do not all have degree 6 – otherwise we could remove the outer ring of boundary faces to obtain a smaller patch. Hence at least one of these vertices must have degree 5.

If we consider the subgraph $\hat{P}$ of P with $v_1, \ldots, v_5$ in its boundary, which is obtained by removing the five boundary vertices (and with this, the 10 boundary faces) of P, we conclude that it has $1 \leq \hat{p} \leq 5$ vertices of degree 5 in its interior. On the other hand $\hat{P}$ has boundary length 5, and this is only possible in case of $\hat{p} = 1$, since the boundary length of any p-patch with $2 \leq p \leq 5$ is at least 6 (corollary 3.3.30 (i)). This implies $\deg(v_i) = 5$ for $i = 1, \ldots, 5$ in P, and consequently $\deg(v_i) = 3$ for $i = 1, \ldots, 5$ in $\hat{P}$. But then we must have $\hat{P} = P_{1,0,0}$ and hence $P = P_{6,0,0}$, in contradiction to our assumption.

□

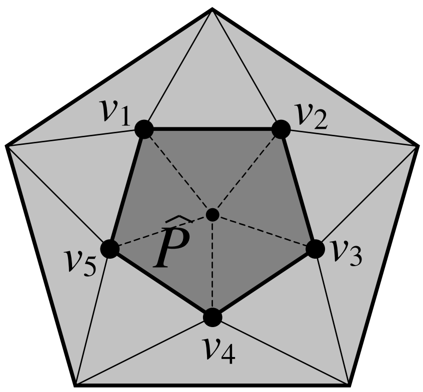

Figure 3.29: The proof of lemma 3.3.33: If P has boundary length 5, consider the patch $\hat{P}$ obtained by removing the boundary vertices of P. It has also boundary length 5, and if at least one of the vertices $v_1, \ldots, v_5$ has degree 5 in P, the subgraph $\hat{P}$ turns out to be equal to $P_{1,0,0}$.

Lemma 3.3.34 *Let P be a 6-patch and P' a 5-patch with $b(P) = b(P')$. Furthermore let $n \in \mathbb{N}$, $S := S(P,n)$, and $S' := S(P',n)$. Then we have*

$$b(S) \leq b(S') \ .$$

PROOF:

Since P is a 6-patch, $b(P^{k+}) = b(P)$ holds for any $k \in \mathbb{N}$ (lemma 3.3.13), so if we let k maximal such that P^{k+} is contained in S and define $a := f(S) - f(P^{k+})$ we have $b(S) = b(P)$ if $a = 0$, $b(S) = b(P) + 1$ if a is odd, and $b(S) = b(P) + 2$ if a is even and $a \neq 0$. Hence we have $b(S) \leq b(P) + 2$.

Furthermore, lemma 3.3.13 implies $b(P'^{+}) = b(P') + 1$ and $f_b(P'^{+}) = 2b(P') + 1$, that means $P'^{+} = S(P', 2b(P') + 1)$. So in case $n > 2b(P') + 1 = 2b(P) + 1$ we must even have $b(S') > b(P') + 1$, or equivalently

$$b(S') \geq b(P') + 2 = b(P) + 2 \geq b(S) \ .$$

For $n \leq 2b(P) + 1$, it is easy to check that $b(S) \leq b(S')$ holds, too: If $n \leq 2b(P) - 1$ we have $b(S) = b(S')$ (both is equal to $b(P) + 1$ in case n is odd, and $b(P) + 2$ in case n even and $n \neq 0$); for $n = 2b(P)$, we have $b(S) = b(P)$ and $b(S') = b(P') + 2 = b(P) + 2 > b(S)$; and in case $n = 2b(P) + 1$ we have $b(S) = 2b(P) + 1 = 2b(P') + 1 = b(S')$.

So $b(S) \leq b(S')$ applies in all cases, and the lemma is proven.

□

Theorem 3.3.35 *Let P be a regular 6-patch and $n \in \mathbb{N}_0$. Then $S(P,n)$ has minimal boundary length among all 6-patches containing P and n further faces.*

PROOF:

In case of $P = P_{6,0,0}$ or $P = P_{6,0,0}^{k+}$ for some $k \in \mathbb{N}$, the theorem already follows from theorem 3.3.28. Otherwise, we have $b(P) \geq 6$ by lemma 3.3.33, so we may assume $b(P) = l$ for some $l \geq 6$. We let Q be an arbitrary 6-patch containing P and n further faces, and define $S := S(P,n)$ – then we have to show $b(S) \leq b(Q)$.

A regular 5-patch P' with boundary length $b(P') = l$ exists for any $l \geq 6$: Just add the appropriate number of rings around $P_{5,0,0}$.

1. At first we assume $V_b(P) \cap V_b(Q) \neq \emptyset$, i.e. there exists a boundary vertex of Q which lies also in the boundary of P. Then we may always replace P by the regular 5-patch P' with $b(P') = b(P)$: Just make sure that the degree 3 vertex of P' lies in the boundary (see figure 3.30). This way we obtain a 5-patch Q' with $b(Q') = b(Q)$.

   If we define $S' := S(P',n)$ we have by lemma 3.3.34 $b(S) \leq b(S')$; and since P' is a 5-patch containing P' and n further faces, theorem 3.3.32 implies $b(S') \leq b(Q')$. All together we obtain:
   $$b(S) \leq b(S') \leq b(Q') = b(Q)$$

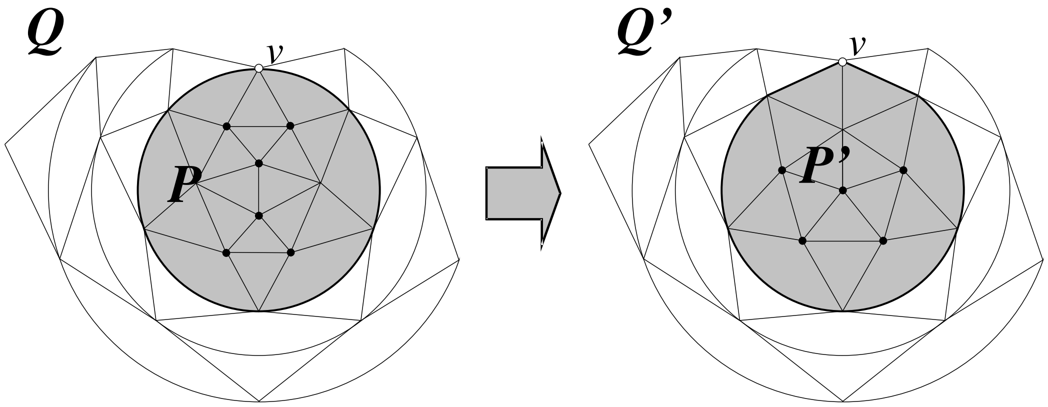

Figure 3.30: An example to demonstrate the proof of theorem 3.3.35, case 1.: If P has a boundary length of at least 6 and is subgraph of Q such that a boundary vertex v of P lies also in the boundary of Q, we may replace P by a regular 5-patch P' (here $P' = P_{5,0,0}$) with the same boundary length.

2. In case of $V_b(P) \cap V_b(Q) = \emptyset$, let k be maximal such that P^{k+} is subgraph of Q. Then we have $V_b(P^{k+}) \cap V_b(Q) \neq \emptyset$, so the first case applies: If $m := f(Q) - f(P^{k+})$ denotes the number of faces in Q that do not lie in P^{k+}, then

$$b(S(P^{k+}, m)) \leq b(Q)$$

holds. But since $S = S(P, n) = S(P^{k+}, m)$ this means $b(S) \leq b(Q)$.

□

3.3.5 Triangle-patches with fixed non-regular subgraphs

In the previous subsection we have shown that given a *regular* p-patch P with $0 \leq p \leq 6$, the spiral $S(P, n)$ has minimal boundary length among all p-patches containing P and n further faces. If P is not regular, it is hard to show a similar statement because it may not be possible to extend P arbitrarily (for instance, if the boundary contains two neighbouring vertices of degree 6). But we could ask the following question: Given a p-patch P that is not regular but has at least a *nice boundary* (this can happen for $0 \leq p \leq 4$), which is the p-patch with minimal boundary length containing P and a given number of n further faces? We will answer this question for the case where n is large enough such that P can be extended to a spiral. At first we show that each patch with a nice boundary can be extended to a regular patch (lemma 3.3.40). For the cases $p = 0$ and $p = 1$ we need also lemma 3.3.37.

Definition 3.3.36 *A p-patch is called* convex *if its boundary contains only vertices of degree* 2*,* 3*, and* 4*.*

In particular, a patch with a nice boundary is also convex. In the following we denote the infinite triangular lattice with one vertex of degree 5 and all others of degree 6 by L_1, and the triangular lattice with all vertices of degree 6 by L_0.

Lemma 3.3.37 *For $p \in \{0, 1\}$, any p-patch P that is convex is subgraph of the lattice L_p.*

PROOF:

We proceed by induction in the boundary length b. The patch with minimal boundary length in case $p = 0$ is the one consisting of only one face, which is obviously subgraph of L_0 and fulfills $b = 3$, and in case $p = 1$ the patch $P_{1,0,0}$, which is subgraph of L_1 and fulfills $b = 5$. All other patches have a longer boundary, so now assume $b > 3$ resp. $b > 5$.

In case there is a degree 2 vertex z in the boundary of P, remove z, and by this the corresponding face. Let x and y be the vertices adjacent to z; then $\{x, y\}$ is now a boundary edge, w.l.o.g. such that the unbounded face lies on the left hand side of the directed edge (x, y). By removing z, the degrees of x and y have been reduced by 1. Because of $b > 3$ none of them could have had degree 2, so the result is still a patch, and since no other vertex degrees have changed it is still convex. Also, all inner vertices remain inner vertices, so in case of $p = 1$ we still have a 1-patch. The boundary length has been reduced by 1 so by induction the patch is subgraph of the lattice L_0 resp. L_1. Consider the position of x and y in the lattice and let z be the vertex adjacent to both of them which lies on the left hand side of (x, y). If we follow the boundary cycle starting with (x, y), we do not make any left turns because the boundary contains no vertices of degree 5 and 6. Hence z does not belong to the patch which is subgraph of the lattice, which means we may extend this subgraph by z and thus obtain the origin patch P as a subgraph in L_0 resp. L_1.

Now assume there is no degree 2 vertex in the boundary, that means we have exactly 6 (in case $p = 0$) resp. 5 (in case $p = 1$) vertices of degree 3 and all others of degree 4. Then choose one side $v_0, v_1, \ldots, v_n$ of P such that the unbounded face lies left of the directed path $v_0, v_1, \ldots, v_n$, and in case $p = 1$ such that none of the vertices $v_0, v_1, \ldots, v_n$ is adjacent to the degree 5 vertex (this is possible because of $b > 5$). We delete these vertices and with them the corresponding faces, which again reduces the boundary length by 1. Let w_0 resp. w_{n+1} be the boundary vertices adjacent to v_0 resp. v_n in P; then the degrees of w_0 and w_{n+1} are reduced by 1, the new boundary vertices $w_1, \ldots, w_n$ on the boundary segment between them have degree 4. Therefore we have again constructed a convex patch, which still contains the inner vertex of degree 5 in case $p = 1$ since it was not adjacent to the removed vertices. By induction this patch is subgraph of the respective lattice. The vertices $w_0, \ldots, w_{n+1}$ form a straight line and we consider the vertices $v_0, \ldots, v_n$ lying left of them such that v_i lies in one face with w_i and w_{i+1}. Then again, since the boundary cycle starting with w_0, w_1 does not make any left turns we may add these vertices to the patch, obtaining the patch P as a subgraph in L_0 resp. L_1.

□

Now we define a simple operation of adding faces to a p-patch with $p \in \{0, \ldots, 4\}$ which has a nice boundary:

Definition 3.3.38 *Let P be a p-patch with $p \in \{0, \ldots, 4\}$ and a nice boundary, and s a side of the boundary with length $k \geq 2$, consisting of the path $v_0, v_1, \ldots, v_k$. By* adding a row to side s *we mean constructing a new p-patch P' with a nice boundary which consists of P and $2k - 1$ further faces, such that all further faces contain at least one of the vertices $v_1, \ldots, v_{k-1}$ (see figure 3.31).*

Applied to a side with length k in a p-patch with $p \leq 3$ and hence three or more sides, this operation obviously yields a new side of length $k-1$ while the lengths of the two neighbouring

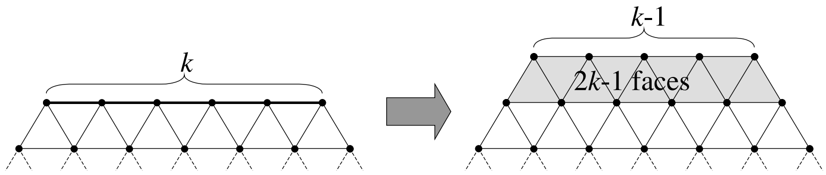

Figure 3.31: Adding a row to a side of length k

sides are extended by 1 and all other sides remain the same. In case of $p = 4$ the length of the side to which the operation is applied is reduced by 1 while the length of the other side grows by 2.

For an easier notation of the changes of the boundary segmentation when adding rows we define the following mapping:

Definition 3.3.39 *Let P be a p-patch with $p \in \{0, \ldots, 4\}$, a nice boundary and boundary segmentation $B(P) = (l_0, \ldots, l_{m-1})$, where $m = 6 - p$ denotes the number of sides.*

If $m \geq 3$ (or equivalently, $p \leq 3$), we define φ_i for $i = 0, \ldots, m-1$ as the mapping that maps $(l_0, \ldots, l_{m-1})$ onto $(l'_0, \ldots, l'_{m-1})$ where

$$l'_j = \begin{cases} l_j - 1 & \textit{if } j = i \\ l_j + 1 & \textit{if } j \in \{(i-1) \bmod m,\ (i+1) \bmod m\} \\ l_j & \textit{else} . \end{cases}$$

In case $m = 2$ and $p = 4$, P has only two sides of lengths l_0 and l_1, and we define ψ_i for $i = 0, 1$ such that $\psi_i(l_0, l_1) = (l'_0, l'_1)$ with $l'_i = l_i - 1$ and $l'_j = l_j + 2$ for $j \neq i$.

This way, $\varphi_i(l_0, \ldots, l_{m-1})$ resp. $\psi_i(l_0, l_1)$ gives the boundary segmentation of the patch we obtain after adding a row to the side corresponding to the $(i+1)$st entry, in this case the side of length l_i.

With the help of this operation we can extend p-patches with nice boundaries to other p-patches with nice boundaries and different boundary segmentation, and finally to regular patches, which will be realized in the proof of the following lemma.

Lemma 3.3.40 *For any p-patch P with $0 \leq p \leq 6$ and a nice boundary there is a regular p-patch $\bar{P}$ containing P.*

PROOF:

For $p = 5$ and $p = 6$ there is nothing to show, because in these cases a p-patch with a nice boundary is regular by definition, so we may choose $\bar{P} = P$. We distinguish the different cases for $p = 0, 1, 2, 3, 4$:

- Assume P is a 0-patch. By lemma 3.3.37 P is subgraph of the lattice L_0, so consider its embedding into the lattice. Choose an arbitrary vertex v in L_0 and let d be the maximal distance of any vertex in P to v. Then define $\bar{P}$ as the subgraph of L_0 containing all vertices whose distance to v is at most d; this yields a regular 0-patch with $B(\bar{P}) = (d, d, d, d, d, d)$ which contains P.

- If P is a 1-patch, it is by lemma 3.3.37 subgraph of the lattice L_1. Let v be the vertex with degree 5 in L_0 and let d be the maximal distance of any vertex in P to v. Now we define $\bar{P}$ as the subgraph of L_1 that contains all vertices with distance to v of at most d and obtain a regular 1-patch with $B(\bar{P}) = (d, d, d, d, d)$ containing P.

- Now consider the case $p = 2$, where the boundary of P consists of 4 sides. Let $B(P) = (a, b, c, d)$ and w.l.o.g. $\max_B(P) = a > 1$. We proceed by induction in $\Delta(P) = \max_B(P) - \min_B(P)$. For $\Delta(P) = 0$ we have four sides of the same length, so we may choose $\bar{P} = P$. In case $\Delta(P) = 1$ there is $k \in \mathbb{N}$ such that one of the following cases applies:

  - $B(P) = (k, k, k, k-1)$: Then we may choose $\bar{P} = P$ as well.
  - $B(P) = (k, k, k-1, k-1)$: Apply φ_0 and afterwards φ_1, so we obtain $\bar{P}$ with
  $$B(\bar{P}) = \varphi_1(\varphi_0(k, k, k-1, k-1)) = \varphi_1(k-1, k+1, k-1, k) = (k, k, k, k)\,.$$
  - $(k, k-1, k, k-1)$: Again we apply φ_0 and obtain $\bar{P}$ with
  $$B(\bar{P}) = \varphi_0(k, k-1, k, k-1) = (k-1, k, k, k)\,.$$
  - $(k, k-1, k-1, k-1)$: Apply φ_0 and afterwards φ_1 to get $\bar{P}$ with
  $$B(\bar{P}) = \varphi_1(\varphi_0(k, k-1, k-1, k-1)) = \varphi_1(k-1, k, k-1, k) = (k, k-1, k, k)\,.$$

  Hence in all cases, we may add faces in order to obtain a p-patch $\bar{P}$ with the required boundary segmentation, which of course contains P.

  Now let $\Delta(P) \geq 2$. The idea is to strictly reduce Δ by applying a finite number of adding-a-row operations.

  For this, we first add a row to the side of length a and obtain a patch P' with boundary segmentation
  $$B(P') = \varphi_0(a, b, c, d) = (a-1, b+1, c, d+1)\ .$$

  (i) Assume that a side with minimal length lies opposite of the side of length a, that means $\min_B(P) = c$. Then we have $\Delta(P) = a - c$ and hence (because $\Delta(P) \geq 2$ holds) $a \geq c + 2$. Furthermore, for symmetry reasons we may assume $b \geq d$.
  This yields $\min_B(P') = c$ and
  $$\max{}_B(P') = \begin{cases} b+1 & \text{if } b > a-2 \\ a-1 & \text{else}\ . \end{cases}$$
  In case $b \leq a-2$ this implies $\Delta(P') = (a-1) - c = \Delta(P) - 1$.
  Otherwise, if $b > a-2$ or equivalently $b \geq a-1$ holds, we have
  $$\Delta(P') = (b+1) - c \geq a - c = \Delta(P)\,.$$
  But then we apply a further operation φ_1 and obtain a p-patch P'' with
  $$B(P'') = \varphi_1(a-1, b+1, c, d+1) = (a, b, c+1, d+1)\,.$$
  We have
  $$\max{}_B(P'') = \begin{cases} d+1 & \text{if } d+1 > a \\ a & \text{else} \end{cases}$$

and $\min_B(P'') = c + 1$, for in this case $c + 1 \leq a - 1 \leq b$ holds.
In case $d + 1 \leq a$ we have

$$\Delta(P'') = a - (c + 1) = \Delta(P) - 1 .$$

Because of $a \geq b \geq d$, the condition $d + 1 > a$, or $d \geq a$, can only be fulfilled if $a = b = d$. Then we apply φ_3 to $(a, b, c+1, d+1) = (a, a, c+1, a+1)$ and obtain P''' with

$$B(P''') = \varphi_3(a, a, c + 1, a + 1) = (a + 1, a, c + 2, a)$$

and

$$\Delta(P''') = (a + 1) - (c + 2) = (a - c) - 1 = \Delta(P) - 1 .$$

(ii) Now assume that c is not minimal among $\{a, b, c, d\}$, and w.l.o.g. $d = \min_B(P)$. Then $c > d$ holds, and we have $\Delta(P) = a - d$ and hence $a \geq d + 2$. Furthermore we may assume $a > b$, because otherwise (i.e. $a = b$) we may choose $B(P) = (b, c, d, a)$ and case (i) applies.
This yields $\min_B(P') = d + 1$ and

$$\max{}_B(P') = \begin{cases} b + 1 & \text{if } b > a - 2 \\ c & \text{if } c > a - 1 \text{ and } b \leq a - 2 \\ a - 1 & \text{else .} \end{cases}$$

Because of $a > b$ we have $b > a - 2$ only in case $b = a - 1$. This implies

$$\Delta(P') = (b + 1) - (d + 1) = a - (d + 1) = \Delta(P) - 1 .$$

In the second case, $c > a - 1$ is only possible if $c = a$ (because of $a \geq c$), which means we have

$$\Delta(P') = c - (d + 1) = a - (d + 1) = \Delta - 1 .$$

Finally, if $b + 1 \leq a - 1$ and $c \leq a - 1$, we even have

$$\Delta(P') = (a - 1) - (d + 1) = (a - d) - 2 = \Delta(P) - 2 .$$

So in all cases there exists a 2-patch $\hat{P}$ with a nice boundary which contains P and fulfills $\Delta(\hat{P}) < \Delta(P)$. By induction, this means there is a 2-patch $\bar{P}$ containing $\hat{P}$ which has a nice boundary and the required boundary segmentation. Since P is subgraph of $\hat{P}$, it is also contained in $\bar{P}$, so the statement is proven for the case $p = 2$.

- Now consider the case $p = 3$. We let $B(P) = (a, b, c)$ and proceed again by induction in $\Delta(P)$. If $\Delta(P) = 0$ we already have $B(P) = (k, k, k)$ so there is nothing left to show. In case $\Delta(P) = 1$ we could have either $B(P) = (k, k, k - 1)$, which allows us to choose $\bar{P} = P$ again, or $B(P) = (k, k - 1, k - 1)$. In the latter case we apply φ_0 to obtain $\bar{P}$ with

$$B(\bar{P}) = \varphi_0(k, k - 1, k - 1) = (k - 1, k, k) .$$

Now let $\Delta(P) \geq 2$. W.l.o.g. we may assume $a \geq b \geq c$, which implies $\Delta(P) = a - c$ and hence $a \geq c + 2$. We apply φ_0 and obtain P' with

$$B(P') = \varphi_0(a, b, c) = (a - 1, b + 1, c + 1) .$$

Observe that $\min_B(P) = c + 1$ and

$$\max_B(P) = \begin{cases} b+1 & \text{if } b+1 > a-1 \\ a-1 & \text{else .} \end{cases}$$

In case $b + 1 \leq a - 1$ this implies $\Delta(P') = (a-1) - (c+1) = \Delta(P) - 2$.

If $b + 1 > a - 1$ holds, we can have (with $a \geq b$) either $b = a - 1$ or $b = a$. In the first case,

$$\Delta(P') = (b+1) - (c+1) = a - (c+1) = \Delta(P) - 1$$

holds. In case of $b = a$ we apply φ_1 to $(a-1, b+1, c+1) = (a-1, a+1, c+1)$ and obtain P'' with

$$B(P'') = \varphi_1(a-1, a+1, c+1) = (a, a, c+2)\ .$$

Then we have $\max_B(P'') = a$, $\min_B(P'') = c + 2$, and hence

$$\Delta(P') = a - (c+2) = \Delta(P) - 2\,.$$

With this we have shown that in any case there exists a 3-patch $\hat{P}$ containing P with a nice boundary and $\Delta(\hat{P}) < \Delta(P)$. By induction, there is a 3-patch $\bar{P}$ containing $\hat{P}$ and hence also P with a nice boundary and the required boundary segmentation, which proves the statement for $p = 3$.

- Now let $p = 4$, $B(P) = (a, b)$, and w.l.o.g. $a \geq b$. Again we proceed by induction in $\Delta(P)$.

  Obviously there is some $k \in \mathbb{N}$ with $B(P) = (k, k)$ in case of $\Delta(P) = 0$, and with $B(P) = (k, k-1)$ if $\Delta(P) = 1$, such that we may choose $\bar{P} = P$.

  So let $\Delta(P) \geq 2$ – then $a \geq b + 2$ holds. We apply ψ_0 to obtain a p-patch P' with $B(P') = \psi_0(a, b) = (a - 1, b + 2)$. In case $a \geq b + 3$ we have

$$\Delta(P') = (a-1) - (b+2) = (a-b) - 3 = \Delta(P) - 3\,.$$

  Otherwise $b + 2 \leq a < b + 3$ holds, that means $a = b + 2$, and hence

$$\Delta(P') = (b+2) - (a-1) = a - (a-1) = 1 < \Delta(P)\,.$$

  So in both cases $\Delta(P')$ is strictly smaller than $\Delta(P)$. Hence by induction there exists a 4-patch $\bar{P}$ containing P' and therefore also P with a nice boundary and the required boundary segmentation, which proves the statement for $p = 4$.

□

A further fundamental observation is that each of the patches $P_{p,s,t}$ that we considered before stands for one particular boundary type, such that for $\bar{p} \leq 4$, any $\bar{p}$-patch P with a nice boundary can be replaced by another patch containing one of the patches $P_{p,s,t}$. We will prove this in lemma 3.3.42.

For the case $p = 3$, the following small lemma turns out to be helpful:

Lemma 3.3.41 *Let P be a 3-patch with a nice boundary. Then it cannot contain two sides of length 1.*

PROOF:

Assume that there exists a counterexample, which we choose minimal with respect to its number of faces. Since there are only three sides, the two of length 1 must be adjacent, which means that the three vertices of degree 3 which lie in the boundary follow upon each other – all other boundary vertices have degree 4.

Let u, v, and w denote the boundary vertices with degree 3, such that $\{u, v\}, \{v, w\} \in E(P)$. Let x be the third vertex adjacent to v. Since all faces are triangles it must also be adjacent to u and v. Furthermore let y be the third vertex adjacent to u, and z the third vertex adjacent to w. These in turn must also be neighbours of x since the respective faces form triangles, and both lie in the boundary because of $\deg(u) = \deg(w) = 3$, such that we have $\deg(y) = \deg(z) = 4$. Now assume $\deg(x) = 6$. Then we may remove u, v, and w to obtain a smaller counterexample where y, x, and z have degree 3 (see figure 3.32, left picture).

This is a contradiction to the assumption, so we must have $\deg(x) = 5$. But then – again with the requirement that all faces have to be triangles – we conclude that the edge $\{y, z\}$ must exist. Since y and z both have degree 4 this means they can only have one further neighbour which must be the same for both vertices because it has to form a triangle with x and y (see figure 3.32, right picture). But then this vertex either has degree 2 or is a cutvertex, both yielding a contradiction. Hence the counterexample does not exist.

□

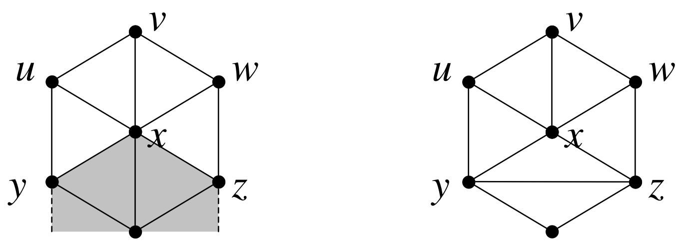

Figure 3.32: The situation in the proof of lemma 3.3.41: Left the case $\deg(x) = 6$, right the case $\deg(x) = 5$

Lemma 3.3.42 *Let P be a $\bar{p}$-patch with a nice boundary, and $0 \leq \bar{p} \leq 4$. Then there exists $(p, s, t) \in \{(0,0,0), (1,0,0), (2,0,0), (3,0,0), (4,0,0), (0,1,0), (1,1,0), (2,1,0)\}$ such that $D(p, s, t) = \bar{p}$, and a (p, s, t)-patch P' with a nice boundary and the same boundary segmentation as P that contains the (p, s, t)-patch $P_{p,s,t}$ as a subgraph.*

PROOF:

For $\bar{p} = 0$ and $\bar{p} = 1$, the lemma is obviously true, for in these cases the patch P itself has to contain $P_{0,0,0}$ or $P_{1,0,0}$, respectively. The cases $\bar{p} = 2$, $\bar{p} = 3$, and $\bar{p} = 4$ are going to be solved separately:

- The case $\bar{p} = 2$:

  Let P be a 2-patch, that means it contains two degree 5 vertices x and y. Since P is convex, the set of shortest paths between x and y spans a 'parallelogram' as depicted in figure 3.33 which is a subgraph of the triangular lattice and has only boundary vertices of degree 4 except two of degree 2 (that are x and y) and two of degree 3, inducing four boundary segments where the respective opposite lying segments have the same length. This way, we may transfer the concept of Coxeter coordinates (see definition 2.3.1) also to this case and assume that x and y have 'Coxeter coordinates' (p, q) or (q, p), meaning the lengths of the sides of the parallelogram induced by them.

  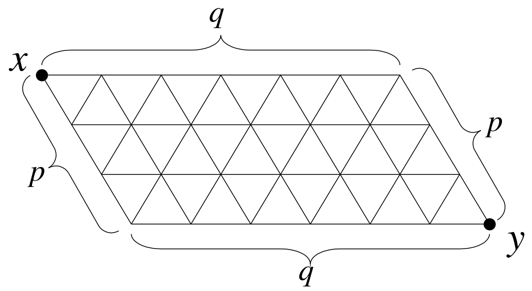

  Figure 3.33: A parallelogram spanned by x and y

  W.l.o.g. we assume $q \geq p$; otherwise we just exchange the parts of p and q in the following.

  In case $(q-p) \bmod 3 = 0$, that means $\frac{q-p}{3} \in \mathbb{N}_0$, we may construct a $(0,1,0)$-patch $\hat{P}$ with a nice boundary and boundary segmentation $B(\hat{P}) = (p, q, p, q)$: Start with $P_{0,1,0}^{(k-1)+}$, where $k = \frac{2}{3}p + \frac{1}{3}q = \frac{q-p}{3} + p$, and add $\frac{q-p}{3}$ rows to two opposite lying sides. Then these sides obtain length $k - \frac{q-p}{3} = p$, the other two $k + 2\frac{q-p}{3} = q$. We replace the parallelogram in P by $\hat{P}$. Note that in $\hat{P}$ the vertices where two sides meet have degree 3 and not 2, so the replacement increases the degrees of x and y by 1. Hence we obtain a $(0,1,0)$-patch P' with the same boundary segmentation as P that contains $P_{0,1,0}$ as a subgraph.

  In case $(q-p) \bmod 3 = 1$, we have $\frac{q-p-1}{3} \in \mathbb{N}_0$ and choose $P_{2,0,0}^{(k-2)+}$ with $k = \frac{2p+q+2}{3} = \frac{q-p-1}{3} + p + 1$. It fulfills $B(P_{2,0,0}^{(k-2)+}) = (k, k-1, k, k-1)$. To both sides of length $k-1$ we add $\frac{q-p-1}{3}$ rows. Then these sides obtain length $k - 1 - \frac{q-p-1}{3} = p$ while the other two sides get length $k + 2\frac{q-p-1}{3} = q$. Thus we have constructed a $(2,0,0)$-patch $\hat{P}$ with a nice boundary which contains $P_{2,0,0}$ and has the boundary segmentation $B(\hat{P}) = (p, q, p, q)$. Again we replace the parallelogram in P by $\hat{P}$ and obtain the desired patch P' with $B(P') = B(P)$.

  Finally let $(q-p) \bmod 3 = 2$ – then we have $\frac{q-p+1}{3} \in \mathbb{N}$. Consider $P_{2,0,0}^{(k-2)+}$ with $k = \frac{2p+q+1}{3} = \frac{q-p+1}{3} + p$; it fulfills $B(P_{2,0,0}^{(k-2)+}) = (k, k-1, k, k-1)$. To both sides of length k we add $\frac{q-p+1}{3}$ rows. Then these sides obtain length $k - \frac{q-p+1}{3} = p$, the other two sides length $k - 1 + 2\frac{q-p+1}{3} = q$. Again we have a $(2,0,0)$-patch $\hat{P}$ containing $P_{2,0,0}$ with $B(\hat{P}) = (p, q, p, q)$ and replace the parallelogram in P by $\hat{P}$, obtaining a patch P' with the boundary segmentation $B(P') = B(P)$.

- The case $\bar{p} = 3$:

  Now let P be a 3-patch with a nice boundary. Let $B(P) = (a, b, c)$ be its boundary segmentation, w.l.o.g. with $a \leq b \leq c$. By lemma 3.3.41 we cannot have $a = b = 1$ so $b \geq 2$ must hold.

  At first we show that in case a, b, c are all even or odd, we can construct a 3-patch P' containing $P_{3,0,0}$ with $B(P') = (a, b, c)$: Let $k = \frac{a+b}{2}$. Since a, b are both even or both uneven, we have $k \in \mathbb{N}$, and $k \geq 2$ holds because of $b \geq 2$. So $P_{3,0,0}^{(k-2)+}$ is well-defined and fulfills $B(P_{3,0,0}^{(k-2)+}) = (k, k, k)$. Then we add $\frac{c-b}{2} \in \mathbb{N}_0$ rows to one side, obtaining the new boundary segmentation $(k + \frac{c-b}{2}, k - \frac{c-b}{2}, k + \frac{c-b}{2})$. Afterwards we add $\frac{c-a}{2} \in \mathbb{N}_0$ rows to one of the sides with length $k + \frac{c-b}{2}$. The boundary segmentation of the resulting patch P' is:

$$\begin{aligned} B(P') &= (k + \frac{c-b}{2} - \frac{c-a}{2}, k - \frac{c-b}{2} + \frac{c-a}{2}, k + \frac{c-b}{2} + \frac{c-a}{2}) \\ &= (\frac{a+b}{2} + \frac{c-b}{2} - \frac{c-a}{2}, \frac{a+b}{2} - \frac{c-b}{2} + \frac{c-a}{2}, \frac{a+b}{2} + \frac{c-b}{2} + \frac{c-a}{2}) \\ &= (a, b, c) \ = \ B(P) \end{aligned}$$

  Now consider the other case where not all of a, b, c are even neither odd. Then we show that there exists a $(1, 1, 0)$-patch P' containing $P_{1,1,0}$ with $B(P') = (a, b, c)$:

  First assume we have either a and b even (and hence c odd), or a and b odd (and c even). Then let $k = \frac{a+b}{2} \in \mathbb{N}$ and consider $P_{1,1,0}^{(k-2)+}$, which fulfills $B(P_{1,1,0}^{(k-2)+}) = (k, k, k-1)$. We add $\frac{c-b+1}{2} \in \mathbb{N}$ rows to one of the sides with length k and obtain the boundary segmentation $(k + \frac{c-b+1}{2}, k - \frac{c-b+1}{2}, k - 1 + \frac{c-b+1}{2})$. Next we add $\frac{c-a+1}{2} \in \mathbb{N}$ rows to the side of length $k + \frac{c-b+1}{2}$, yielding a patch P' with boundary segmentation

$$\begin{aligned} B(P') &= (k + \frac{c-b+1}{2} - \frac{c-a+1}{2}, k - \frac{c-b+1}{2} + \frac{c-a+1}{2}, \\ &\qquad k - 1 + \frac{c-b+1}{2} + \frac{c-a+1}{2}) \\ &= (\frac{a+b}{2} + \frac{c-b+1}{2} - \frac{c-a+1}{2}, \frac{a+b}{2} - \frac{c-b+1}{2} + \frac{c-a+1}{2}, \\ &\qquad \frac{a+b}{2} - 1 + \frac{c-b+1}{2} + \frac{c-a+1}{2}) \\ &= (a, b, c) \ = \ B(P) \ . \end{aligned}$$

  Secondly, let either a odd, b and c even, or a even, b and c odd. Then we define $k = \frac{a+b+1}{2} \in \mathbb{N}$ and start with $P_{1,1,0}^{(k-2)+}$, again with $B(P_{1,1,0}^{(k-2)+}) = (k, k, k-1)$. Adding $\frac{c-b}{2} \in \mathbb{N}_0$ rows to one of the sides with length k yields the boundary segmentation $(k + \frac{c-b}{2}, k - \frac{c-b}{2}, k - 1 + \frac{c-b}{2})$. Afterwards we add $\frac{c-a-1}{2}$ rows to the side of length $k + \frac{c-b}{2}$ and obtain a patch P' with boundary segmentation

$$\begin{aligned} B(P') &= (k + \frac{c-b}{2} - \frac{c-a-1}{2}, k - \frac{c-b}{2} + \frac{c-a-1}{2}, k - 1 + \frac{c-b}{2} + \frac{c-a-1}{2}) \\ &= (\frac{a+b+1}{2} + \frac{c-b}{2} - \frac{c-a-1}{2}, \frac{a+b+1}{2} - \frac{c-b}{2} + \frac{c-a-1}{2}, \\ &\qquad \frac{a+b+1}{2} - 1 + \frac{c-b}{2} + \frac{c-a-1}{2}) \\ &= (a, b, c) \ = \ B(P) \ . \end{aligned}$$

- The case $\bar{p} = 4$:

  Finally we assume that P is a 4-patch with a nice boundary. Let $B(P) = (a, b)$ be its boundary segmentation and w.l.o.g. $a \leq b$. By lemma 3.3.29 we have $b(P) = a+b \geq 6$. At first let $(b-a) \bmod 3 = 0$, that means $\frac{b-a}{3} \in \mathbb{N}_0$. Then we define $k = \frac{2}{3}a + \frac{1}{3}b = \frac{b-a}{3} + a$, which must be in $\mathbb{N}_0$. Furthermore we have $k = \frac{2}{3}a + \frac{1}{3}b = \frac{1}{3}(a+b) + \frac{1}{3}a \geq \frac{7}{3}$ because $a + b \geq 6$ and $a \geq 1$, and hence $k \geq 3$. Consequently, the patch $P_{4,0,0}^{(k-3)+}$ is well-defined and we have $B(P_{4,0,0}^{(k-3)+}) = (k, k)$. If we add $\frac{b-a}{3}$ rows to one side we get the desired 4-patch P' with boundary segmentation

$$\begin{aligned} B(P') &= (k - \frac{b-a}{3},\ k + 2\frac{b-a}{3}) \\ &= (\frac{2a+b}{3} - \frac{b-a}{3},\ \frac{2a+b}{3} + 2\frac{b-a}{3}) \\ &= (a, b) \ = \ B(P)\ . \end{aligned}$$

  Now suppose that $(b-a) \bmod 3 = 1$ holds, and hence $\frac{b-a-1}{3} \in \mathbb{N}_0$. Then we define $k = \frac{2a+b+2}{3}$, which is equal to $\frac{b-a-1}{3} + a + 1$ and thus in $\mathbb{N}$. With $a \geq 1$ and $a + b \geq 6$ we have $k = \frac{a+(a+b)+2}{3} \geq \frac{9}{3} = 3$, so $P_{2,1,0}^{(k-3)+}$ is well-defined. Obviously $B(P_{2,1,0}^{(k-3)+}) = (k-1, k)$ holds. We add $\frac{b-a-1}{3}$ rows to the side of length $k-1$ and obtain a $(2,1,0)$-patch P' with the boundary segmentation

$$\begin{aligned} B(P') &= (k - 1 - \frac{b-a-1}{3},\ k + 2\frac{b-a-1}{3}) \\ &= (\frac{2a+b+2}{3} - 1 - \frac{b-a-1}{3},\ \frac{2a+b+2}{3} + 2\frac{b-a-1}{3}) \\ &= (a, b) \ = \ B(P)\ . \end{aligned}$$

  Finally let $(b-a) \bmod 3 = 2$, that means $\frac{b-a+1}{3} \in \mathbb{N}_0$. Then we choose $k = \frac{2a+b+1}{3} = \frac{b-a+1}{3} + a \in \mathbb{N}$. Because of $a + b \geq 6$ and $a \geq 1$ we have $k = \frac{a+(a+b)+1}{3} \geq \frac{8}{3}$ and hence even $k \geq 3$, which means $P_{2,1,0}^{(k-3)+}$ is well-defined. Again $B(P_{2,1,0}^{(k-3)+}) = (k-1, k)$ holds. Adding $\frac{b-a+1}{3}$ rows to the side of length k yields a $(2,1,0)$-patch P' with the boundary segmentation

$$\begin{aligned} B(P') &= (k - \frac{b-a+1}{3},\ k - 1 + 2\frac{b-a+1}{3}) \\ &= (\frac{2a+b+1}{3} - \frac{b-a+1}{3},\ \frac{2a+b+1}{3} - 1 + 2\frac{b-a+1}{3}) \\ &= (a, b) \ = \ B(P)\ . \end{aligned}$$

□

Lemma 3.3.43 *Let P be a regular (p,s,t)-patch with $D(P) = D(p,s,t) \in \{2,3,4\}$, v a vertex in the boundary of P with degree 3 that lies in a side of P with minimal length, C_v its boundary cycle split up at the vertex v, and φ an embedding of C_v into the triangular lattice L (see definition 2.3.6).*

Furthermore let x be the starting point of $\varphi(C_v)$ and y the ending point. Then if α is a clockwise rotation by $D(P) \cdot 60$ degrees around a center c such that $\alpha(y) = x$, c is a vertex of the lattice if and only if $\Delta(P) = 0$.

PROOF:

We distinguish the different cases for $D(P)$ and $\Delta(P)$.

(1) $D(P) = 2$, $\Delta(P) = 0$: Then we have $B(P) = (k, k, k, k)$ for some $k \in \mathbb{N}$. Considering the embedding of C_v we observe that in this case, $\text{Cox}(\{x, y\}) = (k, k)$ must hold (see also figure 3.34,(1)). Since α is a rotation by 120 degrees, c can be determined as the center of the regular hexagon with all sides of length k that is obtained by extending the embedding of C_v, or equivalently, as the center of a regular triangle where x and y are two vertices. Due to lemma 2.3.2 this means that c is a vertex of the lattice.

(2) $D(P) = 2$, $\Delta(P) = 1$: Then there is $k \in \mathbb{N}$ with $B(P) = (k-1, k, k, k)$. Extending $\varphi(C_v)$ to a hexagon, we obtain one further side of length $k-1$ and one of length $k+1$, such that $\text{Cox}(\{x, y\}) \in \{(k-1, k+1), (k+1, k-1)\}$ (figure 3.34,(2)). Since c must have equal distances to x and y and the angle formed by the lines joining c with x and c with y must be of 120 degrees, c can be determined as the center of a regular triangle with the line joining x and y as one side. Then the Coxeter coordinates of x and y imply that c lies in the center of a face of the lattice (lemma 2.3.2) – so it is *not* a vertex of the lattice.

(3) $D(P) = 3$, $\Delta(P) = 0$: Then $B(P) = (k, k, k)$ holds for some $k \in \mathbb{N}$. This means for the embedding of C_v that x and y lie on a straight line that coincides with a line of the lattice and have distance $2k$ (see figure 3.34,(3)), so we have $\text{Cox}(\{x, y\}) = (2k)$. Since the angle corresponding to α is now of 180 degrees, c must lie on the center of the line joining x and y, which is obviously the vertex with distance k to both x and y – so c is a vertex of the lattice.

(4) $D(P) = 3$, $\Delta(P) = 1$: Then we have $B(P) = (k-1, k, k)$ with $k \in \mathbb{N}$. We observe that $\text{Cox}(\{x, y\}) \in \{(k-1, k+1), (k+1, k-1)$ (figure 3.34,(4)), and again c must lie on the center of the straight line joining x and y, which is the center of an edge in this case – meaning that c does not coincide with a vertex of the lattice.

(5) $D(P) = 4$, $\Delta(P) = 0$: Then $B(P) = (k, k)$ holds for $k \in \mathbb{N}$, which obviously means $\text{Cox}(\{x, y\}) = (k, k)$. Now the angle formed by α is of 240 degrees, implying that c lies again in the center of a regular triangle where x and y form one side (figure 3.34,(5)), and since $\text{Cox}(\{x, y\}) = (k, k)$ this means that c must be a vertex of the lattice (lemma 2.3.2).

(6) $D(P) = 4$, $\Delta(P) = 1$: Then we have $B(P) = (k-1, k)$ and hence $\text{Cox}(\{x, y\}) \in \{(k-1, k), (k, k-1)\}$. As in the previous case c lies in the center of a regular triangle with x and y as vertices (figure 3.34,(6)), and now the Coxeter coordinates of x and y imply that c lies in the center of a face (lemma 2.3.2) and therefore does not coincide with a vertex of the lattice.

□

Lemma 3.3.44 *Let $(p, s, t) \in \{(2,0,0), (3,0,0), (4,0,0), (0,1,0), (1,1,0), (2,1,0)\}$, and consider two regular (p, s, t)-patches P and P', where P' is subgraph of P. Then we have*

$$\Delta(P) = \Delta(P') .$$

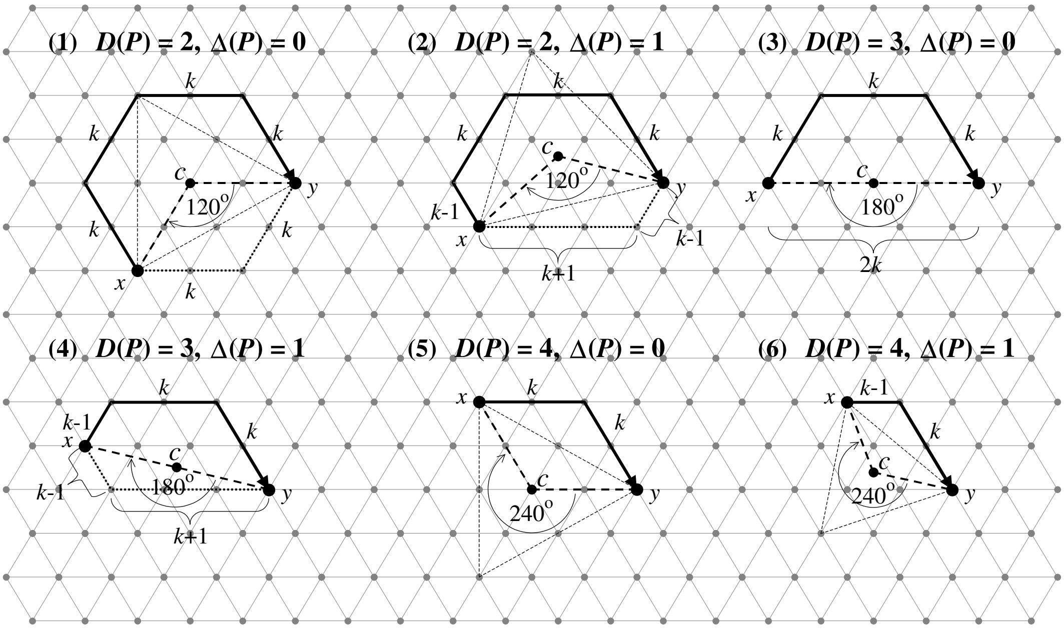

Figure 3.34: Determining the position of c in the cases (1) to (6) that are discussed in the proof of lemma 3.3.43 (for the picture we chose $k = 2$)

PROOF:

Let v be a vertex in the boundary of P with degree 3 that lies in a side of P with minimal length, and w a vertex in the boundary of P' with degree 3 that lies in a side of $\hat{P}$ with minimal length. We consider a cutpath in P with respect to P', v, and w (see definition 2.5.1). Let C_v be the boundary cycle split up at the vertex v, and φ an embedding of C_vXYZ into the triangular lattice L.

Then by lemma 2.5.2 (note that $D(P) \bmod 6 \neq 0$ applies) we have that the inverse path of $\varphi(Z)$ is the image of a clockwise rotation α of $\varphi(X)$ by $D(P) \cdot 60$ degrees around a uniquely determined center c.

In particular, if v_1 denotes the starting vertex of $\varphi(X)$, v_2 the ending vertex of $\varphi(X)$ and starting vertex of $\varphi(Y)$, v_3 the ending vertex of $\varphi(Y)$ and starting vertex of $\varphi(Z)$, and v_4 the ending vertex of $\varphi(Z)$, this means $\alpha(v_1) = v_4$ and $\alpha(v_2) = v_3$ (see figure 3.35).

Since the inverse path of $\varphi(Y)$ (with starting vertex v_3 and ending vertex v_2) is an embedding of the boundary cycle of P' split up at w, lemma 3.3.43 can be applied: α is a clockwise rotation by $D(P) \cdot 60$ degrees around a center c which fulfills $\alpha(v_2) = v_3$ – so by lemma 3.3.43 we get that c is a vertex of the lattice if and only if $\Delta(P') = 0$.

On the other hand, v_4 is the starting vertex and v_1 the ending vertex of $\varphi(C_v)$, and we have $\alpha(v_1) = v_4$. So again by lemma 3.3.43, c is a vertex of the lattice if and only if $\Delta(P) = 0$.

But this means that in case c is a vertex of the triangular lattice we must have $\Delta(P') = 0 = \Delta(P)$, and in case it is no vertex of the lattice $\Delta(P') = 1 = \Delta(P)$; so in any case $\Delta(P') = \Delta(P)$ holds.

□

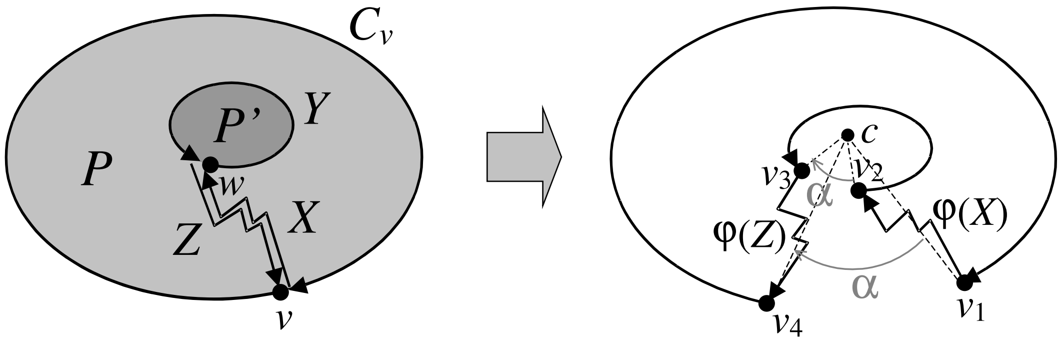

Figure 3.35: The sketch of a cutpath in P with respect to P', v, and w, and its embedding into the lattice

Now we have prepared everything to prove the main theorem of this section:

Theorem 3.3.45 *Given a p-patch P with a nice boundary, $0 \leq p \leq 4$, and a regular p-patch $\bar{P}$ containing P. Furthermore let $n \in \mathbb{N}$ with $n \geq f(\bar{P}) - f(P)$, and $m := n - (f(\bar{P}) - f(P))$. Then the spiral $S(\bar{P}, m)$ has minimal boundary length among all p-patches containing P and n further faces.*

PROOF:

Since P is a subgraph of $\bar{P}$, the spiral $S(\bar{P}, m)$ contains P and has $m + f(\bar{P}) = n + f(P)$ faces in total, and hence n faces apart from the faces in P.

By lemma 3.3.42 there exists a (p', s, t)-patch P' with

$$(p', s, t) \in \{(0,0,0),(1,0,0),(2,0,0),(3,0,0),(4,0,0),(0,1,0),(1,1,0),(2,1,0)\}$$

that contains $P_{p',s,t}$ as a subgraph and fulfills $B(P') = B(P)$.

Hence we may replace P in $\bar{P}$ by P'. This yields a regular (p', s, t)-patch $\hat{P}$ containing $P_{p',s,t}$ (see figure 3.36). Then by lemma 3.3.44, $\hat{P}$ fulfills

$$\Delta(\hat{P}) = \Delta(P_{p',s,t}) = \Delta(P^{k+}_{p',s,t})$$

for any $k \in \mathbb{N}$. Hence there is $k \in \mathbb{N}$ with $B(\hat{P}) = B(P^{k+}_{p',s,t})$. By theorem 2.5.3 from chapter 2, this implies

$$f(\hat{P}) = f(P^{k+}_{p',s,t}) \ . \tag{3.52}$$

Since we replaced P in $\bar{P}$ by P' to obtain $\hat{P}$, the number of faces in $\bar{P}$ that do not lie in P is equal to the number of faces in $\hat{P}$ that do not lie in P', so we have:

$$f(\bar{P}) - f(P) = f(\hat{P}) - f(P') \tag{3.53}$$

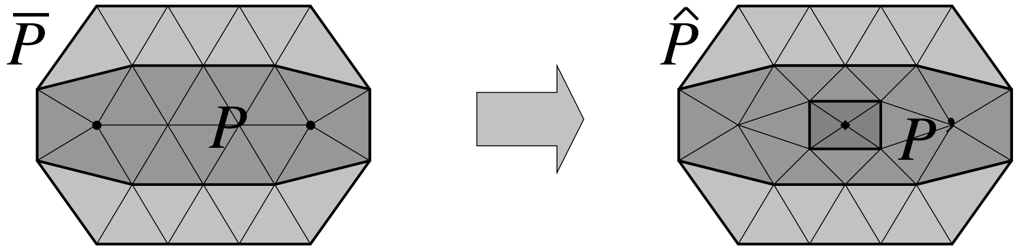

Figure 3.36: An example of a p-patch P with a nice boundary which is subgraph of a regular p-patch $\bar{P}$ (here $p = 2$), and the patch $\hat{P}$ obtained by replacing P in $\bar{P}$ by a patch P' that contains $P_{p',s,t}$ (here $P_{0,1,0}$) as a subgraph.

Now let Q be an arbitrary p-patch containing P and n further faces, that means we have $f(Q) = f(P) + n$. Replacing P in Q by P' yields a (p', s, t)-patch Q'.

Since Q' contains P' and n further faces, its number of faces is given by

$$f(Q') = f(P') + n = f(P_{p',s,t}) + (f(P') - f(P_{p',s,t}) + n) \; .$$

Therefore the spiral

$$S' := S\left(P_{p',s,t},\; f(P') - f(P_{p',s,t}) + n\right)$$

containing $P_{p',s,t}$ and $f(P') - f(P_{p',s,t}) + n$ further faces has the same number of faces as Q', that means $f(S') = f(Q') = f(P') + n$. Then by theorem 3.3.28 we have $b(S') \le b(Q')$. Moreover, S' does not only contain $P_{p',s,t}$ but even $P^{k+}_{p',s,t}$: We have

$$\begin{aligned} f(S') &= f(P') + n \\ &\overset{(3.53)}{=} f(\hat{P}) - (f(\bar{P}) - f(P)) + n \\ &= f(\hat{P}) + m \qquad\qquad \text{(by definition of } m\text{)} \\ &\overset{(3.52)}{=} f(P^{k+}_{p',s,t}) + m \end{aligned}$$

and since $m \ge 0$ this implies $S' = S(\hat{P}, m)$.

Now replace $P^{k+}_{p',s,t}$ in S' by $\bar{P}$. We obtain the spiral $S(\bar{P}, m)$ with

$$b(S(\bar{P}, m)) = b(S') \le b(Q') = b(Q) \; .$$

□

Figure 3.37 visualizes the main ideas of the proof of this theorem.

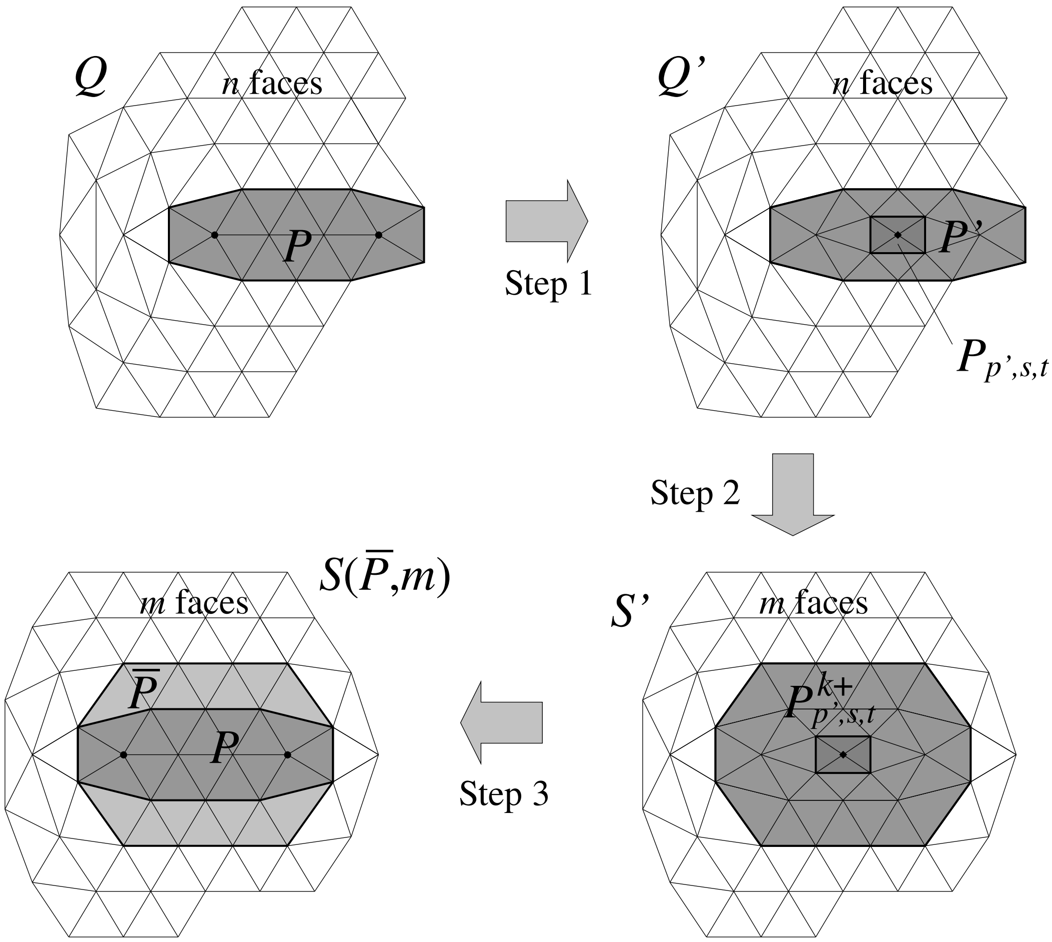

Figure 3.37: The idea of the proof of theorem 3.3.45. Step 1: Replace P in Q by P' to obtain Q'. Step 2: Define S' as the spiral with respect to $P_{p',s,t}$ that has the same number of faces as Q' (then a former theorem implies $b(S') \leq b(Q')$), and show that it contains even $P^{k+}_{p',s,t}$ with $B(P^{k+}_{p',s,t}) = B(\bar{P})$ and that m is the number of additional faces. Step 3: Replace $P^{k+}_{p',s,t}$ by $\bar{P}$ to obtain $S(\bar{P}, m)$.

So we have now shown that given a p-patch P with a nice boundary and $0 \leq p \leq 6$ (the cases $p = 5$ and $p = 6$ have already been examined in the previous subsection because then having a nice boundary is equivalent to being regular), a minimal boundary length for a fixed number of faces is obtained by extending P to a regular patch and afterwards adding faces around it in a spiral way as before – if the number of faces is large enough such that this construction is possible. In case the desired total number of faces is smaller than the number of faces in the respective regular patch, we have not proven how a patch with minimal boundary length containing P looks like.

However, formulas giving a lower bound on the boundary length can be developed in the same way as in the section before, even if the given number of faces is small: Just replace P by the patch P' with the same boundary containing a patch of the type $P_{p',s,t}$, whose existence is guaranteed by lemma 3.3.42, and apply the known formula for (p', s, t). This method does even work for arbitrary p-patches with $0 \leq p \leq 5$ and the property that a patch P' with the same boundary and containing a patch of the type $P_{p',s,t}$ exists! We give an example:

Let P be the 3-patch that is shown in figure 3.38 on the left. There exists a $(1,1,0)$-patch P' with the same boundary that contains $P_{1,1,0}$ (figure on the right). We have $f(P) = 11$ and $f(P') = 13$.

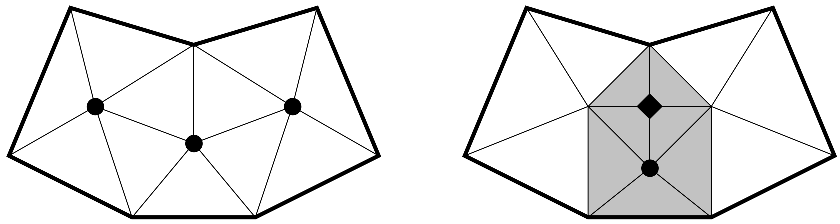

Figure 3.38: A 3-patch P (left) and a $(1,1,0)$-patch P' with the same boundary that contains $P_{1,1,0}$ (right)

Now let Q be an arbitrary 3-patch containing P which has $n := f(Q)$ faces. Then we may replace P by P' and obtain a $(1,1,0)$-patch Q' with $b(Q') = b(Q)$ and $n' := f(Q') = f(Q) + 2 = n + 2$. Applying the boundary formula for $(1,1,0)$-patches given in table 3.2 to Q' yields:

$$\begin{aligned}
b(Q) \;=\; b(Q') &\geq 2\lceil \frac{1}{2}(n' + \sqrt{3n'+4})\rceil - n' \\
&= 2\lceil \frac{1}{2}((n+2) + \sqrt{3(n+2)+4})\rceil - (n+2) \\
&= 2\lceil 1 + \frac{1}{2}(n + \sqrt{3n+10})\rceil - n - 2 \\
&= 2\lceil \frac{1}{2}(n + \sqrt{3n+10})\rceil - n
\end{aligned}$$

Note that this lower bound we obtained for the boundary length of Q is better than the bound we obtain from table 3.2 for general 3-patches, which would be

$$b(Q) \geq 2\lceil \frac{1}{2}(n + \sqrt{3n+6})\rceil - n\ .$$

Chapter 4

Possible boundaries of cones

4.1 Introduction

A *nanotube* is a special fullerene with a tubetype shape that consists of two *caps*, both containing hexagons and exactly six pentagons, and a long body consisting only of hexagons, which can be imagined like a sheet of graphite lattice rolled up into a seamless cylinder. While a nanotube has a diameter of only a few nanometers, its length can be many thousands of times longer.

Nanotubes were first discovered by Sumio Iijima in 1991 [28] and since then, they have been the subject of many studies. Their remarkable electrical properties and extraordinary strength make them useful in many applications in nanotechnology, electronics, optics and other fields of materials science (see e.g. [41], [42], [46]).

Considering the graph of a nanotube, it is of course not exactly determined where the cap 'ends' and the body 'begins'. But it has been shown that the body can be cut into two parts – each containing one cap – in a certain way: There is always a patch with exactly 6 pentagons where all boundary vertices have, alternately, degrees 2 and 3 except possibly two places where once two vertices of degree 2 and once two vertices of degree 3 follow upon each other (see [14] and [17]). More precisely, there exist $k, l \in \mathbb{N}_0$ such that the boundary sequence of the patch is given by $(2,3)^k, (3,2)^l$. These numbers k and l are uniquely determined and already define the structure of the body (except its length).

Since adding a ring of hexagons around such a patch does not change the boundary sequence, the boundary path can be 'shifted' along the body of the tube; so in particular, we may choose a boundary of this kind such that it includes at least one edge which lies in a pentagon. Now one application of [3] is that there is only a finite number of caps that can fill out such a boundary – provided that at least one pentagon lies in the boundary of the cap. This way a classification of all nanotubes is enabled. As a result, in [10] an algorithm is presented to construct all non-isomorphic nanotube caps for given parameters k and l describing the structure of the body.

If we just consider a *halftube*, that is a single cap together with an infinite body – or in mathematical terms an infinite 3-regular plane graph with six pentagons and all other faces hexagons – the result mentioned above implies that we can always find a finite subgraph of such a halftube containing the six pentagons with a boundary of the described type (see examples in figure 4.1). This gives us the possibility to classify these infinite graphs with the help of a finite number of patches.

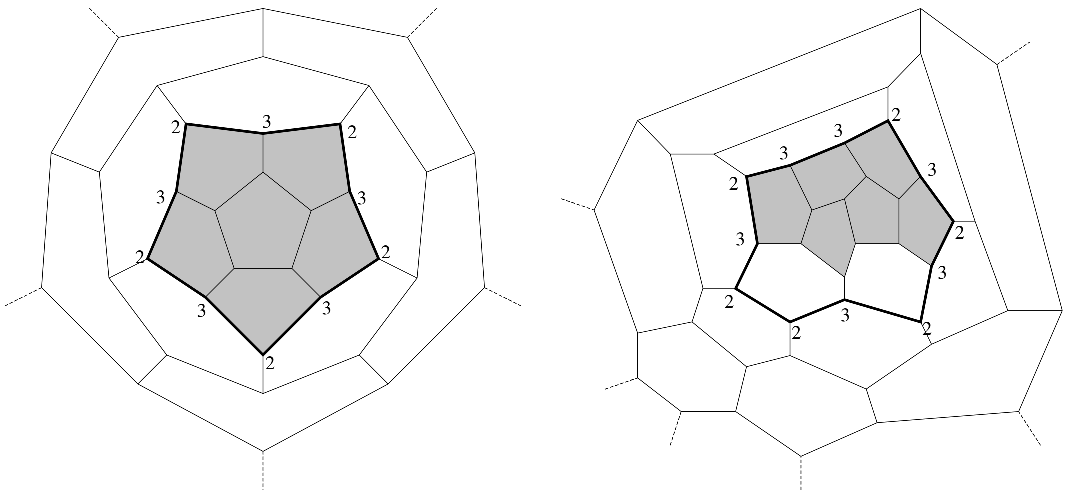

Figure 4.1: Two half-tubes with caps that have a boundary sequence of the type $(2,3)^k,(3,2)^l$: In the left figure we have $k = 5, l = 0$, in the right figure $k = 2, l = 4$. The pentagons in both figures are shaded grey.

Now the question arises whether a similar classification is possible for *nanocones*, that are infinite 3-regular plane graphs with $p < 6$ pentagons and all other faces hexagons. If we were able to find parameters that describe the boundary of a patch in such a nanocone, it would be possible to represent all nanocones by finite structures as well, because [3] implies also that for a given boundary of a p-patch with $p < 6$ there is only a finite number of non-isomorphic patches with that boundary.

What we will show here is that for a given cone with p pentagons, there is always a subpatch containing the pentagons which has a boundary sequence where vertices of degree 2 and 3 are alternating, except $6-p$ places where two vertices of degree 2 follow each other. We will even prove that the distances between these succeeding vertices of degree 2 can be chosen in a certain way such that it is the inner dual of a triangle-patch that does not only have a nice boundary, but is even regular – then we will call the hexagon-pentagon-patch regular, too. We will see that this allows us to describe the boundary with only two parameters.

In particular, in case $p = 5$ we always have a patch with a boundary sequence $(3,2)^k, 2$ and we may choose k minimal with the property that such a patch exists. Therefore in this case, even a *single* parameter (k, or just the boundary length of the patch) is sufficient to characterize the structure of the cone (see figure 4.2). Note that in contrast to the case $p = 6$, we do not have to allow succeeding vertices of degree 3.

At first, we will solve the corresponding question in the dual, since useful techniques for this have already been developed in the previous chapters: We will show that an infinite triangle-cone, that is an infinite triangulation with $0 \leq p \leq 5$ vertices of degree 5 and all others of degree 6, always contains a p-patch which is regular. In the section afterwards, we will transfer this result to hexagon-cones.

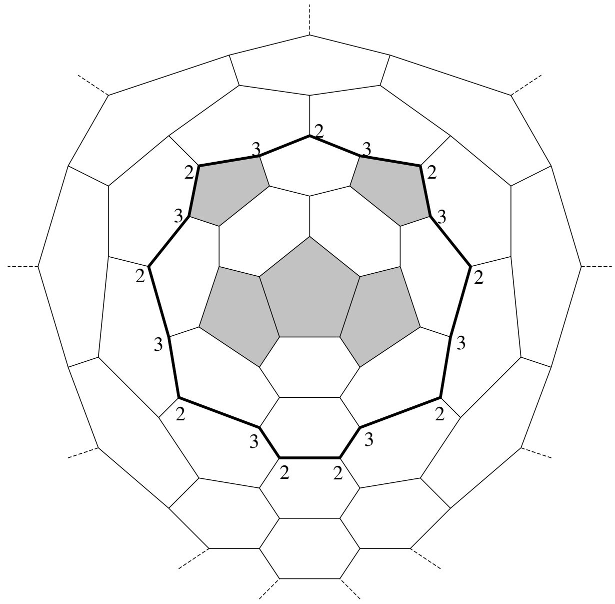

Figure 4.2: An infinite cone with $p = 5$ pentagons, and a subgraph containing all pentagons that has the boundary sequence $(3,2)^8, 2$. If we could find a patch with boundary sequence $(3,2)^k, 2$ (where we choose k minimal) for *any* cone with 5 pentagons, then this would provide a possibility to classify these cones with the help of that parameter.

4.2 Boundaries of triangle-cones

Definition 4.2.1 *An* infinite triangle-cone *is an infinite triangulation of the plane with* $0 \leq p \leq 5$ *vertices of degree* 5 *and all others of degree* 6.

Theorem 4.2.2 *Given an infinite triangle-cone* C *with* $0 \leq p \leq 5$ *vertices of degree* 5. *Then* C *contains a regular* p*-patch* P *as a subgraph.*

PROOF:

The cases $p = 0$ and $p = 1$ are obvious, since we may choose $P = P_0$ or $P = P_1$, respectively. So assume $2 \leq p \leq 5$.

We start with an arbitrary finite 2-connected subgraph P' of C that contains all p vertices of degree 5 in its interior (i.e. P' is a p-patch).

Let v be a boundary vertex of P', and C_v the directed path starting and ending at v which consists of the boundary edges of P' directed in a way that P' lies on their right hand side. Then we consider an embedding φ of C_v into the regular triangular lattice L equipped with a standard coordinate system (compare chapter 2, definitions 2.3.3 and 2.3.6).

As before, we note that it is important to consider a drawing of the triangular lattice in the plane where all basic triangles are equilateral.

Now we let e_0 denote the starting edge of C_v, and $\varphi'(e_0)$ the closure of the embedding (see again definition 2.3.6). Then according to lemma 2.3.8, $\varphi'(e_0)$ is the image of a $p \cdot 60$ degree counterclockwise rotation α of $\varphi(e_0)$ around a center c which is uniquely determined. In particular, if x denotes the starting vertex of $\varphi(C_v)$ (that is the starting vertex of $\varphi(e_0)$) and y the ending vertex of $\varphi(C_v)$ (that is the starting vertex of $\varphi'(e_0)$), we have $y = \alpha(x)$. Moreover we know (also due to lemma 2.3.8) that in case $p \in \{2, 4\}$ c can be a vertex or the center of a face, in case $p = 3$ it can be a vertex or the center of an edge, and in case $p = 5$ it must be a vertex.

Now we determine a hexagon H in L (that is a subgraph with a nice boundary, i.e. exactly 6 boundary vertices of degree 3 and all others of degree 4) that contains all vertices of $\varphi(C_v)$, has a special rotational symmetry with c as rotation center, and a special boundary segmentation: In case c is a vertex of the lattice, we may choose a regular hexagon with c in the center, i.e. H has symmetry group C_6 and six sides of the same length. In case c lies in the center of a face, we choose H to be of symmetry C_3 with boundary segmentation $B(H) = (k, k-1, k, k-1, k, k-1)$ for some $k \in \mathbb{N}$, and in case c coincides with the center of an edge, we may construct H such that it has symmetry group C_2 and boundary segmentation $B(H) = (k, k, k-1, k, k, k-1)$ for some $k \in \mathbb{N}$ (see figure 4.3).

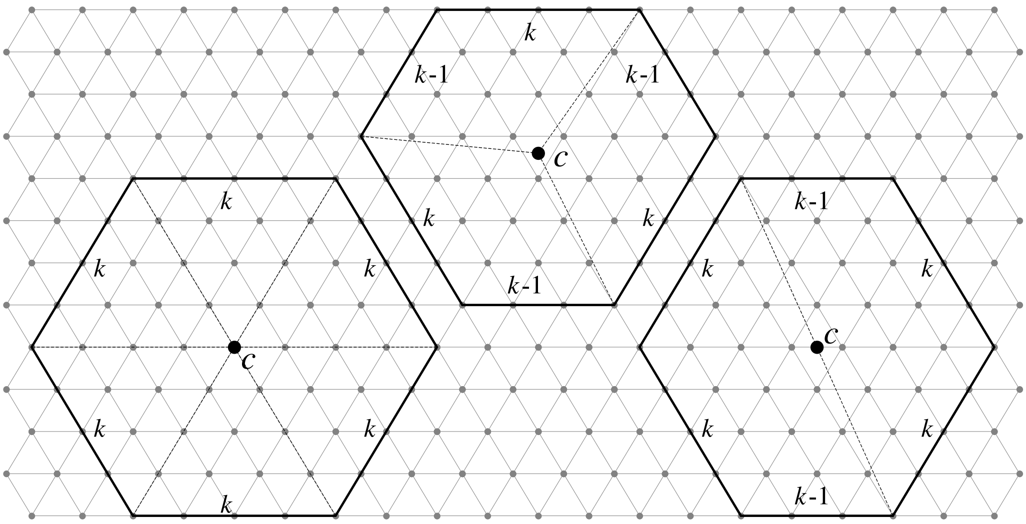

Figure 4.3: Given the position of a point c in the lattice, we may construct a hexagon H with $B(H) = (k, k, k, k, k, k)$ and symmetry group C_6 with respect to c in case c is a vertex (left figure), with $B(H) = (k, k-1, k, k-1, k, k-1)$ and symmetry group C_3 with respect to c in case c is the center of a face (figure in the middle), and with $B(H) = (k, k, k-1, k, k, k-1)$ and symmetry group C_2 with respect to c in case c is the center of an edge (right figure).

W.l.o.g. we may choose H small enough such that at least one vertex of $\varphi(C_v)$ lies in its boundary – otherwise all boundary faces can be removed to obtain a smaller hexagon with the same symmetry group and a boundary segmentation of the same type (only with $k - 1$ instead of k) which also contains $\varphi(C_v)$. Moreover, we may w.l.o.g. even assume that x, the starting vertex of $\varphi(C_v)$, lies in the boundary of H: If this is not the case, let u be a vertex in the boundary of P' such that $\varphi(u)$ lies in the boundary of H. Then if A denotes the subpath of $\varphi(C_v)$ from x to $\varphi(u)$, and B the subpath of $\varphi(C_v)$ from $\varphi(u)$ to y, we have that $B\,\alpha(A)$ forms an embedding of C_u. Because of the symmetry of H, the path $\alpha(A)$ lies still in H. Consequently we may choose u as the boundary vertex of P' instead of v and get the desired property that x, the starting vertex of $\varphi(C_v)$, lies in the boundary of H.

This means that the ending vertex $y = \alpha(x)$ of $\varphi(C_v)$ has to lie in the boundary of H, too: Since α is a rotation of $p \cdot 60$ degrees, i.e. a multiple of 60 degrees, this is obvious if H has symmetry group C_6, which is the case if c is a vertex in L. In case c is the center of a face we must have $p = 2$ or $p = 4$, so α is a rotation of 120 or 240 degrees, and H is chosen to be of symmetry group C_3, implying that y lies in the boundary of H. Finally, if c is the center of a face we must have $p = 3$ such that α is a rotation of 180 degrees, and H has symmetry group C_2, again yielding that y is a boundary vertex of H.

So if we orientate the edges of H such that $\varphi(C_v)$ lies on their right hand side, there exists a directed path $x = v_0, v_1, \ldots, v_n = y$ in L from x to y using only these directed edges. We now define a mapping ψ from this path onto a path in the cone: First, we let $v := \psi(x)$. Furthermore, if $\varphi(e_0) = (x, z)$ is the first directed edge in $\varphi(C_v)$, consider the edges (x, v_1) (the first edge in the path along H) and (x, z) in the rotational system of x, which we interpret as clockwise, and assume that there are l edges between them (that means, if $(x, v_1) \in E_j$ then $(x, z) \in E_{(j+l+1) \bmod 6}$). Then we choose $\psi(v_1)$ in the cone such that in the rotational system of v, there are l edges between $(v, \psi(v_1))$ and e_0.

If for $1 \leq i \leq n-1$ the edge $(\psi(v_{i-1}), \psi(v_i))$ is determined, we choose $\psi(v_{i+1})$ as a neighbouring vertex of $\psi(v_i)$ such that the number of edges between $(\psi(v_i), \psi(v_{i-1}))$ and $(\psi(v_i), \psi(v_{i+1}))$ in the rotational system of $\psi(v_i)$ is equal to the number of edges between (v_i, v_{i-1}) and (v_i, v_{i+1}) in the rotational system of v_i. This way – according to the definition of 'embedding' – the vertices $v = \psi(v_0), \psi(v_1), \ldots, \psi(v_n)$ form a directed path in the cone, which we will denote by $\bar{P}$, such that the directed path $v_0, v_1, \ldots, v_n$ is an embedding of $\bar{P}$ into L. Because of the way we choose the vertex $\psi(v_1)$, we even have that the cycle $\varphi(C_v)^{-1}, v_1, \ldots, v_n$ in L is an embedding of $C_v^{-1}\bar{P}$. But since this cycle only encloses vertices of degree 6, it must form a cycle in the cone, too, so we conclude that v is not only the starting vertex of the path $\bar{P}$, but also its ending vertex, meaning that $\bar{P}$ is a closed cycle in the cone.

Now we show that $\bar{P}$ encloses a p-patch P with a nice boundary, which is even regular except if $p = 2$ and c lies in a face (then we have to make a slight adjustment to obtain a regular patch): Since we chose the corresponding path in L to be a path on a hexagon, we get by construction of $\bar{P}$ that in the rotational system of any interior vertex $\psi(v_i)$ of the path, there are either one or two edges between $(\psi(v_i), \psi(v_{i+1}))$ and $(\psi(v_i), \psi(v_{i-1}))$ (that means in the angle on the 'right hand side' of two succeeding directed edges).

Furthermore we know due to the size of the angle corresponding to α that the path from x to y contains exactly $6-p$ or $6-p-1$ vertices with degree 3 in H (the first case applies if x and y are vertices with degree 4 in H, the second if they have degree 3 in H). So the number of vertices in $\bar{P}$ where there is only one edge in the respective angle is $6-p$ or $6-p-1$, respectively. Now by construction, P' and hence all vertices with degree 5 lie on the right hand side of $\bar{P}$. Since we already know that $\bar{P}$ is a closed cycle, it must enclose a p-patch P, and by formula 3.3.7 the vertex v must have degree 4 in P in the first case and degree 3 in the second. Hence all boundary vertices of P have degree 3 or 4, and consequently it has a nice boundary.

Then the lengths of succeeding sides in P correspond to the lengths of succeeding sides in H. This means that in case c is a vertex in the lattice, all sides of P have the same length, so it is definitely regular. If we have $p = 3$ and c lies in the center of an edge, we must have – due to the way we choose the boundary segmentation of H – two sides of length k and one of length $k-1$, so P is regular, too (but with $\Delta(P) = 1$). In case $p = 4$ and c lies in a face we have only two sides which must have length k and $k-1$, again implying that P is regular with $\Delta(P) = 1$. Only in case $p = 2$ and c lying in a face we obtain $B(P) = (k, k-1, k, k-1)$, such that P is not regular at first. But then we just add a row of faces to one side of length k (i.e. we include all faces containing interior vertices of the respective boundary segment between the two degree 3 vertices to P) which yields the boundary segmentation $(k, k, k, k-1)$, such that the resulting patch is regular.

□

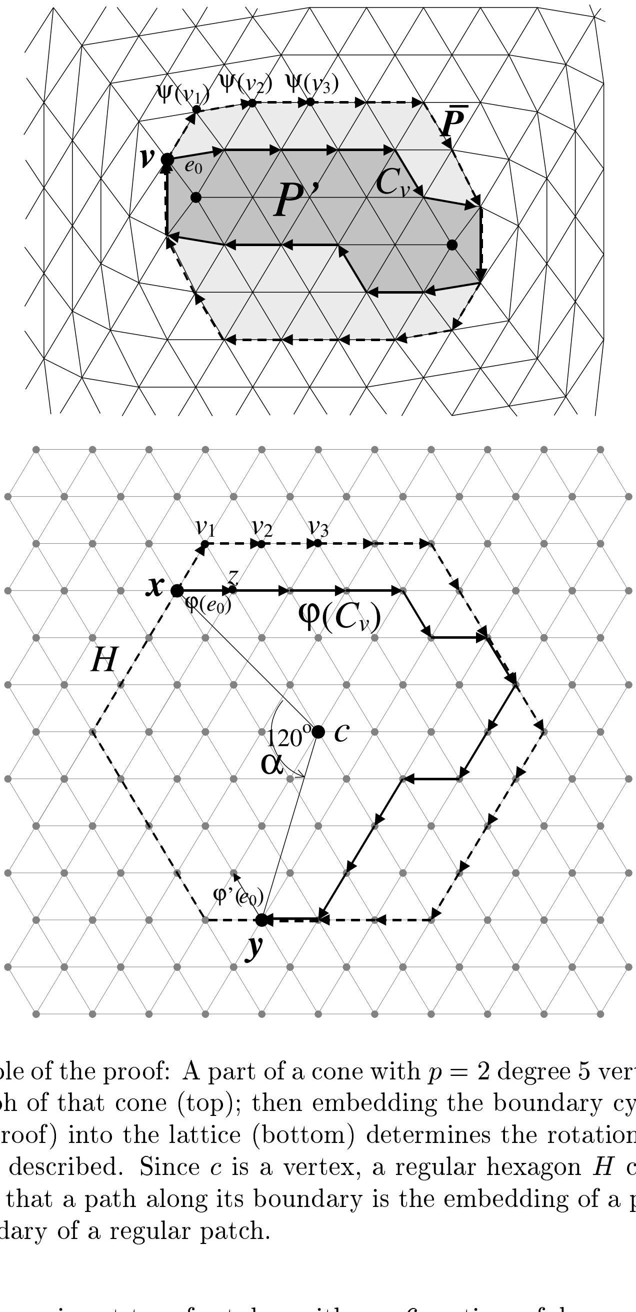

Figure 4.4: Example of the proof: A part of a cone with $p = 2$ degree 5 vertices and a 2-patch P' that is subgraph of that cone (top); then embedding the boundary cycle C_v (where v is chosen as in the proof) into the lattice (bottom) determines the rotation center c – in this case a vertex – as described. Since c is a vertex, a regular hexagon H can be constructed in the lattice such that a path along its boundary is the embedding of a path $\bar{P}$ in the cone which is the boundary of a regular patch.

Note that the theorem is not true for tubes with $p = 6$ vertices of degree 5: Trying to apply the proof for that case, we observe that we would have to choose a path from x to y without any turns – which is not always possible. Figure 4.5 shows an example of a half-tube where indeed no regular subpatch (or – in this case equivalently – with a nice boundary) exists.

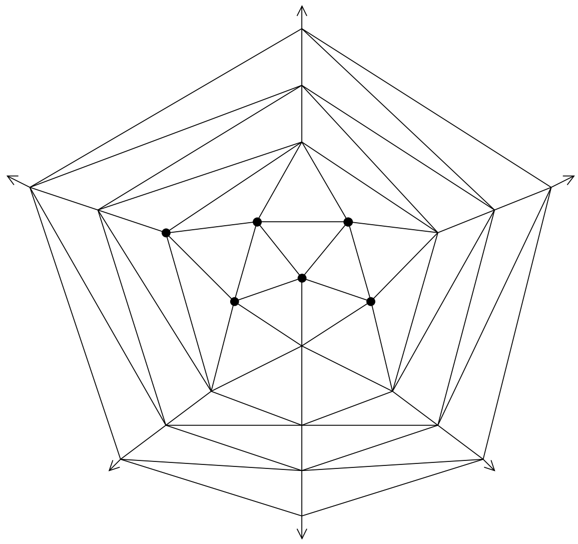

Figure 4.5: A cap with $p = 6$ degree 5 vertices where it is not possible to find a subgraph that is a 6-patch with a nice boundary

Now a result of theorem 4.2.2 is that to a given triangle-cone C with $0 \leq p \leq 5$ vertices of degree 5, we may always assign a pair (k, Δ) with $k \in \mathbb{N}$, $\Delta \in \{0, 1\}$ as follows:

We know that C contains a regular p-patch. Among all possible regular p-patches that are subgraphs of C, we choose one where the maximal length of the sides is minimal, that means we choose P with $k := \max_B(P)$ such that for all other regular p-patches P' that are subgraphs of C we have $\max_B(P') \geq k$. Furthermore we let $\Delta := \Delta(P)$. (Then we have even $\Delta = \Delta(P')$ for all other regular p-patches P' that are subgraphs of C due to lemma 3.3.44.)

On the other hand, the pair (k, Δ) also describes the boundary sequence of a 'cap' in a unique way if p is known. And for given $p < 6$ and (k, Δ), there is only a finite number of p-patches with exactly the respective boundary sequence – this follows from the computations in chapter 3:

By corollary 3.3.4 we have an upper bound for the number of faces of P with respect to its boundary length (3.34), namely

$$f(P) \leq \frac{b(P)^2}{6 - p} .$$

Since for each n there is only a finite number of patches with n faces this means that there is only a finite number of p-patches with $p < 6$ that have a certain boundary length. In particular, for a given boundary sequence that belongs to a p-patch with $p < 6$, there is only a finite number of p-patches with the same boundary sequence.

Consequently, the parameters (k, Δ) can be used for the classification of infinite triangle-cones. Note that in the cases $p = 0$, $p = 1$, and $p = 5$ we must have $\Delta = 0$, such that the structure of these cones can even be described by one single parameter k.

4.3 Boundaries of hexagon-cones

Transferring the result of theorem 4.2.2 to the dual, we obtain a similar result for hexagonal cones:

Definition 4.3.1 *An* infinite hexagon-cone *is a plane* 3*-regular graph with* $0 \leq p \leq 5$ *pentagons and all other faces hexagons.*

For easier notation, a $(p, 0, 0)$*-hexagon-patch (see section* 3.2*) will now be referred to as a hexagon-p-patch. A hexagon-p-patch is called* regular *if it is the inner dual of a regular (triangle-)p-patch.*

Remark 4.3.2 *Due to the definition of 'regular' for triangle-patches, the definition above implies that a hexagon-p-patch P is regular if there is* $k \in \mathbb{N}$ *such that the boundary sequence of P is either*

$$\left((3,2)^k, 2\right)^{6-p},$$

or (only in case $p \in \{2,3,4\}$*)*

$$\left((3,2)^k, 2\right)^{6-p-1}, (3,2)^{k-1}, 2$$

– see also figure 4.6*.*

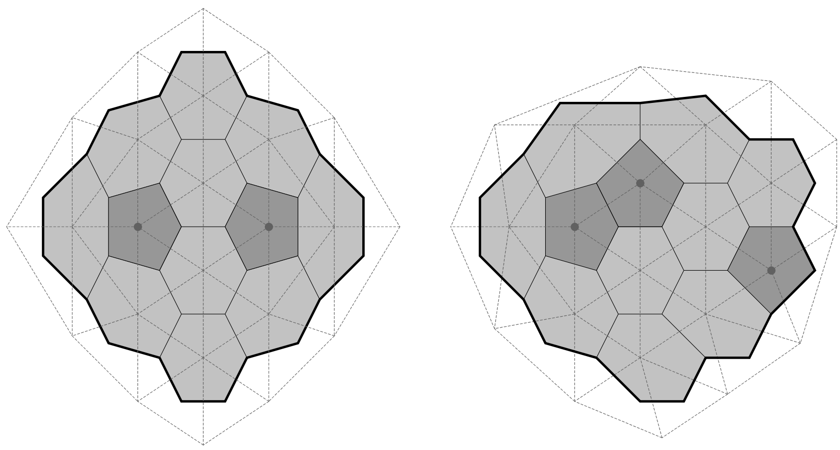

Figure 4.6: Two examples of regular hexagon-p-patches: A regular hexagon-2-patch with boundary sequence $\left((3,2)^2,2\right)^4$ (left), and a regular hexagon-3-patch with boundary sequence $\left((3,2)^3,2\right)^2,(3,2)^2,2$

Theorem 4.3.3 *Given an infinite hexagon-cone with* $0 \leq p \leq 5$ *pentagons. Then it contains a hexagon-p-patch that is regular.*

PROOF:

By definition, the dual of a hexagon-cone with p pentagons is a triangle-cone with p vertices of degree 5. According to theorem 4.2.2, that triangle-cone contains a regular p-patch P. So we consider the set of faces F in the hexagon-cone that are dual to the set of *inner* vertices $V_i(P)$ of P in the triangle-cone. Let P' be the patch in the hexagon-cone that consists of exactly that set of faces, i.e. $F(P') = F$ (see figure 4.7.) Then by construction, P' is the inner dual of P and contains p pentagons, and since P is regular this means by definition 4.3.1 that P' is a regular hexagon-p-patch.

□

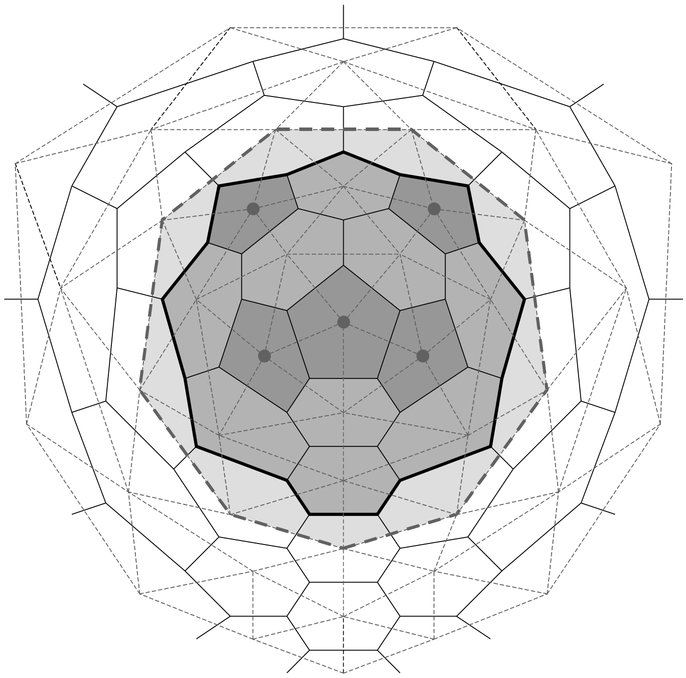

Figure 4.7: A hexagon-cone (here with $p = 5$ pentagons) and its dual, a triangle-cone (dotted lines), containing a regular p-patch; then the faces in the hexagon-cone corresponding to the inner vertices of that p-patch form a regular hexagon-p-patch.

Again we note that this theorem does not hold for a hexagon-tube with $p = 6$ pentagons – for a counterexample see figure 4.1, right picture.

Now similar to the triangular case, theorem 4.3.3 implies that we may characterize hexagon-cones with the help of two parameters (k, Δ): We choose a regular hexagon-p-patch P' in a given hexagon-cone with a boundary length as small as possible, that means the parameter k that occurs in remark 4.3.2 is as small as possible, and we define Δ to be 0 in the first case and to be 1 in the second case of remark 4.3.2. (Then if P denotes the regular triangle-patch whose inner dual is P', we have $\max_B(P) = k + 1$ and $\Delta(P) = \Delta$.)

According to [3], there is an upper bound for the number of faces of a hexagon-p-patch with $p < 6$ depending only on its boundary length (compare also table 3.1), such that there is also only a finite number of hexagon-p-patches (with $p < 6$) for a given boundary sequence. So again, the parameters k and Δ can be the foundation for a classification of infinite hexagon-cones.

Chapter 5

The expander constant of fullerenes

5.1 Introduction

For many applications, graphs are wanted that are *highly connected* yet *sparse*. These apparently contradictory properties make such graphs very useful. Their main applications lie in theoretical computer science where they are important for various problems concerned with information transmission and network design [38], complexity theory [43], coding theory [44], derandomization [36] and many more; even in pure mathematics, see e.g. [32], they are of interest (references taken from [39]).

The 'connectivity' of a graph $G = (V, E)$ can be measured by the *expander* or *Cheeger constant*, which traces back to a similar value for Riemannian manifolds by Jeff Cheeger [11]. It is defined as

$$ch(G) \ := \ \min_{\emptyset \subset U \subset V} \frac{|\partial U|}{\min(|U|,\, n - |U|)} \tag{5.1}$$

where $n := |V|$ denotes the number of vertices, and

$$\partial U := \big\{\{u, v\} \mid u \in U, v \in V - U\big\} \tag{5.2}$$

the set of all edges connecting U with $V - U$, i.e. those with exactly one endpoint in U. If G represents a network, then $ch(G)$ measures its quality: If $ch(G)$ is small, we have a large subset of vertices with relatively few edges leading out, which means that a large part of the network can easily be cut from the rest – so the network is of bad quality. On the other hand, if $ch(G)$ is high, large subsets must be connected with the rest by many edges, implying that the network is 'stable'; and moreover, if we view it for instance as a network transmitting information, then information propagates well. Davidoff, Sarnak and Valette demonstrate this observation in [13] with the help of two extreme examples:

First, consider the complete graph K_n on n vertices (see figure 5.1 for $n = 5$). In order to determine its expander constant, we can w.l.o.g. restrict to those subsets U with $|U| \leq \frac{n}{2}$, because the quotient in (5.1) is always equal for U and $V(K_n)-U$. For any such $U \subset V(K_n)$ we have

$$\frac{|\partial U|}{|U|} = \frac{|U| \cdot (n - |U|)}{|U|} = n - |U|$$

which is minimal for $|U| = \lfloor \frac{n}{2} \rfloor$, so we get $ch(K_n) = n - |U| = \lceil \frac{n}{2} \rceil$. In our example with $n = 5$, we choose an arbitrary vertex set U with $|U| = 2$, and obtain $ch(K_5) = \frac{|\partial U|}{|U|} = 3$.

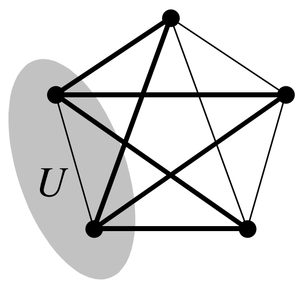

Figure 5.1: The complete graph K_5 with a vertex set U such that $\frac{|\partial U|}{|U|} = 3 = ch(K_5)$; the six fat edges are the ones in ∂U.

The second example is the cycle C_n on n vertices; see figure 5.2 for $n = 6$. For any non-trivial vertex set $\emptyset \subset U \subset V(C_n)$ we have $|\partial U| \geq 2$. So if we choose U as the vertices of a path in C_n with $|U| = \lfloor \frac{n}{2} \rfloor$, we have $|\partial U| = 2$ and hence the quotient $\frac{|\partial U|}{|U|}$ must be minimal under the restriction $|U| \leq \frac{n}{2}$. Therefore we obtain $ch(C_n) = \frac{2}{\lfloor \frac{n}{2} \rfloor}$. In case $n = 6$ we have $ch(C_6) = \frac{2}{3}$, as indicated in the figure.

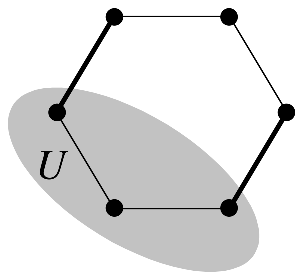

Figure 5.2: The cycle C_6 with U such that $\frac{|\partial U|}{|U|} = ch(C_6)$ holds, and the two fat edges lying in ∂U.

Now if we let the number n of vertices grow, we observe that the expander constant of the complete graph grows proportionately in n, while the expander constant of the cycle decreases to zero. In this sense, the complete graph is ‘highly connected’ while the cycle is not. So if we want to have a graph with a large expander constant, we could just choose the respective complete graph.

But the problem is that the complete graph is not ‘sparse’: For n vertices we have $e(K_n) = \frac{n(n-1)}{2}$, so the number of edges grows quickly with the number of vertices, which makes the network become very expensive. In contrary to this, the cycle on n vertices has $e(C_n) = n$ edges, so with every vertex we have to add only one single edge, which makes it very ‘sparse’.

Consequently, the complete graph is, although 'highly connected', not desirable for networks because it is too expensive. On the other hand the cycle is 'sparse' but not suitable either, since it has a small expander constant. For this reason we are looking for graphs that are both highly connected *and* sparse.

The property to be 'sparse' can be guaranteed by restricting to k-regular graphs, that are graphs with all vertices of the same degree k: The number of edges of a k-regular graph G is $e(G) = \frac{n \cdot k}{2}$ and hence grows linearly with the number of vertices.

It is known that the expander constant of a graph is connected with the eigenvalues of its adjacency matrix. A main result is the following (see Alon/Milman [2] and Tanner [45]): If G is k-regular and A denotes its adjacency matrix, then k is an eigenvalue of A, all eigenvalues of A are real and lie in the interval $[-k, k]$; and if $\lambda_1(A)$ denotes the second largest eigenvalue of A, then the following inequality holds:

$$\frac{k - \lambda_1(A)}{2} \;\leq\; ch(G) \;\leq\; \sqrt{2k(k - \lambda_1(A))}$$

Obviously both bounds are large if $k - \lambda_1(A)$, the gap between the largest and the second largest eigenvalue, is large. Research focuses on algebraic constructions of graphs where this is the case (see e.g. [33], [35], [37]). In case $\lambda_1(A) \leq 2\sqrt{k-1}$ the graph is called *Ramanujan* ([1], [33]); these graphs are optimal as far as the spectral gap measure of expansion is concerned. However, all results connecting eigenvalues and expander constants provide only bounds and do not give precise values. Therefore, in this thesis we disregard this algebraic aspect and choose a different, combinatorial approach that concentrates on definition (5.1) of the expander constant.

We define a *fullerene* as a 3-regular plane graph with all faces of sizes 5 or 6, where due to Euler's formula this requires the number of pentagons to be 12. Since fullerenes are 3-regular and therefore 'sparse', it makes sense to apply the concept of the expander constant to these graphs. On the one hand, we have in mind that for given n there is typically a large number of mathematically possible fullerenes with n vertices, so a criterion to distinguish these fullerenes due to their connectivity would be desirable and might give a hint regarding the stability of the – possibly existing – corresponding chemical molecules. On the other hand, expander graphs have so many applications and fullerenes are not only sparse but have such an interesting structure that they are mainly 'highly connected', so that their graphs might serve for instance as good networks.

It has already been managed to compute the expander constants of single, highly symmetrical fullerenes as the one with 80 vertices (see [40]) which is shown in figure 5.3: The shaded area indicates a subset U that minimizes

$$\frac{|\partial U|}{\min(|U|, n - |U|)}$$

with $|U| = 40$ and $|\partial U| = 10$, which implies that the expander constant of that graph is $\frac{1}{4}$.

However, in general it is very difficult to compute the expander constant of a graph because a priori one has to consider a large number of subsets to find the minimum of the quotient over all U. Therefore, in order to be able to determine the expander constant of a given fullerene without checking all those subsets, which is too expensive even for a small number of vertices, we first investigate the structure of the subgraphs that determine the expander constant of a fullerene.

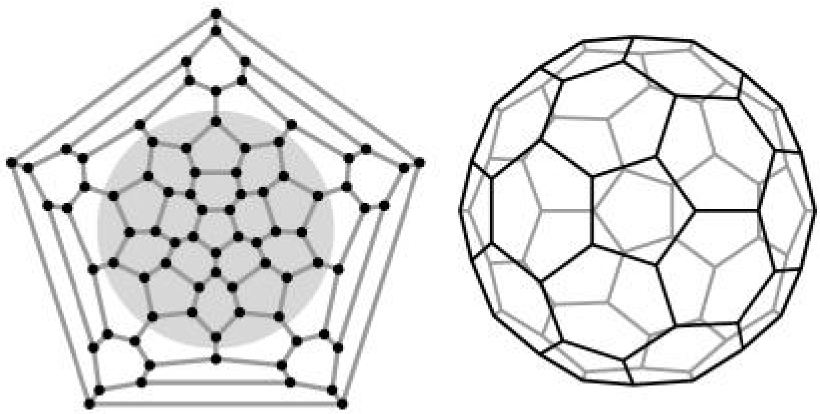

Figure 5.3: A fullerene with 80 vertices and expander constant $\frac{1}{4}$ (taken from [40])

The section 5.2 of this chapter provides some basic results that suggest to focus on the duals of fullerenes, the *geodesic domes*, and examine triangle-patches in geodesic domes instead of vertex sets in fullerenes. This is what we do in section 5.3: We deduce some properties on those triangle-patches in a geodesic dome that have a minimal ratio of boundary length and face number and thus determine the expander constant of the dual fullerene.

Finally, in section 5.4 we apply the obtained knowledge for actually determining the expander constants of fullerenes. In 5.4.1 we present a method that allows to verify the expander constant of classes of symmetrical fullerenes by hand. The arguments that we apply are mainly based on the theoretical results about the boundary lengths of triangle-patches that we developed in chapter 3. This way, we determine and prove in detail the expander constants of all fullerenes that are of the same type as the Buckminster fullerene, that are all fullerenes with icosahedral symmetry where two pentagons that are adjacent in the signature graph have Coxeter coordinates (q, q) for some $q \in \mathbb{N}$.

Furthermore, in section 5.4.2, we present a very different approach to determine the expander contant of a fullerene: We describe an algorithm that is based on results obtained in the sections 5.2 and 5.3 and has been implemented as a computer program. This program is not only able to determine the expander constant of single fullerenes, but can even compute the expander constants of e.g. all 1812 fullerenes on 60 vertices in a few seconds and thus determine the fullerenes with the best expander constants – and hence the highest connectivity – among all fullerenes with a given number of vertices. We present a complete list of the maximal expander constants of fullerenes with up to 140 vertices that have been calculated by that program. For instance we will see that the highly symmetrical fullerene shown in figure 5.3 with its expander constant $\frac{1}{4}$ is actually *not* optimal since there are other fullerenes on 80 vertices with a strictly larger expander constant. Moreover, we list the maximal expander constants of isolated-pentagon fullerenes with certain numbers of vertices, and compare them with the data obtained for all fullerenes. As a surprising result we obtain that there is not always an isolated-pentagon fullerene among the fullerenes with highest expander constant.

5.2 First results

Definition 5.2.1 *A* fullerene *is a* 3*-regular plane graph where all faces have size* 5 *or* 6*. We denote a fullerene by* $G = (V, E, F)$*, where* V *stands for the set of vertices,* E *for the set of edges, and* F *for the set of faces.*

Note that in contrast to the definition of patches, we do not distinguish one outer face, and we let now F be the set of *all* faces in a fullerene!

In the following, we consider a fullerene $G = (V, E, F)$ with $|V| = n$. Euler's formula implies that it consists of exactly 12 pentagons and $\frac{n}{2} - 10$ hexagons. So n must be even and the smallest fullerene is the dodecahedron with $n = 20$ vertices, 12 pentagons and no hexagon. It is known [23] that for any even $n \geq 20$ with the exception of $n = 22$ there exists a fullerene with n vertices – at least one that is mathematically possible.

We let $ch(G)$ denote the expander constant of G (see (5.1)), ∂U the set of edges with exactly one endpoint in $U \subset V$ (see (5.2)), and define the ratio

$$r(U) := \frac{|\partial U|}{\min(|U|,\, n - |U|)} \tag{5.3}$$

for any subset U of V with $\emptyset \neq U \neq V$.

Note that there is always a subset U with $r(U) = ch(G)$ and $|U| \leq \frac{n}{2}$, since $r(U) = r(V - U)$. In this case, we just have $ch(G) = r(U) = \frac{|\partial U|}{|U|}$, and we say '*$U$ determines the expander constant of G*'.

Lemma 5.2.2 *Let* $G = (V, E, F)$ *be a fullerene with* $|V| = n$*, and let* $U \subset V$ *with* $|U| \leq \frac{n}{2}$ *such that* $r(U) = ch(G)$*. Then*

(i) $ch(G) < 1$*;*

(ii) $\frac{|\partial U| - k}{|U| - l} < \frac{|\partial U|}{|U|}$ *for all integers* $0 < l \leq k$*;*

(iii) ∂U *is an independent edge set.*

PROOF:

(i) Let U' be the set of vertices of two adjacent faces. Then $|U'| \leq 10 \leq \frac{n}{2}$ and $|\partial U'| = |U'| - 2$, so $r(U') = \frac{|\partial U'|}{|U'|} < 1$. But since the ratio is minimal for U we get $ch(G) = r(U) \leq r(U') < 1$.

(ii) Now let $k, l \in \mathbb{N}$ with $0 < l \leq k$. Due to (i) we have $|U| > |\partial U| > 0$ and hence

$$\begin{aligned} & k\,|U| > l\,|\partial U| \\ \Leftrightarrow\quad & -k\,|U| + |\partial U|\,|U| < -l\,|\partial U| + |\partial U|\,|U| \\ \Leftrightarrow\quad & (|\partial U| - k)\,|U| < (|U| - l)\,|\partial U| \\ \Leftrightarrow\quad & \frac{|\partial U| - k}{|U| - l} < \frac{|\partial U|}{|U|} \end{aligned}$$

(iii) Suppose ∂U is *not* independent, i.e. there are edges $\{u, v_1\}, \{u, v_2\} \in \partial U$. Let v_3 be the third vertex adjacent to U.

a) In case $u \in U$ we must have $v_1, v_2 \in V - U$. Define $U' := U - u$, so obviously $|U'| = |U| - 1$ holds. If $v_3 \in U$, we have $\partial U' = \partial U - \{\{u, v_1\}, \{u, v_2\}\} \cup \{u, v_3\}$ and hence $|\partial U'| = |\partial U| - 1$. If $v_3 \notin U$ we even get $|\partial U'| = |\partial U| - 3$ since $\partial U' = \partial U - \{\{u, v_1\}, \{u, v_2\}, \{u, v_3\}\}$. So in any case there is some $k > 0$ with $|\partial U'| = |\partial U| - k$, so we obtain with (i)

$$r(U') = \frac{|\partial U'|}{|U'|} = \frac{|\partial U| - k}{|U| - 1} < \frac{|\partial U|}{|U|} = r(U)$$

which is a contradiction to $r(U) = ch(G)$.

b) In case $u \notin U$, the vertices v_1 and v_2 must lie in U. If $|U| < \frac{n}{2}$ we define $U' := U \cup \{u\}$; then $|U'| = |U| + 1 \le \frac{n}{2}$ and

$$r(U') = \frac{|\partial U'|}{|U'|} = \frac{|\partial U| - k}{|U| + 1} < \frac{|\partial U|}{|U|} = r(U)$$

with $k = 1$ if $v_3 \notin U$ and $k = 3$ if $v_3 \in U$ – again a contradiction. If $|U| = \frac{n}{2}$ consider $U'' := V - U'$, which fulfills $|U''| = |U| - 1$ and $|\partial U''| = |\partial U'|$, so we get $r(U'') < r(U)$ just like in a).

□

Sometimes it is useful to consider the *dual* of a fullerene rather than the fullerene itself. We denote the dual of a fullerene $G = (V, E, F)$ as $G^* = (V^*, E^*, F^*)$, and ψ as the mapping that maps the vertices, edges and faces of G on the respective dual faces, edges and vertices of G^*. Then G^* is a triangulation with all vertices of degree 5 or 6 (see figure 5.4) which is also called *geodesic dome*.

Given a fullerene $G = (V, E, F)$ and its dual $G^* = (V^*, E^*, F^*)$, we say that a set of vertices, edges or faces *corresponds* to the respective set of dual faces, edges or vertices it is mapped on by ψ or ψ^{-1}.

For a vertex set $U \subset V$ in G we define $U^* := \psi(U) \subset F^*$ as the corresponding set of faces in G^*, and furthermore $\partial U^* := \psi(\partial U) \subset E^*$ as the set of edges in G^* that corresponds to the edge set ∂U in G. Then we have

$$\frac{|\partial U|}{|U|} = \frac{|\partial U^*|}{|U^*|}.$$

The following lemma provides useful information on the set of faces U^* corresponding to a vertex set U that determines the expander constant of a fullerene:

Lemma 5.2.3 *Let G be a fullerene with n vertices, G^* its dual, and $U \subset V$ with $|U| \le \frac{n}{2}$ such that $r(U) = ch(G)$. Then*

(i) the subgraph S of G^* that is spanned by the edges of ∂U^* consists of disjoint elementary cycles;

(ii) U may be selected such that S forms a single elementary cycle.

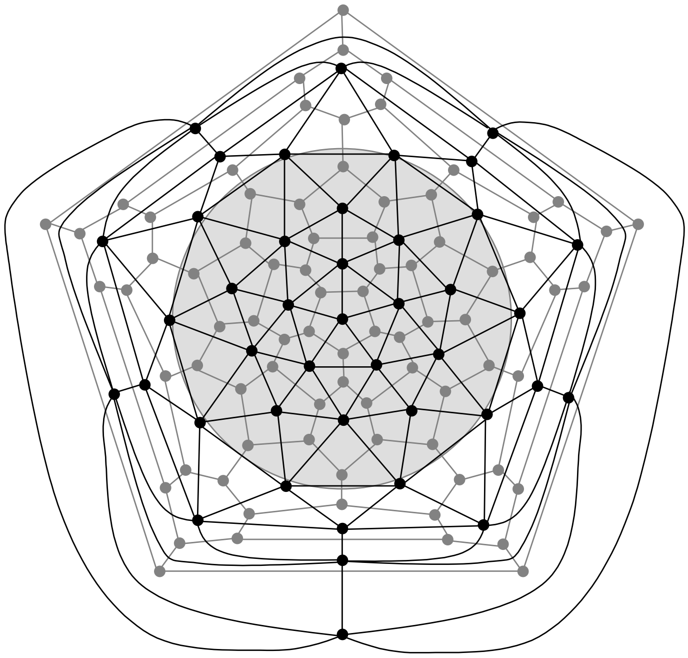

Figure 5.4: The fullerene C_{80} (grey lines – see also figure 5.3) with its dual graph (black lines)

PROOF:

(i) In order to show that S consists of disjoint cycles, we show that all vertices in S have degree 2:

Due to lemma 5.2.2(iii), there cannot be any two edges in ∂U that share a common vertex. This means for the dual that there are no edges in ∂U^* lying in the same triangle. So for each vertex $v \in V^*$, there can be at most 3 edges in ∂U^* adjacent to v (at most 3 in case it has degree 6 and at most 2 in case it has degree 5).

But since every edge $e \in \partial U$ has one endpoint in U and one endpoint in $V - U$, the corresponding edge $\psi(e) \in \partial U^*$ lies between one face in U^* and one face in $F^* - U^*$. So considering the edges around one vertex $v \in V^*$, we 'change sides' with every edge in ∂U^*, which means there must be an even number of those edges. Since there are at most 3, there can either be 0 or 2 edges of ∂U^* adjacent to v – so all vertices in S must have degree 2.

(ii) At first we prove the following *observation*: Let $a, a_1, a_2, b, b_1, b_2 > 0$ with $a = a_1 + a_2$, $b = b_1 + b_2$, and $\frac{a}{b} \leq \frac{a_i}{b_i}$ for $i = 1, 2$; then

$$\frac{a}{b} = \frac{a_1}{b_1} = \frac{a_2}{b_2} \ . \tag{5.4}$$

Proof: We have $a \cdot b_i \leq b \cdot a_i$ for $i = 1, 2$, hence $(a_1 + a_2) \cdot b_1 \leq (b_1 + b_2) \cdot a_1 \Leftrightarrow a_2 b_1 \leq b_2 a_1$ and on the other hand $(a_1 + a_2) \cdot b_2 \leq (b_1 + b_2) \cdot a_2 \Leftrightarrow a_1 b_2 \leq b_1 a_2$, so it follows that

$a_1b_2 = b_1a_2$. Furthermore we get $a \cdot b_1 = (a_1 + a_2) \cdot b_1 = a_1b_1 + a_2b_1 = a_1b_1 + a_1b_2 = a_1 \cdot (b_1 + b_2) = a_1 \cdot b$ and therefore $\frac{a}{b} = \frac{a_1}{b_1} = \frac{a_2}{b_2}$.

Now suppose that S consists of two or more elementary cycles. Each cycle has faces of U^* on one side and faces of $F^* - U^*$ on the other, so U^* or $F^* - U^*$ (maybe even both) must consist of at least two isolated components.

At first assume that $U^* = U_1^* \cup U_2^*$ such that the faces in U_1^* and U_2^* have no common vertices and w.l.o.g. U_1^* has a simple boundary cycle ∂U_1^*. Because of $ch(G) = r(U) = \frac{|\partial U|}{|U|} = \frac{|\partial U^*|}{|U^*|}$ we have

$$\frac{|\partial U^*|}{|U^*|} \leq \frac{|\partial U_i^*|}{|U_i^*|}$$

for $i = 1, 2$. (Note that $|U_i^*| \leq |U^*| \leq \frac{n}{2}$!)

With $|\partial U^*| = |\partial U_1^*| + |\partial U_2^*|$ and $|U^*| = |U_1^*| + |U_2^*|$ it follows from (5.4) that

$$\frac{|\partial U^*|}{|U^*|} = \frac{|\partial U_1^*|}{|U_1^*|} = \frac{|\partial U_2^*|}{|U_2^*|} .$$

This means that with U_1 as the vertex set in G corresponding to U_1^*, we have $ch(G) = r(U) = r(U_1)$, so instead of U we may choose U_1, which corresponds to a *single* cycle in the dual.

Now consider the case where $F^* - U^*$ consists of two or more components and U^* of only one. Let $F^* - U^* = W_1^* \cup \ldots \cup W_l^*$. Assume that an arbitrary non-trivial subset of those components $W^* \subset \{W_1^*, \ldots, W_l^*\}$ with $W^* \neq \{W_1^*, \ldots, W_l^*\}$ contains more than $\frac{n}{2}$ faces. Then $U_1^* := F^* - W^*$ contains less than $\frac{n}{2}$ faces and fulfills $|U_1^*| > |U^*|$ and $|\partial U_1^*| = |\partial W^*| < |\partial U^*|$, hence

$$\frac{|\partial U_1^*|}{|U_1^*|} < \frac{|\partial U^*|}{|U^*|}$$

holds in contradiction to the minimality of U resp. U^*.

Therefore we may assume $F^* - U^* = W_1^* \cup W_2^*$ with $|W_i^*| \leq \frac{n}{2}$ for $i = 1, 2$ where W_1^* is a single component with an elementary boundary cycle and W_2^* the set consisting of the other components of $F^* - U^*$. Then we have

$$\frac{|\partial U^*|}{|U^*|} \leq \frac{|\partial W_i^*|}{|W_i^*|}$$

for $i = 1, 2$, so again with (5.4) we get

$$\frac{|\partial U^*|}{|U^*|} = \frac{|\partial W_1^*|}{|W_1^*|} = \frac{|\partial W_2^*|}{|W_2^*|} .$$

So instead of U we may now choose W_1, the vertex set in G that corresponds to W_1^* which has a single boundary cycle.

□

5.3 Triangle-patches and geodesic domes

In order to determine the expander constant of a fullerene $G = (V, E, F)$ with n vertices, we need to find a vertex set $U \subset V$ with $|U| \leq \frac{n}{2}$ and $r(U) = ch(G)$. According to lemma 5.2.3, among all $U \subset V$ with $|U| \leq \frac{n}{2}$ and $r(U) = ch(G)$ there is at least one where in the dual $G^* = (V^*, E^*, F^*)$, the edge set $\partial U^* \subset E^*$ corresponding to $\partial U \subset E$ forms a simple cycle. Since we have

$$r(U) = \frac{|\partial U|}{|U|} = \frac{|\partial U^*|}{|U^*|}$$

this implies that we may restrict ourselves to subgraphs of the dual that are bounded by a single elementary circuit (that means that are 2-connected).

Hence the task to find a vertex set $U \subset V$ with $|U| \leq \frac{n}{2}$ and minimal ratio of $\frac{|\partial U|}{|U|}$ can be modified into the task to find a face set $U^* \subset F^*$ with $|U^*| \leq \frac{n}{2}$ and minimal ratio of $\frac{|\partial U^*|}{|U^*|}$. The face set U^* then forms a triangle-patch in the dual, and $|\partial U^*|$ is nothing but its boundary length.

Since the boundary length of a patch is easier to handle than the edge set ∂U relative to a vertex set U, we now switch from investigating vertex sets in fullerenes to patches in geodesic domes. Because we need to examine the ratio of boundary length and face number of these patches, the results from the previous chapters will prove helpful.

5.3.1 Optimal patches

As we are now dealing with patches in geodesic domes, we apply the term 'p-patch' as introduced in chapter 2. We will stick to the definitions and notations made in definition 2.2.1. Moreover, since no other types of disordered patches occur in this chapter, by abuse of notation a p-patch is sometimes simply referred to as a *patch* in case the number p of vertices with degree 5 is not important in that context.

Definition 5.3.1 *A* geodesic dome *is a triangulation $T = (V, E, F)$ of the plane (i.e. a 2-connected plane graph with all faces triangles) where all vertices have degree 5 or 6.*

For a geodesic dome T with n faces, we define the expander quotient *of T as*

$$q(T) := \min \left\{ \frac{b(P)}{\min(f(P), n - f(P))} \mid P \textit{ is patch in } T \right\}$$

where $b(P)$ denotes the boundary length (see definition 2.2.1) and $f(P)$ the number of faces of P.

A patch P that is subgraph of a geodesic dome T with $|V| = n$ faces is called optimal *with respect to T if $f(P) \leq \frac{n}{2}$ and $\frac{b(P)}{f(P)} = q(T)$; that means for any other patch P' in T with $f(P') \leq \frac{n}{2}$ we have*

$$\frac{b(P')}{f(P')} \geq \frac{b(P)}{f(P)} .$$

Remark 5.3.2 *Since a geodesic dome is the dual of a fullerene, it contains – due to Euler's formula – exactly 12 vertices with degree 5. Furthermore, if n is its number of faces, the number of vertices with degree 6 must be $\frac{n}{2} - 10$.*

Remark 5.3.3 *The expander constant of a fullerene G is equal to the expander quotient of the geodesic dome T that is dual to the fullerene; in particular, if P is optimal with respect to T, then the set of vertices U in G that corresponds to $F(P)$ determines the expander constant of G, i.e.*

$$ch(G) = \frac{|\partial U|}{|U|} = \frac{b(P)}{f(P)} = q(T) .$$

Definition 5.3.4 *A* boundary labeling *of P with respect to T is a mapping L that assigns integers (*boundary labels*) to the boundary vertices of P such that for every boundary vertex $v \in V_b(P)$ we have*

$$L(v) = \deg_T(v) - \deg_P(v) ,$$

that means $L(v)$ is the number of edges in $T - P$ that are incident to v (see figure 5.5).

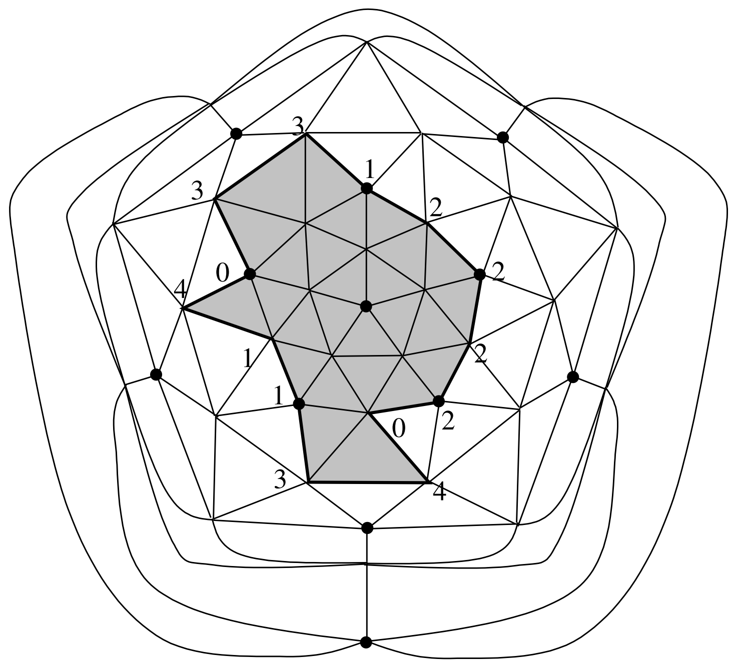

Figure 5.5: An example of a geodesic dome T containing a p-patch P (here with $p = 1$) and a boundary labeling of P with respect to T. Note that the labels are *not* determined by the degrees of the boundary vertices in P, since the boundary vertices of P may have degree 5 or 6 in T.

The following lemma already provides very useful information on the boundary of optimal patches: It says that it cannot contain any vertices with degree 2 or 6, nor any with label 0 or 4. This means that the boundary cycle does not make any 'sharp turns', i.e. if we consider two succeeding edges in the boundary cycle, there must always be at least one edge between them in the rotational system of the common vertex.

Lemma 5.3.5 *Let P be a p-patch that is subgraph of a geodesic dome T. Then possible boundary degrees of P are $2, 3, 4, 5, 6$, and possible boundary labels with respect to T are $0, 1, 2, 3, 4$. In case P is optimal with respect to T, its only possible boundary degrees are $3, 4, 5$, and the only possible boundary labels are $1, 2, 3$.*

PROOF:

Since P is 2-connected, there are no vertices with degree 1, which implies already the first statement.

Now let G denote the fullerene which is dual to T, and U the set of vertices in G that corresponds to $F(P)$. Then according to lemma 5.2.2(iii), the edge set ∂U in G consists of independent edges. Since the dual edges of ∂U are the boundary edges of P, this means there cannot be any two boundary edges of P lying in the same face of T. Consequently there cannot exist any boundary vertices of P with degree 2 or degree 6, and furthermore no boundary labels 0 and 4; so the only possible degrees are $3, 4, 5$ and the only possible labels $1, 2, 3$.

□

5.3.2 Bounds on the expander constant

In lemma 5.2.2 it has already been shown that the expander constant of a fullerene is always smaller than 1. This can even be improved by $\frac{2}{3}$, which also gives us a bound on the boundary length of an optimal patch:

Lemma 5.3.6 *Let P be an optimal patch in a geodesic dome T that consists of n faces. Then we have*

$$q(T) = \frac{b(P)}{f(P)} \leq \frac{2}{3} \tag{5.5}$$

and

$$b(P) \leq \frac{n}{3}\,. \tag{5.6}$$

PROOF:

We may choose a patch P' in T consisting of exactly three inner vertices which form a triangle and among them at least one degree 5 vertex (see figure 5.6).

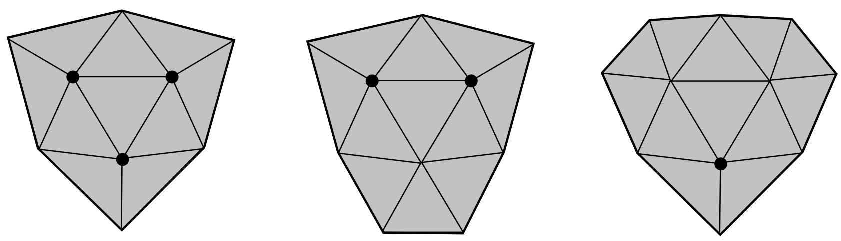

Figure 5.6: Three possible patches with 3, 2 or 1 degree 5 vertex

Then P' contains at most $\frac{n}{2}$ faces: The smallest possible n is $n = 20$, where the geodesic dome consists of 12 degree 5 vertices forming an icosahedron. In this case P' must have 3 inner vertices of degree 5 and hence contains exactly $10 = \frac{n}{2}$ faces. Otherwise we have $n \geq 24$, since n must be even and $n = 22$, i.e. one degree 5 vertex, is not possible (this follows from the possible number of vertices in a fullerene, see 5.2). But in any of the three cases P' contains not more than 12 faces, so it fulfills $f(P') \leq \frac{n}{2}$.

Now if we consider the three possible patches for P' we get that the boundary length divided by the number of faces is either $\frac{6}{10}$, $\frac{7}{11}$, or $\frac{8}{12} = \frac{2}{3}$, and hence in any case smaller than $\frac{2}{3}$. So if P is optimal, it has to fulfill

$$\frac{b(P)}{f(P)} \leq \frac{b(P')}{f(P')} \leq \frac{2}{3}.$$

Since $f(P) \leq \frac{n}{2}$, this also implies:

$$b(P) \leq \frac{2}{3} \cdot f(P) \leq \frac{2}{3} \cdot \frac{n}{2} = \frac{n}{3}$$

□

The bound $\frac{n}{3}$ is of great importance for the later computer program. Also, (5.7) in the following remark will be very helpful:

Remark 5.3.7 *Similarly to the proof of lemma* 5.3.6*, we may even deduce a better bound on the boundary length of an optimal patch in case a patch with a smaller quotient than* $\frac{2}{3}$ *is already known: If in a geodesic dome* T *with* n *faces,* $\bar{P}$ *is an arbitrary patch with* $f(\bar{P}) \leq \frac{n}{2}$*, then an optimal patch* P *must fulfill*

$$\frac{b(P)}{f(P)} \leq \frac{b(\bar{P})}{f(\bar{P})},$$

and with $f(P) \leq \frac{n}{2}$ *this particularly implies:*

$$b(P) \leq \frac{b(\bar{P})}{f(\bar{P})} \cdot \frac{n}{2} \tag{5.7}$$

So we have shown that $\frac{2}{3}$ is one upper bound for the expander constant of a fullerene. On the other hand it is easy to see that the expander constant of a fullerene – which is clearly strictly larger than 0 – can yet be arbitrarily small, i.e. smaller than any $\varepsilon > 0$:

A *nanotube* is a tube-type fullerene which consists of two *caps* each containing six pentagons, and one body consisting of hexagonal rings (see chapter 4). If we maintain the caps and enlarge the body of a nanotube, the expander constant becomes smaller, because the same cut can be used to split more vertices. So in order to achieve an expander constant smaller than a given $\varepsilon > 0$, we just have to add sufficiently many hexagonal rings.

Of course this can easily be transferred to the dual, where the tubes contain two 6-patches as caps and a body of triangles and all vertices with degree 6. For an example we study the dual of the nanotube whose caps consist of just the six pentagons:

We start with the patch that contains exactly six interior vertices of degree 5 and add rings of 10 triangles each (see figure 5.7). The boundary length stays 5, not depending on how many rings we add. Eventually we complete with a cap again, such that the number of rings is even. Then we can split the tube half-and-half by a cycle of length 5, which obviously yields an optimal patch since a smaller boundary length than 5 is not possible except for patches consisting only of one or two faces. So the optimal patch has boundary length 5 and contains half the number of faces. For $2k$ rings we have in total $30 + 20k$ faces, i.e. $15 + 10k$ faces in the optimal patch and hence an expander quotient of $\frac{1}{3+2k}$. For k large enough this quotient becomes arbitrarily small.

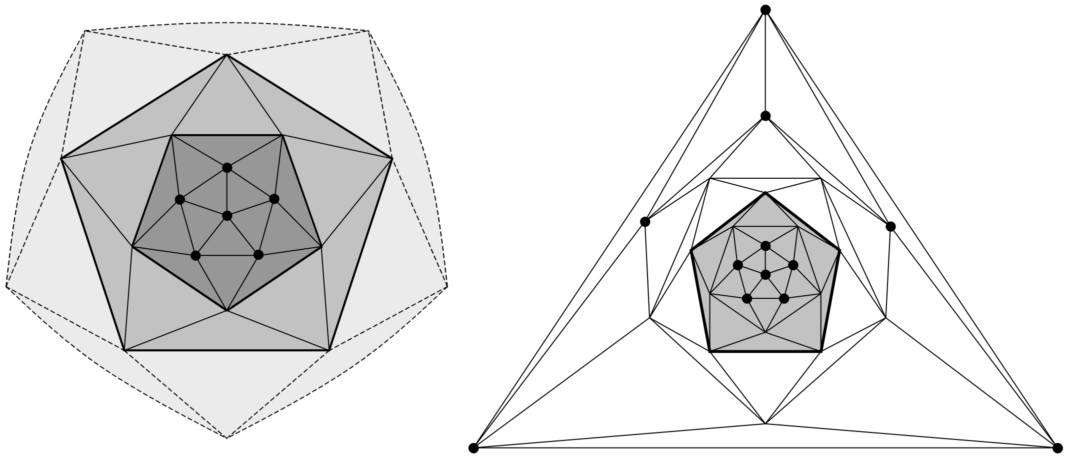

Figure 5.7: The construction of a patch of arbitrary size with boundary length 5 (left), and an example of a geodesic dome with 50 faces constructed in the described way (right) where an optimal patch with 25 faces and boundary length 5 is marked

5.3.3 The boundary of optimal patches

In this section we collect further information on the boundary of optimal patches, apart from the information contained in lemma 5.3.5.

At first remember the following formula concerning the boundary degrees in p-patches:

Remark 5.3.8 *For any p-patch P we have*

$$\sum_{v \in V_b(P)} (4 - \deg(v)) \;=\; 6 - p \tag{5.8}$$

due to lemma 2.2.3 *and remark* 2.2.2.

Corollary 5.3.9 *Let P be a p-patch where all boundary vertices have degree* 3, 4 *or* 5, *and $D_i(P)$ the number of boundary vertices with degree i. Then formula* (5.8) *implies*

$$D_3(P) - D_5(P) \;=\; 6 - p\,. \tag{5.9}$$

Lemma 5.3.10 *Let P be a p-patch that is subgraph of a geodesic dome T with a boundary labeling L, and p_B the number of boundary vertices of P that have degree* 5 *in T. Then we have*

$$\sum_{v \in V_b(P)} (L(v) - 2) \;=\; 6 - (p + p_B). \tag{5.10}$$

PROOF:

Consider $P' := T - P$ and assume it is a p'-patch. Since in total there must be 12 vertices of degree 5 in T, which distribute over the interior of P, the interior of P', and the boundary of P, we have

$$p' = 12 - (p + p_B)\,. \tag{5.11}$$

Furthermore, for every boundary vertex $v \in V_b(P)$ of P (which is obviously also boundary vertex of P') we have $\deg_{P'}(v) + \deg_P(v) = \deg_T(v) + 2$, because by adding the incident edges in the respective patches we obtain the two boundary edges twice; therefore we get with the definition of boundary labeling:

$$\deg_{P'}(v) = \deg_T(v) - \deg_P(v) + 2 = L(v) + 2 \tag{5.12}$$

Now we apply formula (5.8) to P':

$$\begin{aligned} & \sum_{v \in V_b(P)} (4 - \deg_{P'}(v)) = 6 - p' \\ \overset{(5.12),(5.11)}{\Leftrightarrow} \quad & \sum_{v \in V_b(P)} (4 - (L(v) + 2)) = 6 - (12 - (p + p_B)) \\ \Leftrightarrow \quad & \sum_{v \in V_b(P)} (2 - L(v)) = -6 + (p + p_B) \\ \Leftrightarrow \quad & \sum_{v \in V_b(P)} (L(v) - 2) = 6 - (p + p_B) \end{aligned}$$

□

Corollary 5.3.11 *Let P be a p-patch in a geodesic dome T that has only boundary labels* 1, 2 *and* 3, p_B *the number of boundary vertices of P that have degree* 5 *in T, and L_i the number of boundary vertices with label i. Then we have by formula* (5.10)

$$L_3(P) - L_1(P) = 6 - (p + p_B)\,. \tag{5.13}$$

In the following we will have a closer look on the number and order of the labels 1, 2 and 3 in the boundary of an optimal patch.

Remark 5.3.12 *Let P be an optimal patch in a geodesic dome T and $\overline{p} := p + p_B$ the number of both inner and boundary vertices of P with degree* 5*. By remark* 5.3.5*, P contains only boundary labels* 1, 2 *and* 3*, so corollary* 5.3.11 *can be applied and yields that we have $L_1(P) = L_3(P)$ iff $\overline{p} = 6$, $L_1(P) < L_3(P)$ iff $\overline{p} < 6$, and $L_1(P) > L_3(P)$ iff $\overline{p} > 6$. Because of $0 \leq \overline{p} \leq 12$ we know especially that $-6 \leq L_3(P) - L_1(P) \leq 6$ holds.*

Definition 5.3.13 *Given a p-patch P that is subgraph of a geodesic dome T, and L a labeling of its boundary. The cyclic sequence of vertex labels as they occur in the boundary cycle of P is called the* boundary label sequence *of P. Two boundary label sequences are identified with each other if one can be obtained from the other by a cyclic reordering or inversion. If the boundary label sequence contains a subsequence $l, l, \ldots, l$ of equal succeeding labels l occurring i times, we also write l^i instead of $l, l, \ldots, l$.*

The visual meaning of the following lemma is that the boundary cycle of an optimal patch (if we view it as a directed cycle where the patch lies on its right hand side) cannot contain two succeeding 'left turns' (i.e. a label subsequence $1, 2^i, 1$) *and* two succeeding 'right turns' (i.e. a label subsequence $3, 2^j, 3$), unless there are only these four 'turns' and the right and left follow immediately upon each other.

Lemma 5.3.14 *Let P be an optimal patch in a geodesic dome T. If its boundary label sequence contains a subsequence $1, 2^i, 1$ as well as a subsequence $3, 2^j, 3$, where $i, j \in \mathbb{N}_0$, then the whole boundary label sequence is given by $1, 2^i, 1, 3, 2^j, 3$.*

PROOF:

Assume there are the subsequences $1, 2^i, 1$ and $3, 2^j, 3$, but not both follow immediately upon each other – w.l.o.g. there is a vertex following on the second label 1 vertex of the first subsequence which is different from the first label 3 vertex of the second subsequence.

Let $v_0, v_1, \ldots, v_k, \ldots, v_l, \ldots, v_m, v_{m+1}$ denote the succeeding boundary vertices such that $L(v_1) = L(v_k) = 1$, $L(v_l) = L(v_m) = 3$, and $L(v_h) = 2$ for $h = 2, \ldots, k-1, l+1, \ldots, m-1$, as indicated in figure 5.8 (where $k = i + 2$ and $m - l = j + 1$). Then by assumption we have $\{v_k, v_{k+1}\} \neq \{v_{l-1}, v_l\}$, while the case $\{v_0, v_1\} = \{v_m, v_{m+1}\}$ cannot be excluded.

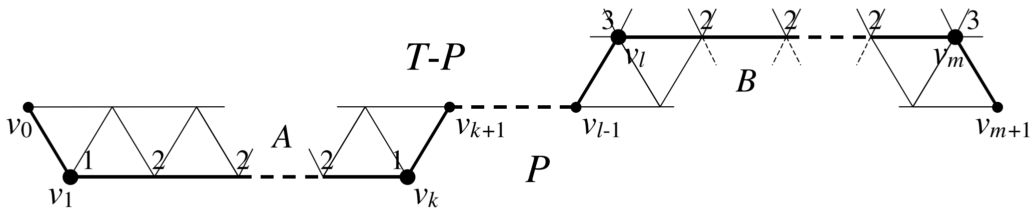

Figure 5.8: The subsequences $1, 2^i, 1$ and $3, 2^j, 3$ in the boundary of P

Now we let

$$A := \{f \in F(T - P) : \exists\, i \in \{1, \ldots, k\} \text{ such that } v_i \in f\}$$

be the set of triangles in $T - P$ that lie 'between' v_1 and v_k, and

$$B := \{f \in F(P) : \exists\, i \in \{l, \ldots, m\} \text{ such that } v_i \in f\}$$

the set of triangles in P lying 'between' v_l and v_m (see also figure 5.8). Then A contains an odd number of triangles (namely $2k + 1$), while $|B|$ can be even or odd, depending on the number of vertices with degree 5 among the label 2 vertices.

First we assume that $|A| \geq |B|$. Then we may remove all the triangles in B from P and add the same number of triangles of A to P, starting with the one that contains $\{v_k, v_{k+1}\}$ and continuing with the neighbours. (Note that because of $\{v_k, v_{k+1}\} \neq \{v_{l-1}, v_l\}$, the triangle in P that contains $\{v_k, v_{k+1}\}$ remains !)

If the boundary of the resulting graph still forms a simple cycle, we obtain a patch P' where the length of the boundary segment between v_{l-1} and v_{m+1} is reduced by at least 1. The length of the segment between v_0 and v_{k+1} stays either the same (in case $|B|$ even) or grows by 1 (in case $|B|$ odd) – compare figure 5.9. In the first case, P' has a smaller quotient of boundary length divided by face number, which is a contradiction to the assumption that P

was optimal. In the second case, the boundary length (and hence the quotient) of P' might be the same as in P, but then P' has a vertex of degree 2 which means that P' cannot be optimal and neither can P.

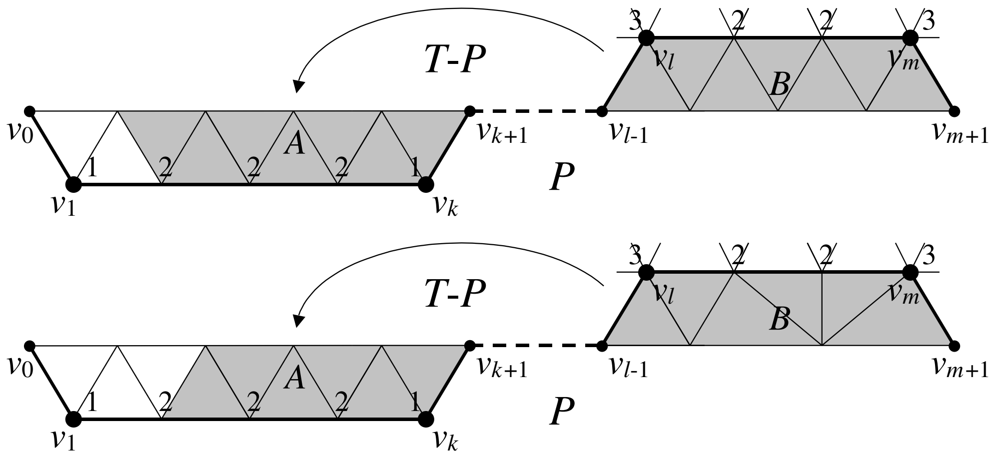

Figure 5.9: The situation $|A| \geq |B|$ in the proof of lemma 5.3.14, where the $|B|$ faces are removed from P and the same number of faces from A are included. In the upper figure we see the case where $|B|$ is odd, in the lower case $|B|$ is even.

Now it might be the case that either removing the faces in B results in a graph that is not 2-connected anymore, or that by adding faces in A we touch the boundary somewhere else, so that the new boundary consists of distinct cycles. But its boundary length is even smaller, so the quotient is reduced again and because of lemma 5.2.3, there is a 2-connected patch with the same (or even smaller) quotient.

Finally consider $|A| < |B|$. Then we include all faces of A to P and delete $|A|$ faces in B, starting with the one that contains $\{v_{l-1}, v_l\}$ and continuing with the neighbours. Hence the length of the boundary segment between v_0 and v_{k+1} is reduced by 1, and the length of the segment between v_{l-1} and v_{m+1} might be less or equal, which reduces the quotient, or grows by 1, but then we have again a vertex of degree 2 – see also figure 5.10. (This holds again even if the new boundary does not form a simple cycle, as demonstrated in the case before.) So again P cannot be optimal.

□

A similar technique can be applied in order to exclude a boundary label sequence containing two succeeding 'right turns', that means a subsequence $3, 2^k, 3$, and at the same time a label 1 vertex with 'too many' label 2's next to it, that means a subsequence $1, 2^{k+1}$ or $2^{k+1}, 1$, unless the label 1 vertex is adjacent to one of the label 3 vertices.

Lemma 5.3.15 *Given a geodesic dome T containing an optimal patch P. If the boundary label sequence of P contains a subsequence $3, 2^k, 3$, and additionally there exists a vertex with label 1, then either the label 1 vertex is adjacent to one of the two label 3 vertices of the subsequence, or there are at most k vertices with label 2 next to the label 1 vertex in both directions of the boundary cycle.*

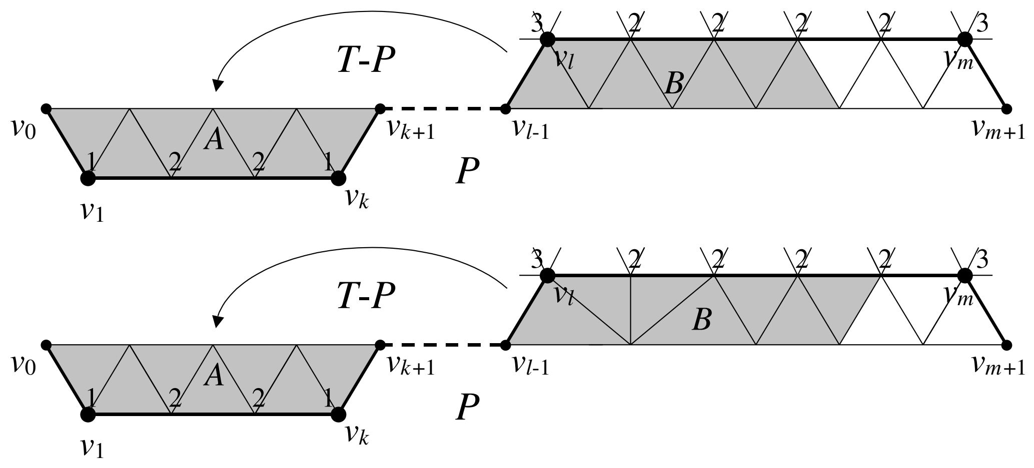

Figure 5.10: The situation $|A| < |B|$ in the proof of lemma 5.3.14: Remove $|A|$ faces from B and include all faces of A. In the upper figure this induced a boundary vertex of degree 2, in the lower figure the boundary length is strictly reduced.

PROOF:

Assume the contrary, i.e. the label 1 vertex is *not* adjacent to one of the label 3 vertices, and there are at least $k+1$ label 2 vertices next to the label 1 vertex, that means there is a boundary label subsequence $2^{k+1}, 1$. Then we may remove all the faces 'between' the two label 3 vertices (i.e. all that contain one of the respective vertices – that are at most $2k+3$ faces) and add the same number of faces at the $2^{k+1}, 1$ subsequence next to the label 1 vertex, that means we include the appropriate number of those faces to P that lie in $T-P$ but contain one of the vertices corresponding to the $2^{k+1}, 1$ subsequence, starting with the face that contains only the label 1 vertex and continuing with its neighbours. It is possible to add up to $2k+4$ faces this way. Then in case the number of faces is odd, we obtain a degree 2 vertex while the boundary length stays the same or is even reduced, so the new patch and therefore also the original one cannot be optimal; and in case the number of faces is even, the boundary length is strictly reduced so the original patch could not have been optimal either (compare also the proof of lemma 5.3.14). Figure 5.11 gives an example of either case. Hence we have a contradiction and the lemma is proved.

□

Combining the two previous lemmas, we immediately obtain the following corollary:

Corollary 5.3.16 *Given a geodesic dome T containing an optimal patch P. Then the boundary label sequence of P cannot contain a subsequence of one of the types*

$$1, 2^i, 1, x, \ldots, 3, 2^j, 3$$
$$3, 2^i, 3, x, \ldots, 1, 2^j, 1$$
$$3, 2^k, 3, x, \ldots, 1, 2^{k+1}$$
$$3, 2^k, 3, \ldots, 2^{k+1}, 1, x$$

where $i, j, k \in \mathbb{N}_0$, x denotes an arbitrary boundary label, and $\ldots$ may be filled by an arbitrary sequence of boundary labels but may also be empty.

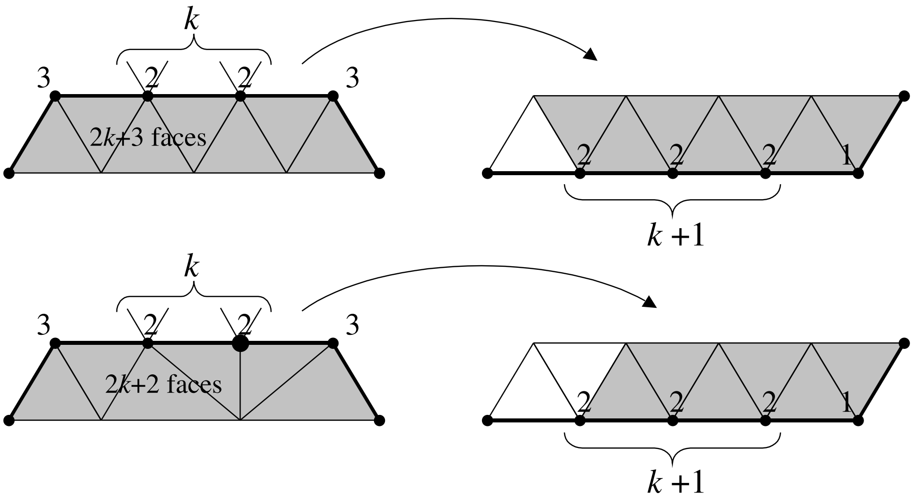

Figure 5.11: The situation in a counterexample to lemma 5.3.15: If there is a subsequence $3, 2^k, 3$ and additionally a vertex with label 1 which appears in a subsequence $2^{k+1}, 1$ and is not adjacent to one of the considered label 3 vertices, we may shift faces such that either we obtain a degree 2 vertex while the boundary length does not grow (upper figure), or the boundary length is strictly reduced (lower figure).

5.3.4 Numbers of faces in optimal patches

The question that we discuss in this section is: How close is the number of faces in an optimal patch to half of the number of faces in the geodesic dome? (Note that the number of faces in the geodesic dome is always even since it is the number of vertices in the dual fullerene.) If we were able to show that an optimal patch in a geodesic dome with n faces always has to contain $\frac{n}{2}$, or maybe $\frac{n}{2} - 1$ faces, this would simplify the task to find optimal patches a lot. Unfortunately we will see that this is not the case and that we also have to consider patches whose numbers of faces are remarkably smaller than $\frac{n}{2}$.

However, the following lemma implies that for a geodesic dome with n faces, an optimal patch often contains $\frac{n}{2}$ or $\frac{n}{2}-1$ faces; otherwise its boundary label sequence must not contain any label 1.

Lemma 5.3.17 *Let P be an optimal patch with respect to a geodesic dome T, and let n be the number of faces in T. If the boundary of P contains a vertex with label 1, then*

$$\frac{n}{2} - 1 \leq f(P) \leq \frac{n}{2} .$$

PROOF:

Let v be the vertex with label 1. Then we either have $\deg_P(v) = 5$ and $\deg_T(v) = 6$, or $\deg_P(v) = 4$ and $\deg_T(v) = 5$. In any case there are two triangles adjacent to v that are lying in T but not in P.

Now $f(P) \leq \frac{n}{2}$ already holds by definition of an optimal patch; so assume that $f(P) \leq \frac{n}{2} - 2$. Then if we define a patch P' as the patch P together with the two triangles from $T - P$ (see figure 5.12), it still fulfills $f(P') \leq \frac{n}{2}$. Obviously we have $b(P') = b(P)$ and $f(P') = f(P)+2$, and hence

$$\frac{b(P')}{f(P')} < \frac{b(P)}{f(P)} .$$

So P was not optimal, that means the assumption was wrong and we must have $f(P) \geq \frac{n}{2} - 1$.

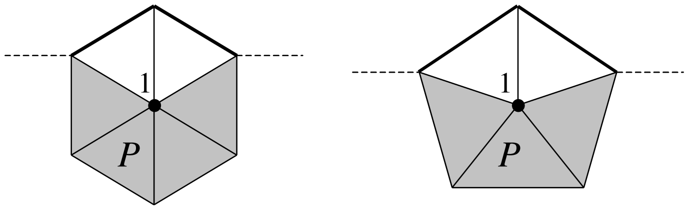

Figure 5.12: Two label 1 vertices in P – one with degree 6 and one with degree 5 in T. In both cases, one can add two triangles without changing the boundary length

□

If P does *not* contain a label 1 vertex, i.e. there are only boundary labels 2 and 3, it is not possible to establish a bound on the number of faces in a similar way, since we cannot add any faces without changing the boundary length: Adding 3 faces at a label 2 vertex will for example extend the boundary length by 1 (see figure 5.13). This might not be enough to reduce the quotient $\frac{b(P)}{f(P)}$: If $3b(P) \leq f(P)$, the new patch P' still fulfills $\frac{b(P')}{f(P')} = \frac{b(P)+1}{f(P)+3} \geq \frac{b(P)}{f(P)}$. So an optimal patch might consist of less than $\frac{n}{2} - 2$ faces in this case.

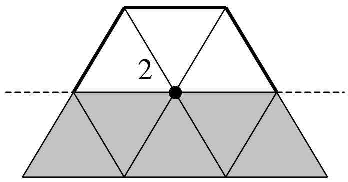

Figure 5.13: Adding 3 triangles to a regular patch at a label 2 vertex with degree 6

We will now demonstrate that indeed the difference between $\frac{n}{2}$ and the number of faces in an optimal patch can even be arbitrary large by constructing an appropriate class of geodesic domes.

At first we choose a 6-patch P_1 where all boundary vertices have degree 4. Such a patch can be constructed fulfilling $b(P_1) \geq m$ for any given $m \in \mathbb{N}$ – for example in the following way:

Let $s := \lceil \frac{m}{6} \rceil$ and consider the subgraph of the triangular lattice which forms a regular hexagon with boundary length $6s$ and $6s^2$ triangles. Then add further faces around it such that the six boundary vertices of degree 3 get degree 5 in the patch (see figure 5.14). The resulting patch P_1 fulfills $b(P_1) = 6s \geq m$, and all boundary vertices have degree 4.

Now we take two such patches as caps and insert k additional rings of $2b(P_1)$ faces each, such that we obtain a tube with $n = 2f(P_1) + 2kb(P_1)$ faces and hence $\frac{n}{2} = f(P_1) + kb(P_1)$.

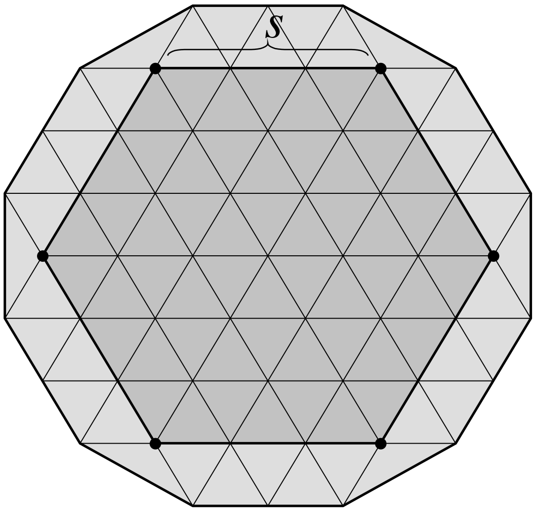

Figure 5.14: A patch with boundary length $6s$ (here $s = 3$), and only degree 4 vertices in the boundary

If k is even, the tube can be cut into two equal-sized halves, both containing $\frac{n}{2}$ faces and having the same boundary length $b(P_1)$ as the two caps (compare also section 5.3.2).

However, this is not possible if k is odd. In this case consider the patch P consisting of one cap and $\frac{k-1}{2}$ rings. It has the boundary length $b(P) = b(P_1)$ and contains $f(P) = f(P_1) + (k-1)b(P) = \frac{n}{2} - b(P)$ faces. Nevertheless P could already be an optimal patch: Since all boundary labels are 2, no faces can be added without changing the boundary length. However, we may add an odd number of up to $b(P)$ faces to this patch such that the boundary length is extended by 1. Then the quotient of boundary length divided by face number of the resulting patch P' is at least $\frac{b(P')}{f(P')} = \frac{b(P)+1}{f(P_1)+kb(P)}$.

Supposing that this quotient is strictly larger than the respective quotient $\frac{b(P)}{f(P)}$ of P, we develop the following condition:

$$\begin{aligned}
& \frac{b(P)+1}{f(P_1)+kb(P)} > \frac{b(P)}{f(P_1)+(k-1)b(P)} \\
\Leftrightarrow\quad & b(P)f(P_1) + (k-1)b(P)^2 + f(P_1) + (k-1)b(P) > b(P)f(P_1) + kb(P)^2 \\
\Leftrightarrow\quad & f(P_1) + (k-1)b(P) > b(P)^2 \\
\Leftrightarrow\quad & \frac{f(P_1)}{b(P)} + k - 1 > b(P) \\
\Leftrightarrow\quad & k > b(P) - \frac{f(P_1)}{b(P)} + 1
\end{aligned}$$

That means if relative to the boundary length $b(P) = b(P_1)$ and the number of faces $f(P_1)$ of the cap P_1, we choose the number of rings k large enough such that $k > b(P) - \frac{f(P)}{b(P)} + 1$ holds, adding more faces to P does *not* reduce the quotient of boundary length divided by face number. And since there is no other possibility to split the body of such a tube such that the boundaries of the resulting patches are strictly smaller than $b(P_1)$, we conclude that the patch P with $\frac{n}{2} - b(P)$ faces indeed must be an optimal patch in the constructed geodesic dome. Because the starting patch P_1 can be chosen with $b(P_1)$ arbitrarily large, this gives us a way to construct a geodesic dome with n faces and an optimal patch whose number of faces is arbitrarily far from $\frac{n}{2}$.

An example: A geodesic dome with n faces where an optimal patch contains $\frac{n}{2} - 5$ faces can be constructed by choosing a cap P_1 with boundary length $b(P_1) = 5$ like in figure 5.7. We add k rings of $2b(P_1) = 10$ faces such that k is odd and $k > b(P_1) + 1 - \frac{f(P_1)}{b(P_1)} = 5 + 1 - \frac{15}{5} = 3$, e.g. $k = 5$. Then we have in total $2 \cdot 15 + 5 \cdot 10 = 80$ faces, and the patch P consisting of one cap with 2 rings contains 35 faces and is optimal: Any patch that contains more faces has a longer boundary and even adding 5 more faces does not reduce the quotient ($\frac{5}{35} < \frac{6}{40}$!) – see figure 5.15.

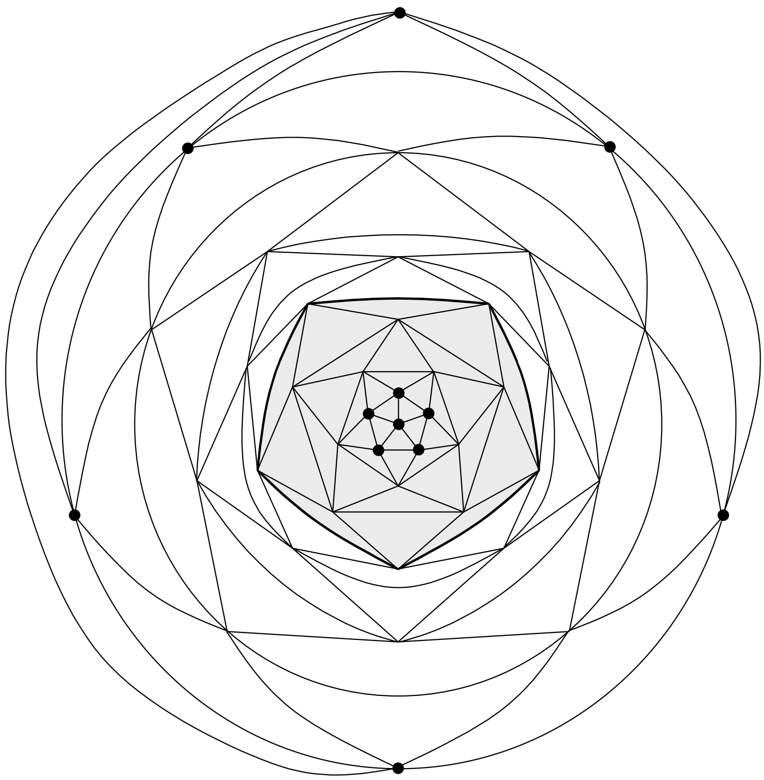

Figure 5.15: A geodesic dome with 80 faces and an optimal patch consisting of 35 faces

So this way we can construct tube-type geodesic domes where the difference between the number of faces $f(P)$ in an optimal patch P and half of the number of total faces $\frac{n}{2}$ is arbitrarily large. However, in order to obtain a larger difference we have to construct a larger geodesic dome. So a further interesting question, which we do not discuss here, would be whether the difference between $f(P)$ and $\frac{n}{2}$ can be determined by the number of faces n.

5.4 Determination of expander constants of fullerenes

Now we want to apply the established results in order to determine the expander constant of a given fullerene. We offer two different approaches: At first we demonstrate how to prove the expander constant of a class of symmetrical fullerenes by hand; afterwards we introduce a computer program that is able to compute the expander constant if the graph of the geodesic dome is given, and present some of its results.

5.4.1 A theoretical approach

In this section we develop some useful techniques of how one can verify the expander constant of a given fullerene (or the expander quotient of the corresponding geodesic dome), preferably with a high symmetry, with the help of results from chapter 3. We proceed such that at first an optimal patch in the given geodesic dome must be guessed, and then we prove that it is optimal by showing that no other patches with a smaller quotient of boundary length and face number exist, where we distinguish between the different possible numbers of degree 5 vertices. For this, the formulas that have been derived for the boundary lengths of patches with respect to their number of faces in chapter 3 will be essential, as well as the method introduced in 3.3.4 and 3.3.5 to determine such formulas in case a fixed subpatch is given.

We demonstrate the approach by determining and discussing the expander constant of a certain group of fullerenes with icosahedral symmetry, including the famous Buckminster fullerene.

The following lemmas are based on results from chapter 3 and provide a very simple and effective possibility to exclude p-patches with small p (and also with very large p) from being candidates for optimal patches in a given geodesic dome.

Lemma 5.4.1 *For any p-patch P with $0 \leq p \leq 5$ we have:*

$$\frac{b(P)}{f(P)} \geq \sqrt{\frac{6-p}{f(P)}}$$

PROOF:

By corollary 3.3.4 we have $b(P) \geq \sqrt{(6-p)f(P)}$. This implies:

$$\frac{b(P)}{f(P)} \geq \frac{\sqrt{(6-p)f(P)}}{f(P)} = \sqrt{\frac{(6-p)f(P)}{f(P)^2}} = \sqrt{\frac{6-p}{f(P)}}$$

□

Lemma 5.4.2 *Let T be a geodesic dome with $2n$ faces, and P' a patch in T with $f(P') \leq n$ and $a := \frac{b(P')}{f(P')}$. Then if there exists $\bar{p} \in \{0, 1, \dots, 5\}$ with*

$$\sqrt{\frac{6-\bar{p}}{n}} > a \, , \tag{5.14}$$

all optimal patches in T must be p-patches with $\bar{p} < p < 12 - \bar{p}$.

PROOF:

At first assume there is an optimal p-patch P with $p \le \bar{p}$. Then we have $6 - p \ge 6 - \bar{p}$, $f(P) \le n$, and with lemma 5.4.1 and the assumption (5.14) we get:

$$\frac{b(P)}{f(P)} \ge \sqrt{\frac{6-p}{f(P)}} \ge \sqrt{\frac{6-p}{n}} \ge \sqrt{\frac{6-\bar{p}}{n}} > a = \frac{b(P')}{f(P')}$$

But this is a contradiction to the assumption that P was optimal.

Now suppose P is an optimal p-patch with $p \ge 12 - \bar{p}$. Then it fulfills $f(P) \le n$. Moreover, $Q := T - P$ is a q-patch with $q \le 12 - p = \bar{p} \le 5$, that means also $6 - q \ge 6 - \bar{p}$; furthermore $b(Q) = b(P)$ and $f(Q) = 2n - f(P) \ge n \ge f(P) = 2n - f(Q)$. All together we obtain with corollary 3.3.4:

$$\begin{aligned}\frac{b(P)}{f(P)} = \frac{b(Q)}{2n - f(Q)} &\overset{(3.33)}{\ge} \frac{\sqrt{(6-q)f(Q)}}{2n - f(Q)} \\ &\ge \frac{\sqrt{(6-\bar{p})f(Q)}}{2n - f(Q)} \\ &\ge \frac{\sqrt{(6-\bar{p})\,n}}{n} = \sqrt{\frac{6-\bar{p}}{n}} > a = \frac{b(P')}{f(P')}\end{aligned}$$

This means again that P could not have been optimal.

□

In [12], Coxeter classifies highly symmetric geodesic domes that have the full rotational group of the icosahedron. These geodesic domes can be obtained by filling each of the 20 faces of the icosahedron with an equilateral triangle that is subgraph of the regular triangular lattice of the plane. In [19], Graver extends Coxeter's approach to other geodesic domes. He uses a plane *signature graph* which consists of the icosahedron together with a labeling of the edges and angles, such that the vertices correspond to the 12 vertices of degree 5 in the geodesic dome and the filling of the 20 faces can be reconstructed by the labeling. In [21] and [20] he uses this approach to give a full parameterization of all fullerenes resp. geodesic domes with ten or more symmetries. In particular, the signature graph of a geodesic dome is supposed to give information about how far two vertices of degree 5 lie apart. Such a distance can be expressed by the *Coxeter coordinates* (see definition 2.3.1).

For instance, all geodesic domes with icosahedral symmetry have the icosahedron as signature graph where all edges are equipped with the same label. According to [21] we distinguish between three cases: In the first case, all edges of the signature graph have Coxeter coordinates (r), in the second (q, q), and in the third case $(q + r, q)$ for arbitrary $q, r \in \mathbb{N}$.

The second of the mentioned groups contains the dual of the Buckminster fullerene (case $q = 1$), which we will call *Buckminster dome.* In the following, we will examine the members of that group with regard to their expander quotient and as a result show:

Theorem 5.4.3 *Let $q \in \mathbb{N}$, and consider the geodesic dome whose signature graph is the icosahedron with all labels being (q, q). Then its expander quotient, and hence the expander constant of the corresponding fullerene, is $\frac{3}{10q}$ in case q is even, and $\frac{3}{10q} + \frac{1}{30q^2}$ in case q is odd. In particular, the expander constant of the Buckminster fullerene (with $q = 1$) is $\frac{1}{3}$.*

Figure 5.16 shows the graph of the Buckminster dome; in order to obtain the graph of another geodesic dome of this group with $q > 1$, we may just insert vertices such that each edge in the Buckminster dome is replaced by a path of length q, and replace each triangle in the Buckminster dome by a large triangle consisting of q^2 small triangles, as indicated in the figure on the right.

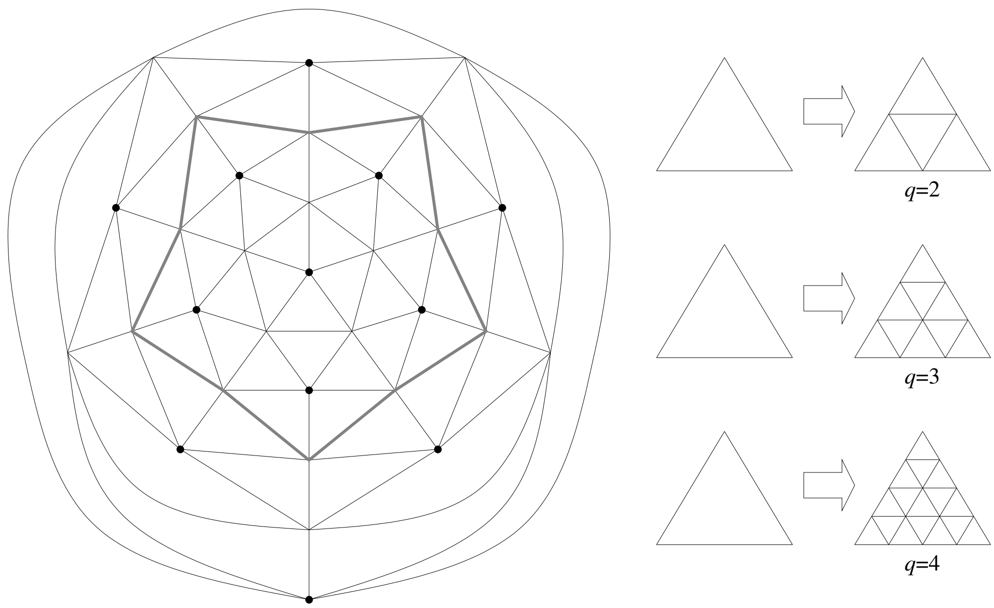

Figure 5.16: The graph of the Buckminster dome (left), and operations that can be applied to its faces in order to obtain the respective dome with $q = 2$, $q = 3$, and $q = 4$ (right)

In the following we will denote the geodesic dome of this group where all labels in the signature graph are (q, q) by T_q, relative to the given parameter $q \in \mathbb{N}$. Since the Buckminster dome T_1 contains 60 faces, the geodesic dome T_q obviously has $60q^2$ faces.

In figure 5.16 we also indicated one possible split (the fat grey line) of the graph into two equal halves – for general q they contain $30q^2$ faces each – which seems likely to produce a small quotient of boundary length and face number for the corresponding patches. The boundary length of such a patch is $10q$ and hence its quotient is $\frac{10q}{30q^2} = \frac{1}{3q}$. Therefore $\frac{1}{3q}$ can be established as an *upper* bound for the expander constant of the dual of T_q. In case of $q = 1$ we will see that the expander constant is $\frac{1}{3}$, such that the patch with the boundary drawn in figure 5.16 is indeed optimal for the Buckminster dome; however, for $q > 1$ this is not the case, as we will see in the following.

In case q is even, all triangles of q^2 faces can be obtained from the triangle consisting of 4 small triangles (case $q = 2$) by drawing further lines. Hence, T_q with q even can be constructed from T_2 by the replacements described above. In particular, each path in T_2 can be transferred to a path in T_q, where the path in T_q is k times as long if $q = 2k$.

Now in T_2 there exists a 6-patch with boundary length 18 which contains $120 = \frac{1}{2}f(T_2)$ faces, as can be seen from figure 5.17.

The corresponding quotient is $\frac{18}{120} = \frac{3}{20}$ which is strictly smaller than $\frac{1}{6} = \frac{1}{3q}$. We will show that this patch is optimal in T_2. Moreover, if we consider the corresponding path in T_q with

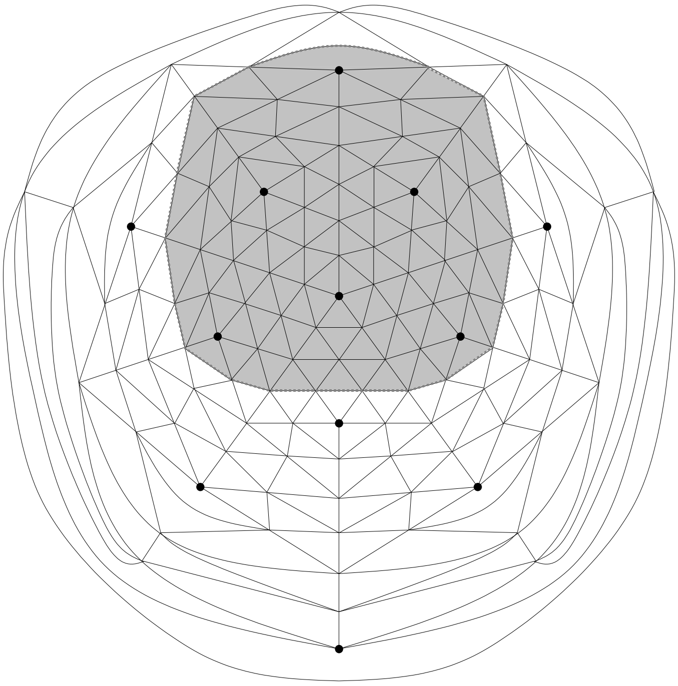

Figure 5.17: The geodesic dome T_2 with an optimal patch (shaded area)

$q = 2k$ it has the length $18k = 9q$ and still splits the graph half-and-half, and hence leads to the quotient

$$\frac{9q}{30q^2} = \frac{3}{10q} .$$

We will prove that this is indeed the expander constant of the dual of T_q in case q is even.

Figure 5.18 shows again the optimal patch in T_2 resp. T_q with q even: It contains 21 triangles of q^2 faces each, and the faces around it – that are $\frac{q}{2}$ rings of $18q$ faces each – can be rearranged to form 9 further triangles.

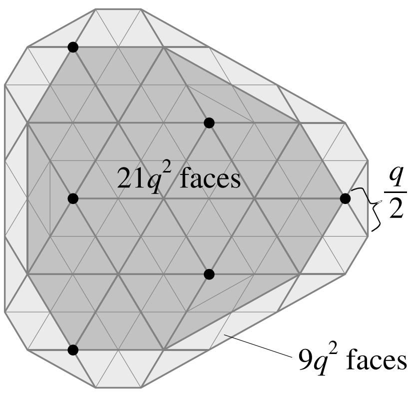

Figure 5.18: A 6-patch that is optimal with respect to T_2

In case q is odd, it is not possible to build a number of rings around the patch consisting of 21 triangles such that exactly $30q^2$ faces are contained. We may only take $\frac{q-1}{2}$ rings – then the boundary length is still $9q$ but the number of faces is $21q^2 + \frac{q-1}{2}18q = 30q^2 - 9q$. It is also possible to add $9q$ more faces of the next ring and thereby extend the boundary length by 1; then the quotient is

$$\frac{9q+1}{30q^2} = \frac{3}{10q} + \frac{1}{30q^2} .$$

This is smaller than $\frac{9q}{30q^2-9q}$ for any $q \in \mathbb{N}$, and we will prove that in case q is odd, the corresponding patch is even optimal. Figure 5.19 shows that patch for the case $q = 3$ and indicates how the other cases can be constructed; however, note that now the figures for the other cases can *not* be obtained by some triangle replacements.

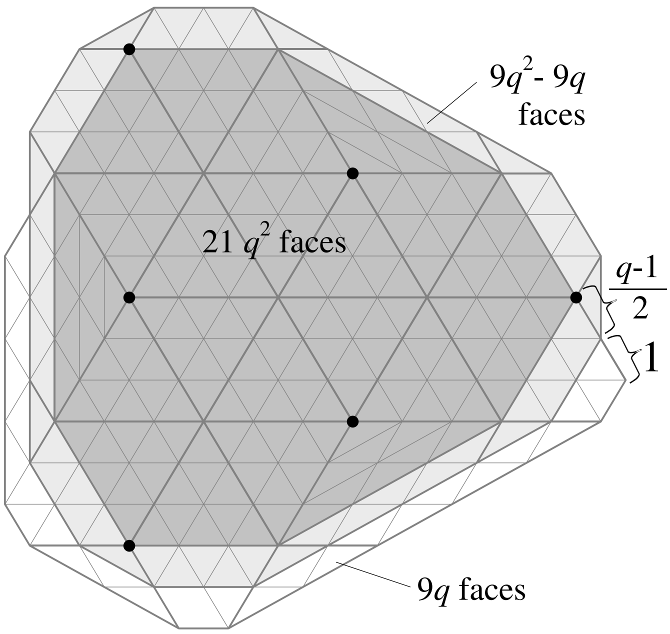

Figure 5.19: A 6-patch that is optimal with respect to T_3

Moreover, note that the case $q = 1$ is a special case: We may construct the patch as described, but – since no ring is added – then we obtain either a 4- or a 5-patch as a result (see figure 5.20). Indeed all these patches lead to the quotient $\frac{3}{10} + \frac{1}{30} = \frac{10}{30} = \frac{1}{3}$.

In order to prove for all cases that the constructed patches are optimal in T_q, we will proceed as follows: The idea is to distinguish between the number p of degree 5 vertices in possible optimal patches. If we are able to show that for certain p, *all* possible p-patches would have a quotient larger than the quotient of an existing patch with not more than $30q^2$ faces, then we conclude that no p-patches can be optimal in T_q. The existing patch with the quotient to compare could be the one which we claim to be optimal, or sometimes (for easier computation) also the one with quotient $\frac{1}{3q}$.

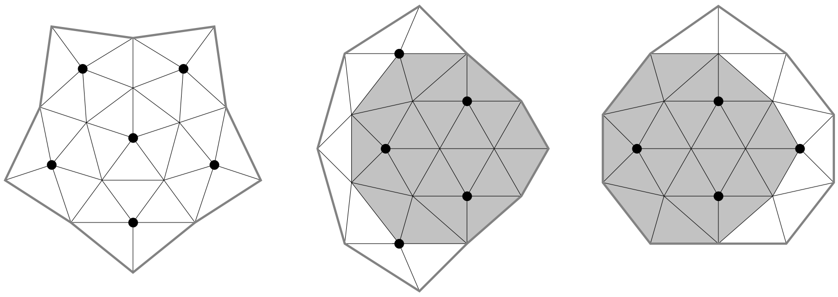

Figure 5.20: A 6-, a 5- and a 4-patch that are all subgraph of T_1, have boundary length 10 and contain 30 faces, where the 5- and the 4-patch can be constructed in the way described above by adding 9 faces around the shaded patch consisting of 21 triangles; as we will show that $\frac{1}{3}$ is the expander constant of the Buckminster fullerene, all these patches turn out to be optimal in the Buckminster dome.

The cases $p \leq 3$ and $p \geq 9$:

First, with the help of lemma 5.4.2, we are able to exclude all p-patches with $p \leq 3$ and $p \geq 9$ from being optimal in T_q, for q even as well as for q odd:

We already know that in any case T_q contains a patch with $30q^2$ faces and a quotient $a_q := \frac{1}{3q}$ of boundary length divided by face number. Now for $\bar{p} = 2$ we have

$$\sqrt{\frac{6-\bar{p}}{n}} = \sqrt{\frac{4}{30q^2}} = \frac{2}{\sqrt{30}\,q} > \frac{1}{3q} = a_q$$

which implies by lemma 5.4.2 that all optimal patches in T_q must be p-patches for some $2 < p < 10$.

Moreover, if q is even there is a patch with quotient $b_q := \frac{3}{10q}$, and if q is odd there exists a patch with quotient $c_q := \frac{3}{10q} + \frac{1}{30q^2}$. For $\bar{p} = 3$ we get

$$\sqrt{\frac{6-\bar{p}}{n}} = \sqrt{\frac{3}{30q^2}} = \frac{1}{\sqrt{10}\,q} > \frac{3}{10q} = b_q \ ;$$

furthermore, for $q \geq 3$ we have $(30 - 9\sqrt{10})q^2 \geq 3(30 - 9\sqrt{10})q > \sqrt{10}q$ and hence

$$\frac{1}{\sqrt{10}\,q} > \frac{9q+1}{30q^2} = \frac{3}{10q} + \frac{1}{30q^2} = c_q \ .$$

That means by lemma 5.4.2 that we may also exclude all 3-and 9-patches in case q is even, and in case q is odd with the exception $q = 1$.

The case $q = 1$ can be considered separately: We know that there exists a patch in T_1 with 30 faces and boundary length 10. Now if there was a 3-patch with up to 30 faces and a strictly smaller quotient, it could only have boundary length 9 or less. It is easy to see that such a patch would have to contain 3 degree 5 vertices with pairwise Coxeter coordinates $(1, 1)$, since all other configurations of degree 3 vertices require longer boundaries; but the largest 3-patch with boundary length 9 contains only 21 faces, and $\frac{9}{21} = \frac{3}{7} > \frac{1}{3}$. Furthermore, if there was an optimal 9-patch in T_1, it would have to contain at most 30 faces; however, any

9-patch in T_1 has to contain at least 45 faces, because for each of the inner degree 5 vertices it has to contain 5 faces, since no two degree 5 vertices are adjacent. So this leads to a contradiction, too, and we get that also for $q = 1$ there cannot be any optimal 3- or 9-patch in T_q.

The case $p = 4$*:*

Unfortunately we cannot apply lemma 5.4.2 for this case, since

$$\sqrt{\frac{2}{30q^2}} = \frac{1}{\sqrt{15}q} < \frac{3}{10q} \ .$$

The reason for this is that the lemma is based only on the inequations holding for *all* p-patches, where the minimal boundary length is obtained when the degree 5 vertices are close together, and does not make use of the information we have on the special configurations of degree 5 vertices for the current class of geodesic domes, where no adjacent degree 5 vertices exist. Therefore we have to investigate the boundary length of 4-patches that do actually occur in T_q. A further argument which becomes useful now is that the existing patches in T_q already provide an upper bound for the boundary length of an optimal patch:

We already know that in case q is even, there exists a patch with boundary length $9q$ containing $30q^2$ faces, and in case q is odd, there is one with boundary length $9q + 1$ and $30q^2$ faces. Hence if there was a patch with a strictly smaller quotient, it would have to have a boundary length strictly smaller than $9q$ or $9q + 1$, respectively.

There are only two possible configurations of 4 degree 5 vertices which allow such a boundary length for a 4-patch containing them; these are shown in figure 5.21. It is easy to check that all other configurations of degree 5 vertices that occur in T_q require that 4-patches containing them must have a boundary length of at least $9q + 1$.

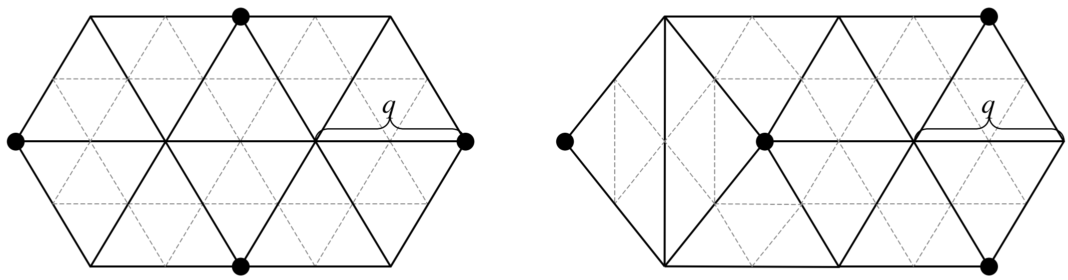

Figure 5.21: Two possible configurations of 4 degree 5 vertices in T_q (the dotted lines indicate the case $q = 2$ as an example)

At first we consider the left configuration of 4 degree 5 vertices where one pair has Coxeter Coordinates $(3q)$ and all other (q, q). We let $\bar{P}_q$ be the smallest regular 4-patch containing such a configuration, which has the boundary length $8q + 2$ (see figure 5.22 on the left for the case $q = 2$). It contains $14q^2$ inner faces (the interior consists of 14 triangles with q^2 faces each) and $16q + 2$ boundary faces, such that

$$f(\bar{P}_q) = 14q^2 + 16q + 2 \ .$$

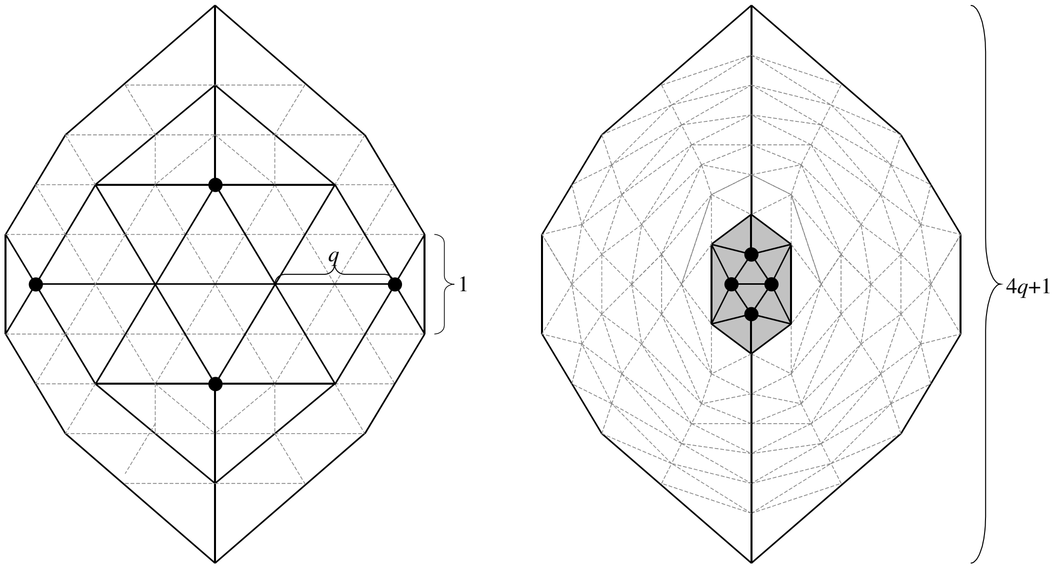

Figure 5.22: A regular 4-patch $\bar{P}_q$ which occurs in T_q (left picture), and the 4-patch $\hat{P}_q$ with the same boundary that contains $P_{4,0,0}$ (right picture)

Note that $f(\bar{P}_q) = 14q^2 + 16q + 2 \geq 30q^2$ for $q \geq 2$, but not for $q = 1$. Therefore we consider the case $q = 1$ separately: We know that in that case there exists a patch with boundary length 10 and 30 faces. Furthermore we observe that already the smallest patch containing the four degree 5 vertices (figure 5.23 left picture) has a boundary length of 10 and that adding any faces cannot reduce the boundary length; hence there can be no 4-patch with that configuration of degree 5 vertices which has a quotient *strictly* smaller than $\frac{1}{3}$. However, there is indeed a 4-patch in T_1 which has boundary length 10 and contains 30 faces; it can be obtained from the regular patch with 32 faces by removing two faces adjacent to one of the degree 3 vertices (see figure 5.23 middle and right picture). This is the same patch that we constructed in figure 5.20, right picture, and indeed it will turn out to be optimal in T_1.

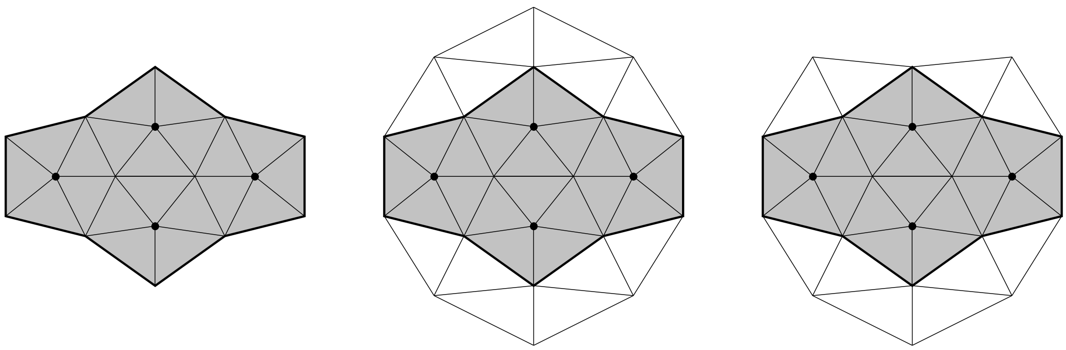

Figure 5.23: A configuration of four degree 5 vertices as it occurs in T_1 (left); the smallest regular patch $\bar{P}_q$ containing the configuration, which has 32 faces (middle), and a patch with a total number of 30 faces and boundary length 10 (right)

Now let $q \geq 2$; then we may assume that if there was an optimal 4-patch containing that configuration of degree 5 vertices, then it contains even $\bar{P}_q$, because otherwise we could always add faces without enlarging the boundary length.

So suppose there exists an optimal 4-patch P_q in T_q which contains $\bar{P}_q$. In order to develop a lower bound on the boundary length of P_q with respect to its number of faces that is sharper than the one obtained from corollary 3.3.3, we proceed exactly as demonstrated in section 3.3.4: We replace the 4-patch $\bar{P}_q$ in P_q by a 4-patch $\hat{P}_q$ with the same boundary that contains $P_{4,0,0}$ (see figure 5.22, right picture). Now we determine the number of faces in $\hat{P}_q$ with respect to $f(\bar{P}_q)$: With $f(\bar{P}_q) = 14q^2 + 16q + 2$ we get that the number of faces in $\hat{P}_q$ is

$$f(\hat{P}_q) \;=\; 2(4q+1)^2 - 6 \;=\; 32q^2 + 16q - 4 \;=\; f(\bar{P}_q) + 18q^2 - 6 \; .$$

So applying corollary 3.3.3 to P'_q, we get the following formula for P_q:

$$\begin{aligned} b(P_q) \;=\; b(P'_q) \;&\geq\; \sqrt{2f(P'_q) + 12} \\ &=\; \sqrt{2(f(P_q) + 18q^2 - 6) + 12} \\ &=\; \sqrt{2f(P_q) + 36q^2} \end{aligned} \tag{5.15}$$

Furthermore, since P_q was assumed to be optimal, we have $f(P_q) \leq 30q^2$. It follows that

$$\begin{aligned} \frac{b(P_q)}{f(P_q)} \;&\overset{(5.15)}{\geq}\; \frac{\sqrt{2f(P_q) + 36q^2}}{f(P_q)} \\ &=\; \sqrt{\frac{2}{f(P_q)} + \frac{36q^2}{f(P_q)^2}} \\ &\overset{f(P_q)\leq 30q^2}{\geq}\; \sqrt{\frac{2}{30q^2} + \frac{36q^2}{(30q^2)^2}} \\ &=\; \sqrt{\frac{96q^2}{(30q^2)^2}} \;=\; \frac{\sqrt{96}\,q}{30q^2} \;=\; \frac{\sqrt{96}}{30} \cdot \frac{1}{q} \end{aligned} \tag{5.16}$$

Now we have $\frac{\sqrt{96}}{30} > \frac{3}{10}$, and for $q \neq 1$ we even have $\frac{\sqrt{96}}{30q} > \frac{9q+1}{30q^2}$. That means P_q cannot be optimal – neither if q is even, nor if q is odd, with the exception $q = 1$ which has been examined above.

Note that even if a patch contained the four degree 5 vertices but not the whole regular graph $\bar{P}_q$, we could have replaced the patch by a patch with the same boundary containing $P_{4,0,0}$ and this way obtained the same results.

Next we consider the second possible configuration of 4 degree 5 vertices, where two pairs have Coxeter Coordinates $(3q)$ and the four other (q,q). Again we let $\bar{P}_q$ be the smallest regular 4-patch containing such a configuration, which has also boundary length $8q+2$ (see figure 5.24 for the case $q = 2$). As before we may assume that if there was an optimal 4-patch containing these degree 5 vertices, then it contains $\bar{P}_q$.

Now the 4-patch $\bar{P}_q$ contains only $10q^2$ inner faces and $16q+2$ boundary faces, such that

$$f(\bar{P}_q) = 10q^2 + 16q + 2 \; .$$

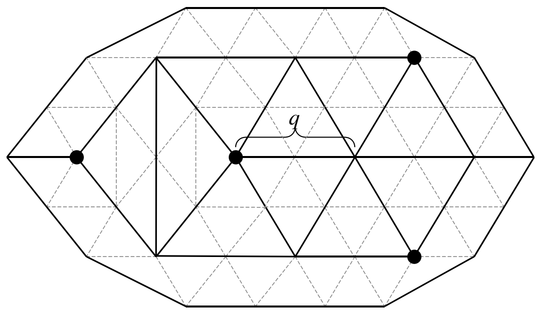

Figure 5.24: A regular 4-patch $\bar{P}_q$ which occurs in T_q (here with $q = 2$ as an example)

If $\hat{P}_q$ denotes the same 4-patch containing $P_{4,0,0}$ as in the first case, we now have

$$f(\hat{P}_q) \;=\; 32q^2 + 16q - 4 \;=\; f(\bar{P}_q) + 22q^2 - 6\ .$$

Hence, if P_q contains $\bar{P}_q$ and P'_q is obtained by replacing $\bar{P}_q$ by $\hat{P}_q$, we get:

$$\begin{aligned} b(P_q) \;=\; b(P'_q) &\geq \sqrt{2f(P'_q) + 12} \\ &= \sqrt{2(f(P_q) + 22q^2 - 6) + 12} \\ &= \sqrt{2f(P_q) + 44q^2} > \sqrt{2f(P_q) + 36q^2} \end{aligned}$$

So with $f(P_q) \leq 30q^2$ it follows from (5.16) that $\frac{b(P_q)}{f(P_q)} \geq \frac{\sqrt{96}}{30} \cdot \frac{1}{q}$.

Since $\frac{\sqrt{96}}{30q} > \frac{9q+1}{30q^2} > \frac{3}{10}$ for $q \neq 1$, we get again that P_q cannot be optimal except in case $q = 1$. But if $p = 1$ we have again that the smallest possible patch has already boundary length 10, so there can be no patch with a quotient strictly smaller than $\frac{1}{3}$. For this configuration, there is even no patch with a quotient equal to $\frac{1}{3}$, since the regular patch from figure 5.24 contains only 28 faces, and adding more faces increases the boundary length.

The case $p = 8$:

Suppose there exists an optimal 8-patch P_q in T_q. In particular we must have $f(P_q) \leq 30q^2$. But this is already a contradiction in case $q = 1$, because such a patch would have to contain at least $8 \cdot 5 = 40$ faces (5 faces for each inner vertex of degree 5). So assume $q \neq 1$. Now $\bar{P}_q := T_q - P_q$ must be a $\bar{p}$-patch with $\bar{p} \leq 4$ and $f(\bar{P}_q) \geq 30q^2$.

By (3.33) we have $b(\bar{P}_q) \geq \sqrt{(6-\bar{p})f(\bar{P}_q)}$, so in particular for $\bar{p} \leq 3$ we have $b(\bar{P}_q) \geq \sqrt{3f(\bar{P}_q)}$ and hence:

$$\frac{b(P_q)}{f(P_q)} = \frac{b(\bar{P}_q)}{f(P_q)} \geq \frac{\sqrt{3f(\bar{P}_q)}}{f(P_q)} \geq \frac{\sqrt{90q^2}}{30q^2} = \frac{\sqrt{10}}{10q} > \frac{3}{10q}$$

This is an immediate contradiction in case q is even. In case q is odd we can assume $q \geq 3$ since we already excluded $q = 1$; but then we have even $\frac{\sqrt{10}}{10q} > \frac{9q+1}{30q^2}$, so we get a contradiction, too. Left is the case $\bar{p} = 4$. Then by (5.15) we have $b(\bar{P}_q) \geq \sqrt{2f(\bar{P}_q) + 36q^2}$ and hence

$$\frac{b(P_q)}{f(P_q)} = \frac{b(\bar{P}_q)}{f(P_q)} \geq \frac{\sqrt{2f(\bar{P}_q) + 36q^2}}{f(P_q)} \geq \frac{\sqrt{96q^2}}{30q^2} = \frac{\sqrt{96}}{30q} > \frac{3}{10q}\ .$$

In case $q \neq 1$ we even have $\frac{\sqrt{96}}{30q} > \frac{9q+1}{30q^2}$, so in any case we obtain that P_q cannot be optimal in T_q.

The case $p = 5$:

Considering all possible configuration of degree 5 vertices in T_q, we see that all have a boundary length of at least $10q$. Since $10q \geq 9q + 1 > 9q$ for all $q \in \mathbb{N}$, we obtain immediately that there can be no 5-patch in T_q with a quotient strictly smaller than $\frac{9q+1}{30q^2}$. For $q \neq 1$ we even have $10q > 9q + 1$ so there can be no optimal 5-patch at all; in case $q = 1$ we have $10q = 9q + 1$ and there exists indeed a 5-patch with quotient $\frac{1}{3}$, which is the one in figure 5.20 (middle).

The case $p = 7$:

Now we assume that there is an optimal 7-patch P_q in T_q. Again $f(P_q) \leq 30q^2$ is already a contradiction in case $q = 1$ since the patch would have to contain at least $7 \cdot 5 = 35$ faces. Now $\bar{P}_q := T_q - P_q$ must be a $\bar{p}$-patch with $\bar{p} \leq 5$ and $f(\bar{P}_q) \geq 30q^2$. But $\bar{p} \leq 4$ has already been excluded in case $p = 8$, and $\bar{p} = 5$ cannot be the case because then the boundary length of $\bar{P}_q$ and hence also of P_q would be $9q + 1$ or larger.

The case $p = 6$:

In T_q there exists only one configuration of degree 5 vertices where a 6-patch containing it may have boundary length $9q$, and one where the boundary length $10q$ is possible. Figure 5.25 shows the respective patches in case $q = 1$.

All other configurations require even longer boundaries. Now as we already discussed at the beginning of this section, the first mentioned configuration is contained in a 6-patch with boundary length $9q$ and $30q^2$ faces only in case q is even; if q is odd, we have either boundary length $9q$ and $30q^2 - 9q$ faces, or boundary length $9q + 1$ and $30q^2$ faces, where the latter leads to a smaller quotient. Patches containing the other configuration have even a longer boundary, except in case $q = 1$, where the patch in the figure indeed shows an optimal patch.

Consequently there are no 6-patches in T_6 with a quotient strictly smaller than $\frac{9q}{30q^2}$ in case q even and $\frac{9q+1}{30q^2}$ in case q odd.

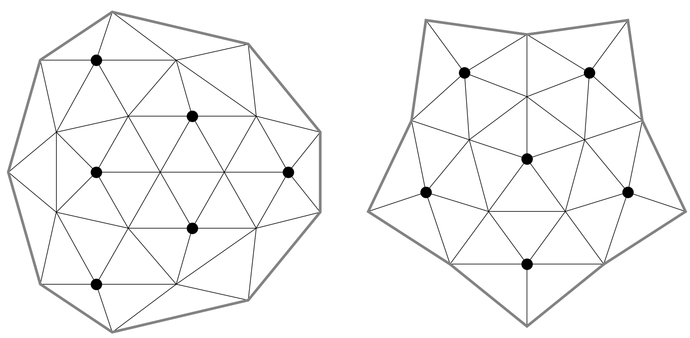

Figure 5.25: Two 6-patches that occur in T_1

5.4.2 A program and its results

We conclude the study on the expander constant of fullerenes with presenting an algorithm for computing the expander constant of any given fullerene, using some of the results that were proven in this chapter. A program based on this algorithm has been implemented in C and independently tested by a second program.

An interesting question for application is: For a given number n of vertices, which are the fullerenes on n vertices with a maximal expander constant? This would give us candidates for particularly stable fullerenes of the respective size. And moreover, do all fullerenes that have a maximal expander constant fulfill the isolated-pentagon rule? Or at least, is there always an isolated-pentagon fullerene among those that have a maximal expander constant?

We will at first describe the algorithm, then we present and discuss the results of the program.

The basic algorithm

For the input we use a generator for planar polycyclic hydrocarbons *CaGe* [4] that provides the adjacency lists as well as images of the geodesic domes. All figures of geodesic domes that occur in this section and in the appendix are generated with *CaGe*.

So assume we have a geodesic dome T with n faces. We will use the adjacency list in order to build paths in T that yield the boundary of a patch in case they close to a cycle. We are looking for a patch P with minimal quotient

$$q(P) := \frac{b(P)}{\min(f(P), n - f(P))} .$$

Now due to lemma 5.3.6, an optimal patch $\bar{P}$ must have a quotient $q(\bar{P}) \leq \frac{2}{3}$; so at the beginning we may set $q_{\min} := \frac{2}{3}$ as a starting value for the minimal quotient. Also by lemma 5.3.6 we have $b(\bar{P}) \leq \frac{n}{3}$ for the boundary length of an optimal patch $\bar{P}$ in T, so in the beginning we only have to construct paths with up to $\frac{n}{3}$ edges in order to find optimal patches. Therefore we set $b_{\max} := \frac{n}{3}$ as a first upper bound on the length of any path that we construct in the current fullerene. We will see that this bound can be improved during the execution whenever a smaller quotient is found.

Moreover, lemma 5.3.5 states that the boundary of an optimal patch cannot contain degrees 2 and 6, nor labels 0 and 4. Consequently we may exclude the possibility that our path contains succeeding vertices x, y, z with $\{x, z\} \in E(T)$ because such a 'sharp turn' yields one of the cases from above. So if the previous vertices in the path are x and y, we may, when choosing the next vertex of the path, restrict to those neighbours of y that are not adjacent to x and not x itself. This leaves only three possibilities for succeeding vertices in case of $\deg(y) = 6$, and even only two if $\deg(y) = 5$. In the following we will denote all vertices that are adjacent to a vertex v in T by $N(v)$.

The algorithm proceeds as follows: Choose a starting vertex v_0. The set of possibilities for the next vertex in the path is denoted by S_1 and can be set to be $N(v_0)$ in the beginning. If a vertex $v_1 \in S_1$ is chosen, remove it from S_1. The set of possibilities for the vertex v_2 is then defined as

$$S_2 := N(v_1) - N(v_0) - \{v_0\} ,$$

where the vertices in $N(v_0)$ may be excluded due to the observation on 'sharp turns' mentioned above.

Now for $i \geq 2$, where a path $v_0, \ldots, v_{i-1}$ is already constructed and the set S_i determined, the following steps are carried out:

1. In case $S_i = \emptyset$, reduce i by 1 and go back to 1.

2. Choose a vertex $v_i \in S_i$ and afterwards, delete it from S_i.

3. Check if v_i already lies in the interior path $v_1, \ldots, v_{i-2}$ – if so, it does not have to be considered further because we only want to construct paths that close again at the starting vertex without crossing the already constructed path. Therefore we may immediately go back to 1.

4. Check if $v_i = v_0$ – if so, a cycle has been found. Then we let P denote the patch in T that lies left of the cycle and has that cycle as boundary cycle.

   - At first determine the number of faces in P. For this, we compute the degrees of the boundary vertices in P and determine all vertices that lie in the interior of P. Now we have

   $$3f(P) + b(P) \;=\; \sum_{v \in V(P)} \deg_P(v) \quad \Leftrightarrow \quad f(P) \;=\; \frac{\sum_{v \in V(P)} \deg_P(v) - b(P)}{3}$$

   because counting each vertex with respect to its degree yields each bounded face three times and the outer face $b(P)$ times. Hence we are able to determine $f(P)$ with respect to the boundary length – which is simply the length of the cycle – and the vertex degrees in P and its boundary. Then we compute the quotient

   $$q(P) = \frac{b(P)}{\min(f(P), n - f(P))} \, .$$

   - Now remark 5.3.7 yields

   $$b(\bar{P}) \;\leq\; q(P) \cdot \frac{n}{2}$$

   for any optimal patch $\bar{P}$. Therefore we may make use of the new information and adjust the bound on the boundary length of optimal patches in order to accelerate further computation:
   If $q(P) \leq q_{\min}$ we set

   $$q_{\min} \;=\; q(P)$$

   and

   $$b_{\max} \;=\; q_{\min} \cdot \frac{n}{2} \; .$$

   - Afterwards go back to 1. without changing i.

5. Check if the boundary length is exceeded: If $i > b_{\max}$, we decrease i by 1 and go to 1.

6. Determine the possible vertices for the next step: The set of possibilities for the vertex v_{i+1} is defined as

   $$S_{i+1} := N(v_i) - N(v_{i-1}) - \{v_{i-1}\} \, ,$$

   where again $N(v_{i-1})$ can be excluded in order to avoid 'sharp turns'. Then increase i by 1 and continue with 1.

These steps are carried out for the starting edge (v_0, v_1) as long as $i \geq 2$. If $i < 2$ is reached, all cycles containing (v_0, v_1) have been constructed. Then we choose the next vertex in S_1, delete it from S_1 and proceed in the same way. If $S_1 = \emptyset$, all cycles containing v_0 have been constructed.

Now one after another, we choose the other vertices of the graph as starting vertices and proceed as described. Additionally, if $v_0^1, v_0^2, \dots, v_0^i$ have already been chosen as starting vertices, we exclude these vertices in the computations for all following starting vertices of the graph, since all cycles containing them have already been constructed. So we add the following step:

3.b) Check if v_i has already been chosen as a starting vertex – if so, go back to 1.

This way, the later starting vertices can be examined in a very short time, because on the one hand $b_{\max}$ has usually been decreased, and furthermore there are not many vertices left that can be chosen for the path.

When all vertices have been chosen as starting vertices, the program stops. Then the current value of $q_{\min}$ gives the minimal quotient of the geodesic dome, that is the expander quotient, and hence the expander constant of the corresponding fullerene. All closed paths for which the quotient $q_{\min}$ was computed indicate the possible optimal patches.

Further improvements

Further improvement of the program has been achieved by considering the following items:

- The set of possibilities for the second vertex in the path can even be set as

$$S_1 := N(v_0) - \{x, y\}$$

  where x, y are chosen as two arbitrary vertices in $N(v_0)$ with $\{x, y\} \in E(T)$. The reason why we may exclude x and y is that we do not care about the direction of the cycles – actually the algorithm described above constructs each cycle twice, namely once for each direction – so all cycles starting with (v_0, x) or (v_0, y) and ending with (z, v_0) for any $z \notin \{x, y\}$ can be excluded because the cycles with opposite directions are already constructed when z is chosen as second vertex. The only cycles that are completely left out are those starting with (v_0, x) resp. (v_0, y) and ending with (v_0, y) resp. (v_0, x) – but they can be excluded because they contain a 'sharp turn' at v_0 since x and y have been chosen as neighbouring vertices.

- Furthermore, we observe that sometimes it is not possible for a path to return to the starting vertex because none of its neighbours can be chosen anymore, or that the only possibility to return yields a sharp turn at the starting vertex. Then we can stop the construction of the current path. So if v_0, v_1 are the first two vertices of a path, we determine the set of 'possible return vertices' as $N(v_0) - N(v_1) - \{v_1\}$. In step i we investigate – after checking if $v_i = v_0$ – whether the path $v_2, \dots, v_{i-1}$ contains all of these return vertices, and if this is the case, we go back to 1.

- Moreover, even if it is still possible to choose neighbours of the starting vertex, it might be the case that the path cannot return to the starting vertex in a number of steps such that the total bound of the path length is not exceeded. Therefore we assign, after the starting edge (v_0, v_1) has been chosen, 'returning distances' to certain directed edges in the graph: For $1 \leq k \leq b_{\max}$, a directed edge e gets distance k if the shortest path from e to (v_0, v_1) edge without sharp turns has length k, where by length we mean the number of inner vertices of the path including e and (v_0, v_1) – see also figure 5.26. Then, whenever a vertex v_i is chosen, we determine the sum of the path length up to v_{i-1}, that is $i - 1$, and the distance of (v_{i-1}, v_i) to the starting vertex, and in case it exceeds the current bound $b_{\max}$, we return to 1.

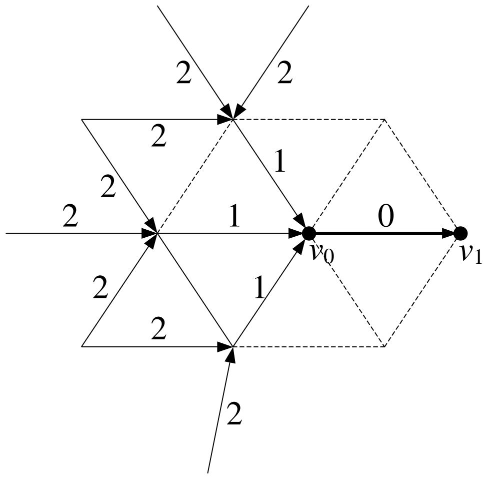

Figure 5.26: An example of how to assign distances up to 2 to directed edges with respect to the starting edge (v_0, v_1)

- Finally, corollary 5.3.16 can be used to exclude paths with certain labels: When constructing a path we compute a label for each vertex in the path after its successor has been chosen, giving the number of edges in the angle left of the vertex. With the help of variables that count the number of succeeding labels we may stop the construction of a path whenever a label sequence of one of the types listed in corollary 5.3.16 occurs.

The algorithm that is described here computes the expander constant of a single fullerene. However, it can of course also be used to compute the expander constants of a large set of fullerenes, for instance all fullerenes on n vertices. *CaGe* also produces such lists of fullerenes that can be used for a repeated application of the described procedure.

In case we have such a list and are only interested in the fullerenes with *largest* expander constant, we may simplify the program further by immediately stopping the whole computation for one fullerene where a quotient has been detected that is strictly smaller than the current maximal expander constant of the already examined fullerenes.

Results

The question that we focus on is: If we consider all fullerenes on n vertices, which of them have the largest expander constants and are hence the 'most stable' in the sense of the expander constant? A program based on the described algorithm has been used to determine all maximal expander constants for all fullerenes with up to 140 vertices, where a second program validated the figures for up to 100 vertices.

Furthermore, we are interested in the expander constants of the isolated-pentagon fullerenes; since chemists consider them to be particularly stable, it would be interesting to compare them with other fullerenes with the same number of atoms in order to see if the isolated-pentagon fullerenes are most stable in the sense of the expander constant, too.

As a first result, we computed the expander constants of all fullerens with 60 vertices. We obtained that the largest possible expander constant among them is $\frac{1}{3}$, and that there are exactly two fullerenes on 60 vertices with that expander constant – the Buckminster fullerene and one further fullerene. The dual graphs of both with examples of optimal patches can be seen in figure 5.27. In table 5.1, the numbers of the C_{60} fullerenes with the respective expander constants are given.

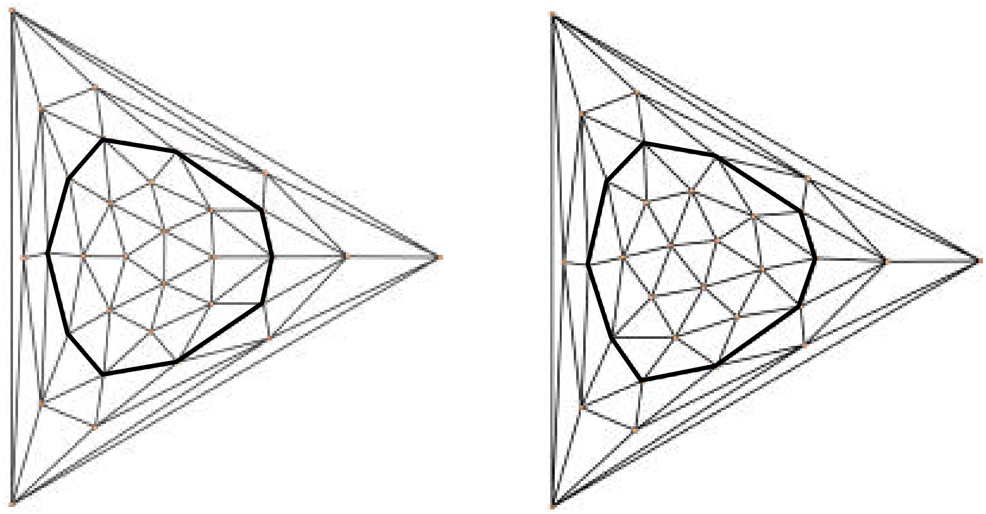

Figure 5.27: The two geodesic domes with 60 faces whose duals have the maximal expander constant $\frac{1}{3}$ (the left one is the Buckminster dome).

The main results of our program can be found in tables 5.2 and 5.3: For each possible n until 140, we determined the largest expander constant that occurs among all fullerenes with n vertices.

For easier notation we define

$$ch_{\max}(n) := \max\{ch(G) \mid G \text{ is a fullerene on } n \text{ vertices}\}$$

as the maximal expander constant of all fullerenes with n vertices. In the tables we give the expander constants as values rounded to 4 digits. Furthermore, we let $b_{\max}(n)$ and $f_{\max}(n)$ denote the boundary length and number of faces of an optimal patch in one of the respective geodesic domes, such that $ch_{\max}(n) = b_{\max}(n) / f_{\max}(n)$; in case $ch_{\max}(n)$ is obtained by patches of different sizes, we choose the quotient such that $f_{\max}(n)$ is maximal. Additionally, we give the number of fullerenes with n vertices whose expander constant is maximal, denoted as $full_{\max}(n) := |\{G \mid ch(G) = ch_{\max}(n)\}|$, and in comparison the total number of fullerenes $full(n)$ with n vertices, which can be found in [6].

The table indicates that larger graphs tend to have a smaller expander constant, although the expander constant is not monotonously decreasing. Consequently, among two fullerenes with the same expander constant we could interpret the one with the larger number of faces

Expander constant	Number of C_{60} fullerenes with that expander constant
$\frac{10}{30} \approx 0.3333$	2
$\frac{9}{29} \approx 0.3103$	665
$\frac{8}{26} \approx 0.3077$	164
$\frac{8}{28} \approx 0.2857$	146
$\frac{8}{30} \approx 0.2666$	736
$\frac{7}{27} \approx 0.2593$	16
$\frac{7}{29} \approx 0.2414$	77
$\frac{6}{28} \approx 0.2143$	2
$\frac{6}{30} = 0.2$	4

Table 5.1: The expander constants that occur when considering fullerenes with 60 vertices, and the number of these fullerenes that have the respective expander constant

as 'more stable'. In other words, we view a fullerene with n vertices as 'particularly stable' if it has not only a maximal expander constant among all fullerenes on n vertices, but also among all fullerenes with n or more vertices. The maximal expander constants where – at least in the table – no larger fullerenes with the same or a larger expander constant occur are marked with a star.

Considering $b_{\max}(n)$ and $f_{\max}(n)$, we observe that both the boundary lengths and the numbers of faces of the optimal patches seem to increase monotonously.

A further interesting observation is that the number $full_{\max}(n)$ of fullerenes with maximal expander constant seems to follow a special pattern: It is monotonously increasing within a certain range where it reaches a comparatively high value, followed by a very small number which marks again the beginning of a new increasing process.

Moreover, we applied the same program to the subset of all isolated-pentagon fullerenes with the same number of vertices n until $n = 140$ and thus determined the largest expander constant that occurs among all isolated-pentagon fullerenes with n vertices, which exist for $n = 60$ and each even $n \geq 70$. The results can be found in the tables 5.4 and 5.5, where the maximal expander constants are denoted by $ch^{\mathrm{IP}}_{\max}(n)$ and the numbers of isolated-pentagon fullerenes with n vertices whose expander constant is maximal by $full^{\mathrm{IP}}_{\max}(n)$.

We immediately see that there exist non-isolated-pentagon fullerenes which have a strictly larger expander constant than certain isolated-pentagon fullerenes with the same number of vertices: For instance we have that in case $n = 76$, only one of the two possible isolated-pentagon fullerenes has the maximal expander constant $\frac{11}{37}$, while there are in total 10 fullerenes with 76 vertices and that expander constant – consequently, 9 of them must be non-isolated pentagon fullerenes with a better expander constant than one of the isolated-pentagon fullerenes.

Above that, comparing the maximal expander constants $ch_{\max}(n)$ for n vertices with the maximal expander constants $ch_{\max}^{\mathrm{IP}}(n)$ of isolated-pentagon fullerenes with n vertices, we observe that in the cases $n = 90$ and $n = 108$, we have

$$ch_{\max}(n) > ch_{\max}^{\mathrm{IP}}(n)$$

which means that in these cases, none of the fullerenes with expander constant $ch_{\max}(n)$ does fulfill the isolated-pentagon-rule. In all other case up to $n = 140$ we have $ch_{\max}(n) = ch_{\max}^{\mathrm{IP}}(n)$, so the set of isolated-pentagon fullerenes with maximal expander constant must be a subset of all fullerenes with maximal expander constant of the same number of vertices.

Thus we have shown that it is *not* true that there is always an isolated-pentagon fullerene among the fullerenes with maximal expander constant – although it seems to hold in most of the cases. Figure 5.28 shows the duals of the two only C_{90} fullerenes with maximal expander constants $\frac{12}{44}$, where it can easily be verified that both are no isolated-pentagon fullerenes.

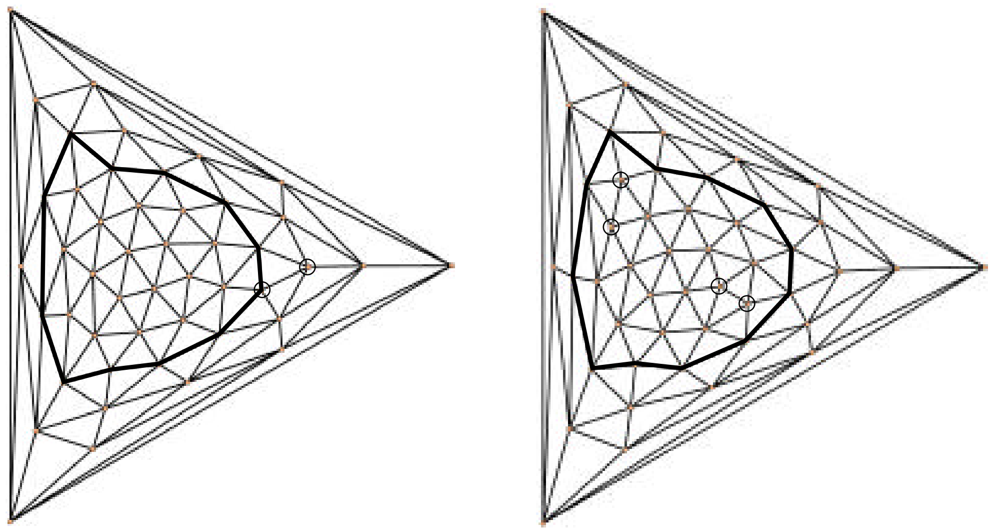

Figure 5.28: The two geodesic domes with 90 faces whose duals have the maximal expander constant $\frac{12}{44}$; both contain adjacent vertices of degree 5 (marked with cycles), so the corresponding fullerenes do not fulfill the isolated-pentagon-rule.

For application it is also of interest which fullerenes actually are those with the largest expander constants. Considering the values of $full_{\max}(n)$ and $full_{\max}^{\mathrm{IP}}(n)$, it is obvious that we cannot depict all of them here. Instead, we chose for each $n \leq 100$ one isolated-pentagon fullerene with maximal expander $ch_{\max}^{\mathrm{IP}}(n)$ constant among all isolated-pentagon fullerenes with n vertices, and additionally for each $n \leq 100$ one fullerene with maximal expander constant $ch_{\max}(n)$ among all fullerenes with n vertices.

The corresponding geodesic domes of these fullerenes can be found in appendix A, where we also depicted one optimal patch for each geodesic dome.

n	$ch_{\max}(n)$	$b_{\max}(n)$	$f_{\max}(n)$	$full_{\max}(n)$	$full(n)$
20	0.6 ∗	6	10	1	1
24	0.5	6	12	1	1
26	0.5	6	12	1	1
28	0.5385 ∗	7	13	1	2
30	0.4667	7	15	1	3
32	0.4667 ∗	7	15	3	6
34	0.4118	7	17	4	6
36	0.4118	7	17	10	15
38	0.4444 ∗	8	18	1	17
40	0.4	8	20	9	40
42	0.4 ∗	8	20	9	45
44	0.3636	8	22	40	89
46	0.3636	8	22	60	116
48	0.3636 ∗	8	22	1	199
50	0.36	9	25	7	271
52	0.36 ∗	9	25	23	437
54	0.3333	9	27	93	580
56	0.3333	9	27	211	924
58	0.3103	9	29	368	1 205
60	0.3333	10	30	2	1 812
62	0.3333 ∗	10	30	3	2 385
64	0.3125	10	32	31	3 465
66	0.3125 ∗	10	32	75	4 478
68	0.2941	10	34	475	6 332
70	0.2941	10	34	799	8 149
72	0.2777	10	36	2 501	11 190
74	0.2973	11	37	2	14 246
76	0.2973 ∗	11	37	10	19 151
78	0.2821	11	39	52	24 109
80	0.2821 ∗	11	39	225	31 924

Table 5.2: The maximal expander constants $ch_{\max}(n) = b_{\max}(n)/f_{\max}(n)$ of all fullerenes with $n \leq 80$ vertices, the number $full_{\max}(n)$ of fullerenes with n vertices whose expander constant is maximal, and the total number of fullerenes $full(n)$ with n vertices (taken from [6]). Cases where these fullerenes are 'particularly stable' are marked with *.

n	$ch_{\max}(n)$	$b_{\max}(n)$	$f_{\max}(n)$	$full_{\max}(n)$	$full(n)$
82	0.2683	11	41	1 325	39 718
84	0.2683	11	41	2 910	51 592
86	0.2558	11	43	7 798	63 761
88	0.2727	12	44	1	81 738
90	0.2727 *	12	44	2	99 918
92	0.2609	12	46	55	126 409
94	0.2609 *	12	46	120	153 493
96	0.25	12	48	1 220	191 839
98	0.25 *	12	48	3 220	231 017
100	0.24	12	50	12 700	285 914
102	0.24	12	50	22 222	341 658
104	0.2308	12	52	51 920	419 013
106	0.2308	12	52	79 491	497 529
108	0.2453 *	13	53	2	604 217
110	0.2364	13	55	136	713 319
112	0.2364 *	13	55	835	860 161
114	0.2281	13	57	6 014	1 008 444
116	0.2281 *	13	57	14 654	1 207 119
118	0.2203	13	59	44 209	1 408 553
120	0.2203	13	59	79 165	1 674 171
122	0.2131	13	61	176 894	1 942 929
124	0.2258	14	62	4	2 295 721
126	0.2258 *	14	62	11	2 650 866
128	0.2186	14	64	273	3 114 236
130	0.2186 *	14	64	1 412	3 580 637
132	0.2121	14	66	10 088	4 182 071
134	0.2121	14	66	22 921	4 787 715
136	0.2059	14	68	80 038	5 566 948
138	0.2059	14	68	148 782	6 344 698
140	0.2174 *	15	69	1	7 341 204

Table 5.3: The maximal expander constants $ch_{\max}(n) = b_{\max}(n)/f_{\max}(n)$ of all fullerenes with $82 \leq n \leq 140$ vertices, the number $full_{\max}(n)$ of fullerenes with n vertices whose expander constant is maximal, and the total number of fullerenes $full(n)$ with n vertices (taken from [6]). Cases where these fullerenes are 'particularly stable' are marked with *.

n	$ch^{\mathrm{IP}}_{\max}(n)$	$b^{\mathrm{IP}}_{\max}(n)$	$f^{\mathrm{IP}}_{\max}(n)$	$full^{\mathrm{IP}}_{\max}(n)$	$full^{\mathrm{IP}}(n)$
60	0.3333	10	30	1	1
70	0.2941	10	34	1	1
72	0.2777	10	36	1	1
74	0.2973	11	37	1	1
76	0.2973	11	37	1	2
78	0.2821	11	39	2	5
80	0.2821	11	39	3	7
82	0.2683	11	41	4	9
84	0.2683	11	41	10	24
86	0.2558	11	43	14	19
88	0.2727	12	44	1	35
90	0.2444	11	45	38	46
92	0.2609	12	46	8	86
94	0.2609	12	46	4	134
96	0.25	12	48	25	187
98	0.25	12	48	52	259
100	0.24	12	50	209	450
102	0.24	12	50	299	616
104	0.2308	12	52	525	823
106	0.2308	12	52	784	1 233
108	0.2222	12	54	1 457	1 799
110	0.2364	13	55	36	2 355
112	0.2364	13	55	83	3 342
114	0.2281	13	57	334	4 468
116	0.2281	13	57	695	6 063
118	0.2203	13	59	1 967	8 148
120	0.2203	13	59	3 263	10 774
122	0.2131	13	61	5 686	13 977
124	0.2258	14	62	3	18 769
126	0.2258	14	62	5	23 589

Table 5.4: The maximal expander constants $ch^{\mathrm{IP}}_{\max}(n) = b^{\mathrm{IP}}_{\max}(n)/f^{\mathrm{IP}}_{\max}(n)$ of all isolated-pentagon fullerenes with $n \leq 126$ vertices, the number $full^{\mathrm{IP}}_{\max}(n)$ of isolated-pentagon fullerenes with n vertices whose expander constant is maximal, and the total number of isolated-pentagon fullerenes $full^{\mathrm{IP}}(n)$ with n vertices (taken from [6]).

n	$ch^{\mathrm{IP}}_{\max}(n)$	$b^{\mathrm{IP}}_{\max}(n)$	$f^{\mathrm{IP}}_{\max}(n)$	$full^{\mathrm{IP}}_{\max}(n)$	$full^{\mathrm{IP}}(n)$
128	0.2188	14	64	72	30 683
130	0.2188	14	64	240	39 393
132	0.2121	14	66	1 252	49 878
134	0.2121	14	66	2 659	62 372
136	0.2059	14	68	7 943	79 362
138	0.2059	14	68	13 483	98 541
140	0.2174	15	69	1	121 354

Table 5.5: The maximal expander constants $ch^{\mathrm{IP}}_{\max}(n) = b^{\mathrm{IP}}_{\max}(n)/f^{\mathrm{IP}}_{\max}(n)$ of all isolated-pentagon fullerenes with $128 \leq n \leq 140$ vertices, the number $full^{\mathrm{IP}}_{\max}(n)$ of isolated-pentagon fullerenes with n vertices whose expander constant is maximal, and the total number of isolated-pentagon fullerenes $full^{\mathrm{IP}}(n)$ with n vertices (taken from [6]).

Chapter 6

Conclusions and outlook

Here we shortly summarize the main outcomes of the present work and point out some possibilities for further research.

In this thesis, we have developed a number of results concerning the boundaries of patches. We have shown that the number of faces of a disordered triangle-patch P is uniquely determined by its boundary sequence and a fixed subpatch Q that contains all defective vertices in case $D(Q) \bmod 6 \neq 0$, that means the disorder of Q does not correspond to a trivial rotation. The proof works similarly for hexagon- and quadrangle-patches and even in case the disorder consists also in defective faces, where the condition that describes the degree of rotation has to be adjusted appropriately. With this we have found a general approach that includes previous results which have been achieved in this context ([26], [5], [29], [9]). For the cases corresponding to trivial rotations it is known that the result is generally not true; however, it would be desirable to understand these cases better and see whether under certain circumstances, similar results could hold (compare also section 2.6). This could be the subject of future research.

A further contribution of this work is the systematic investigation of patches with minimal boundaries. The tables 3.1 and 3.2 provide formulas for the minimal boundaries of hexagonal and triangular patches with defective vertices resp. faces of degree 3, 4 and 5 relative to their numbers of faces. While for the hexagonal case it has already been shown that the minimal boundaries are attained when arranging the faces in a certain spiral way, we have shown similar results for the triangular case. Furthermore, we have extended the problem to triangle-patches where the defective vertices may not be arbitrarily placed but are given in a fixed subpatch. We have proven that in case the boundary of that subpatch is *regular*, minimal boundaries are again obtained by appropriate spiral constructions. Moreover, we have shown that patches with *nice boundaries* can always be extended to regular patches, and that patches with minimal boundary lengths containing a given subpatch with nice boundary and a given face number which is large enough can be built by first extending the nice boundary patch to a regular patch, and then constructing spirals around that regular patch. We also have introduced a method of how to develop optimal formulas for minimal boundaries of patches when such a fixed subpatch is given. Further research could concentrate on allowing disordered subpatches with more general boundaries, where one problem is that some boundaries do not allow to add an unlimited number of faces in a spiral way. Also, it would be interesting to examine patches with minimal boundaries and a fixed number of n faces that contain a nice boundary subpatch in case n is too small to enable the extension to a regular patch. We conjecture that a construction of such patches could be based on adding rows of faces to the respective longest sides of the patch.

These investigations form also the basics for the chapters 4 and 5 which provide results with immediate applications. We have shown that in triangle- and hexagon-cones, that are infinite triangle- and hexagon-patches with $p < 6$ degree 5 vertices resp. pentagons, always a boundary of a certain type can be chosen: In a triangle-cone we always have a regular subpatch containing the degree 5 vertices, in a hexagon-cone there is always a subpatch containing the pentagons with a boundary sequence where vertices of degree 2 and 3 are alternating except $6 - p$ places with two succeeding vertices of degree 2. Similarly to the boundary of regular triangle-patches, the subpatch in the hexagon-cone can also be chosen such that either all segments between succeeding degree 2 vertices are of the same length, or one is by 1 shorter than the others. If we choose the patch with minimal boundary length, we conclude that the boundary can be described by two parameters (for $p \in \{0, 1, 5\}$ even by only one). This enables a parameterization of possible 'caps' of cones and hence a classification of the cones themselves, since such a cap boundary can only be filled with a finite number of patches. Of course this result can easily be generalized to cones with other defective vertex degrees or faces. However, the case with hexagons and pentagons is most interesting for application in chemistry.

Finally, one of the main results of the present thesis consists in the determination of the expander constants of fullerenes. We translated the problem to the duals, that are geodesic domes, where the task can be formulated as follows: Given a geodesic dome with n faces, determine among all subpatches with at most $\frac{n}{2}$ faces one where the ratio of boundary length and number of faces is minimal. We have presented two different approaches of how to deal with that problem. The first one allows to verify the expander constants of classes of symmetric fullerenes by hand and is essentially based on the results on minimal boundaries obtained in this thesis. This way we proved the expander constant of the fullerene with icosahedral symmetry where all edges of the signature graph have Coxeter coordinates (q, q) to be $\frac{3}{10q}$ in case q is even, and $\frac{3}{10q} + \frac{1}{30q^2}$ in case q is odd – obviously decreasing to 0 for q going to infinity. We assume that with similar arguments, the expander constants of the other two classes of fullerenes with icosahedral symmetry can be determined. An interesting task for future work could also be to apply the technique to other symmetric classes of fullerenes listed in [21], where all parameters for fullerenes with 10 or more symmetries can be found.

A second approach regarding the determination of the expander constant of fullerenes is based on an algorithm and its implementation. With the help of a computer program we obtained many interesting results and answers to questions posted in the beginning: We list for each $n \leq 140$ the maximal expander constant among all fullerenes with n vertices and the number of fullerenes where this constant is reached (tables 5.2 and 5.3). Examples of such fullerenes can be found in the appendix. The numbers of fullerenes with maximal expander constants show a pattern for which we cannot offer any explanation, but which could be the subject of further research. Also, it would be interesting to see whether the boundary length and face number of optimal patches is indeed monotonically increasing, as our outcome suggests, and how the expander constant develops for larger n. For this it would be helpful to continue the list even further.

Moreover, we analyzed the maximal expander constants for isolated-pentagon fullerenes (see tables 5.4 and 5.5). An important outcome is that not only there exist fullerenes which do not fulfill the isolated-pentagon-rule and have a larger expander constant than isolated-pentagon fullerenes of the same size, but that there are even cases ($n = 90$ and $n = 108$) where *none* of the fullerenes with highest expander constant is an isolated-pentagon fullerene. This is rather surprising because in chemistry, isolated-pentagon fullerenes are considered to be most stable. It would surely be worthwhile to investigate further in this context and compare the computed values and the particular fullerenes with findings from chemistry in order to see whether a connection between the expander constant and the chemical stability of fullerenes exist.

A further direction for future research could lie in combining the precise values that we computed with the results connecting the expanding properties of a graph with the eigenvalues of its adjacency matrix. An interesting task could be to consider the spectral gap of the fullerenes that we determined to have particularly large expander constants, or the other way around to compute with our program the expander constants of fullerenes for which the spectral gap has been shown to be particularly large. We hope that the results from this thesis could provide new insights in this very interesting and applicable research field.

Acknowledgement

The preparation of this thesis has been enabled by many people. In particular, I would like to thank Gunnar Brinkmann for all his support over the last years, for taking the time to read large parts of this work, making many useful comments, and for contributing to the present outcome with a computer program which provided the results for the larger numbers. An important part played also Jack Graver, whom I wish to thank for the interesting topic, his exceptional hospitality during my stay in Syracuse, and a lot of helpful advice in email conversation in all the time since then. Moreover, I thank Prof. Carstens for his support and for giving me the opportunity to write this doctoral thesis at the University of Bielefeld. Very special thanks go to Markus Ruschhaupt for many helpful discussions, useful comments, help with the programming and all his support and encouragement.

Financial support is gratefully acknowledged from the German Academic Exchange Service (DAAD), the rectorate of Bielefeld University, the department of mathematics of Bielefeld University, the former 'Graduiertenkolleg Strukturbildungsprozesse', and the German Research Foundation (DFG).

Appendix A

Figures

In the following, geodesic domes can be found whose duals are fullerenes with maximal expander constants. The figures are created with *CaGe* and are results of the program described in section 5.4.2. In most cases, there is more than one fullerene with that expander constant (compare the tables in section 5.4.2); then we chose an arbitrary one.

First, the figures A.1 and A.2 show duals of *isolated-pentagon* fullerenes with n vertices – one for each $n \leq 100$ for which isolated-pentagon fullerenes exist – where each is one with a maximal expander constant among all isolated-pentagon fullerenes of the same size. Actually, in all cases except $n = 90$ the expander constant is even maximal among *all* fullerenes with n vertices.

Furthermore, in the figures A.3 until A.7 one geodesic dome is given for each number n of faces with $n \leq 100$ where a geodesic dome exists, such that the dual fullerene on n vertices has a maximal expander constant among all fullerenes of the same size. There we chose, if possible, one where the respective fullerene does not fulfill the isolated-pentagon rule; this was always possible except in case $n = 88$, where the only fullerene with maximal expander constant is an isolated-pentagon fullerene.

In every geodesic dome pictured here, one cycle is indicated by fat lines, which determines one possible, arbitrarily chosen optimal patch on its bounded side. The respective expander constant is given as a fraction such that its numerator is the boundary length of that patch and its denominator the number of faces.

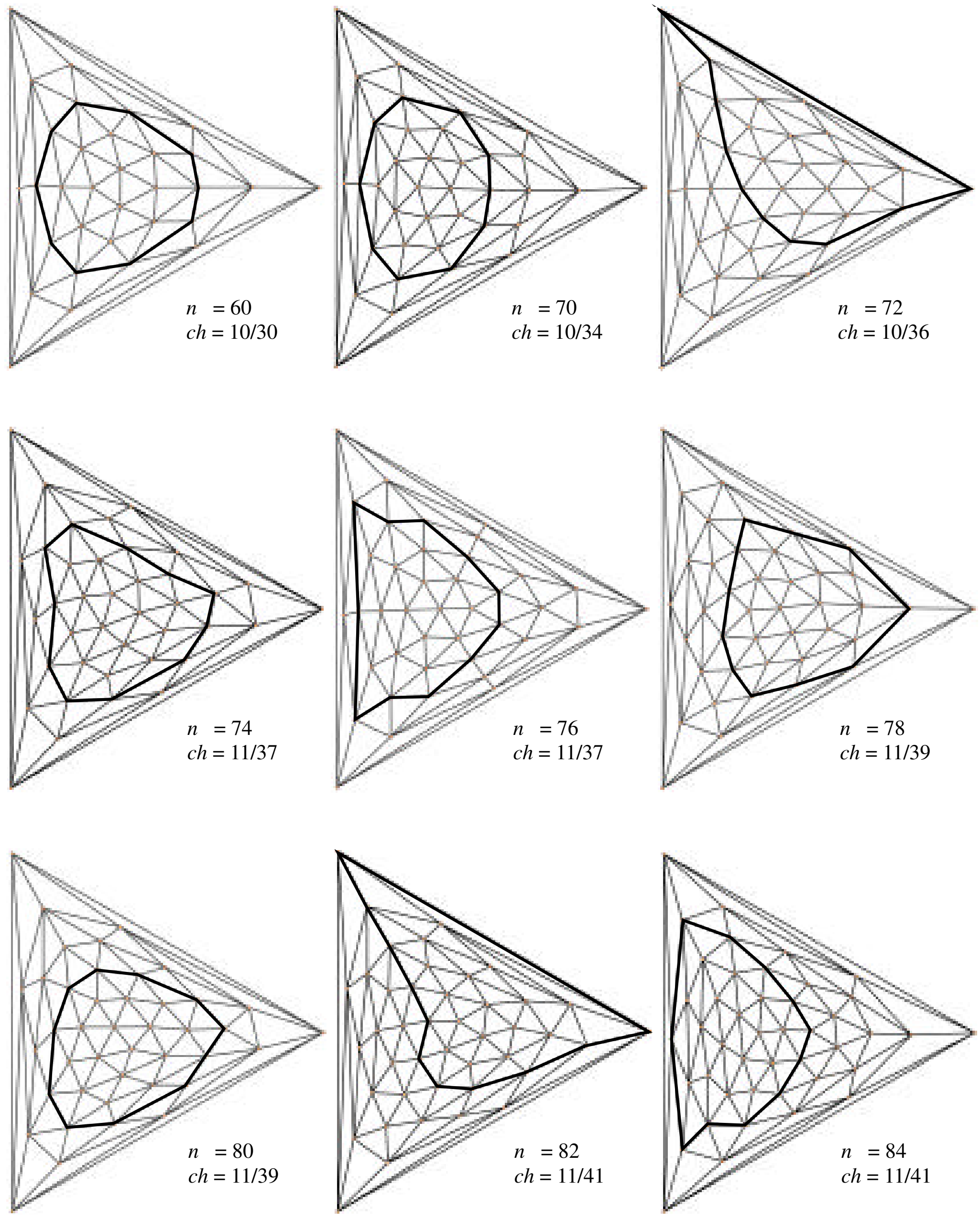

Figure A.1: Geodesic domes with $n \leq 84$ faces whose duals are isolated-pentagon fullerenes with maximal expander constants. The value ch gives the expander constant as a fraction which indicates the boundary length and face number of an optimal patch, and for each geodesic dome, one possible optimal patch is shown.

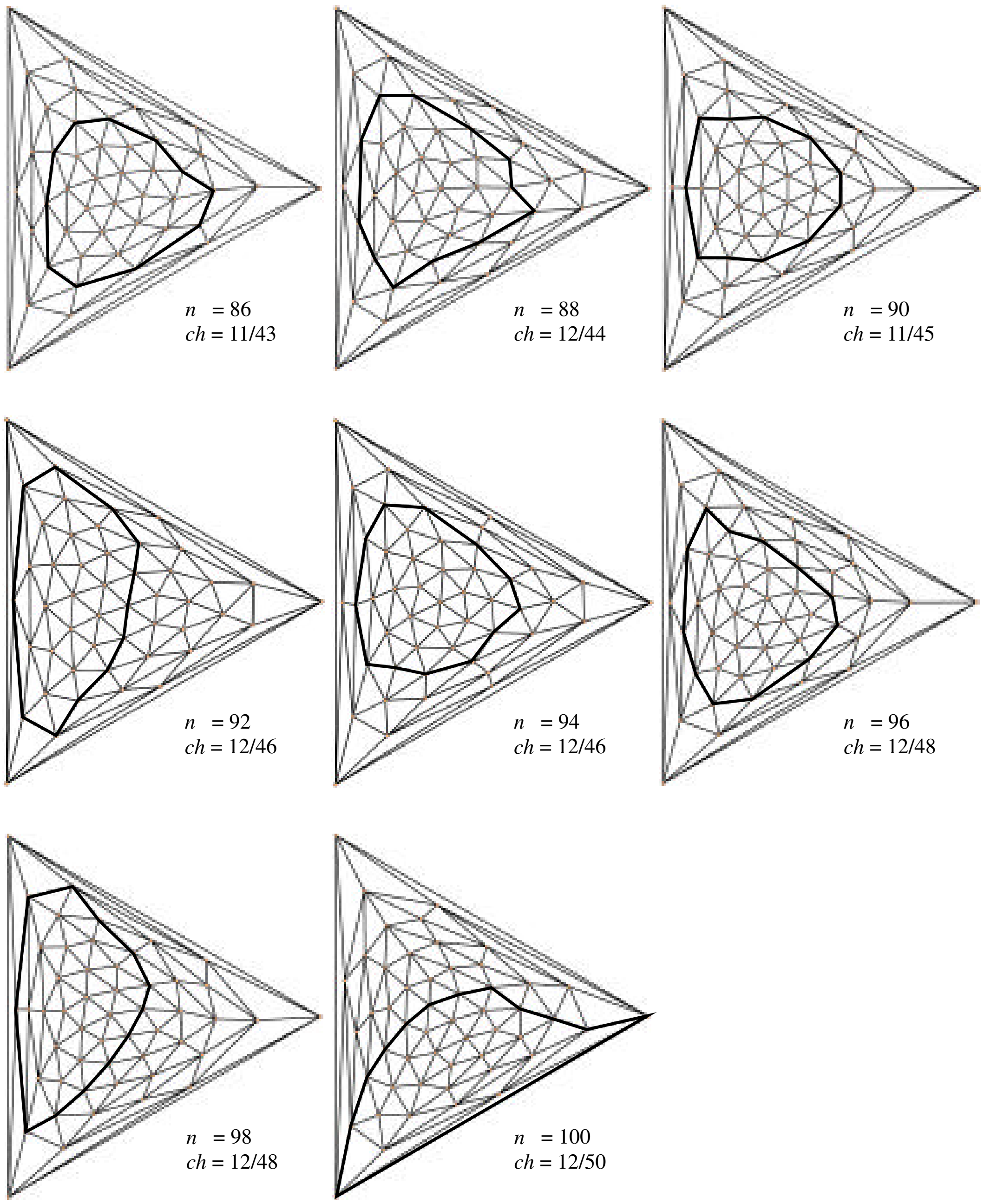

Figure A.2: Geodesic domes with $86 \leq n \leq 100$ faces whose duals are isolated-pentagon fullerenes with maximal expander constants. The value ch gives the expander constant as a fraction which indicates the boundary length and face number of an optimal patch, and for each geodesic dome, one possible optimal patch is shown.

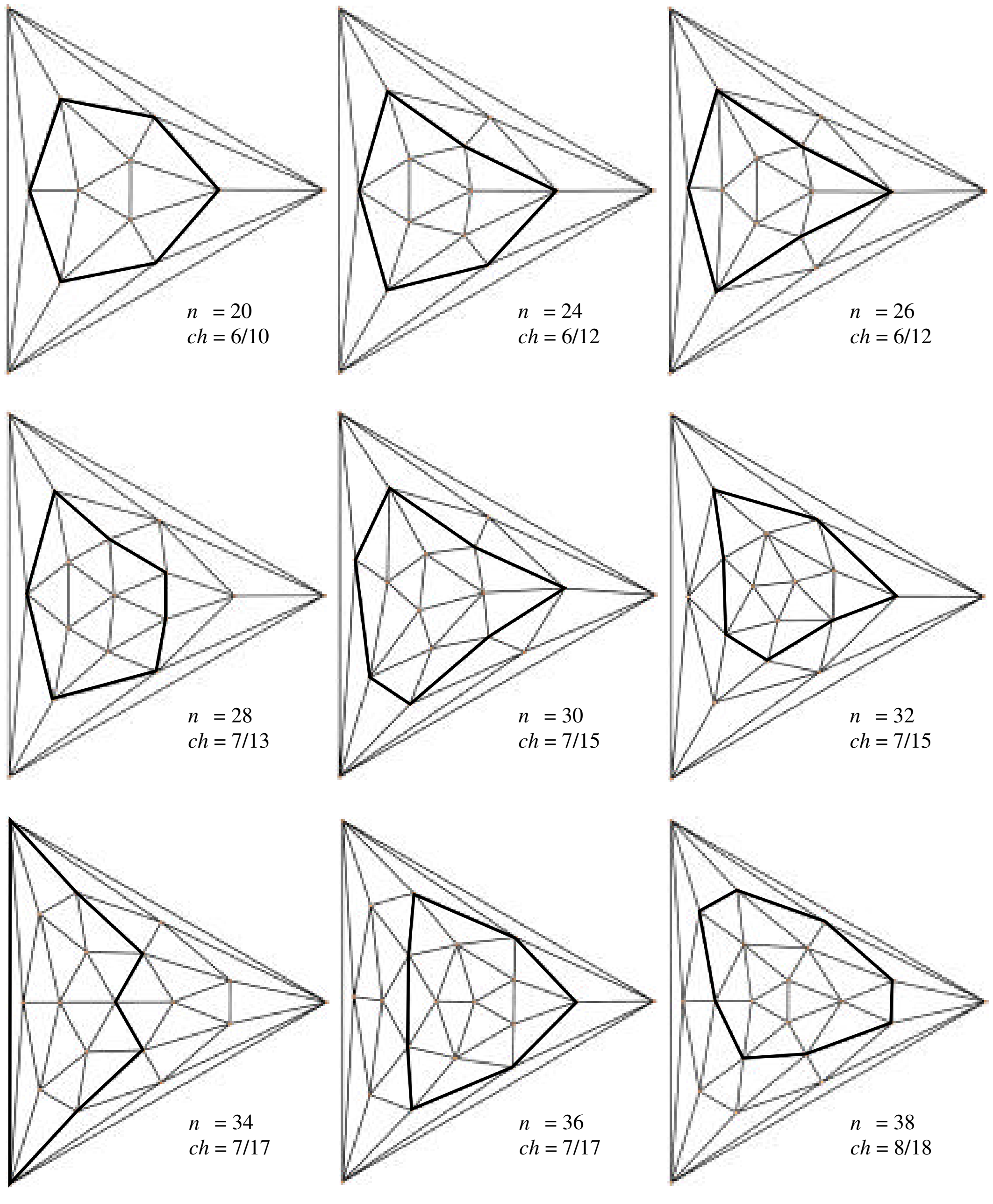

Figure A.3: Geodesic domes with $n \leq 38$ faces where the corresponding fullerenes have maximal expander constants. The value ch gives the expander constant as a fraction which indicates the boundary length and face number of an optimal patch, and for each geodesic dome, one possible optimal patch is shown.

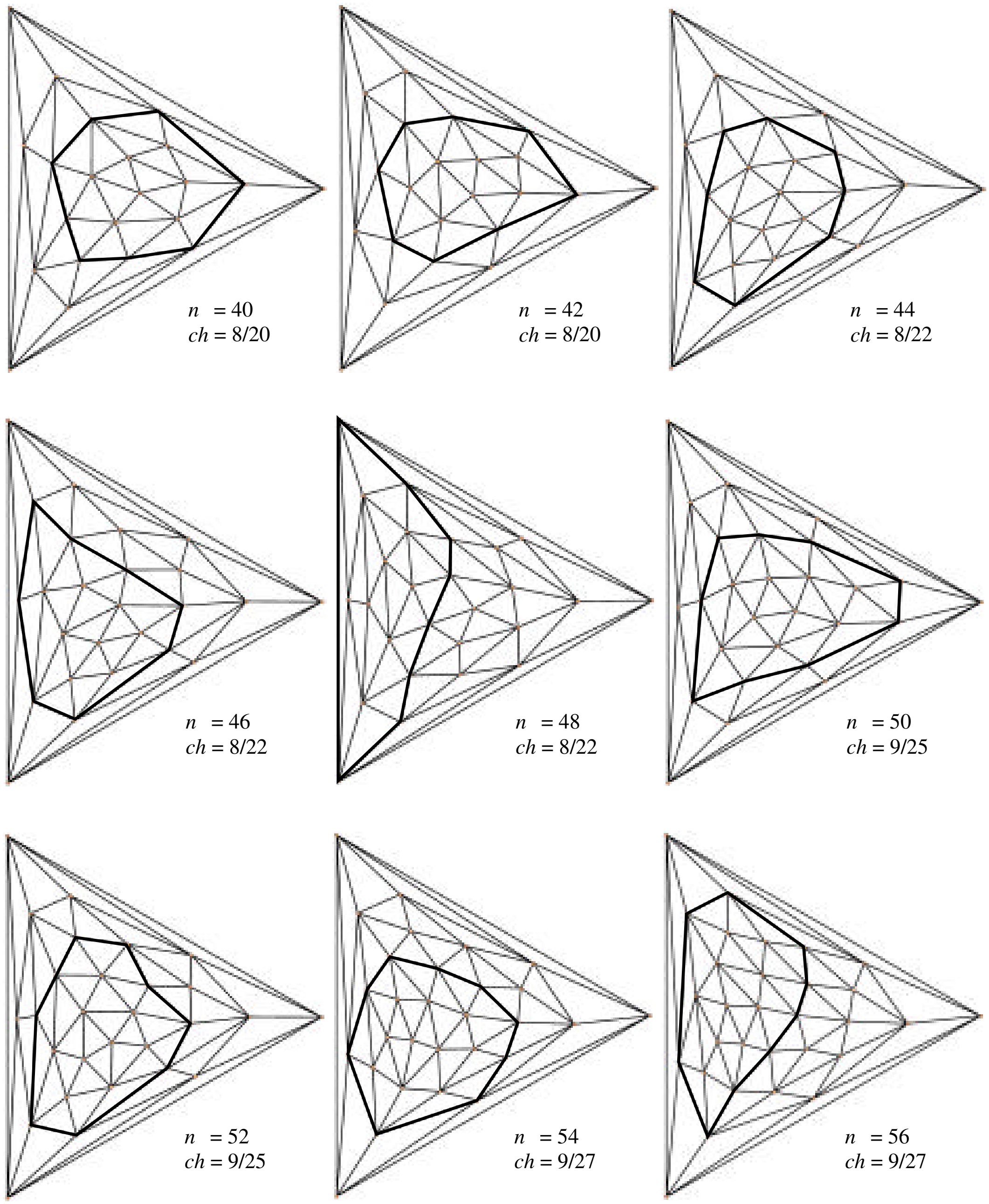

Figure A.4: Geodesic domes with $40 \leq n \leq 56$ faces where the corresponding fullerenes have maximal expander constants. The value ch gives the expander constant as a fraction which indicates the boundary length and face number of an optimal patch, and for each geodesic dome, one possible optimal patch is shown.

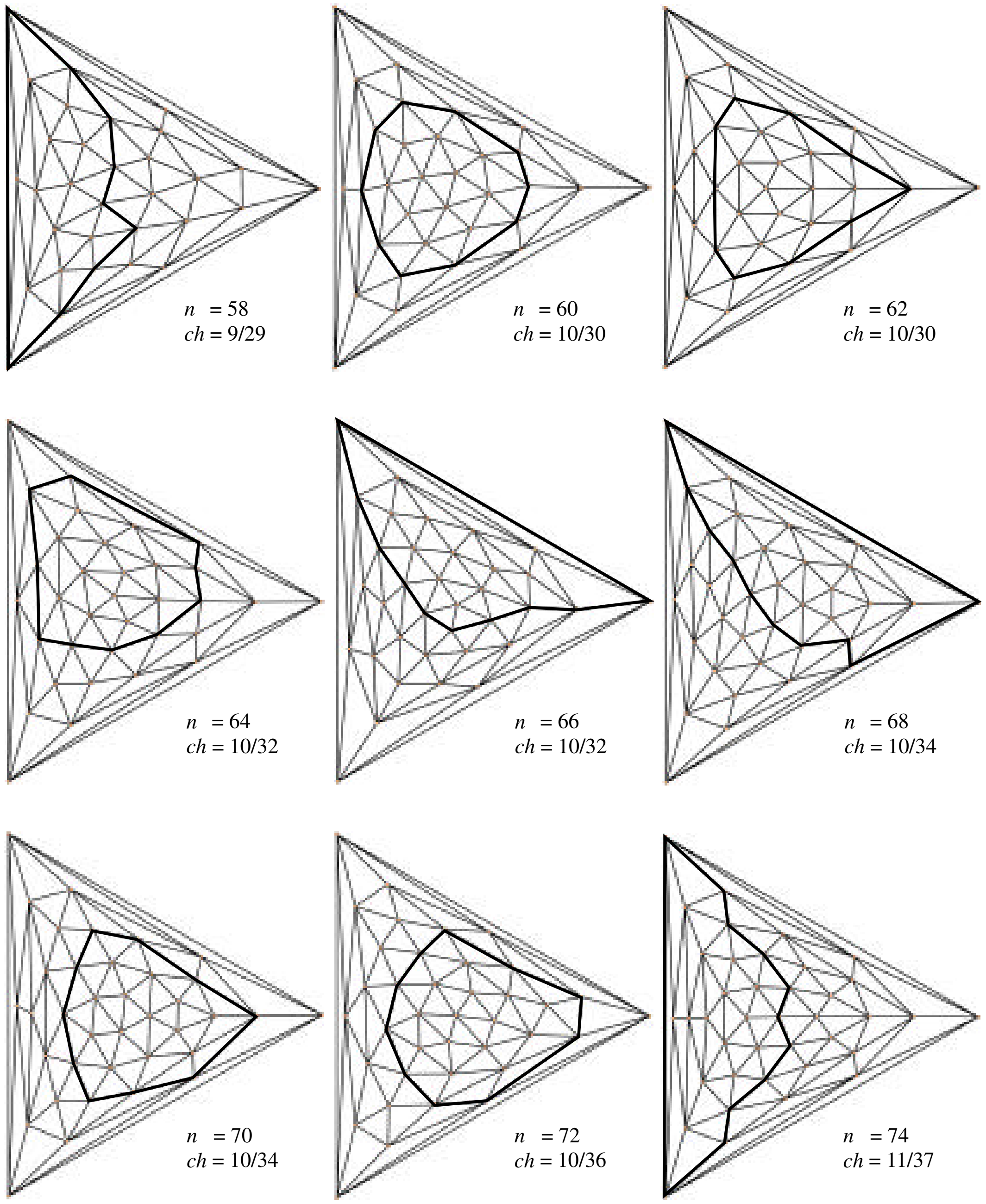

Figure A.5: Geodesic domes with $58 \leq n \leq 74$ faces where the corresponding fullerenes have maximal expander constants. The value ch gives the expander constant as a fraction which indicates the boundary length and face number of an optimal patch, and for each geodesic dome, one possible optimal patch is shown.

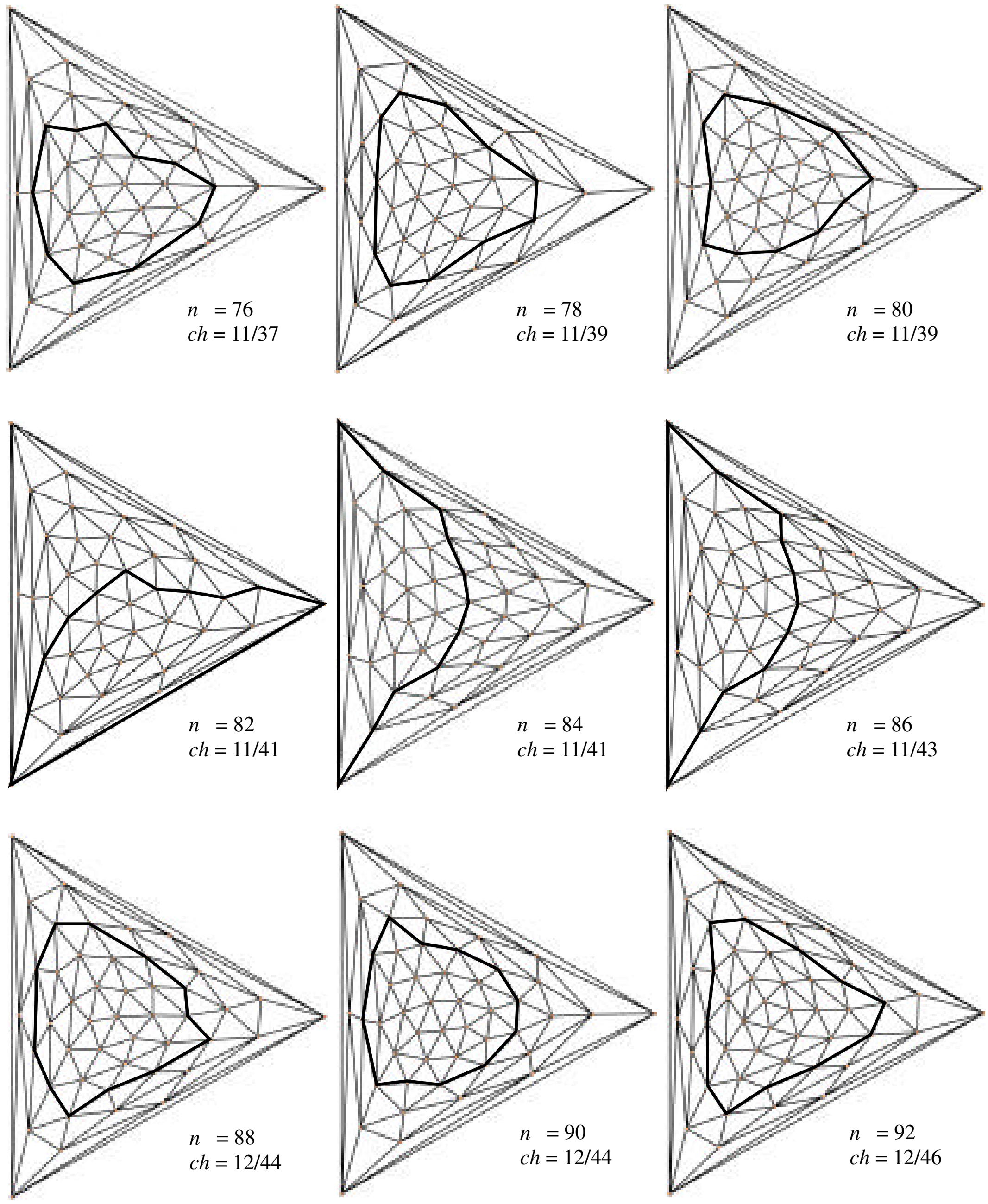

Figure A.6: Geodesic domes with $76 \leq n \leq 92$ faces where the corresponding fullerenes have maximal expander constants. The value ch gives the expander constant as a fraction which indicates the boundary length and face number of an optimal patch, and for each geodesic dome, one possible optimal patch is shown.

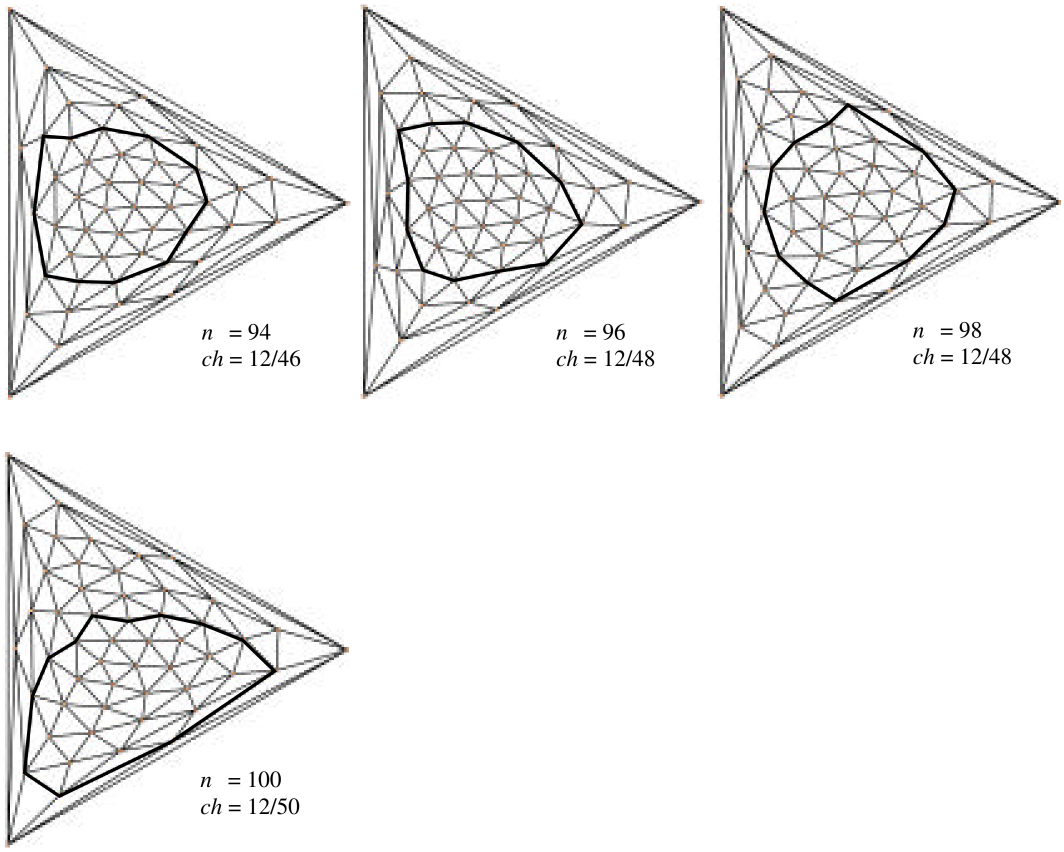

Figure A.7: Geodesic domes with $94 \leq n \leq 100$ faces where the corresponding fullerenes have maximal expander constants. The value ch gives the expander constant as a fraction which indicates the boundary length and face number of an optimal patch, and for each geodesic dome, one possible optimal patch is shown.

List of Tables

Bibliography

[1] N. ALON, Eigenvalues and Expanders, *Combinatorica* 6(2) (1986), 83-96.

[2] N. ALON and V.D. MILMAN, λ_1, isoperimetric inequalities for graphs and superconcentrators, *Journal of combinatorial theory* (Series B) 38 (1985), 73-88.

[3] J. BORNHÖFT, G. BRINKMANN, and J. GREINUS, Pentagon-hexagon-patches with short boundaries, *European Journal of Combinatorics* 24 (2003), 517-529.

[4] G. BRINKMANN, O. DELGADO FRIEDRICHS, A. DRESS, and T. HARMUTH, Cage – a virtual environment for studying some special classes of large molecules, *Match* 36 (1997), 233-237. See http://www.mathematik.uni-bielefeld.de/~CaGe

[5] G. BRINKMANN, O. DELGADO FRIEDRICHS, and U. VON NATHUSIUS, Numbers of faces and boundary encodings of patches, *Graphs and Discovery* – Proceedings of the DIMACS workshop on *Computer-Generated Conjectures from Graph Theoretic and Chemical Databases*, 2001.

[6] G. BRINKMANN and A. DRESS, A constructive enumeration fo fullerenes, *Journal of Algorithms* 23 (1997), 345-358.

[7] G. BRINKMANN, P.W. FOWLER, and C. JUSTUS, A catalogue of isomerisation transformations of fullerene polyhedra, *Journal of Chemical Information and Computer Science* 43 (2003), 917-927.

[8] G. BRINKMANN and P.W. FOWLER, A catalogue of growth transformations of fullerene polyhedra, *Journal of Chemical Information and Computer Science* 43 (2003), 1837-1843.

[9] G. BRINKMANN, J.E. GRAVER, and C. JUSTUS, Numbers of faces in disordered patches. Appears in: *Journal of Mathematical Chemistry.*

[10] G. BRINKMANN, U. VON NATHUSIUS, and A.H.R. PALSER, A constructive enumeration of nanotube caps, *Discrete Applied Mathematics* 116 (2002), 55-71.

[11] J. CHEEGER, A lower bound for the smallest eigenvalue of the Laplacian, in *Problems in Analysis* (edited by R.C. Gunning), Princeton University Press, New Jersey (1970), 195-199.

[12] H.S.M. COXETER, Virus macromolecules and geodesic domes, in *A Spectrum of Mathematics* (edited by J.C. Butcher), Oxford University Press (1971), 98-107.

[13] G. Davidoff, P. Sarnak, and A. Valette, *Elementary number theory, group theory, and Ramanujan graphs*, Cambridge University Press (2003).

[14] M.S. Dresselhaus, G. Dresselhaus, and P.C. Eklund, *Science of Fullerenes and Carbon Nanotubes*, Academic Press, 1996.

[15] A. Egging, Kürzeste Randlängen von Patches mit Drei-, Vier-, Fünf- und Sechsecken, Diplomarbeit, Bielefeld 2005.

[16] M. Endo and H.W. Kroto, Formation of carbon nanofibers, *Journal of Physical Chemistry*, 96 (1992), 6941-6944.

[17] M. Ficon, Die (s,t)-Klassifikation von Halftubes, Diplomarbeit, Bielefeld 2004.

[18] P.W. Fowler, K.M. Rogers, S. Fajtlowicz, P. Hansen, and G. Caporossi, Facts and conjectures about fullerene graphs: Leapfrog, Cylinder and Ramanujan fullerenes, in *Algebraic Combinatorics and Applications* (edited by A. Betten, A. Kohnert, R. Laue, A. Wassermann), Springer, Berlin (2000), 134-146.

[19] J.E. Graver, Encoding fullerenes and geodesic domes, *SIAM Journal on Discrete Mathematics* 17(4) (2004), 596-614.

[20] J.E. Graver, The structure of fullerenes, *DIMACS Series in Discrete Mathematics and Theoretical Computer Science* 69, AMS (2005), 137-166.

[21] J.E. Graver, A catalog of fullerenes with 10 or more symmetries, *DIMACS Series in Discrete Mathematics and Theoretical Computer Science* 69, AMS (2005), 167-188.

[22] J. Greinus, Patches mit minimaler Randlänge, Diplomarbeit, Bielefeld 2000.

[23] B. Grünbaum and T. Motzkin, The number of hexagons and the simplicity of geodesics on certain polyhedra, *Canadian Journal of Mathematics* 15 (1963), 744-751.

[24] B. Grünbaum, *Convex polytopes*, Interscience Publishes, New York (1967).

[25] J.L. Gross and T.W. Tucker, *Topological Graph Theory*, John Wiley and Sons, 1987.

[26] X. Guo, P. Hansen, and M. Zheng, Boundary uniqueness of fusenes, *Discrete Applied Mathematics* 118(3) (2002), 209-222.

[27] F. Harary and H. Harborth, Extremal Animals, *Journal of Combinatorics, Information and System Sciences* 1 (1976), 1-8.

[28] S. Iijima, Helical microtubules of graphitic carbon, *Nature* 318 (1991), 162-163.

[29] C. Justus, Transformationen zwischen Fullerenen und die Flächenzahl von Patches mit gleichem Rand, Diploma thesis, Bielefeld, 2003.

[30] W. Krätschmer, L.D. Lamb, K. Fostiropoulos, and D.R. Huffman, Solid C_{60}: a new form of carbon, *Nature* 347 (1990), 354-358.

[31] H.W. Kroto, J.R. Heath, S.C. O'Brien, R.F. Curl, and R.E. Smalley, C_{60}: Buckminster fullerene, *Nature* 318 (1985), 162-163.

[32] A. Lubotzky and I. Pak, The product replacement algorithm and Kazhdan's property (T), *Journal of the American Mathematical Society* 14(2) (2000), 347-363.

[33] A. Lubotzky, R. Phillips, and P. Sarnak, Ramanujan graphs, *Combinatorica* 8(3) (1988), 261-277.

[34] B. Mohar, Isoperimetric numbers of graphs, *Journal of combinatorial theory*, Series B, 47 (1989), 274-291.

[35] M. Morgenstern, Existence and explicit constructions of q+1 regular Ramanujan graphs for every prime power q, *Journal of Combinatorial Theory* 62 (1994), 44-62.

[36] J. Naor and M. Naor, Small-bias probability spaces: Efficient constructions and applications, *SIAM Journal on Computing* 22 (1993), 838-856.

[37] A. Nilli, On the second eigenvalue of a graph, *Discrete Mathematics* 91 (1991), 207-210.

[38] N. Pippenger, Sorting and selecting in rounds, *SIAM Journal on Computing* 16 (1987), 1032-1038.

[39] O. Reingold, S. Vadhan, and A. Wigderson, Entropy waves, the zig-zag product, and new constant-degree expanders, *Annals of Mathematics* 155 (2002), 157-187.

[40] P. Sarnak, What is an expander? *Notices of the AMS* 51 (2004), 762-763.

[41] R.F. Service, Mixing nanotube structures to make a tiny switch, *Science* 271 (1996), 1232.

[42] R.F. Service, Superstrong nanotubes – Show they are smart, too, *Science* 281 (1998), 940-942.

[43] M. Sipser, Expanders, randomness, or time versus space, *Journal of Computer System Sciences* 36 (1988), 379-383.

[44] M. Sipser and D.A. Spielman, Expander codes, *IEEE Transactions on Information Theory* 42 (1996), 1710-1722.

[45] M. Tanner, Explicit concentrators from generalized n-gons, *SIAM Journal on Algebraic Discrete Methods* 5 (1984), 287-293.

[46] S.J. Tans, M.H. Devoret, H.J. Dai, A. Thess, R.E. Smalley, L.J. Geerligs, and C. Dekker, Individual single-wall carbon nanotubes as quantum wires, *Nature* 386 (1997), 474-477.

Index